GEOLOGICA ULTRAIECTINA

Mededelingen van het
Instituut voor Aardwetenschappen der
Rijksuniversiteit te Utrecht

No. 57

Geochemical and Early Diagenetic Aspects of Interbedded Pelagic/Turbiditic Sediments in Two N. Atlantic Abyssal Plains

Gerrit Jan DE LANGE

STELLINGEN

Observed gradients in solid-phase calcitic-Mn profiles within turbidites are not necessarily related to observed gradients in the pore water concentration of Mn^{2+} from the same samples. (Jarvis & Higgs, 1987; Thomson et al., 1987)

Une cigarette en haute cuisine est un crime culinaire (Maître Antonin Carème, 1784-1833).

Bij de huidige promovendus is het hemd nader dan de rook.

In South Africa Black & White is served from separate bottles.

De gemiddelde verblijftijd van een aio zal vrijwel net zo lang en onzeker zijn als de gemiddelde verblijftijd van water in de Kau Baai, Halmahera (oostelijk Indonesië).

Good appetite is not satisfied by apatite.

Despite the use of complicated mathematical models often simple chemical rules (like mass and charge balance) are not obeyed (Emerson et al., 1982; Bender et al., 1985; Wilson et al., 1986).

Is doctor ande(r)s ?

The K^+-enrichment of interstital water relative to open-ocean bottom water as deduced from the composition of clinoptilolite is in conflict with most observed K^+ pore-water values (Chelishchev, 1986 in : Geokhimiya 4, 540-547).

Genetische manipulatie is geen ethische manipulatie.

The relative enrichment of Fe over Mn in Fe,Mn-rich coatings on recent foraminifera cannot be attributed to selective (early diagenetic) dissolution of Fe (Palmer & Elderfield, 1986).

Aerobic abyssal sediments are in general the least 'aerobic'.

Vergrijzing begint vaak al op jeugdige leeftijd.

The presence of Pb in petrol has a negative influence on all ages (Moorbath et al., 1981)

An organic C content of 3% of a deep red clay (Nares Abyssal Plain) seems to be a large over-estimation (Valin & Morse, 1982).

Public's embarrassment of public embracement has debased.

Subsampling may be a subversive activity.

Gert J. de Lange

Utrecht, 28-11-1988

Addendum

Various (parts of) chapters and some figures have already been published and are included in this thesis by permission of the publishers/journals :

- Oceanologica Acta
- Science
- American Journal of Science
- Pergamon Press
- Geologica Society Publishing House

GEOLOGICA ULTRAIECTINA

Mededelingen van het
Instituut voor Aardwetenschappen der
Rijksuniversiteit te Utrecht

No. 57

Geochemical and Early Diagenetic Aspects of Interbedded Pelagic/Turbiditic Sediments in Two N. Atlantic Abyssal Plains

CIP-GEGEVENS KONINKLIJKE BIBLIOTHEEK, DEN HAAG

Lange, Gerrit Jan de

Geochemical and early diagenetic aspects of interbedded pelagic/turbiditic sediments in two N. Atlantic Abyssal plains / Gerrit Jan de Lange. - [Utrecht : Instituut voor Aardwetenschappen der Rijksuniversiteit Utrecht]. - (Geologica Ultraiectina : no. 57)
Proefschrift Utrecht. - Met lit. opg. - Met samenvatting in het Nederlands en Frans.
ISBN 90-71577-10-4
SISO 562 UDC 550.46(043.3)
Trefw.: geochemie.

ISBN : 90-71577-10-4
Graphic production : Oosterijssel, Alblasserdam

Geochemical and Early Diagenetic Aspects of Interbedded Pelagic/Turbiditic Sediments in Two N. Atlantic Abyssal Plains

Geochemische en Vroeg-Diagenetische Aspecten van Afwisselend Pelagische/Turbiditische Sedimenten in Twee N. Atlantische Abyssale Vlaktes

(met een samenvatting in het Nederlands)

Aspects Géochimiques et Diagenétiques Précoces des Sédiments Interstratifiés Pélagiques et Turbiditiques dans Deux Plaines Abyssales de l'Atlantique du Nord

(avec un résumé en Français)

PROEFSCHRIFT

Ter verkrijging van de graad van doctor aan de Rijksuniversiteit te Utrecht op gezag van de Rector Magnificus, Prof. Dr. J.A. van Ginkel ingevolge het besluit van het College van Dekanen in het openbaar te verdedigen op

maandag 28 november des namiddags te 0.45 uur

1988

door

Gerrit Jan de Lange

geboren op 15 juni 1950, te Harderwijk

PROMOTOR : Prof. Dr. C.H. van der Weijden

C O N T E N T S

Some chapters or parts of chapters have already been published or are accepted for publication.

Chapter 1. In part conveyed at DAHLEM Conference on '*Productivity of the Ocean: Present and Past*'. Berlin, April 1988.

Chapter 2. DE LANGE G.J. (1984[a]) Chemical composition of interstitial water in cores from the Madeira Abyssal Plain (Eastern North Atlantic). Meded. Rijks Geol. Dienst 38, 199-207.

DE LANGE G.J., CRANSTON R.E., HYDES D.H. and BOUST D. (1988[a]) Problems that can be encountered during the extraction of pore water from marine sediments. In: Schüttenhelm R.T.E. et al. (eds), JRC Series (in press).

Chapter 3. DE LANGE G.J. (1984[b]) Shipboard pressure-filtration system for interstitial water extraction. Meded. Rijks Geol. Dienst 38, 209-214.

DE LANGE G.J., CRANSTON R.E., HYDES D.H. and BOUST D. (1988[a]) Problems that can be encountered during the extraction of pore water from marine sediments. In: Schüttenhelm R.T.E. et al. (eds), JRC Series (in press).

Chapter 4. DE LANGE G.J. (1986[b]) Early diagenetic reactions in interbedded pelagic and turbiditic sediments in the Nares Abyssal Plain (western North Atlantic) : Consequences for the composition of sediment and interstitial water. Geochim. Cosmochim. Acta 50, 2543-2561.

Chapter 5. DE LANGE G.J., JARVIS I. and KUIJPERS A. (1987[a]) Geochemical characteristics and provenance of late quaternary sediments from the Madeira Abyssal Plain, North Atlantic. In: Weaver P.P.E. and Thomson J., eds., Geology and Geochemistry of Abyssal Plains. Proc. Geol.Soc. 31, 179-213.

MIDDELBURG J.J. and DE LANGE G.J. (1988[a]) Geochemical characteristics as indicators of the provenance of Madeira Abyssal Plain turbidites. A statistical approach. Oceanol. Acta 11, 159-165.


Differentes Sortes
de BATIMENS
HOLLANDOISES
Dessiné et Gravé

PROLOGUE

In 1980 adequate shipboard facilities for the accurate handling of sediments were not available at the Institute of Earth Sciences. Therefore, during the first years of this study the main attention has been focussed on the development of an appropriate shipboard-handling system and analytical (shipboard and laboratory) procedures.

For the study of pore waters in anoxic/suboxic sediments, it is absolutely necessary to avoid samples to become contaminated with oxygen, prior to or during the pore-water extraction. For that purpose, it is necessary to use a well-designed glove box system. Therefore, a perspex glove box was designed and constructed (see Chapters 2 & 3). For the 1980 expedition to the South Atlantic four high-pressure (up to 50 bar) Manheim-type squeezers (MANHEIM, 1966) could be borrowed.

Due to sampling constraints, to the relatively inefficient handling of this type of squeezers in a glove box and to the limited input of personnel for squeezing (1 person), this expedition has mainly served to gain experience in the anoxic handling and squeezing of deep-sea sediments. Not long after this expedition a squeezing system was designed that would be more easy to operate in a glove box and that would be less costly than the Manheim-type squeezers.

The newly constructed squeezers (after REEBURGH, 1967) were tested during the 1981 expedition to the Norwegian Basin, North Atlantic. Despite the malfunctioning of the on-board analytical system (nutrients) some results of this expedition could be published (DE LANGE, 1983). Next, the analytical facilities were developed, starting in 1982 with a 4-channel auto-analyzer. During the 1982 expedition to the Madeira Abyssal Plain (from hereon referred to as MAP) eastern North Atlantic, the auto-analyzer was used for the first time, and in addition an improved glove box system was installed.

It was only during the 1983 expedition to the eastern Mediterranean that the glove box/ squeezing system (with 2 'squeezing lines') and shipboard analytical techniques both worked satisfactorily. In addition, pH and alkalinity measurements were done on-board. During this expedition the hypersaline Tyro Basin has been discovered (JONGSMA et al., 1983; DE LANGE & TEN HAVEN, 1983). The results of this expedition have been used in the thesis of H.L. TEN HAVEN (1986) and other publications (TEN HAVEN et al., 1985; 1987).

Some expansion of the analytical and squeezing facilities and capacity took place, for the 1984 expedition of the Dutch Geological Survey (RGD) to the Nares Abyssal Plain (from hereon referred to as NAP) western North

Atlantic. In addition the analysis of the pore-water concentration of Si and the measurement of Eh in the sediment were done on board. Part of the results from this expedition are incorporated in this thesis (Chapter 4), another part has been published separately (DE LANGE et al., 1985; DE LANGE, 1986[a]; DE LANGE & RISPENS, 1986; KUIJPERS et al., 1987[a]).
The glove box and squeezing system were subsequently used during the 1985 Snellius II expedition leg K4 of the Working Group Marine Earth Sciences Utrecht, to Kau Bay Halmahera, eastern Indonesia. The results of this expedition will be used in the Ph.D. study of J.J. Middelburg and in other publications (DE LANGE et al., 1988[e]; MIDDELBURG & DE LANGE 1988[c]; MIDDELBURG et al., 1988[a,b]; VAN DER SLOOT et al., 1988; VAN DER WEIJDEN et al., 1988[a]).
Within a month after this expedition the same glove box and squeezing systems were used during the International ESOPE expedition, to the MAP and NAP. In this expedition the glove box, the squeezing and the analytical systems worked excellently (see Chapters 2,3). Meanwhile the on-board geochemical group had expanded from 1 person (1980) to 21 persons (1985), and the total number of squeezed samples per expedition day had increased from 1 to 22, on average. Part of the results originating from this expedition have been published separately (MIDDELBURG & DE LANGE, 1988[b]; MIDDELBURG et al., 1987). Subsequent expeditions to the MAP (1986) and the eastern Mediterranean (1987) have thusfar resulted in other papers that are not included in this thesis (DE LANGE et al., 1987[b]; DE LANGE et al., 1988[b,c,f];HYDES et al., 1988; VAN DER WEIJDEN et al., 1988[b,c]).
Most of the results reported in this thesis are based on samples that have been obtained during the 1984 RGD- and the 1985 ESOPE-expedition.
The financial and technical support given by the RGD for both expeditions (and for other expeditions) is highly appreciated. In addition to thanking the Director of the RGD for this support, I wish to acknowledge all those forming part of the on-board team : R.T.E. Schüttenhelm, K. Adriaanse, F. Clotz, H. Dekker, S. Dijkstra, E. Duin, R. Hoogendoorn, R. Janus, P. van der Klugt, L. Kluwen, P. Kok, A. Kuijpers, C. Laban, C. Mesdag, F. Rispens, T. Van Warmenhoven (all RGD), J. Ebbing (now RGD), J. Schilling, T. Buisman, H. De Porto (all NIOZ), C. Schröder (BRD), D. Boust, B. Chapuy, R. Gandon (all France), S. Colley, D. Hydes, N. Higgs, D. Stanners (all United Kingdom), R. Cranston, B. Fitzgerald (both Canada), R. Delfanti, G. Izzo, C. Papucci (all Italy), K. Shimooka (Japan), H. Boespflug, L. Brush, L. Shephard (all USA).
In addition to shipboard assistance, analytical support has been given by: H. Dekker, T. Bouten, J. Niël, M. Van Alphen, V. Govers, T. Van Zessen, G. Eussen, G. Peters, G. Nobbe, A. Van Dijk, H. Nederloff, P. Anten.
The inventive technical assistance and creative cooperative thinking given by D. Steenbeek and A. Van Genderen, and by P. Kleingeld and H. Van Der

Meer are greatly appreciated.

Working on a ship is team-work, therefore I thank all other team-members that shared expeditions with me, namely : J. Van Bennekom, F. Schilling, T. Van Weering, D. Eisma, S. Van Der Gaast, F. Jansen, J. Kalf, J. Van Iperen, R. Gieles, R. De Vries, G. Berger, M. Van Der Loeff, P. Alkema, R Schmidt, J. Leijtens, A. Balk, W. Polman, W. Van Veen, J. Van Beusekom, R. Groenewegen, I. Timmers (all NIOZ/NCZ), D. Hoede (ECN), R. Dujardin (Belgium), C. Müller (BRD), G. Anastasakis, M. Alexandri, V. Lykousis, A. Sioulas, C. Tziavos, N. Vouloumanos (all Greece), G. Auffret, R. Kerbrat, R. Montarget (all France), D. Buckley (Canada), J. Bonaduce, A. Camerlenghi, G. Catalano, E. Erba (all Italy), T. Freeman, K. Jones, C. Law, T.Newby, P. Schultheiss, I. Steward, P. Weaver, (all United Kingdom), A. Driscoll, G. Luther III, W. Ullman (all USA), K. Bjørklund (Norway), Suharno, Sukardjono, D. Mulyadi, S. Shophiah and S. Latiff (all Indonesia), A. Fortuin, D. Van Harten, W. Huson, D. Jongsma, G. Klaver, D. Kroon, J. Peters, T. Speelman, S. Troelstra, M. Van Gool (all VU/GU), M. Van Der Hoek (TNO), H. Van Aken and W. Boot (both IVOU), L. Belle, H. Boer, H. De Baar, C. Hendriks, E. Henneke, D. Hoede, R. Mattthezing, T. McGee, J. Middelburg, A. Meertens, P. Pruijsers, E. Rohling, D. Steenbeek, L. Ten Haven, A. Van Genderen, W. Van Der Linden, H. Van Der Meer, R. Van Leeuwen, M. Van Vreumingen, C. Van Der Weijden, R. Van Der Weijden, R. Van Ingen, B. Van Os, D. Verwey, O. Werver, J. Zachariasse, (all IVAU).
In addition, I wish to thank C. Van Der Weijden for the support and liberty given during the research, miss S. McNab for linguistic and stylistic advice that made some chapters more readable.
A. Van Genderen, R. Comans & J. Middelburg, deserve special thanks, not only because of cheerfully sharing a room, a telephone and coffee with the author, but also because of their pleasant cooperation and the numerous scientific and other discussions.
Although not directly involved in the results discussed in this thesis, the Dutch Council for Sea-Research (NRZ) has supported the marine geochemical research of the Institute of Earth Sciences Utrecht throughout the years. The Tidal Division of the Public Works Department of the Netherlands kindly lent us their high-pressure squeezers (courtesy J. Al).
Part of the drawings in this thesis were skillfully made by R. Meye and I. Santoe of the Drawing Department. I. Jarvis is thanked for his cooperation in preparing the manuscript for Geol. Soc. volume 31 (see Chapter 5); all other co-authors are thanked for their contribution(s).
The cooperation given by Captain Blok and crew of R.V. Tyro and by Y. Balut, Captain and crew of R.V. Marion Dufresne were greatly appreciated.
In advance I wish to apologize for the unintentional but inevitable

omission of names of (on-board) companions and other partners in science.

Last but not least, I thank Françoise, Erick and Sebastiaan for their moral support and their (almost) endless comprehension during the preparation of this thesis.

Ship figures have been reproduced from GROENEWEGEN (1789).

ABSTRACT

An adequate shipboard system has been developed for the handling and analysis of suboxic sediments and pore waters. The results obtained with this system have been compared with those obtained using another system. Between these two systems large variations have been found in the concentration of some pore-water constituents. These variations could be explained not only by contamination with oxygen, but also by temperatures deviating from the in-situ temperature during the pore-water extraction.

The sediments that have been studied originate from two North Atlantic abyssal plains, namely the Madeira and Nares Abyssal Plains (from hereon referred to as MAP and NAP respectively). Both plains are characterized by interbedded pelagic/turbiditic sediments. The average sedimentation rate for the sediments in the NAP is 10 times higher, and the average turbidite thickness 10 times lower, than those in the MAP. The post-depositional early diagenetic processes that occur in the sediments of both plains are mainly determined by the organic matter content. The organic matter content is in general higher in turbiditic sediments than in pelagic. Therefore, in the former sediments the concentration of NO_3^- generally goes to zero within a sediment depth of 1 m, whereas at 8 m in a pelagic core from the same area (NAP) the concentration of NO_3^- is still higher than it is in the bottom water. The pore-water concentration of Mn^{2+} in the turbiditic sediments of the NAP increases sharply down to a depth of approximately 3 m, and from thereon remains nearly constant due to saturation with respect to Mn,Ca-CO_3. The pore water of the turbiditic sediments is also saturated with respect to calcite. The few "diagenetic spikes" in the pore-water concentration of NO_3^- and Mn^{2+} and the concentration/depth profile of dissolved iron, H_4SiO_4 and phosphate all clearly demonstrate the inhomogeneous nature of interbedded pelagic and turbiditic sediments. The simultaneous occurrence of peaks of dissolved iron/silica and of sediment intervals with a relatively high organic carbon content is attributed to enhanced early diagenetic reactions associated with the decomposition of organic matter in these specific intervals. Due to the unique combination of low porosity and relatively high sedimentation rates, the sediments from the NAP are an ideal basis for the study of the pore-water chemistry in such interbedded sequences of pelagic and turbiditic deposits.

Re-allocation of Fe and P has been demonstrated to occur in the sediments of the NAP. These processes are likely to occur also in the sediments of MAP. The various turbidites in the MAP can be correlated without great problems, whereas for those in the NAP no correlation could be

demonstrated. On the basis of chemical analyses it has been possible to assign provenance areas for most of the turbidites in the MAP. Only two major components could be distinguished for the sediments of the NAP, namely a mainly 'oceanic' and a mainly 'continental' component. The sediments of the MAP have been divided into three main sediment types, namely 'volcanic', 'organic-rich' and 'carbonate-rich'. These different types are related to different provenance areas lying to the **ENE** (Madeira and Canary Islands + possible near-coastal component), **E** (near-coastal) and **W** (Great Meteor-Cruiser Seamount Chain) of the MAP respectively.

Not only the major and trace element composition of the various turbidites is in part determined by their provenance, but also the composition of the various N and P fractions. The exchangeable (N_{ex}), fixed (N_{fix}) and organic (N_{org}) nitrogen content are all related to the organic carbon (C_{org}) content and demonstrate a much lower affinity with the mineral composition of the sediment. Upon postdepositional decomposition of the organic matter N_{ex} decreases but the N_{ex}/C_{org} ratio remains constant. Therefore, N_{ex} seems to be proportional to the amount of C_{org} present in these sediments. N_{fix} and N_{fix}/Al are high in the organic-rich turbidites, but do not change upon postdepositional oxidation of the organic matter. If the carbonate content is taken into account, then the relative % illite in the organic-rich turbidites is much higher than that in the other turbidites. Therefore, N_{fix} is not associated with C_{org}, but with illite. Postdepositional oxidation of organic matter through oxygen leads to a decrease in the C/N ratio of the remaining organic matter in the organic-rich turbidites. The calculated C/N ratio is similar for organic matter which has been decomposed through oxygen in the upper part of organic-rich turbidites, and for that which is decomposing through sulphate reduction below a depth of 35 m in the sediment (C/N of ≈17 and ≈18 respectively). This implies that the C/N ratio of decomposing organic matter is not much influenced by redox conditions in the sediment.

In contrast to N_{ex}, postdepositional oxidation of organic matter does not change the concentration of P_{ex} (exchangeable and carbonate-bound phosphate) or the P_{ex}/Al ratio in the sediment. Most of the P_{ex} can be attributed to carbonate-associated P, although an additional contribution of P (excess-P) to P_{ex} may exist in the organic-rich e-turbidite. The concentration of Fe- and Al-associated phosphate (P_{OH}) in the oxidized part of organic-rich turbidites is slightly higher than that in the reduced part of the same turbidite. This difference is likely to be due to post-depositional oxidation during which Fe and P are dissolved in the reduced intervals followed by their immobilization in the oxidized turbiditic and pelagic intervals. Linked with these reactions is the irregular pore-water concentration of phosphate (NAP), which is shown to originate partly from the oxidation of organic matter, but mainly from the

desorption of phosphate from iron oxide. Potential concentrations of phosphate are calculated from the stoichiometric early diagenetic reactions and compared with measured concentrations. Sediment intervals in which reductive dissolution of Fe (and P) occurs, are green in colour and have a relatively low Eh value, whereas the more oxidized intervals are brown and have a higher Eh. In the sediments of the MAP these processes are likely to occur too.

High P_{OH} values (MAP) are mainly confined to carbonate-free pelagic sediments, which have been deposited at low sedimentation rates. These high values are likely to result for the greater part from adsorption of P on Fe-oxihydroxides during the extended periods of exposure to seawater at deposition of these sediments.

The total phosphorus content of the sediment consists mainly of apatite-P, which is primarily (if not entirely) provenance-related. The average composition of organic matter found in this study is $C_{106}N_{5.9}P_{0.09}$, whereas that for average marine plankton is $C_{106}N_{16}P_{1}$. This depletion of N and P relative to C has been attributed to preferential decomposition of the N- and P-rich organic compounds in these sediments.

SAMENVATTING

Een adequaat systeem is ontwikkeld om aan boord sub-oxysche sedimenten en poriënwaters te kunnen verwerken en analyseren. De resultaten van dit systeem zijn vergeleken met die van een ander systeem. Tussen de systemen zijn verschillen gevonden in de poriënwater samenstelling van enkele componenten. Deze verschillen konden worden toegeschreven aan zuurstof contaminatie en aan temperaturen, tijdens de poriënwater extractie, die afweken van de in-situ temperatuur.
De bestudeerde sedimenten komen uit twee Noord Atlantische abyssale vlaktes, namelijk de Madeira en Nares Abyssale Vlaktes (respectievelijk MAV en NAV). Beide vlaktes worden gekenmerkt door afwisselende lagen van pelagische en turbiditische sedimenten. De gemiddelde sedimentatie snelheid voor de sedimenten van de NAV is 10 keer hoger, en de gemiddelde dikte van de turbidieten 10 keer lager, dan die in de MAV. In beide vlaktes worden de vroeg-diagenetische processen bepaald door het gehalte aan organisch materiaal. Het gehalte aan organisch materiaal is in de turbiditische sedimenten in het algemeen hoger dan in pelagische. Dientengevolge gaat in eerstgenoemde sedimenten de NO_3^- concentratie in het algemeen naar nul, binnen een sediment diepte van 1 m, terwijl op 8 m in een pelagische kern uit hetzelfde gebied (NAV) de nitraat concentratie nog steeds hoger is dan in het bodem water. De poriënwater concentratie van Mn^{2+} in de turbiditische sedimenten van de NAV neemt tot een diepte van 3 m steil toe en blijft daarna vrijwel constant door verzadiging ten opzichte van Mn,Ca-CO_3. Het poriënwater van turbiditische sedimenten is ook verzadigd ten opzichte van calciet. De enkele "diagenetische pieken" in de poriënwater concentratie van NO_3^- en Mn^{2+} en het concentratie/diepte profiel van opgelost ijzer, H_4SiO_4 en fosfaat laten alle duidelijk het inhomogene karakter zien van afwisselend gelaagde pelagische en turbiditische sedimenten. Het tegelijkertijd voorkomen van pieken in de concentraties van opgelost ijzer/silica en van sediment intervallen met een relatief hoog organisch koolstof gehalte is toegeschreven aan verhoogde activiteit van vroeg-diagenetische reacties samenvallend met de afbraak van organisch materiaal in deze specifieke intervallen. Door de unieke combinatie van een lage porositeit en een relatief hoge sedimentatie snelheden vormen de sedimenten van de NAV een ideale basis voor de studie van deze afwisselend gelaagde pelagische en turbiditische sedimenten.
In de sedimenten van NAV is de re-allocatie van Fe en P aangetoond. Het is waarschijnlijk dat in de sedimenten van MAV deze processen ook gebeuren. De verschillende turbidieten in de MAV kunnen zonder grote problemen gecorreleerd worden, terwijl bij die in de NAV geen correlatie aangetoond kon worden. Gebaseerd op chemische analyses is het mogelijk geweest

oorsprongs-gebieden toe te wijzen aan de meeste turbidieten in de MAV. Bij de sedimenten in de NAV konden slechts twee componenten onderscheiden worden, namelijk een voornamelijk 'oceanische' en een voornamelijk 'continentale' component. De sedimenten van de MAV zijn verdeeld in drie groepen, namelijk 'vulkanisch', 'organisch-rijk' en 'carbonaat-rijk'. De verschillende groepen zijn gerelateerd aan de verschillende oorsprongs-gebieden, die respectievelijk ten ONO (Madeira en Canarische eilanden + een mogelijke kust-nabije component), ten O (kust-nabij) en ten W (Great Meteor-Cruiser Seamount Chain) van de MAV liggen. Niet alleen de hoofd- en spoor- element samenstelling van de verschillende turbidieten wordt bepaald door hun oorsprong, maar ook de samenstelling van de verschillende N- en P-fracties. Het gehalte aan uitwisselbare (N_{ex}), gefixeerde (N_{fix}) and organische (N_{org}) stikstof is gerelateerd aan het organisch koolstof gehalte (C_{org}) en vertoont veel minder affiniteit met de mineraal-samenstelling van het sediment. Door afbraak van organisch materiaal na afzetting neemt weliswaar het N_{ex} gehalte af, maar de N_{ex}/C_{org} ratio blijft constant. Het lijkt daarom dat het gehalte aan N_{ex} is evenredig is met het C_{org} gehalte in het sediment. N_{fix} en N_{fix}/Al zijn hoog in de organisch-rijke turbidieten, maar veranderen niet door afbraak van organisch materiaal na afzetting. Als rekening gehouden wordt met het kalk-gehalte, dan hebben de organische turbidieten een relatief illiet gehalte dat hoger is dan dat in de andere turbidieten. Kortom, N_{fix} is niet ge-associeerd met C_{org}, maar met illiet. Wanneer na afzetting het organisch materiaal (micro-biologisch) door middel van zuurstof wordt afgebroken, dan leidt dit tot een afname in de C/N ratio van het overblijvende organische materiaal in de organisch-rijke turbidieten. De berekende C/N ratio voor dit door zuurstof afgebroken organische materiaal is gelijk aan de ratio die door stoichiometrisch modelleren berekend wordt (C/N ratios van respectievelijk ≈17 en ≈18). Dit betekent, dat de C/N ratio van organisch materiaal bij afbraak niet be-ïnvloed wordt door de redox condities in het sediment.
In tegenstelling tot N_{ex} veranderen de concentratie 'uitwisselbaar en carbonaat-gebonden fosfaat' (P_{ex}) en de P_{ex}/Al ratio niet door de afbraak van organisch materiaal na afzetting. Het grootste deel van de P_{ex} kan worden toegeschreven aan carbonaat-gebonden P, alhoewel er vooral voor de e-turbidiet een additionele P-bijdrage aan P_{ex} is (excess-P). De concentratie van Fe- en Al-geassocieerde fosfaat (P_{OH}) in het ge-oxydeerde deel van organisch-rijke turbidieten is iets hoger dan die in het ge-reduceerde deel van dezelfde turbidiet. Dit verschil wordt vermoedelijk veroorzaakt door oxydatie na afzetting gedurende welke Fe en P opgelost worden in de gereduceerde intervallen en vervolgens weer neerslaan in de ge-oxideerde turbiditische en pelagische intervallen. De onregelmatige poriën-water concentratie van fosfaat (NAV) houdt verband met deze reacties. Deze concentratie wordt voor een deel veroorzaakt door de

oxydatie van het organisch materiaal, maar is voor het grootste deel afkomstig van desorptie van fosfaat van ijzer oxyde. Potentiële concentraties van fosfaat zijn berekend uit de stoichiometrische vroeg-diagnetische reacties en vergeleken met gemeten concentraties. Sediment-intervallen waar door reductie Fe (en P) oplost, zijn groen en hebben een relatief lage Eh waarde, terwijl de meer ge-oxydeerde intervallen bruin zijn en een hogere Eh hebben. Het is waarschijnlijk dat deze processen ook in de sedimenten van de MAV gebeuren. Hoge P_{OH} waarden (MAV) worden vooral gevonden in carbonaat-vrije pelagische sedimenten, die bij lage sedimentatie snelheden zijn afgezet. Deze hoge waarden worden voor het grootste deel veroorzaakt door adsorptie van P aan Fe-oxyhydroxydes gedurende de lange periode van contact met zeewater bij lage sedimentatie snelheid.

Het totale fosfor gehalte van het sediment bestaat voor het grootste deel uit apatiet-P, dat voornamelijk (of zelfs geheel) bepaald is door de herkomst. De hier gevonden gemiddelde samenstelling van organisch materiaal is $C_{106}N_{5.9}P_{0.09}$, terwijl die voor marien plankton $C_{106}N_{16}P_1$ is. Deze relatieve afname van N en P ten opzichte van C is toegeschreven aan preferente afbraak van het organisch materiaal in deze sedimenten.

RESUME

Un système a été développé pour la manipulation et l'analyse des sédiments sub-oxyques et des eaux interstitielles à bord. Les résultats obtenus avec ce système-ci ont été comparés à ceux obtenus avec un autre système. Entre ces deux systèmes de grandes différences ont été trouvées dans la concentration de quelques composants de l'eau interstitielle. Ces différences pouvaient être expliquées non seulement par une contamination par oxygène, mais aussi par des températures différentes de la température 'in-situ' pendant l'extraction de l'eau interstitielle.

Les sédiments étudiés descendent de deux plaines abyssales de l'Atlantique Nord, c'est-à-dire la Plaine Abyssale de Madère et celle de Nares (nommées ci-après respectivement PAM et PAN). Les deux plaines sont caractérisées par des sédiments pélagiques/turbiditiques interstratifiés. Le tas de sédimentation moyen pour les sédiments de la PAN est 10 fois plus élevé, et l'épaisseur moyenne des turbidites est 10 fois moins élevée, que celui et celle de la PAM. Les réactions de diagenèse précoce post-dépositionnelles qui ont lieu dans les sédiments des deux plaines, sont déterminées surtout par le contenu de la matière organique. Le contenu de la matière organique est en général plus élevé dans les sédiments turbiditiques que dans les sédiments pélagiques. Pour cette raison, en général, la concentration de NO_3^- s'approche de zéro à une profondeur de moins de 1 m dans les sédiments turbiditiques. Par contre, la concentration de NO_3^- à une profondeur de 8 m dans une carotte pélagique est toujours plus élevée que celle dans l'eau du fond. La concentration de Mn^{2+} dans l'eau interstitielle dans les sédiments turbiditiques de la PAN augmente brusquement jusqu'à une profondeur d'environ 3 m, et à partir de là reste presque constante à cause d'une saturation par rapport à $Mn,Ca-CO_3$. L'eau interstitielle des sédiments turbiditiques est aussi saturée par rapport à la calcite. Les quelques pics dans les profils de la concentration vers la profondeur en NO_3^-, Mn^{2+}, Fe^{2+}, H_4SiO_4 et en phosphate, montrent clairement la nature non-homogène des sédiments pélagiques et turbiditiques interstratifiés. Les présences des pics de fer dissous et de pics de silice, simultanées à des couches de sédiments ayant un contenu élevé de matières organiques, sont attribuées à des réactions accrues de diagenèse précoce associées à la décomposition de la matière organique dans ces couches spécifiques. Grâce à la combinaison unique de faible porosité et des taux de sédimentation relativement élevés, les sédiments de la PAN sont une base idéale pour l'étude de ces séquences de dépôts pélagiques et turbiditiques interstratifiés.

Il a été démontré que la re-allocation de Fe et P se passe dans les sédiments de la PAN. Ces réactions se passent probablement aussi dans les

sédiments de la PAM. Les différentes turbidites dans la PAM peuvent être mises en corrélation sans grandes difficultés, tandis que pour celles de la PAN il est impossible de montrer une corrélation. Sur la base des analyses chimiques il a été possible d'assigner des régions de provenance pour la plupart des turbidites dans la PAM. Seulement deux composants pouvaient être distingués pour les sédiments de la PAN, c'est-à-dire un composant principalement 'océanique' et un principalement 'continental'. Les sédiments de la PAM ont été répartis en trois types de sédiments principaux, c'est-à-dire 'volcanique', riche-en-matière-organique ('organique') et riche-en-carbonate ('carbonate'). Ces types différents sont liés à des régions d'origines différentes, étant situées par rapport à la PAM respectivement à l'**ENE** (îles de Madère et Canaries + un composant littoral possible), à l'**E** (littoral) et à l' O (Great Meteor-Cruiser Seamount Chain). Non seulement la composition des éléments majeurs et traces des turbidites différentes est partiellement déterminée par leur provenance, mais aussi la composition des fractions différentes de N et P. Les concentrations d'azote échangeable (N_{ex}), fixé (N_{fix}) et organique (N_{org}) sont toutes liées à la concentration de carbone organique (C_{org}) et montrent une affinité plus faible avec la composition minérale du sédiment. Sur décomposition post-dépositionnelle de la matière organique, N_{ex} diminue mais le ratio N_{ex}/C_{org} reste constant. C'est pourquoi N_{ex} est directement proportionnel à la concentration de C_{org} dans les sédiments. N_{fix} et N_{fix}/Al sont élevés dans les turbidites organiques, mais ils ne changent pas sur oxydation post-dépositionnelle de la matière organique. Si on tient compte du contenu en carbonate, le pourcentage relatif d'illite dans les sédiments organiques est plus haut que celui des autres turbidites. Pour cette raison, N_{fix} n'est pas associé à C_{org}, mais à l'illite. L'oxydation post-dépositionnelle de matière organique par oxygène mène dans les turbidites organiques à une diminuation du ratio C/N de la matière organique résiduelle. Le ratio C/N calculé est semblable pour la matière organique qui a été décomposée par oxygène dans la partie supérieure des turbidites organiques, et pour celle qui est en décomposition par réduction de sulfate en dessous d'une profondeur de 35 m dans le sédiment (respectivement un C/N de ≈17 et de ≈18). Cela signifie que le ratio C/N de la matière organique en décompostion n'est pas beaucoup influencé par des conditions rédox dans le sédiment.

Par opposition à N_{ex}, l'oxydation post-dépositionnelle ne change pas la composition de P_{ex} (échangeable et carbonate-lié) ou le ratio de P_{ex}/Al dans le sédiment. La plupart du P_{ex} peut-être attribué au P lié-au-carbonate, bien qu'une contribution additionnelle de P (P-excess) à P_{ex} puisse exister dans la turbidite organique de 'e'. La concentration de phosphate associée au Fe et Al (P_{OH}) dans la partie oxydée des turbidites organiques est tant soit peu plus élevée que celle dans la partie

réductrice de la même turbidite. Cette différence est probablement due à l'oxydation post-dépositionelle pendant laquelle Fe et P sont dissous dans les couches réductrices, suivie par leur immobilisation dans les couches oxydantes turbiditiques et pélagiques.

La concentration irrégulière de phosphate dans l'eau interstitielle est liée à ces réactions (PAN); il a été démontré que ceci est provoqué partiellement par l'oxydation de la matière organique, mais pour la plus grande partie par la désorption de l'oxyde de fer. Des concentrations potentielles de phosphate ont été calculées depuis des réactions diagénétiques précoces stoechiométriques et comparées à des concentrations mesurées. Des couches de sédiments dans lesquelles se passent la dissolution réductive de Fe (et P), sont de couleur verte et ont une valeur de Eh relativement basse. Par contre, les couches plus oxydées sont de couleur marron et ont un Eh plus élevé. Il est probable que les mêmes réactions se passent aussi dans les sédiments de la PAM.

Des valeurs élevées de P_{OH} (PAM) sont principalement limitées aux sédiments pélagiques sans carbonate, qui ont été déposés à des taux faibles de sédimentation . Ces valeurs élevées sont probablement pour la plus grande partie le résultat d'adsorption de P aux oxyhydroxydes de fer pendant les périodes étendues d'exposition à l'eau de mer à la déposition de ces sédiments.

Le contenu total du sédiment en phosphate est composé principalement d'apatite-P, ce qui est essentiellement (ou même entièrement) en liaison avec l'origine. La composition moyenne de la matière organique trouvée dans cette recherche est $C_{106}N_{5.9}P_{0.09}$, tandis que celle du plancton marin est en moyenne $C_{106}N_{16}P_{1}$. Ce déficit en N et P par rapport à C a été attribué à la décomposition préférentielle de la matière organique dans ces sédiments.

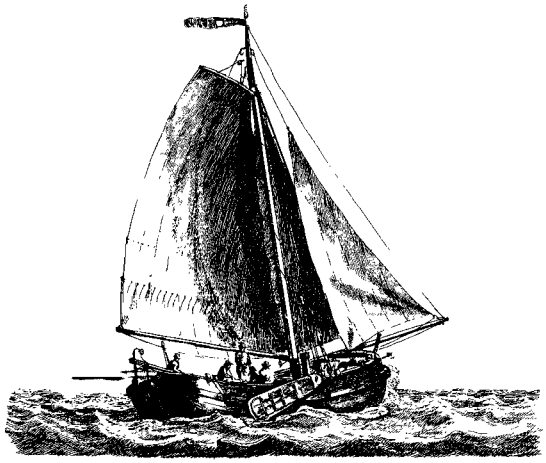

D Schol schuit die zijn Korde uitzeilt 11

Chapter 1

SOME ASPECTS OF THE DECOMPOSITION OF ORGANIC MATTER IN MARINE SEDIMENTS; A BRIEF REVIEW

ABSTRACT

Most early diagenetic reactions described in this thesis are determined by the organic carbon content of the sediment. In this Chapter a brief review is given of the present knowledge of organic matter decomposition rates and its possible dependency on the oxygen content of the sediment.

1-1. INTRODUCTION

Organic matter seems to be the main 'fuel' that allows the 'diagenetic motor' to run, at various 'speeds'. Most early diagenetic processes discussed in this thesis find their origin in the microbial decomposition of organic matter. It is therefore appropriate to briefly summarize some of the present ideas on organic carbon and its decomposition:
The fate of organic carbon and the organic carbon content of the sediment in relation to paleo productivities or to bottom-water oxygen content, have been discussed extensively in the literature (e.g. EMERSON, 1985; REIMERS, 1988 and refs. herein). It is only in the last two decades that some progress has been made on its quantification and on the actual mechanisms that determine its decomposition rates. Some presently known aspects that are appropriate to this study will be briefly summarized here (conveyed at DAHLEM Conference, Berlin, April 1988) :

1-2. ORGANIC MATTER AND ITS DECOMPOSITION RATES

Organic matter reaching the sea floor can be thought to consist of several groups of compounds (multi G model, JØRGENSEN, 1979; BERNER, 1980a; WESTRICH, 1983; WESTRICH & BERNER, 1984) that differ in their reactivity with respect to decomposition. If first order reaction kinetics are assumed, then the overall decomposition rate can be expressed as :

$$-dG_T/dt = \sum_{1}^{n} k_i G_i \qquad (1)$$

in which : i = fraction
G_i = concentration of organic carbon per unit mass of total solids in an organic compound group
G_T = total decomposable organic carbon
k_i = first order rate constant
The value of k_i decreases for each successive fraction. Although the

various fractions of organic matter probably form a continuum, as a simplification organic matter can be thought to consist of three main fractions, being 1. ***very labile***, 2. ***labile*** and 3. ***refractory*** (e.g. BERNER, 1980a; WESTRICH & BERNER, 1984; EMERSON et al., 1987; REIMERS, 1988).

Fraction 1 (***very labile***) is decomposed rapidly in the water column and at the sediment-water interface. Decomposition through oxygen or sulphate under oxidized respectively reduced conditions has been reported to occur at similar rates ($k < 20\ y^{-1}$) within a factor of 2 to 3. This means that for most deep-sea sediments this fraction will be decomposed within a few months after its deposition.

Fraction 2 (***labile***) is decomposed at the sediment-water interface or in the sediment at moderate rates ($k \approx 10^{-2}$ to $10^{-5}\ y^{-1}$); the decomposition rate of part of this fraction seems to be dependent on the presence of oxygen (see below).

Fraction 3 (***refractory***) is the refractory fraction, being virtually non-decomposable under normal low temperature early diagenetic conditions.

Depending on sedimentation rate, bottom-water oxygen content, and the organic carbon content of the sediment in question, part of fraction 2 may be buried in the sediment. Once below the zone of oxygen penetration, decomposition of this fraction will continue only very slowly (orders of magnitude slower than under oxic conditions {$k < 10^{-6}\ y^{-1}$}).
It is mainly fractions 2+3 that make up the organic carbon "paleo signal" in the sediment. The possible difference in organic-matter decomposition rates under oxic and under anoxic conditions has been the subject of discussion for some years (e.g. BERNER, 1980a; MÜLLER & MANGINI, 1980; REIMERS & SUESS, 1983; WESTRICH & BERNER, 1984; EMERSON, 1985; HENRICHS & REEBURGH, 1987; REIMERS, 1988). The question is an important one, as the cycles of organic carbon content that commonly occur in marine sediments may be interpreted as records of paleo productivity and of bottom water oxygen content (e.g. EMERSON, 1985; REIMERS, 1988; THIERSTEIN, 1988). On the basis of a literature review organic matter decomposition rates have recently been reported to be similar under oxic and under anoxic conditions (within a factor of 3) for a wide range of organic matter (HENRICHS & REEBURGH, 1987; CANFIELD, 1988). However, research has mainly been focussed on the ***very labile*** fraction of the organic matter. This fraction forms a large part (> 90%) of the total organic matter in sea water, is rapidly decomposed (within a year) and will therefore rarely be found deeper down in the sediment. In contrast, the decomposition rate of fraction 2 seems to be dramatically influenced by the presence of oxygen.

The interbedded organic-rich (turbiditic) and organic-poor (pelagic and turbiditic) sediments of the MAP form a perfect example for this phenomenon (see also Chapter 4). These sediments demonstrate the result of natural 'in-situ experiments' with a time-scale of 10^4 years. Especially in the organic-rich turbidites (% Org. C>0.5%) a distinct colour change occurs in the upper part of each turbidite. Study of the most recent turbidite has demonstrated that this colour change is related to the depth of oxygen penetration ("oxidation front"). The organic carbon content of the oxidized part is much lower than in the reduced parts of these turbidites. At deposition the organic matter content must have been the same within each turbidite. Therefore, from these observations one must conclude that the decomposition of this organic matter (fraction 2) occurs at much higher rates under oxic than under suboxic conditions. Preliminary calculations of the decomposition rates for this fraction in some of the organic-rich turbidites resulted in values for $k \approx 10^{-2}$ to 10^{-5} y^{-1}.
Another example can be found in the eastern Mediterranean, where some small anoxic basins are found. The oxic-anoxic interface occurs at a water depth of ≈3300 m, and the bottom of the basins lies at ≈3700 m. The organic carbon content of the sediments in these anoxic basins is higher than in the oxic sediments outside the basins (approx. 2% vs. 0.3%). The organic carbon rain being identical, these findings indicate that for at least part of the organic matter the decomposition rates are lower under anoxic than under oxic conditions. It must be noted that this statement is only true if bacterial activity is not suppressed by high salinities such as those found in the basin brines.

The oxidation (through oxygen) of the organic matter in the organic-rich turbidites of the MAP not only affects the Org. C content, but also the concentrations of the various nitrogen (N) compounds, and the C/N ratio (Chapter 6).
Similar phenomena must also occur in the NAP. However, the turbidites deposited here are rather thin (mostly cms to dms, compared to ms in MAP) and are less well defined. Furthermore, the high estimated average sedimentation rates (up to 100 $cm.ky^{-1}$ for turbiditic sediments; KUIJPERS et al., 1987) imply frequent deposition of turbidites. Therefore, the 'burn-down' phenomenon that is so well observed in sediments of the MAP is unlikely to have developed to a similar extent in the NAP. In addition, erosion may occur frequently in the NAP, grain-size variations occur on a small scale and estimated average sedimentation rates are ≈10 times higher than in the MAP. Attempts to correlate the various turbidites between cores have been in vain (Chapter 5). Consequently, the sediments of this area are rather complex in composition. In contrast, the relatively thick individual turbiditic deposits in the MAP offer ample opportunity to study and compare

diagenetic processes in various well-defined interbedded organic-rich/organic-poor sedimentary settings.

Due to the high sedimentation rates and the related young age of deposition, the organic matter is more reactive in the sediments of the NAP than in those of the MAP. In addition the sediments in the NAP have a much lower porosity than those in the MAP. Therefore, the sediments of NAP form an ideal basis for the study of the pore-water chemistry in such interbedded sequences of pelagic and turbiditic deposits.

A comparison of these two abyssal plains both containing numerous turbiditic deposits but of very different deposition rates and frequencies is therefore interesting.

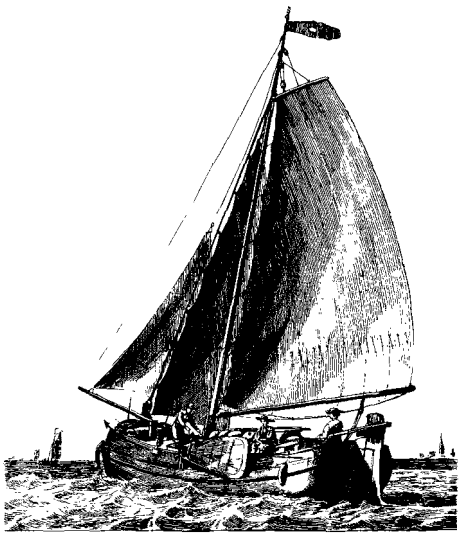

B van Poon 8

Chapter 2

PROBLEMS THAT CAN BE ENCOUNTERED DURING THE EXTRACTION OF PORE WATER FROM MARINE SEDIMENTS

ABSTRACT

Great care must be taken in extracting pore water if results are to be reliable. Errors can arise by inadequate storage conditions prior to pore water extraction, by a difference between extraction temperature and the in situ temperature, by oxygen contamination and possibly by high squeezing pressures. All these errors are discussed and examples are shown; in addition three different extraction techniques are compared.

2-1. INTRODUCTION

Since the early days of pore-water extraction (MURRAY & IRVINE, 1895), many types of systems have been developed to separate pore water from sediment. Only in the last two decades has it become evident that conditions during handling and pore-water extraction of the sediment should be closely controlled, in order to get correct pore-water data (MANGELSDORF et al., 1969; BISCHOFF et al., 1970; FANNING & PILSON, 1971; BRAY et al., 1973; SAYLES et al., 1973a,b; GIESKES, 1973; TROUP et al., 1974; ROBBINS & GUSTINIS, 1976; HOLDREN et al., 1975; LODER et al., 1978; MASUZAWA et al., 1980; DE LANGE 1984[a,b]).

At present squeezing techniques are most widely used; they are relatively simple, they produce reliable pore-water data and the equipment is relatively inexpensive. Centrifugation (POWERS, 1957; RITTENBERG et al., 1963; EDMUNDS and BATH, 1976), leaching (EMERY & RITTENBERG, 1952; SWARZENSKI, 1959) and dilution (MURTHY & FERRELL, 1972), liquid displacement (SCHOLL, 1963; BATLEY & GILES, 1979) and vacuum filtration (JOHNSON, 1967) are other methods that have been used to extract pore water from sediments. Recently, BENDER et al. (1987) have reported that 'whole-core squeezing' of sub-cores may give reliable results with a high depth resolution for the top-most ≈20 cm of sediment recovered by box-corer.

In-situ extraction (e.g. BARNES, 1974; SAYLES et al., 1976; SAYLES, 1985) must be considered as the best possible way of recovering pore water, in that it yields reliable pore-water data, and does not require a complicated, elaborate extraction procedure on board ship. On the other hand, in-situ sampling of pore water in deep-sea sediments is difficult. The in-situ extraction technique avoids amongst other things decompressional effects in the sediment, due to raising the core to the surface from a great depth. Such pressure artifacts have been reported, but these seem to occur only in cores taken in carbonate-ooze sediments, whereas in non-carbonate sediments no such artifacts could be demonstrated (MURRAY et al., 1980; EMERSON et al., 1980; 1982; JAHNKE et al., 1982; DE LANGE, 1986[b]). So far it has not been possible to bring the sediment associated with the in-

situ collected pore-water samples on board ship. Furthermore the number of samples that can be taken per core is relatively limited, as is the depth of penetration (BARNES, 1974; SAYLES et al., 1976), and the price of an in-situ sampler is rather high.
For the on-board extraction procedure, squeezers and centrifuges seem to be the best equipment to use. They are relatively easy to handle and produce pore water of reliable quality, provided that some precautions are taken. Several types of squeezers have been developed, some are gas-operated, others hydraulic (SIEVER, 1962; HARTMANN, 1965; MANHEIM, 1966; REEBURGH, 1967; PRESLEY et al., 1967; KALIL & GOLDHABER, 1973; HOROWITZ et al., 1973; MANHEIM, 1974; ROBBINS & GUSTINIS, 1976; SHISHKINA & TSVETKOV, 1978; ROZANOV et al., 1978; MASUZAWA et al., 1980; RIDOUT, 1981; DE LANGE, 1984[b]). On-board centrifuges need to be fixed in a gimballed structure that compensates for the movements of the ship. Squeezers and centrifuges are mostly operated in combination with a cooling system, and various methods are used to prevent oxygen contamination prior to and during pore-water extraction.

2-2. STUDY AREAS

During the international ESOPE expedition on R.V. Marion Dufresne, high quality cores of up to 34 m in length were taken in the Madeira and Nares Abyssal Plains, eastern and western North Atlantic respectively (Fig. 2-1, Table 2-1). The Madeira Abyssal Plain (from hereon referred to as MAP) is situated approximately half-way between the NW African Continental Shelf and the Mid Atlantic Ridge, ca. 600 km south of the Azores. The average water depth is 5400 m, and the sediments consist mainly of turbiditic material inter-bedded with small pelagic units. The carbonate content varies mostly between 50 and 60% (WEAVER et al., 1986; DE LANGE et al., 1987[a]). The NAP (from hereon referred to as NAP) is located approximately 400 km north of Puerto

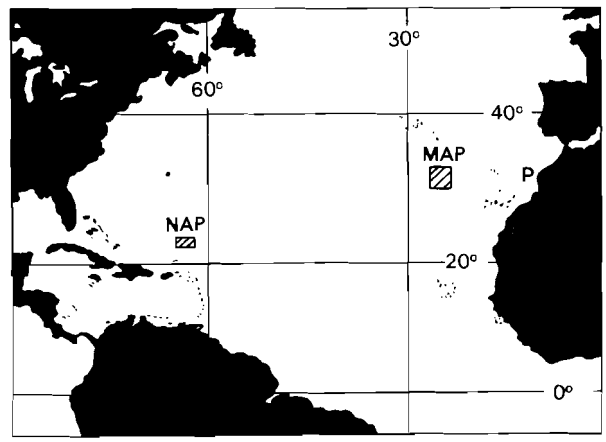

Fig. 2-1. Madeira (MAP) and Nares (NAP) Abyssal Plains study areas. P indicates occurrence of phosphorite nodules; see Chapter 5, (CRONAN, 1980).

TABLE 2-1. Numbers and locations of cores discussed in the text.

core		location		water depth
MD10	(MAP)	31° 16,70' N	25° 23,33' W	5450 m
MD48	(NAP)	22° 54,89' N	63° 26,69' W	5830 m
MD56	(NAP)	23° 59,38' N	64° 30,78' W	5845 m
MD60	(NAP)	23° 34,49' N	63° 31,30' W	5855 m

Rico. The average water depth is 5800 m; the sediments consist of inter-bedded turbiditic / pelagic material and are almost carbonate depleted (KUIJPERS et al. , 1987). The in situ temperature for surfacial sediments of both areas is approximately 1.5°C.

2-3. METHODS

In the present study two types of squeezers, namely gas-operated (DE LANGE, 1984[b]) and hydraulic (RIDOUT, 1981; RIDOUT & PAGETT, 1984), and a centrifuge system have been used simultaneously to extract pore water from sediment samples. Upon recovery of the core the pvc core-liner was cut into 1 m sections which were tightly sealed with plastic tops and tape. These sections were stored, horizontally, in a cooled storage room. Pore-water extraction was started within 12 hours of core collection. The core sections were split lengthwise into two parts, using an electrically operated cutting system. One part was immediately transferred into either of the two nitrogen-filled glove box systems, and processed (see Chapter 3). Each of the two glove box systems (from hereon referred to as A and B) was located in a cooled 20-feet container (from hereon referred to as coollab A and B). In coollab A the hydraulic squeezers (RIDOUT, 1981; RIDOUT & PAGETT, 1984; BOUST, 1986), and centrifuge samples prior to centrifuging, were handled, using glove box system A, whereas in coollab B the gas-operated squeezers were used in combination with glove box system B. (for a description of glove box systems, squeezers and centrifuging system, see Chapter 3). Temperature and oxygen conditions in the A combination appeared to be higher than in the B combination, resulting in obvious differences in pore-water composition, as will be discussed below. After the samples for pore-water extraction had been taken, Eh and pH punch-in measurements were done on the same core half, as closely as possible to the sampled intervals. These measurements were executed at room air-temperature, with the temperature of the sediment being monitored simultaneously. In a third nitrogen-filled glovebox system, operated at room temperature, the extracted pore-water samples were subsampled for various analyses. Immediately after subsampling the on-board analyses for nutrients, dissolved iron and manganese, were done on two different auto analyzer systems, namely Chemlab type AA2 (Fe, Mn, PO_4, SiO_4) and Skalar type SA400 (NO_2, NO_3, PO_4, NH_4); The pH (pore water) and alkalinity determinations were done on 1 ml samples by a method adapted after EDMOND

(1970).
Pore-water subsamples acidified on board were analysed for their major element composition at Utrecht University, using an ICPES system (ARL 34.000), and were analysed for some trace elements (Cu, Ni, Zn) at Bedford Institute of Oceanography, after MIBK/APDC solvent extraction (after BROOKS et al., 1967) using flameless AAS (Varian 975).

2-4. RESULTS and DISCUSSION

Some of the factors reported to have an influence on the reliability of pore-water data are :

a. *decompressional effect*
b. *period and conditions of storage of the sediment prior to pore-water extraction*
c. *squeezing pressure*
d. *temperature during pore-water extraction*
e. *oxygen contamination during pore-water extraction.*

2-4. a. Decompressional effect

Upon recovery, the core is raised from the ocean-floor to the seawater surface. Carbonate equilibria can be especially sensitive to such a change in pressure, which for the MAP and NAP is equivalent to a 550 bar change in pressure. The decompressional effect due to raising of the core to the surface from a great depth, is reported to occur mainly in carbonate-ooze sediments, whereas in non-carbonate sediments no such artifacts have been demonstrated (MURRAY et al., 1980; EMERSON et al., 1980; 1982; JAHNKE et al., 1982; DE LANGE, 1986[b]). Therefore, for the carbonate containing sediments from the MAP, deviations from the in-situ concentration can be expected, whereas for most of the carbonate depleted sediments from the NAP such effect is unlikely. During previous expeditions to the MAP, the concentration of Ca was found to be similar for the pore-water in box cores, and for the bottom water. Therefore, for sediments from the MAP the decompressional effect on the pore-water concentration of Ca cannot have been more than the analytical error of 3%. On the assumption that in the precipitate which may occur due to decompression, the Mn/Ca ratio is similar to the ratio in solution, an identical ultimate deviation of 3% is to be expected for the Mn pore-water concentration in these sediments. In addition, it can be noted that SAWLAN (1982) was not able to show a systematic decompressional effect for Mn

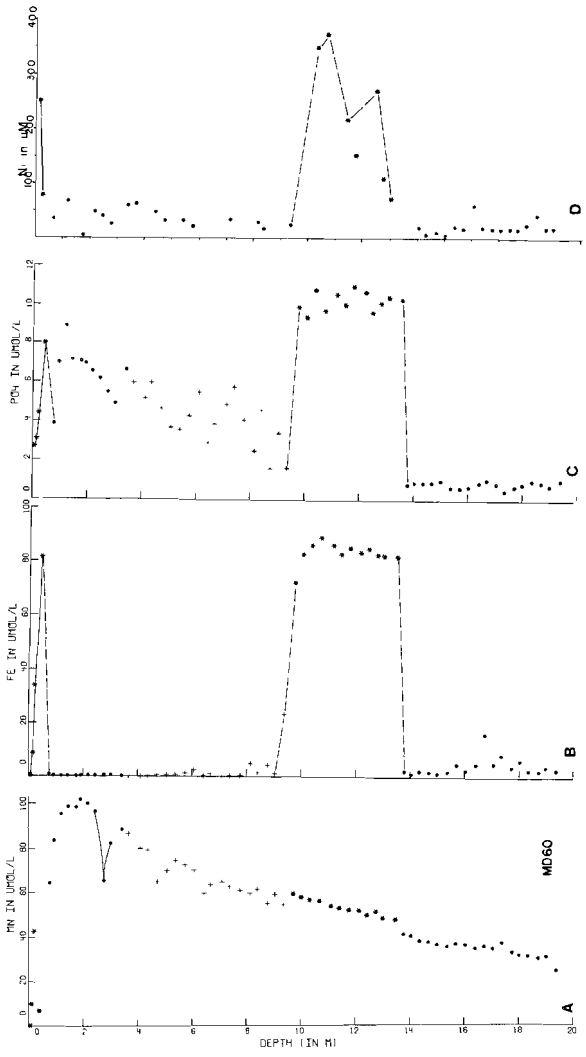

Fig. 2-2. Pore-water concentrations of manganese (a), iron (b), phosphate (c) and nickel (d) in core MD60, NAP. (o): extraction system A1; (+) : extraction system A2; however, in graph (d) : (o) :system A1 and A2; (*) pressure filtration system B (see Chapter 3).

in deep-sea sediments.

For sediments from the NAP, some negative spikes in the Mn pore-water concentration, coinciding with sediment intervals of enhanced $CaCO_3$ content, have been attributed to a decompressional effect (DE LANGE, 1986[b]). Similar spikes are visible in core MD60. However, the large spike at 3 m is to be attributed to a temperature of extraction effect (Fig. 2-2; see also the section on temperature during pore-water extraction).

The only way to avoid these possible decompressional effects is to extract the pore water in situ as briefly discussed in the Introduction.

2-4. b. Period and conditions of storage of the sediment prior to pore-water extraction

In order to prevent possible changes in the pore-water composition due to oxygen contamination or a rise in temperature prior to pore-water extraction, it is necessary to store the tightly closed core sections as quickly as possible near in-situ temperature.

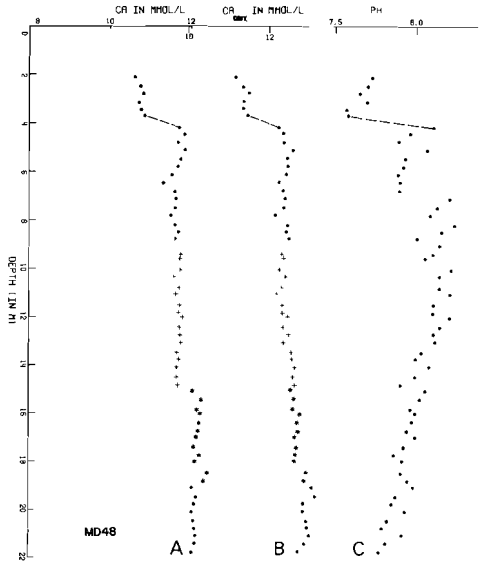

Fig. 2-3. Pore-water concentration of calcium, and punch-in pH measurements for core MD48, NAP. The pH values are raw data which were not corrected for temperature variations (between 10 and 15 °C).

It is possible to store the sediment at the in-situ temperature for a day without there being any detectable alteration in the dissolved element concentration (ROBBINS & GUSTINIS, 1976), with the possible exception of alkalinity (MASUZAWA et al., 1980). However, when the core section is stored for a period of a week or more, significant deviation from the original in-situ concentration may occur (PRESLEY et al., 1967). During the ESOPE expedition we routinely terminated squeezing operations within 48 hours of core collection and between consecutive core sections we didn't find concentration differences that could be attributed to the period of storage. However, for the sediment at 2-4 m in core MD48 a large decrease in the concentration of calcium, and a decrease in alkalinity (not shown in Fig.) and pH was observed (Fig. 2-3). Due to a bent core barrel these two sections remained several hours on deck at air-temperatures of 30°C or more. Upon increasing temperature, reaction 1 was driven to the right.

$$Ca^{2+} + HCO_3^- \longleftrightarrow CaCO_3\downarrow + H^+ \qquad (1)$$

As a consequence calcium-carbonate must have precipitated, and apparently re-equilibration did not happen or was insufficient during the few hours in the cool-storage room prior to pore-water extraction.
Obviously if anoxic samples were stored without the exclusion of oxygen, the same deviations as those described in the section on oxygen contamination during pore-water extraction would have occurred prior to the

extraction of the pore water. Deviations as caused by contamination with oxygen will be described in that section.

2-4. c. Squeezing pressure

The effect of squeezing pressure on the chemical composition of the extracted pore water has also been a subject for research, but is considered to be very small or undetectable for moderate pressures (MANHEIM & SAYLES, 1974; MANHEIM, 1976). With a different set of squeezers ('Manheim-type squeezer', MANHEIM, 1966), we were able to test filtration pressures up to 50 bar, with no significant change in the concentrations of ammonia, nitrite, nitrate, phosphate, silica and iron (unpublished results). At pressures of over 2 to 9 kbar both concentration increases and decreases have been claimed (KRIUKOV & KOMAROVA, 1954; MANHEIM, 1966; SHISHKINA, 1968; SAYLES, 1970; KHARAKA & BERRY, 1973; MANHEIM, 1974). For a fairly complete review, reference can be made to KRIUKOV & MANHEIM (1982). The squeezing pressures for the gas-operated squeezer are up to 15 bar, and for the hydraulic squeezer up to 100 bar. Therefore no effects on the chemical composition of the pore water are to be expected from the squeezing pressures in these systems. Comparison of the pore-water results in alternate sections that were handled by either of the two squeezing systems or the centrifuge, did not reveal any measurable difference in the pore-water composition that could result from a change in squeezing pressure. The data for a change in pore-water composition in core MD48 as presented in Table 2-2 were attributed to a shift in temperature at two interfaces (15 and 19 m) (see next section), although these two interfaces also include a change in extraction technique. At 15 m the change in extraction technique is from high pressure (hydraulic squeezers) to medium pressure (gas-operated squeezers) and at 19 m from the latter to centrifuging. No difference in change of pore-water composition is observed between these two interfaces, therefore a pressure-of-extraction dependency is unlikely for the present extraction systems. In addition, at 9 m in core MD48, the extraction technique changed from centrifuge to high-pressure squeezing without there being a measureable effect on the pore-water composition.

2-4. d. Temperature during pore-water extraction

If the temperature during squeezing deviates from the in-situ temperature of the sediment, then there may be large differences between the concentration of most of the ions in the extracted pore water and

TABLE 2-2. Ranges of average deviation (in %) from the in-situ pore-water concentration due to a squeezing/centrifuging temperature that is 20°C higher than the in-situ temperature.

Pore-water constituent	I	II	III	IV
Na	+ 1 to + 2	+ 1 to + 2	+ 2 to + 4	+ 1 to + 2
Mg	- 2 to - 8	- 6 to - 8	-12 to -16	- 6 to - 8
Ca	0 to - 7	- 6 to -12	- 9 to -15	- 4 to - 8
Sr	0 to -20	< 3	- 9 to -12	- 4 to - 6
K	+20 to +28	+28 to +32	+90 to +120	+45 to +60
B	+ 8 to +60	(+60)	(+60)	(+30)
Li	0 to - 3	+12 to +16	+20 to +50	+10 to +25
Si	+26 to +60	+10 to +20	0 to -90	0 to -45
SO_4	< 0.5	< 2	< 2	< 2
Mn	-	0 to -10	-30 to -75	-15 to -40

I. Average ranges as compiled from MANGELSDORF et al., 1969; BISCHOFF et al 1970; FANNING and PILSON, 1971; SAYLES et al., 1973b; GIESKES, 1973; SAYLES and MANHEIM, 1975; SAYLES et al., 1976; MASUZAWA et al., 1980; DE LANGE, 1984b). II. Average ranges as calculated from data of core MD48 on the assumption of a temperature dependency for B of 60%. III. Average ranges as calculated from data of core MD60 on the assumption of a temperature dependency for B of 60%. IV. Average ranges as calculated from data of core MD60 on the assumption of a temperature dependency for B of 30%.

the in-situ concentration of these ions. The temperature effect is reported to be dependent on the kind of sediment involved. Clay and marly sediment seems to be most sensitive to the temperature of extraction, whereas siliceous oozes are reported to be the least affected (SAYLES et al., 1973[b]; 1976). The direction and quantity of deviation from the in-situ concentrations differ considerably per element. Variations of -20% (Sr) to +60% (Si,B), relative to the in-situ concentration, for a squeezing temperature of approximately 20°C higher than the in-situ temperature, have been reported (MANGELSDORF et al., 1969; BISCHOFF et al., 1970; FANNING & PILSON, 1971;

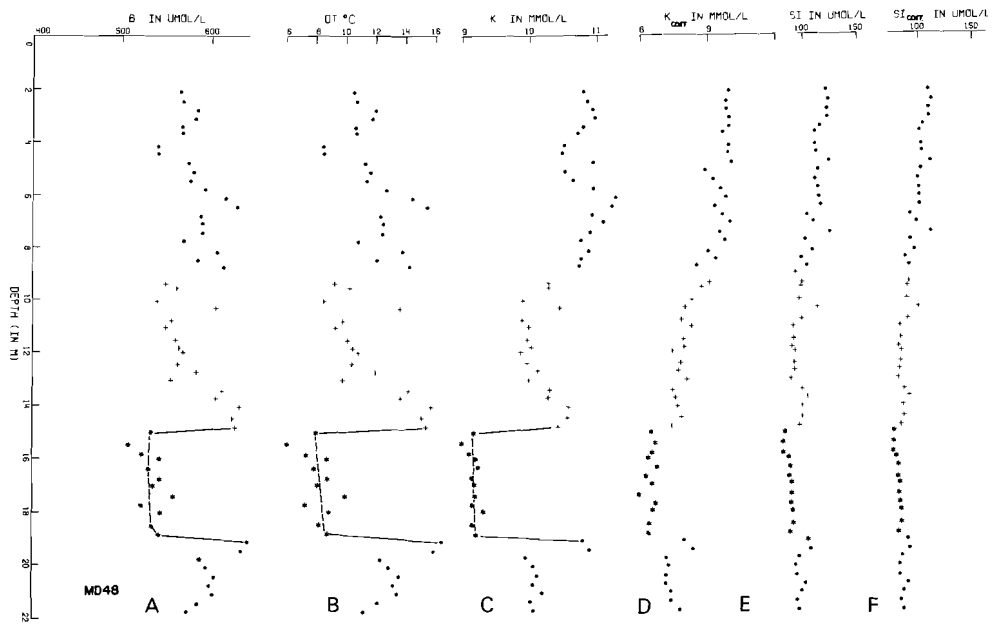

Fig. 2-4. Pore-water concentration of boron (a), the calculated temperature deviation relative to the in-situ temperature (b) (see text), pore-water concentration of potassium (c) and silica (e), corrected pore-water concentrations of potassium (d) and silica (f) for core MD48, NAP. K_{corr} and Si_{corr} refers to a correction for the temperature dependency of K and silica respectively (see Table 2-2 and in text). For ‹o›, ‹+› and ‹› see caption of Fig. 2-2.*

BRAY et al., 1973; SAYLES et al., 1973[a,b]; GIESKES, 1973; TROUP et al., 1974; ROBBINS & GUSTINIS, 1976; HOLDREN et al., 1975; LODER et al., 1978; MASUZAWA et al., 1980; DE LANGE 1984[b]). Data from literature have been summarized in Table 2-2. The difference in temperature between coollabs A and B that were used for pore-water extraction with squeezers and sample preparation for the centrifuge system was estimated on board. For the extraction of sediment samples in the MAP a difference of 2-6°C was noted, whereas, due to higher air temperatures, in the NAP a temperature difference of 5- 10°C was normal. The temperature in coollab A was always higher than in coollab B, and both coollabs were above in-situ temperature. Dissolved boron in deep-sea pore water is reported to be conservative and is reported to demonstrate one of the highest deviations due to a temperature of squeezing that is different from the in-situ temperature (e.g. SAYLES, 1985; see Table 2-2 and discussion below). Therefore, the difference in temperature of pore-water extraction is clearly reflected in the profile of dissolved boron versus depth for core MD48 (Fig. 2-4). Based on reported deviations in the pore-water concentration of boron as caused by squeezing temperatures that differ from the in-situ temperature, we assume here a 60% deviation per temperature difference of 20°C, from hereon referred to as "temperature dependency of 60%" (Table 2-2). From the measured boron (B) pore-water profiles the temperature deviation can then be calculated according to equation 2 :

$$\Delta T = \frac{(B_{meas} - B_{BW})}{B_{BW}} * \frac{20}{60} * 100\% \quad (\text{in } °C) \qquad (2)$$

in which : ΔT = difference of in-situ and calculated temperature
B_{meas} = measured pore-water B concentration
B_{BW} = bottomwater B concentration (430 µM/l)

Two major temperature shifts, namely at 15 and 19 m respectively, are then observed in this core (Fig. 2-4); the inferred temperature difference of approximately 7°C between the two coollabs is in accordance with the on-board observed difference of 5 to 10°C. We have now used these two temperature shifts to deduce the temperature dependency of other pore-water constituents (Table 2-2). The calculated temperature dependencies closely resemble those that were previously reported, with the exception of the values for Si and Li. Although oxidation-during-sampling artifacts have been reported for dissolved silica (LODER et al., 1978), we do not attribute the observed shifts of dissolved silica in core MD48 to this phenomenon, as will be discussed in the section on oxidation effects during pore-water extraction. Note that if a smaller temperature dependency of Boron would have been assumed, not only would the inferred temperature have

deviated from our on-board observations, but also most constituents in Table 2-2 would have demonstrated a much larger temperature dependency than has been reported previously.
The temperature dependency of cations seems to be due to temperature-dependent cation-exchange equilibria between sediment and interstitial water. Assuming a sediment column of homogenous composition, and a 60% temperature dependency for dissolved boron, it might then be possible for example to correct the measured pore-water K^+ concentration for calculated temperature deviations :

$$K_{meas} = K + K * \frac{(\Delta T * TD)}{20 * 100} \qquad (3)$$

in which : K_{meas} = measured pore-water K^+ concentration.
ΔT = difference of in-situ and calculated temperature.
TD = temperature dependency in % per ΔT of 20°C.

after reworking :

$$K_{corr} = \frac{K_{meas} * 2000}{(2000 + \Delta T * TD)} \qquad (4)$$

in which : K_{corr} = K, corrected for temperature dependency TD.

The resulting pore-water concentration/depth profile for core MD48 (Fig. 2-4) demonstrates a much more realistic trend than the uncorrected profile did. However, if an identical temperature dependency of dissolved boron and potassium is applied to the pore-water composition of K^+ in core MD60, this does not result in a similar improvement of the K^+ profile (Fig. 2-5b,c). Apparently the largely turbiditic sediments of core MD60 have a different temperature dependency than the mainly (hemi-)pelagic sediments in core MD48. It is remarkable that for core MD60 the derived temperature difference between coollabs A and B is only half the observed value for the NAP (4° instead of 5-10°C). Furthermore, it appears that all constituents except boron and silica demonstrate a temperature dependency that is twice as large as earlier reported values (Table 2-2). It seems therefore that the boron temperature dependency for the sediment of core MD60 is only half as large as it is for sediment of core MD48 (Table 2-2). On the assumption of a temperature dependency for boron of 30% per 20°C, the calculated temperature shift between the two coollabs is consistent with the on-board observations, and the temperature dependency for all pore-water constituents except silica and K^+ is consistent with earlier reported values (Table 2-2). This deviation of K^+ is difficult

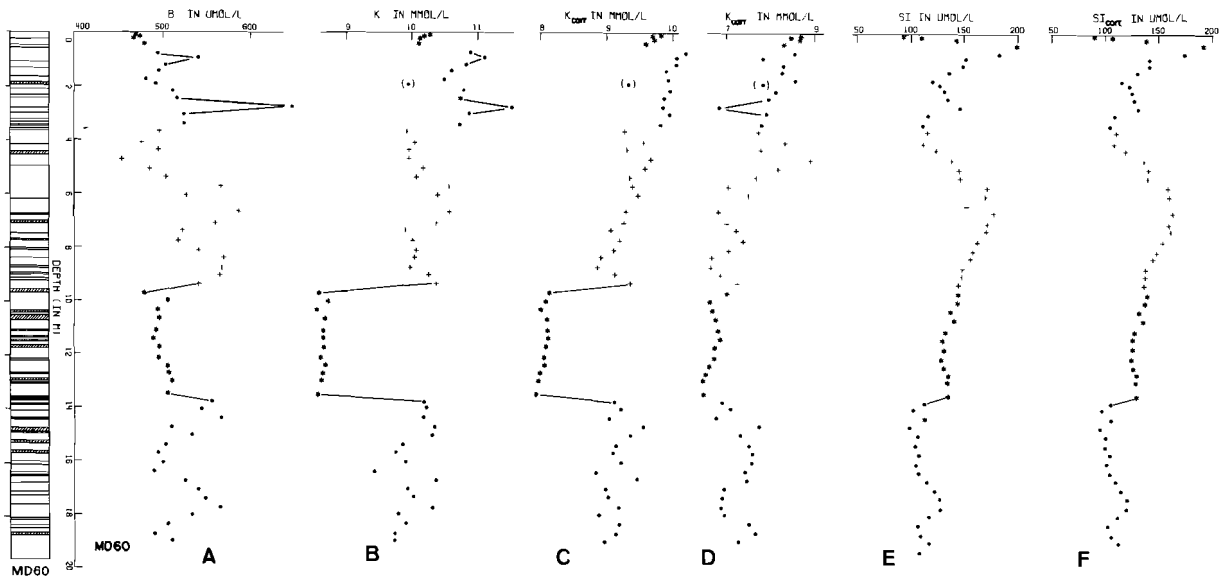

Fig. 2-5. Pore-water concentration of boron (a), of potassium (b) and silica (e), corrected pore-water concentrations of potassium (c) and silica (f) for core MD60, NAP (see caption of Fig. 2-4). In addition a generalized representation of the sediment column is given. For ⟨o⟩, ⟨+⟩ and ⟨⟩ see caption of Fig. 2-2.*

to understand and cannot be explained by a simple temperature dependency. Even an extreme temperature dependency for K^+ of 60% does not produce a smooth profile for dissolved K^+ versus depth in core MD60 (Fig. 2-5d). In addition, it must be noted that after such an extreme temperature correction, the calculated level of the pore-water concentration of K^+ in the top metre of core MD60 is well below the bottom-water concentration for K^+ (10.5 mM). The deviating behaviour of silica and K^+ will be discussed in the next paragraph. The calculated temperature of pore-water extraction deviates less and more irregularly from the in-situ temperature for sediments from the MAP than it does for the sediments from the NAP. The calculated temperatures are again in the same range as the temperatures of extraction that have been observed on board. However, if we apply a 30% and a 50% temperature dependency for the K^+ pore-water concentration, this does not result in a smooth curve for the K^+ concentration with depth in core MD10 (Fig. 2-6). This result is not surprising in view of the large differences in sediment composition within one core in this abyssal plain (DE LANGE et al., 1987[a]). Some of the shifts in the pore-water concentration of K^+ evidently coincide with a change in squeezing temperature. However, the shifts that are observed at 14.5 m and at 29.2 m in core MD10 cannot possibly be attributed to effects associated with a change in extraction technique, such as pressure- or temperature of extraction, or oxygen contamination (Fig. 2-6). Recently, the possible non-conservative behaviour of B in the pore water of some near-coastal sediments has been reported (MACKIN, 1987; MACKIN et al., 1988). In view of the extended period of contact with seawater, for the present sediments no such effects are expected.

If the assumption of conservative behaviour of boron in marine pore waters of deep-sea sediments (SAYLES, 1985) is not valid, then for dissolved boron a smooth, diffusion-controlled concentration versus depth profile would result, which cannot explain the above-mentioned abrupt changes in core MD10. Therefore these shifts cannot be attributed to in-situ conditions, but must arise from artifacts prior to or during pore-water extraction. It must be noted that both shifts do coincide with large compositional differences of the sediment (Fig. 2-6; DE LANGE et al., 1987[a]). It seems likely therefore that the applied overall temperature dependency of the pore-water of K^+ and boron is not valid for sediments of highly variable composition. A more detailed discussion on variations in temperature dependencies relating to changes in sediment composition is beyond the scope of this thesis.

In summary, deviations from the in-situ pore-water composition (as examplified for K^+) that are caused by temperatures of extraction deviating from the in-situ temperature, are dependent on the composition of the sediment that is in contact with the pore water. Corrections for

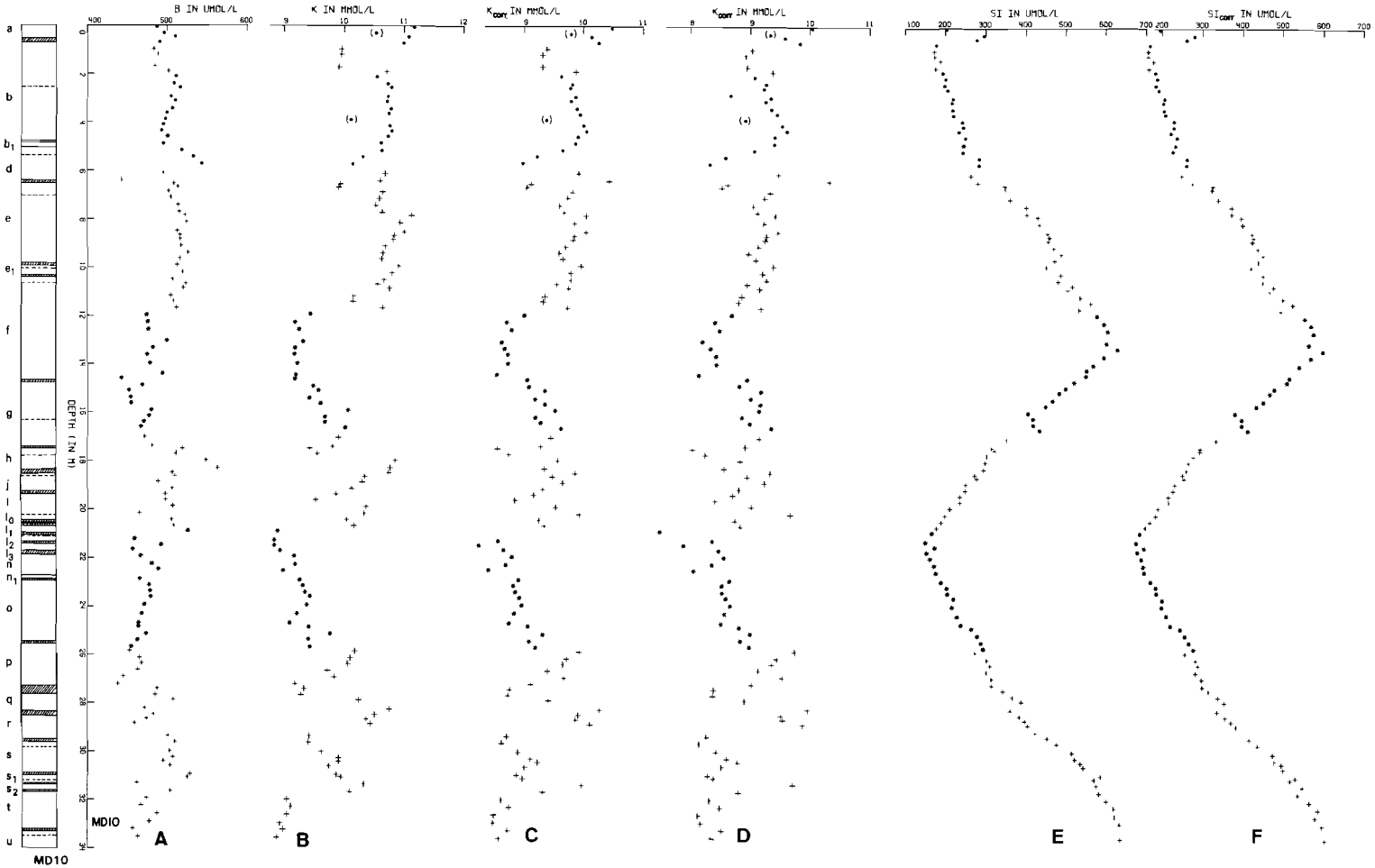
B IN UMOL/L
K IN MMOL/L
K_{CORR} IN MMOL/L
K_{CORR} IN MMOL/L
SI IN UMOL/L
SI_{CORR} IN UMOL/L
DEPTH (IN M)
MD10
MD10
A
B
C
D
E
F

Fig. 2-6. Pore-water concentration of boron (a); pore-water concentration of potassium (b) and silica (e), corrected pore-water concentrations of potassium (c,d) and silica (f) for core MD10 MAP (see caption of Fig. 2-4). In addition a generalized representation of the sediment column is given. Although at 16-17 m an upside-down sediment section is likely (see Si profile), we have no absolute proof for it. For ‹o›, ‹+› and ‹› see caption of Fig. 2-2.*

deviating temperatures can therefore not readily be made.
For dissolved manganese it is difficult to differentiate between a temperature dependency and an oxidation artifact. Note the extreme boron concentration (= high temperature) at 3 m depth in core MD60 (Fig. 2-5a), which is reflected in all other pore-water constituents, such as K_+ (Fig. 2-5b), Ca^{2+} (not shown in Fig.) and Mn^{2+} (Fig. 2-2). In view of the chemical similarity of manganese and calcium, relating to the carbonate system, a similar temperature dependency would be expected for these two pore-water constituents. If the temperature dependency of calcium is applied to the manganese concentration versus depth profile for core MD60 (Fig. 2-2), the resulting temperature-corrected manganese profile suggests that only a minor measurable oxidation artifact occurs at 10-14 m depth (not shown in Fig.). In addition a decompressional effect is suggested for manganese in some limited intervals in core MD60 (see section on decompressional effect). The behaviour of dissolved manganese in this respect is in sharp contrast to that of dissolved iron, as discussed in the next section.

2-4. e. Oxygen contamination during pore-water extraction

Oxidation artifacts during sampling procedures have been reported to severely affect the concentration of iron and phosphate in pore water that is rich in dissolved Fe^{2+} (BRAY et al., 1973; TROUP et al., 1974; HOROWITZ et al., 1973). Upon oxidation of such a solution, precipitation of iron(III) hydroxide occurs (equation 4) which can be accompanied by co-precipitation of phosphate, silicate, and trace metals. From the pore-water profiles of dissolved iron and phosphate in cores MD56 (not shown in Fig.) and MD60 (Fig. 2-2) it is obvious that besides the observed temperature differences between the glovebox systems A and B (see Chapter 3) an oxidation artifact occurred as well. Cores MD56 and MD60 contain suboxic, mainly turbiditic, sediments. Core MD48 is more oxidizing and consists of (hemi-)pelagic sediments mainly; in this core no oxidation artifact is observed for dissolved iron and phosphate. Oxidation artifacts are much less evident in core MD10 from the MAP; for dissolved iron and phosphate only at 26 m such artifacts can be observed without any doubt (Fig. 2-7).
The pore water profiles of dissolved silica are also interesting in this context. In core MD48 the two shifts in the silica pore-water profile

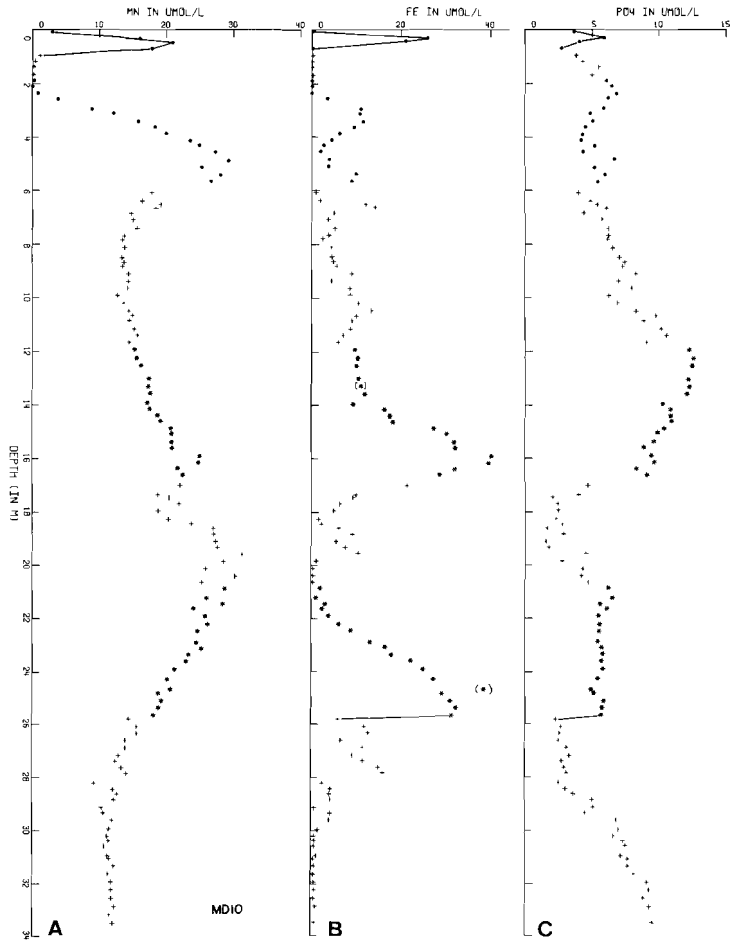

Fig. 2-7. Pore-water concentration of manganese (a), iron (b) and phosphate (c) for core MD10, MAP.

(Fig. 2-4) were attributed to shifts in temperature (Table 2-2). However, if in core MD60 the shift in dissolved silica at ≈13.6 m (Fig. 2-5) were to be attributed to a temperature dependency, then the calculated dependency would be largely negative (-45%/20°C, see Table 2). Such a temperature dependency for silica would be in sharp contrast to previously reported values. In core MD60 the shift in the pore-water silica concentration in core MD60 is better explained by an oxidation effect (LODER et al., 1978). How then to explain the absence of such an effect in core MD48 ? One of the differences between cores MD48 and MD60 is the punch-in Eh measured on board, which in general is somewhat higher (more oxidizing) in the former (Figs. 2- 8,9). The oxidation effect would not only add oxygen to the sediment, but raise the Eh as well. If our results are comparable to

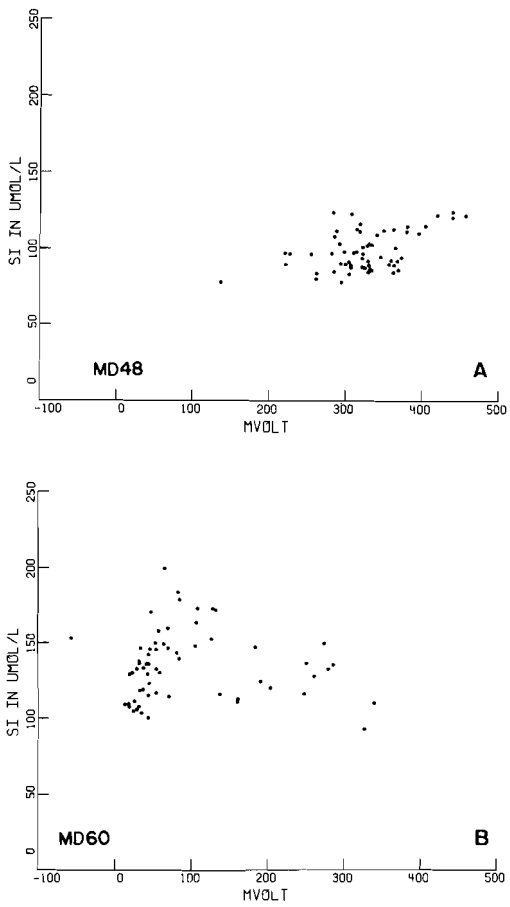

Fig. 2-8. Redox potential versus pore-water concentration of silica for cores MD48 (a) and MD60 (b). Both cores are from the NAP.

those previously reported for the same area (DE LANGE, 1986[b]), then for a redox potential of above +250 mV (such as in core MD48) a rise in Eh would not result in a decrease of the silica pore-water concentration, whereas it would for a lower Eh (such as in core MD60). Indications for such a redox-dependent relationship were found during experiments with Californian borderland sediments (J.BOUCHER, 1986, pers. commun.). Unfortunately this Eh effect on the silica pore-water concentration cannot always be distinguished from an often simultaneous effect of precipitation of iron(III)-oxihydroxide during oxidation. In core MD48 dissolved iron concentrations are always below 1 µM (not shown in Fig.), whereas for sediment of core MD60 there obviously is an oxidation problem relating to iron, as discussed above (Fig. 2-2). Oxidation-induced precipitation of 80 µM/l of iron in core MD60 would then be accompanied not only by a removal of approximately 10 µM/l of phosphate, but also by nearly 30 µM/l of silica. During the precipitation of Fe(III)oxihydroxides, variable amounts of silica can be incorporated (HARDER, 1965; 1978; HARDER & FLEHMIG, 1970; DE LANGE & RISPENS, 1986). In addition the co-precipitation of trace metals and of rare earth elements is likely to occur, as for example is demonstrated for nickel (Fig. 2-2). The fact that no measurable oxidation artifact for Mn^{2+} occurs in core MD48 in the presence of a much higher pore-water concentration of Mn^{2+}, strongly suggests that the possible oxidation artifact for Mn^{2+} in cores MD56 and MD60 may also be caused by co-precipitation with Fe(III)oxihydroxide. This difference in behaviour between Fe and Mn can be understood by the much slower oxidation kinetics of dissolved Mn^{2+} relative to dissolved Fe^{2+} (STUMM & MORGAN, 1970).

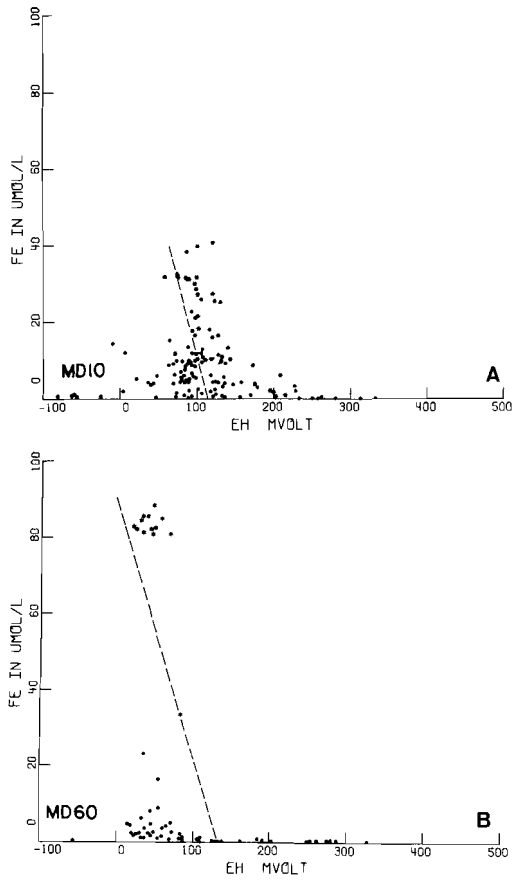

Fig. 2-9. Redox potential versus pore-water concentration of iron for cores MD48 (a) and MD60 (b). Both cores are from the NAP [o] : extraction systems A1 and A2; [*] : extraction system B. Dashed lines taken from the Fe^{2+}/Eh plot of DE LANGE (1986[b]); see Chapter 4).

The occurrence of oxidation artifacts in core MD10 is much less evident. The pore-water silica profile does not demonstrate a clear oxidation effect (Fig. 2-6), and also from the iron- and phosphate pore-water profiles in core MD10 (Fig. 2-7) oxidation artifacts are not so evident as they are in core MD60. There is no reason to assume less significant oxygen contamination during the extraction of core MD10 than during extraction of core MD60; therefore we need to search for other differences between the two cores. The low Eh of core MD10, and the much higher pore-water silica concentration relative to core MD60 would only tend to make an oxidation effect more likely to be visible, and can thus be ruled out as a possible explanation. If any effect would occur due to the sediment composition, then it should be visible at 14.7 m depth in core MD10. At this interface the sediment composition is the only parameter that changes, and involves a dramatic change from the diatom-rich f-turbidite to the volcanic g-turbidite (DE LANGE et al., 1987[a]). However, no change in the silica pore-water concentration is observed at this particular horizon. The observed shifts in dissolved silica in cores MD56 and MD60 do coincide with major oxidation artifacts observed for iron and phosphate. Therefore, the relation of dissolved silica with the oxidation artifacts of dissolved iron seems to be the main reason for shifts in the silica profile in core MD60. In core MD10 a visible oxidation artifact for iron and phosphate occurs only at 26 m depth. If a ratio of co-precipitation of silica and iron(III)-oxihydroxide similar to the ratio in core MD60 is assumed to occur in core MD10 , then a shift of 10 µM in dissolved silica would be expected at this depth. Being close to the analytical error this shift in

dissolved silica is only just visible (Fig. 2-6).
The shift in the concentration of dissolved K^+ that remains visible at 14 m in core MD60, even after an extreme temperature correction, is much more difficult to understand. A similar problem exists for the difference after temperature correction in the concentration of K^+ between bottom water (10.5 mM/l) and the pore water from the top section of suboxic core MD60 (Fig. 2-5). Similar shifts remain, after temperature correction, in the K^+ profile of suboxic core MD56 (not shown in Fig.), whereas a much smaller (if any) shift remains in the oxic core MD48. There is no evidence for an unusually large analytical error, and there is no obvious major change in sediment composition at these particular sediment horizons. Therefore, also for K^+ an oxidation artifact needs to be assumed to explain this difference between oxic and suboxic sediments. The exact nature of such an artifact is unknown. A possible relation with the oxidation artifacts of dissolved iron and silica can only explain this phenomenon to a limited extent :

$$4\ Fe^{2+} + O_2 + 10\ H_2O \longrightarrow 4\ Fe(OH)_3 \downarrow + 8\ H^+ \qquad (4)$$

Assuming that rapid equilibration with a carbonate phase would not occur, and assuming that all H+ that could be formed during reaction 4 would only exchange for adsorbed K^+, this would still account for an increase of 0.16 mM in K^+ only. This represents less than 20% of the total shift that is observed after temperature correction. However, a rise of Eh, such as caused by the introduction of oxygen in a suboxic environment, could result in different mineral equilibria. If as a consequence the concentration of K^+ would increase, or the concentration of dissolved boron would decrease, then the effect on the temperature-corrected K^+ concentration is similar. Therefore, the observed discrepencies in the pore-water concentration of K^+ cannot unequivocally be explained. Although we cannot explain the exact nature, oxidation artifacts for dissolved K and/or boron seem likely to occur.

2-5. CONCLUSIONS

If no great care is taken prior to and during the extraction of pore water from marine sediments, large deviations from the in-situ pore-water concentration may occur :

1. Due to transport of the sediment from great depths to the sea water surface, decompressional effects may occur.
2. A too long time of storage of the sediment prior to pore-water extraction, or storage of the sediment under inadequate conditions,

including oxygen contamination, and temperature deviations, may cause changes in the pore-water composition.

3. Deviations from the pore-water concentration occur if the temperature of extraction differs from the in-situ temperature of the sediment. The magnitude of the deviation is dependent not only on the pore-water constituent that is considered, but also on the composition of the sediment that is in contact with the pore water. Therefore corrections for deviating temperatures of extraction cannot readily be made.
4. Minor contamination with oxygen during handling of the samples and during extraction of the pore water may lead to large deviations in the pore-water concentration of Fe, Si, PO_4, some trace metals and possibly REE.
5. No changes in the pore-water composition could be demonstrated as caused by large differences in the pressure of extraction.
6. Although large differences in some pore-water constituents were found between samples that were handled in the two glove box systems (A and B), no systematic deviations in the pore-water concentration could be demonstrated to be due to either of the three different extraction techniques, namely centrifuging, low- and high- pressure squeezing.

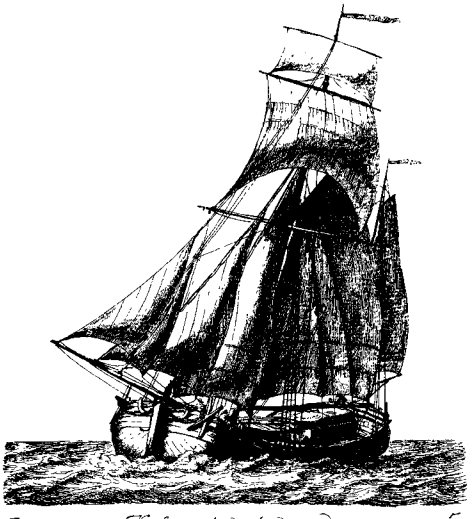

E Kof zeylende by de wind 5

Chapter 3

SHIPBOARD ROUTINE AND PRESSURE-FILTRATION SYSTEM FOR PORE-WATER EXTRACTION FROM SUBOXIC SEDIMENTS

ABSTRACT

A description is given of a shipboard pressure-filtration system that gives reliable results for the extraction of pore waters from sub-oxic sediments. In addition, two other systems that are mentioned in Chapter 2 are briefly reported in the Appendix.

3-1. INTRODUCTION

Before pore water can be extracted from sediment, an accurate procedure for the handling of the sediment is necassary in order to obtain reliable samples. During the shipboard handling, undesirable changes may occur in the pore-water composition due to :

1. *period and conditions of storage of the sediment prior to pore-water extraction*
2. *temperature during pore-water extraction*
3. *oxygen contamination during or prior to pore-water extraction*

These factors have been discussed extensively in Chapter 2. In order to prevent these factors from causing possible deviations in the in-situ pore-water concentrations, a pressure-filtration system and an adequate ship-board routine have been developed. The results using this filtration system and following this routine have been discussed in Chapter 2, and have been compared to two other systems (see also Appendix 3-1).

3-2. PRESSURE-FILTRATION SYSTEM

This system consists of slightly modified Reeburgh type squeezers (Reeburgh, 1967) made of Delrin, with a teflon supporting screen, and a 0.2 µm cellulose-acetate membrane filter (Fig. 3-1). The dental dam has been glued to the rubber O-ring, thus providing a quick and secure sealing system. During squeezing the pressure of the nitrogen gas forces the rubber diaphragm against the sediment, which is thus squeezed. On both sides of the teflon supporting screen a 0.1 mm-thick teflon-sheet has been glued. This reduces the force to be applied by the 'slide-rod-clamp', to ensure complete sealing up to at least 15 bar. The supporting screen, besides supporting the membrane filter, also permits the squeezed pore water to

pass through, and minimizes the 'dead volume' of pore water. Previous tests that were done to compare acid-washed and unwashed membrane filters did not demonstrate a difference in concentration of any of the analysed pore-water constituents. Six slide-rod clamps attached to a rilsan-coated iron frame, are used to fix the squeezers (Fig. 3-2). Six 3-way cocks (Whitney) permit the squeezers to be operated independently. For the "fixed" part of the high pressure nitrogen-gas system, copper tubing (coated with plastic) has been used, whereas nylon tubing has been used for the part connected to the squeezer top, allowing greater flexibility. The frame is fixed inside a 10 mm perspex glove box, which during operation is kept under a low oxygen atmosphere (generally O_2 < 0.003%) by means of high purity nitrogen-gas (O_2 < 0.0005%). Sluices on both sides permit the introduction of samples and flasks, without any significant introduction of oxygen (Fig. 3-3). Special sluice doors have been constructed to ensure tight closing and easy handling. Metal parts of the doors have been covered with a plastic layer. All glass- and plastic-ware, squeezers, spatulas etc. are

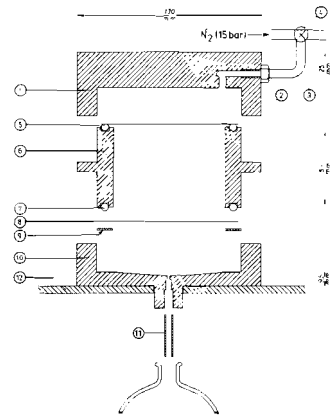

Fig. 3-1. Cross-section of the squeezer used in the pressure-filtration system (for explanation of numbers, see Fig. 3-4).

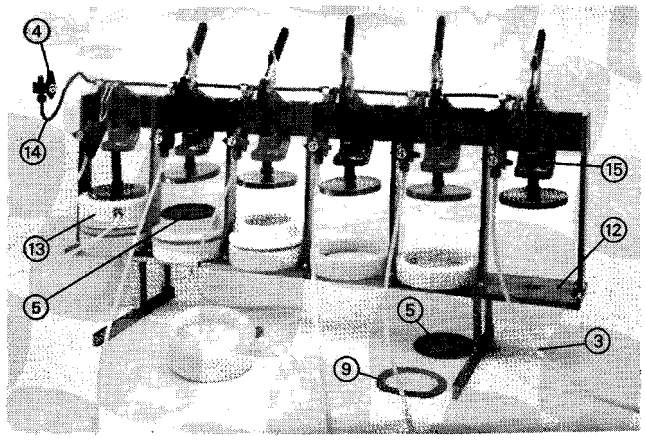

Fig. 3-2. Frame and squeezers of the pressure-filtration system (for explanation of numbers, see Fig. 3-4).

introduced through the large sluice (Fig. 3-3) only after an introduction procedure of at least 3 cycles : "vacuum (<1 mbar)-nitrogen (O_2<0.0005%) ". Membrane filters are left in the sluice, under vacuum, for 12 hours, before continuing with the introduction procedure. The glove box is operated under nitrogen atmosphere, with a continuous flow of high-purity nitrogen, and a slight overpressure. The oxygen concentration and temperature inside the glove box are monitored continuously. The whole pore-water pressure-filtration system is operated in a 20-feet container, which is normally kept at, or slightly below, the in-situ temperature. Unfortunately, during the ESOPE expedition we were not able to maintain such low temperatures, as is discussed in the text.

3-3. SHIPBOARD WORKING PROCEDURE

The following procedure is carried out on board ship, schematically represented in Figure 3-4 :
Immediately after collection of the core the pvc liner is cut into 1 m sections, that are stored, horizontally, at 3-4°C. After lengthwise splitting of a core section, one half is immediately transferred to coollab B into a nitrogen-filled glove bag, which is then flushed 3-4 times with high purity nitrogen gas (< 0.0005% oxygen). The bag's end is closed, so as to allow a light overpressure and flux of nitrogen. The upper few millimetres of sediment are removed before samples are taken for pore water extraction. These samples are taken with a bone spatula and put into poly-ethylene beakers, which are subsequently transported into the glove box via a sluice system (Figs. 3-3,4). With a bone spatula the sediment is transferred from a beaker to a squeezer. After fixing the squeezer in the frame by the slide-rod clamps, squeezing is started at a low pressure (1-2 bar). Higher pressures (up to 15 bar) are applied gradually so as to prevent formation of a thin dry sediment-cake immediately above the filter, which would slow down the extraction of the pore water. Depending on the water content of the sediment and the amount of pore water required, squeezing times range from 15 minutes to 4 hours. Generally portions of approximately 150 cm^3 of sediment are squeezed, which usually yield a sufficient amount of pore water (20 to 50 ml). Portions of up to 300 cm^3 of sediment can be handled, but this would require too large a lithological section of average-sized piston cores.

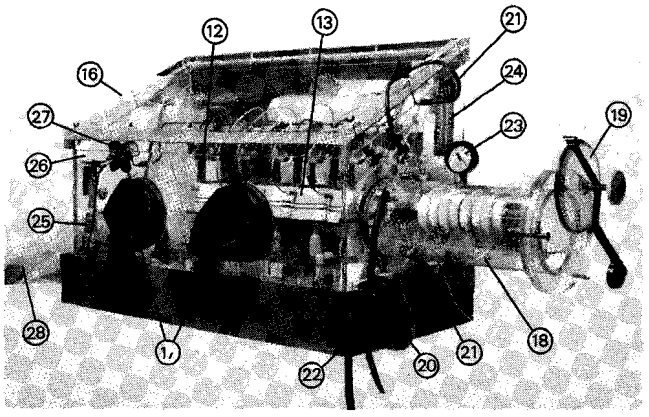

Fig. 3-3. Glove box made of Delrin (for explanation of numbers, see Fig. 3-4).

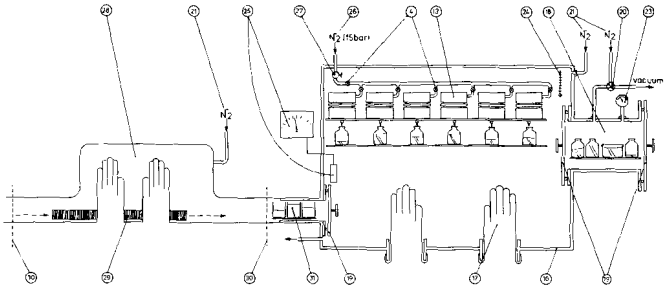

Fig. 3-4. Schematic representation of the shipboard pore-water extraction (not to scale) : 1. Delrin top; 2. Stainless steel plug (Swagelok 6MO-14RT); 3. Nylon tubing; 4. Three-way cock (Whitey 43XS4); 5.Viton rubber O-ring glued to a dental dam rubber diaphragm; 6. Delrin middle part; 7. Viton rubber O-ring; 8. Cellulose-acetate 0.2 µm membrane filter; 9. Teflon supporting screen, with a 0.1 mm thick teflon ring glued to each side for optimal sealing; 10. Delrin base; 11. Sample drain tube; 12. Nickel coated 5 mm iron frame, covered with rilsan; 13. Squeezer; 14. 6 mm copper tubing coated with plastic; 15. Slide-rod clamp (AMF); 16. Glove box made of 10 mm perspex; 17. Neoprene gloves (Labconco); 18. Large sluice; 19. Sluice door; 20. Three-way cock (Whitey 44XS10mm), permitting either nitrogen influx to the sluice or the creation of vacuum in the sluice; 21. Low-pressure high purity nitrogen tubing (oxygen less than 0.0005%); 22. Vacuum tubing; 23. Manometer; 24. Thermometer (min/max); 25. Oxygen probe; 26. High pressure nitrogen tubing (oxygen less than 0.0005%); 27. Pressure regulator; 28. Glove bag (I^2R, both sides extended with polyethylene tubing); 29.split core section; 30. Quick-closing clamps; 31. Polyethylene beakers with samples for pore-water extraction.

APPENDIX 3-1

Extraction system A

1. Centrifuging system

Two refrigerated centrifuges (Sorvall RC-2B), suspended in gimbal systems to compensate for ship motion, were used to recover pore water. Extraction temperatures varied, depending on the temperature of the sediment when placed in the centrifuge, and the length of time the samples were in contact with the cold centrifuge head (at -2 to +2°C) before extraction occurred. Sediment subsamples were transferred into 50 ml acid-cleaned polyethylene centrifuge tubes in a nitrogen-filled glovebox in cold room A. Each capped tube provided 5-10 ml of pore water after spinning for 1 hour at a gravitational force of 10.000 g. Two to 4 tubes were filled for each subsample in order to recover 20 to 30 ml of pore water, depending on the porosity of the sediment.

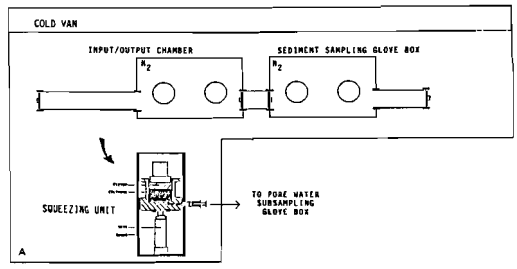

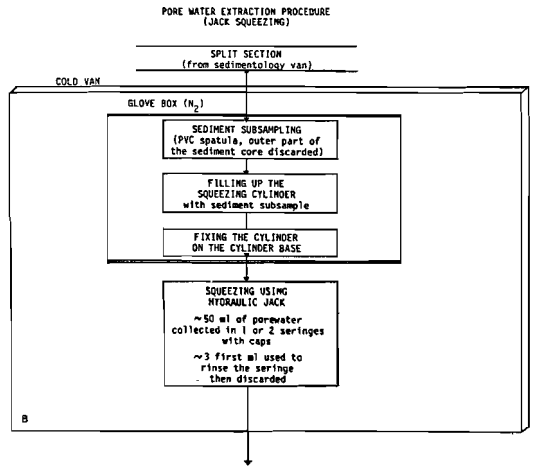

2. High-pressure squeezing system

The hydraulic squeezers of this system were previously described by RIDOUT (1981); RIDOUT and PAGETT (1985) and BOUST (1986) and will therefore not be discussed in detail. Glove box system A is schematically represented in Fig. a, the shipboard procedure in Fig. b.

E Barkentyn Zeylonder by de wind 7

Chapter 4

EARLY DIAGENETIC REACTIONS IN INTERBEDDED PELAGIC AND TURBIDITIC SEDIMENTS IN THE NARES ABYSSAL PLAIN (WESTERN NORTH ATLANTIC) : CONSEQUENCES FOR THE COMPOSITION OF SEDIMENT AND INTERSTITIAL WATER.

Measured pore-water concentrations of iron in interbedded pelagic and turbiditic sediments from the Nares Abyssal Plain are in excellent agreement with sediment colour and measured redox potential. The organic carbon content of these sediments appears to define the redox conditions and consequently the pore-water and solid-phase concentration of constituents that are involved in early diagenetic reactions. In the turbiditic sediments the concentration of NO_3^- generally goes to zero within a sediment depth of 1 m, whereas at 8 m in the pelagic core from the same area the concentration of NO_3^- is still higher than it is in the bottom water. The pore-water concentration of Mn^{2+} in the turbiditic sediments increases sharply down to a depth of approximately 3 m, and from thereon remains nearly constant due to saturation with respect to Mn,Ca-CO_3. The pore water of the turbiditic sediments is also saturated with respect to calcite. The few "diagenetic spikes" in the pore-water concentration of NO_3^- and Mn^{2+} and the concentration/depth profile of dissolved iron, H_4SiO_4 and phosphate all clearly demonstrate the inhomogeneous nature of interbedded pelagic and turbiditic sediments. The simultaneous occurrence of peaks of dissolved iron/silica and of sediment intervals with a relatively high organic carbon content is attributed to enhanced early diagenetic reactions associated with the decomposition of organic matter in these specific intervals. Linked with these reactions is the irregular pore-water concentration of phosphate, which is shown to originate partly from the oxidation of organic matter, but mainly from the desorption of phosphate from iron oxide. Potential concentrations of phosphate are calculated from the stoichiometric early diagenetic reactions and compared with measured concentrations. Due to the unique combination of low porosity and relatively high sedimentation rates, the sediments from the Nares Abyssal Plain are an ideal basis for the study of such interbedded sequences of pelagic and turbiditic deposits.

4-1. INTRODUCTION

Turbiditic sediments of continental origin are known to occur at distances of up to several thousands of km from the continent. Diagenetic processes in these sediments differ greatly from those in the pelagic sediments (e.g. WILSON et al., 1985). Study and comparison of the two types of sediments in a similar environment will enhance our knowledge and understanding of the diagenetic processes that occur in deep-sea sediments.

A number of recent studies on sediments in Atlantic abyssal plains emphasize the importance of processes relating to the presence of organic-

rich sediment layers which are interbedded with intervals of pelagic sediment low in organic carbon (e.g. KUIJPERS, 1982; 1985; THOMSON et al., 1984[a]; DE LANGE 1986[b]; WILSON et al., 1985). Post-depositional migration of some trace elements and a close similarity of the profiles of dissolved phosphate and the organic carbon in the solid phase have been reported (COLLEY et al., 1984; DE LANGE, 1984[a]).

The sediments in the Nares Abyssal Plain show a wide variability, ranging from red-brown clay, interpreted as pelagic deposition, to grey silt, attributed to turbiditic deposition. Sedimentation rates of 0.5cm/kyr have been calculated for pelagic sediments in the Nares Abyssal Plain (THOMSON et al., 1984[b]). A similar or even lower rate was found for the 'average' sedimentation of the sediment in core 84P39 (0.9 cm/kyr; DE LANGE et al., in preparation). The turbiditic sediments are thought to originate from the Hatteras Abyssal Plain, the Vema Gap being the major passage (TUCHOLKE, 1980). The eastward flow of turbidites spreads out irregularly in time and space over the southern Nares Abyssal Plain, the average sedimentation rates being several decimetres per 1000 years (KUIJPERS & DUIN, 1986). For the sediments of core 84P1 (Fig. 4-1) an average sedimentation rate of 45 cm/kyr was found (DE LANGE, 1986[a]), which is extremely high for abyssal plain sediments. The coincidence of high sedimentation rates and low porosity in sediments from the Nares Abyssal Plain means that the situation is ideal for a study of pore-water profiles of such a setting of alternating sediment layers of very different composition. The cores which consist mainly of sediments of turbiditic origin will be referred to from here onwards as "turbiditic cores". In the same area it was possible to study a core consisting mainly of pelagic sediments. This core (84P39), referred to as "pelagic core", was taken on the top of an abyssal hill approximately 300 m above the Plain sediments.

4-2. MATERIALS AND METHODS

In the present study results will be discussed from 8 piston cores, recovered during the 1984 cruise with the R.V.Tyro to the Nares Abyssal Plain (Fig. 4-1; Table 4-1). Most of these cores consisted of turbiditic sediments with some pelagic intervals (KUIJPERS, 1985; KUIJPERS & DUIN, 1986). Great care must be taken TAB 4-1 in handling deep-sea sediment samples and in controlling temperature and oxygen conditions during squeezing to prevent alterations in pore-water chemistry (MANGELSDORF et al., 1969;

TABLE 4-1. Positions and details of piston cores used in this study.

STATION NO.	POSITION	DEPTH(m)
84P1	23°.32'.30 N 63°.31'.48 W	5855
84P7	23°.09'.30 N 64°.28'.06 W	5847
84P10	22°.57'.30 N 64°.10'.12 W	5847
84P11	23°.01'.12 N 64°.16'.00 W	5847
84P17	22°.40'.30 N 63°.26'.54 W	5838
84P22	22°.30'.30 N 63°.40'.54 W	5836
84P31	22°.13'.24 N 63°.15'.18 W	5791
84P39	22°.01'.06 N 62°.32'.06 W	5531

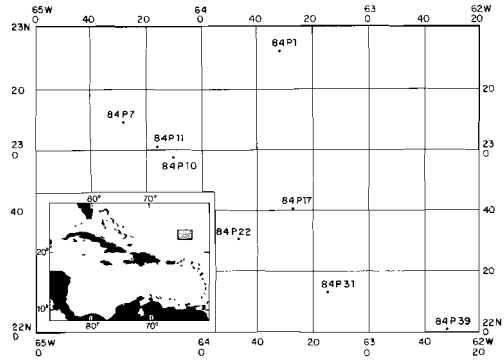

Fig. 4-1. Sampling area. Cores from which sediment samples have been extracted for pore water have been indicated.

BISCHOFF et al., 1970; FANNING & PILSON, 1971; BRAY et al., 1973; MASUZAWA et al., 1980). A shipboard routine was deveveloped in order to prevent these factors from causing deviations in the in situ pore-water concentration. Another possible source of error is de-compression, which can result in $CaCO_3$ precipitation (MURRAY et al., 1980). The shipboard routine has been described in detail elsewhere (DE LANGE, 1984[b]; see also Chapter 3). The shipboard analyses were started within 12 hours of the extraction of the pore water. These included the determination of the alkalinity by a modified titration method (after STRICKLAND & PARSONS, 1968) and analyses of nitrate, nitrite, phosphate and ammonium. These nutrients were measured on a Skalar SA-400 AutoAnalyzer, ammonium according to the phenol-hypochlorite method (HELDER & DE VRIES, 1979), the others by automated STRICKLAND & PARSONS (1968) methods. Dissolved reactive silicate was analysed after the method of STRICKLAND & PARSONS. All on-board nutrient determinations were done in duplicate; the analyses of the major cations at the University laboratory were done in triplicate. The major cations were measured by flame atomic absorption spectrometry (Perkin-Elmer 2380), with Cs and La as spectroscopic stabilizers; manganese and iron were measured by flameless atomic absorption spectrometry (on a Perkin-Elmer 5000 with an AS40 autosampler and HGA 400 graphite furnace and Zeeman background correction). The organic carbon content was determined partly by a standard sulphuric acid/dichromate oxidation (after SIMS & HABY, 1971) and by a volumetric method after HARTMANN et al. (1971); the difference between the results of the two methods was negligible.

4-3. RESULTS AND DISCUSSION

Before variations in the element composition of sediments can be discussed, it is important to assess if large fluctuations occur in the grain size distribution and/or major element composition. The association of trace metals and organic matter with fine-grained particles is well-known, as is the correlation between particle size and major element composition (e.g. SALOMONS & FÖRSTNER, 1984). The major part of the sediment in the Nares Abyssal Plain has a relatively constant composition

TABLE 4-2. Main elements and element/Al for samples from core 84P1

SAMPLE NO.	DEPTH (cm)*	Si %	Al %	Fe %	Mn ‰	Ca %	org.C %	Fe/Al	Mn/Al x100
4070	7-15	26	9.1	5.8	1.4	2.6	0.36	0.63	1.5
4071	17-27	27	8.3	5.1	1.2	3.3	0.40	0.61	1.4
4072	50-60	30	7.9	4.8	2.6	1.0	0.24	0.61	3.3
4073	97-106	28	7.8	4.9	0.6	2.2	0.64	0.62	0.8
4074	136-143	28	7.4	4.0	0.7	3.1	0.45	0.54	0.9
4075	174-182	29	8.7	5.9	0.7	0.9	0.59	0.67	0.8
4076	216-226	28	8.3	5.3	1.0	2.0	0.38	0.64	1.2
4077	247-257	27	9.0	5.9	1.8	1.2	0.44	0.66	2.0
4078	260-270	27	9.2	5.9	1.2	0.8	0.21	0.64	1.3
4079S	315-323	31	5.7	3.0	3.7	4.1	0.24	0.53	6.5
4080	326-334	28	9.2	5.4	0.9	0.7	0.40	0.59	1.0
4081	363-370	28	9.1	5.5	1.0	1.4	0.27	0.61	1.1
4082	418-429	27	9.7	6.2	1.0	1.4	0.33	0.64	1.1
4083	454-465	29	7.6	4.5	2.3	2.2	0.25	0.59	3.1
4084	485-495	27	10.5	6.0	0.9	1.6	0.60	0.58	0.9
4085	529-540	27	9.6	6.4	1.3	3.2	0.34	0.67	1.3
4086	557-567	27	9.8	6.6	1.4	1.8	0.38	0.68	1.4
4087S	581-592	29	8.2	4.7	1.6	2.5	0.19	0.57	1.9
4088	601-610	28	8.6	5.4	1.3	1.4	0.35	0.64	1.5
4089S	623-632	30	7.0	4.0	1.0	5.0	0.23	0.57	1.4
4090	646-655	28	9.1	5.8	1.1	1.1	0.27	0.64	1.2
4091	671-681	28	8.4	5.3	1.0	1.0	0.23	0.63	1.2
4092	736-747	29	6.3	4.0	1.1	3.8	0.23	0.64	1.7
4093	782-793	28	6.4	3.6	1.0	5.4	0.60	0.56	1.6

Samples marked with S contain silt-stringers. * depth interval. Al, Fe, Mn, Ca and Si analysed by standard ICP and XRF techniques.

with respect to the grain-size fraction <16 µm (90% ± 10). The main deviation in grain-size and major element composition (Table 4-2) occurs in the silt stringers that have only 60%(±20) of the grain-size fraction <16µm (F. B. RISPENS pers. comm.). The sediment is carbonate depleted except for some intervals of limited extent that have up to 16% $CaCO_3$. Therefore one can not expect major variations in the trace element composition as a consequence of changes in the grain size distribution or major element composition (with the exception of the silt stringers). However, the Fe and especially the Mn content of the sediment, as shown for core 84P1 in Table 4-2, demonstrate that large changes do occur. These changes can be attributed to diagenetic reactions that are accompanied by changes in redox conditions as will be discussed below.

Redox potential / Organic carbon content

Eh / Colour of the sediment

For many years brown-coloured sediments have been interpreted as being pelagic, oxidized sediments, whereas the green colour of sediment was attributed to more reducing conditions. Local discoloration due to more reducing micro areas within highly oxidizing sediments has been demonstrated by HARTMANN (1979). In a recent article LYLE (1983) demonstrates that the colour of the sediment is indicative for the oxidation state of iron, and thus for the redox condition of the sediment. The generally assumed sequence in the consumption of oxidants is O_2 > MnO_2 NO_3^- > Fe_2O_3 > SO_4^{2-} (Table 4-3) (e.g. FROELICH et al., 1979; EMERSON et al., 1980; 1982; LYLE, 1983). This is accompanied by a decrease in redox potential (e.g. BRECK, 1974; TURNER et al., 1981; TEBO et al., 1984). Lyle predicts that the nitrate concentration in the pore water approaches zero Eat the brown/green colour transition in the sediment. The implicit assumption made by LYLE (1983), FROELICH et al. (1979) and others is that

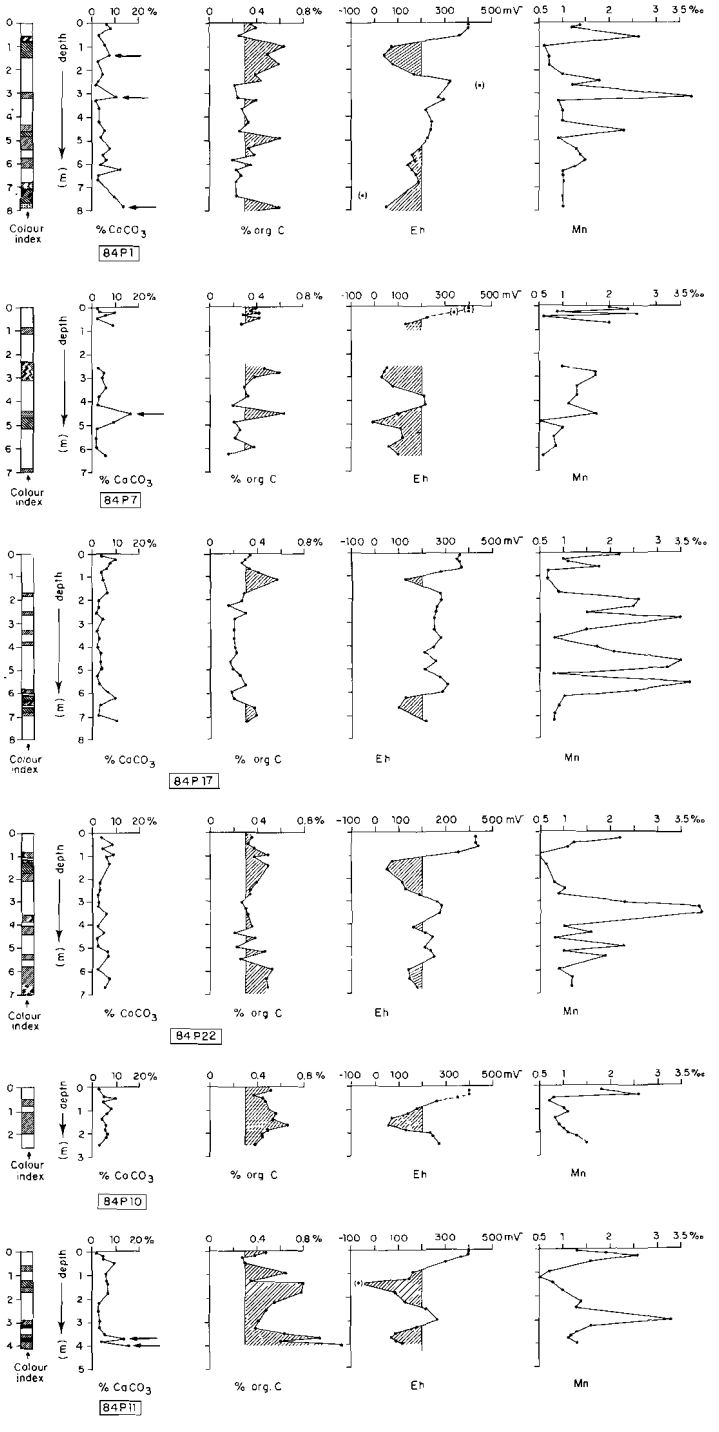
Colour index
depth (m)
% CaCO3
% org C
Eh
Mn
84P1
84P7
84P17
84P22
84P10
84P11

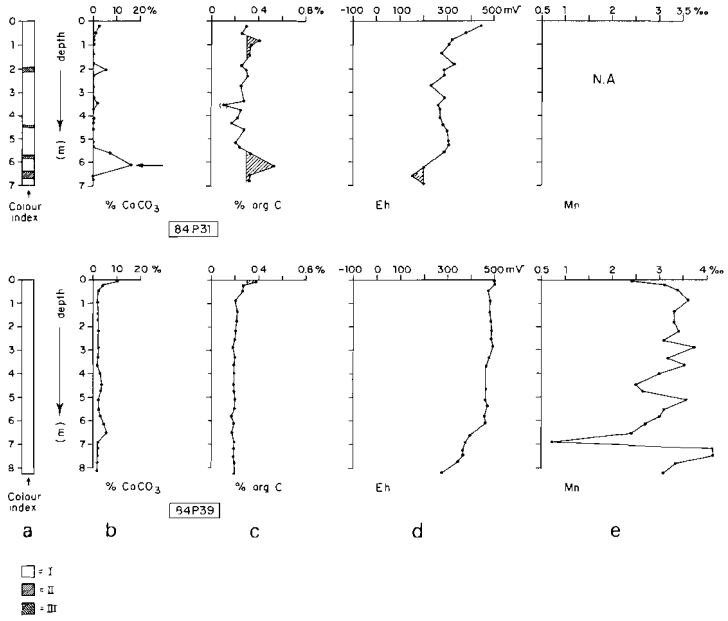

Fig. 4-2. a.Generalized colour index of the sediments; [I]= 10YR ("yellowish brown"), [II]=2.5Y4-6/2-5 ("greyish yellow"), [III]=5Y4-6/2-5 ("greyish olive") (After KUIJPERS, 1985, according to Munsell colour chart) b. Total Ca content of the sediment (which includes non-carbonate Ca) converted into $CaCO_3$ content; for core 84P31 Ca was determined from the acid-leach; c. Organic carbon content, values over 0.3% have been arbitrarily shaded; d. Redox potential, values less than +200 mV relative to the H_2 electrode have been arbitrarily shaded; e. Total manganese content of the solid phase, NA = not analysed. Note missing section in core 84P7. Horizontal arrows indicate sediment intervals with enhanced carbonate content.

the sediment composition is homogeneous. With regard to the turbiditic sediments from the Nares Abyssal Plain this is not the case and this work does not support any simple relation between colour and pore-water nitrate. The generalized colour-index, as shown in Fig. 4-2, clearly demonstrates the inhomogeneous character of the deposited sediments. The relation of sediment colour and redox potential as deduced by LYLE (1983) was actually measured in these sediments (Fig. 4-2). Comparison of the profiles of redox potential and organic carbon (Fig. 4-2) shows that in the turbiditic cores the organic carbon profile fluctuates considerably, high organic carbon values coinciding both with greenish-coloured sediment and low Eh values. Upon oxidation of the sediment in the laboratory the greenish colour changed to brown and upon reduction it changed back to green again (see LYLE, 1983). Therefore the colour is not caused directly by the organic carbon content, but by the oxidation state of iron.
Core 84P39, consisting mainly of pelagic sediment, has a relatively low and nearly constant organic carbon content. Only in the lower part of this core does the Eh value drop gradually, simultaneously with a decrease in the

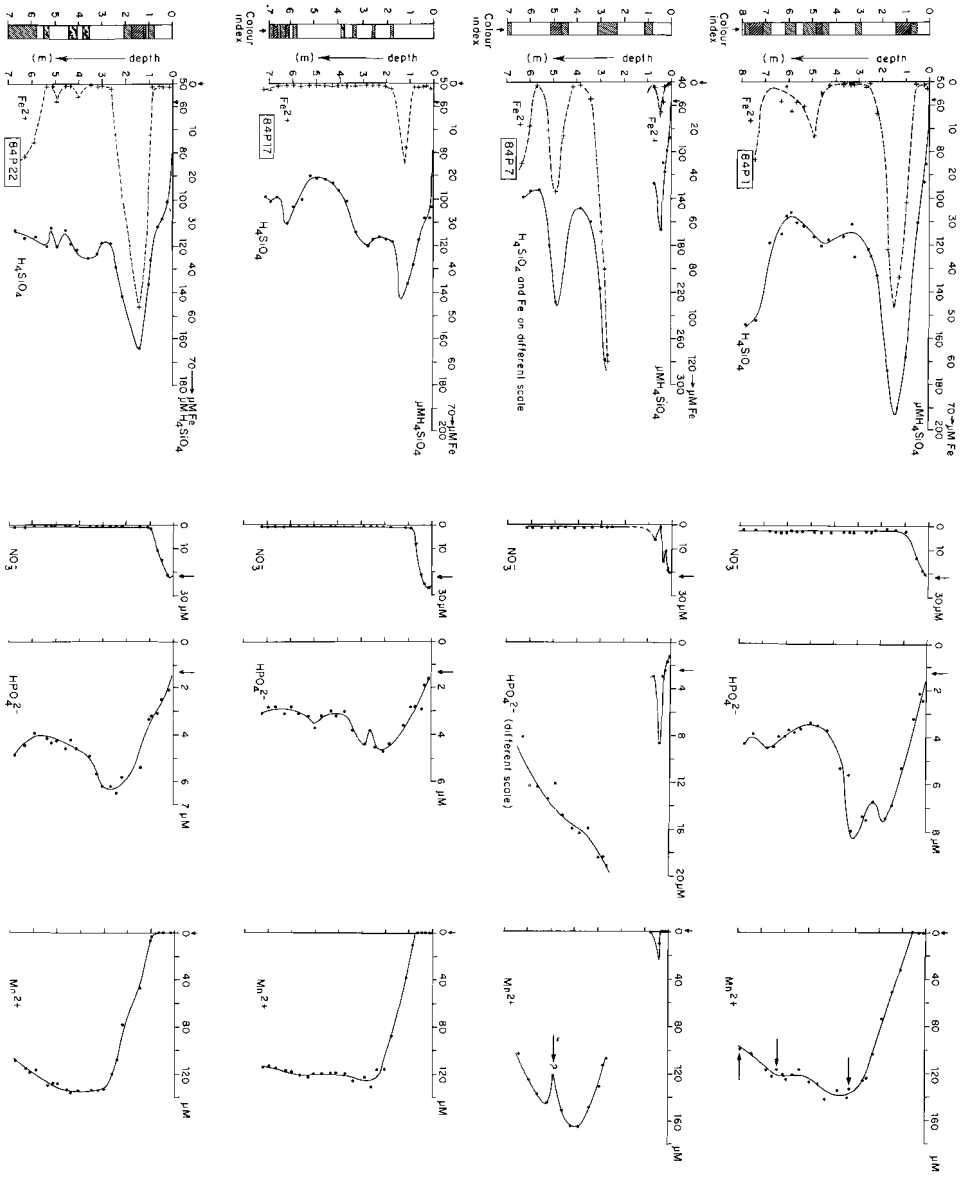
Colour index
(m) depth
84P1
84P7
84P17
84P22
Fe2+
H4SiO4
μMH4SiO4
70→μM Fe
120→μM Fe
H4SiO4 and Fe on different scale
NO3-
30 μM
HPO42-
8 μM
HPO42- (different scale)
20 μM
Mn2+
160 μM

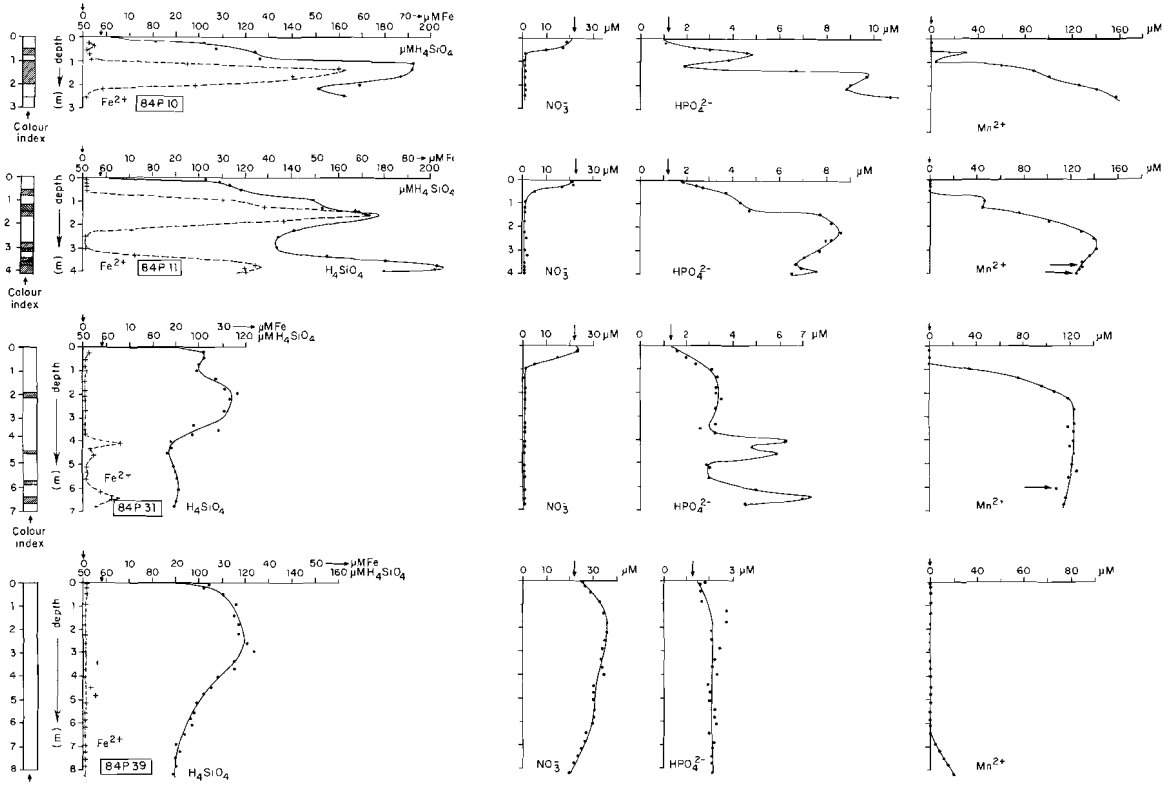

Fig. 4-3. Pore-water concentrations of : a.Iron and reactive silica; b. Nitrate; c. Phosphate; d. Manganese; vertical arrows indicate bottom-water concentrations (see Table 4-4); horizontal arrows indicate samples originating from sediment intervals with enhanced carbonate content.

interstitial nitrate concentration and an increase in dissolved manganese (Fig. 4-3).

TABLE 4-3. Oxidation reactions of organic matter in marine sediments.

1. Oxygen reduction :

$138\ O_2 + C_{106}H_{263}O_{110}N_{16}P + 18\ HCO_3^- \longrightarrow 124\ CO_2 + 16\ NO_3^- + HPO_4^{2-} + 140\ H_2O$

2. Nitrate reduction :

$94.4\ NO_3^- + C_{106}H_{263}O_{110}N_{16}P \longrightarrow 13.6\ CO_2 + 92.4\ HCO_3^- + 55.2\ N_2 + 84.8\ H_2O + HPO_4^{2-}$

3. MnO_2 reduction :

$236\ MnO_2 + C_{106}H_{263}O_{110}N_{16}P + 364\ CO_2 + 104\ H_2O \longrightarrow 470\ HCO_3^- + 8\ N_2 + 236\ Mn^{2+} + HPO_4^{2-}$

4. Fe_2O_3 reduction :

$212\ Fe_2O_3 + C_{106}H_{263}O_{110}N_{16}P + 740\ CO_2 + 316\ H_2O \longrightarrow 846\ HCO_3^- + 424\ Fe^{2+} + 16\ NH_3 + HPO_4^{2-}$

5. Sulphate reduction :

$53\ SO_4^{2-} + C_{106}H_{263}O_{110}N_{16}P \longrightarrow 39\ CO_2 + 67\ HCO_3^- + 16\ NH_4^+ + 53\ HS^- + 39\ H_2O + HPO_4^{2-}$

6. Calcium-carbonate dissolution/precipitation :

$CO_2 + H_2O + CaCO_3 \longleftrightarrow Ca^{2+} + 2\ HCO_3^-$

Eh / Pore-water composition

The concentration/depth profile of dissolved iron and silica for the turbiditic cores (Fig. 4-3) indicates a close relationship between the dissolved iron and silica and the organic carbon content and Eh values (Fig. 4-2), whereas the concentration/depth profiles of dissolved phosphate and manganese (Fig. 4-3) seem to be only indirectly related to the Eh. Comparing the redox potential data for all cores with the concentration of dissolved nitrate, manganese, iron and silica, it appears that there is a certain relation between these parameters in the highly variable sediments discussed here (Fig. 4-4). There is quite a large scatter in the plots of the redox potential (Fig. 4-4), which in the absence of variations in the pH, may be attributed partly to the fact that the time allowed for equilibration during the Eh measurements was insufficient.

Despite the fluctuating data of Eh and the rapid changes in the concentration of NO_3 (Fig. 4-3) a good correlation between the two parameters was found (Fig. 4-4[a]). Therefore the concentration of dissolved nitrate can be considered to be a good indicator of redox conditions in the sediment.

TABLE 4-4. Mean concentrations of 22 bottom water samples, taken at approximately 1 m above the sediment/water interface.

NH_4^+ (*)	NO_2^- (*)	NO_3^- (*)	HPO_4^{2-} (*)	H_4SiO_4 (*)	O_2 (*)	Na^+ (+)	Mg^{2+} (+)	K^+ (+)	Ca^{2+} (+)	Cl^- (+)
<1 (-)	<0.05 (-)	20.2 (.9)	1.3 (.2)	58.5 (.9)	130 (1)	485 (5)	54.5 (.9)	10.5 (.2)	10.5 (.2)	560 (.5)

(*) : concentration in µM; (+) : concentration in mM; standard deviations are indicated between brackets.

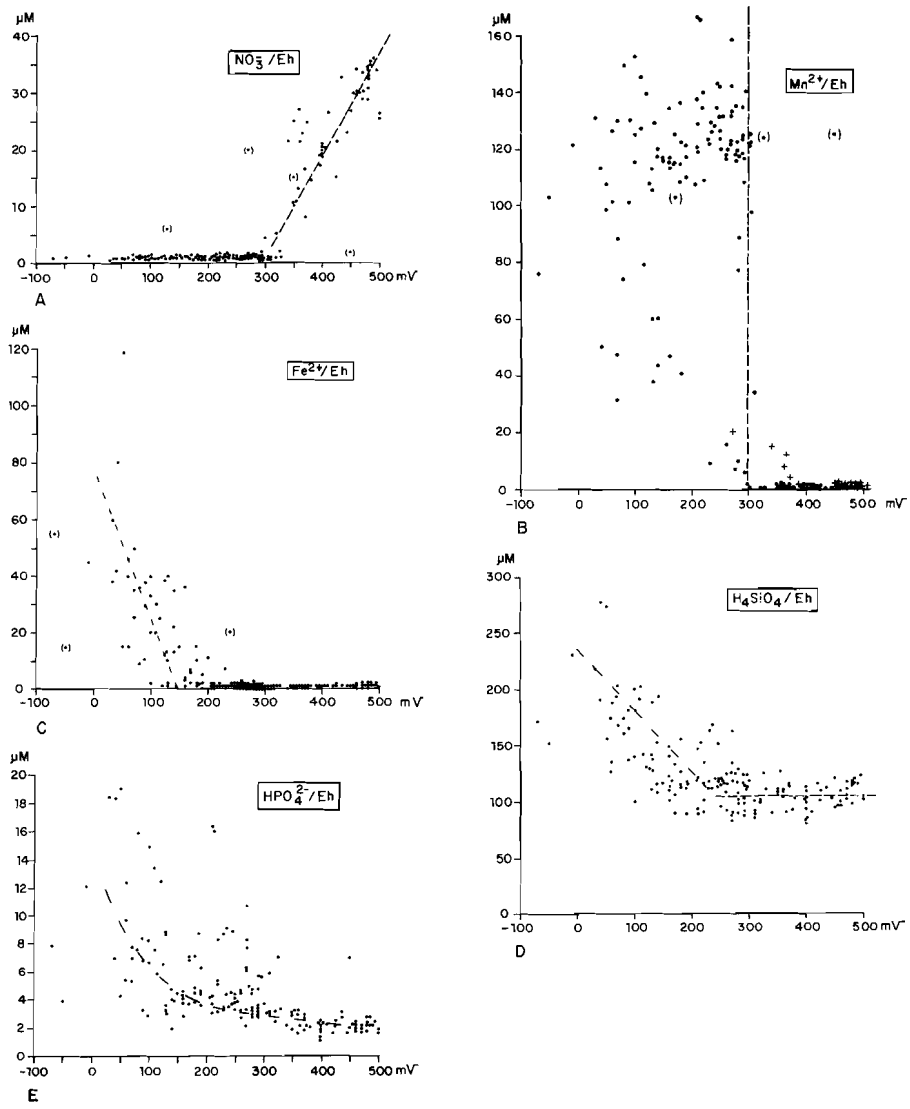

Fig. 4-4. Redox potential versus pore-water concentration of : a. Nitrate; b. Manganese; c. Iron; d. Silica; e. Phosphate.

The Eh value found for the boundary where nitrate approaches zero (325 mV) (Fig. 4-4[a]) is close to the value for the redox couple NO_3^-/NH_4^+ (270-330 mV) (BILLEN, 1975; GARRELS & CHRIST, 1965; STUMM & MORGAN, 1970; WHITFIELD & JAGNER, 1981).

Within each turbiditic core there is no clear correlation between dissolved manganese and the redox potential or the organic carbon content in the

sediment. However, when the redox potential and the manganese content of the solid phase within each core are compared, a relation becomes evident (Fig. 4-2) : a low redox potential corresponds with a low manganese content in the solid phase. If the composition of the sediment at deposition is assumed to be relatively constant, then the levels of low manganese content in the solid phase indicate an enhanced reduction of manganese at lower Eh conditions. If all the data of redox potential and dissolved manganese are plotted (Fig. 4-4^b) it appears that reduction of manganese oxide takes place only at an Eh of less than 300 mV, which is similar to the value for the Mn(IV)/Mn(II) redox couple (270-340 mV) (GARRELS & CHRIST, 1965; VAN DER WEIJDEN et al., 1970; HARTMANN et al., 1976; LYLE, 1983). There is a fairly direct correlation between the distribution of dissolved iron and redox conditions too (Fig. 4-4^c). The limiting redox potential found for iron (150-200 mV; Fig. 4-4) is lower than that found for manganese and for nitrate, which is in accordance with observed and theoretical findings (e.g. STUMM & MORGAN, 1970; BRECK, 1974; FROELICH et al., 1979; WHITFIELD & JAGNER, 1981; TEBO et al., 1984).

Decomposition of organic matter

Early diagenetic reactions relating to the decomposition of organic matter have a major influence on processes and element distribution in the upper part of deep-sea sediments. The over-all stoichiometric equations for the sequence of oxidants during such a decomposition are summarized in Table 4-3 (FROELICH et al.,1979; EMERSON et al.,1980; 1982). The mobility of dissolved manganese, its ability to consume oxygen, and the almost identical redox potential or thermodynamic properties at which degradation of organic matter by either nitrate or manganese oxide takes place (FROELICH et al., 1979; EMERSON et al., 1980; 1982) could easily change the detected sequence of these reactions. The order of reduction may also depend on sediment and interstitial water properties. Apparently in the sediments that are discussed here the reduction of nitrate precedes that of manganese oxide in the degradation of organic matter. The reduction of sulphate in all cores that are discussed here is of no significance. Dissolved sulphide was not detectable (<1 µM), although the concentration of sulphate decreases slightly with depth in the turbiditic cores ($SO_4 \approx 1$ mM per 8 m sediment depth); this is probably due to diffusive processes only. Some of the above-mentioned oxidants as well as some products of the degradation of organic matter will be discussed below.

Pelagic sediments

In the pelagic core 84P39 oxygen is thought to be present in more than a trace amount down to a sediment depth of more than 2 metres (nitrate maximum). The sedimentation rate of the sediments in core 84P39 is very low, so that most of the organic carbon has been decomposed by dissolved oxygen as oxidant. The organic carbon content in core 84P39 diminishes rapidly from 0.4% at the top to half this value at less than a metre depth. The remaining 0.2% of organic matter is probably more refractory and is decomposed at a minimal rate only. The continuing decomposition of organic matter in core 84P39 can only be confirmed by the decrease in the concentration of dissolved nitrate in the pore water (Fig. 4-3) and by the decrease in the redox potential (Fig. 4-2). It is likely that the generation of reduced manganese (Table 4-3) only takes place at sediment depths below 8 m in this core, and that the profile of dissolved reduced manganese (Fig. 4-3) merely indicates the upward diffusion and oxidation of dissolved manganese (see also Fig. 4-4^{b}) (BURDIGE & GIESKES, 1983). The presence of dissolved manganese at a sediment depth of 6- 8 m will remove any remaining traces of dissolved oxygen, and thus enhance the reduction of nitrate. A silt layer of low porosity (0.5) at a depth of approximately 660 cm in this core probably limits the penetration of oxygen and nitrate to a greater depth, thus causing an increased slope of nitrate from 6 m sediment depth downwards. The concentration of dissolved silica in the pelagic core 84P39 is at its maximum at approximately 200-300 cm. This depth was mentioned before as the interval where the oxygen concentration falls below a critical value, and the denitrification starts to be of importance. Lower down in this core the concentration of dissolved silica seems to remain constant at a level of approximately 90 µM. This value is very close to the value indicated for equilibrium with quartz (100 µM; BROECKER & PENG, 1982; MACKENZIE & GEES, 1971; and others). The authigenic formation of quartz in sediments of similar age has been demonstrated in the Pacific Ocean (SINGER et al., 1984), and could possibly also limit the concentration of dissolved silica in the sediment of core 84P39 at a depth of more than 6 metres.

Turbiditic sediments

In the turbiditic cores it is the amount of organic matter above the refractory part in combination with a high sedimentation-rate which causes both oxygen and nitrate to be rapidly exhausted, generally within a depth of one metre (Fig. 4-3). Subsequently the reduction of manganese oxi-hydroxide (Table 4-3) starts at or slightly below the depth at which the

concentration of nitrate approaches zero. In all turbiditic cores initially the concentration of dissolved manganese increases sharply but seems to reach a nearly constant value at greater depths; the latter will be discussed in the next section which is on Mn,Ca-CO_3. After the available dissolved oxygen and nitrate, and Mn(IV) oxide have been consumed, the oxidation of organic matter proceeds with the reduction of iron(III) oxide (Table 4-3).

A number of simultaneous sharp maxima in the concentration of dissolved silica and iron occur in all turbiditic cores. Such a variable profile for the concentration of dissolved silica and iron with depth deviates from the generally assumed behaviour of these constituents during early diagenetic reactions in (homogeneous) deep-sea sediments (e.g. HURD, 1973; FROELICH et al., 1979; TEBO et al., 1984).

Reduction of iron oxide occurs at lower Eh values than does the reduction of manganese oxide (see also discussion above). Therefore the reduction of iron during the decomposition of organic matter in the interbedded pelagic and turbiditic sediments under discussion only takes place in very limited intervals. The sediment in these intervals is characterised by the presence of low levels of manganese oxide as a potential oxidant, by a relatively high organic carbon content, and by relatively low redox conditions, as compared with the sediment above and below these intervals (Fig. 4-2).

The behaviour of iron seems to be different from that of manganese, but, in view of the "early diagenetic spikes" of manganese (see below) this apparent difference can be attributed partly to different redox conditions. Further-more manganese is known to be a much more mobile ion than iron, because of its slower oxidation kinetics (STUMM & MORGAN, 1970; POSTMA, 1985).

The "early diagenetic spikes" that occur in the top part of cores 84P7 and 84P10 (Fig. 4-3) originate from limited sediment intervals with enhanced decomposition of organic matter. The latter is reflected in the pore-water concentration of nitrate, manganese, reactive silica, iron and phosphate (Fig. 4-3) and by the reverse spikes in the manganese content of the solid phase in these intervals (Fig. 4-2). It should be noted that it is not possible to explain these features by oxidation artifacts, should any have occurred despite our accurate shipboard handling procedure.

The increasing concentration of dissolved silica with depth in marine sediments is generally attributed to the dissolution of amorphous silica (WOLLAST, 1974; SAYLES, 1979; 1981), which at a depth of 140 cm in core 84P1 was demonstrated by electron microscopy (DE LANGE & RISPENS, 1986).

The concentration of dissolved silica seems to be related to redox conditions in almost the same way as dissolved iron. This relation, however, probably reflects the fact that silica dissolution depends on the reduction of iron. The apparent relation between the concentration of

silica and iron is caused by the simultaneous oxidation of organic matter and the related increased dissolution of biogenic silica. Removal of organic matter and/or iron oxide from the surface of amorphous silica particles enlarges the specific surface area and thus enhances their dissolution. Diffusion from the horizon of production and subsequent precipitation of $Fe(OH)_3$ and $FeSiO_3$ above and below this horizon (WINTERS & BUCKLEY, 1986; DE LANGE & RISPENS, 1986) determine the shape of the Fe,Si profiles in Figure 4-3.
The pH of the sediment as determined by punch-in measurements on-board ship and the pH measured in the interstitial water show little variation; the pH varies only between 7.70 and 7.90. Apparently the large changes in redox conditions are not accompanied by major changes in pH.
The bottom part of core 84P22 forms an exception to this general phenomenon of coinciding peaks in the concentrations of dissolved reactive silica and dissolved iron in the interstitial water. At present no satisfactory explanation can be given for this deviation, but possible causes are the absence of amorphous silica at this depth in core 84P22 or equilibrium with other minerals.

Mn,Ca-CO_3

The almost constant level of dissolved manganese at depths greater than approximately 3 m in all turbiditic cores, together with the low levels of dissolved iron at these depths, could mean that decomposition of organic matter has ceased. Since the concentration of manganese oxide in the sediment seems to be sufficient (Fig. 4-2) to allow a continuing decomposition of organic matter as inferred from the increase in alkalinity (Fig. 4-5) and since no detectable sulphate reduction seems to occur, the concentration/depth profile of dissolved manganese must indicate a limitation within the interstitial water itself. At high levels the concentration of dissolved manganese in the interstitial water of suboxic sediments is most likely to be limited by the solubility of rhodochrosite ($MnCO_3$) or at least of a mixed Mn,Ca-CO_3 (LI et al., 1969; SUESS, 1979; PEDERSEN & PRICE, 1982; JOHNSON, 1982; SAWLAN & MURRAY, 1983; MIDDELBURG et al., 1987)). The saturation state with respect to rhodochrosite ($MnCO_3$) as well as calcite ($CaCO_3$) has been calculated (Appendix 4-1). In all turbiditic cores there is an apparent equilibrium with respect to rhodochrosite as well as calcite below a depth of about 250 cm in the sediment (Fig. 4-6). Pressure artifacts have been reported, but these seem to occur only in cores taken in carbonate-ooze sediments, whereas in non-carbonate sediments no such artifacts could be demonstrated (EMERSON et al., 1980; 1982; MURRAY et al., 1980; JAHNKE et al., 1982). Except for some

intervals of limited extent that can have up to 15% $CaCO_3$, the sediments of this study contain virtually no carbonate; therefore no pressure artifact is expected for these sediments. A closer examination of the Ca^{2+} and alkalinity profiles (Fig. 4-5) suggests a possible minor decrease of both parameters (of approximately 0.1 mM and 0.2 meq/l respectively) at sediment intervals where the $CaCO_3$ content exceeds 10% (Fig. 4-2). The presence of "seed crystals" in these specific intervals could explain such a phenomenon

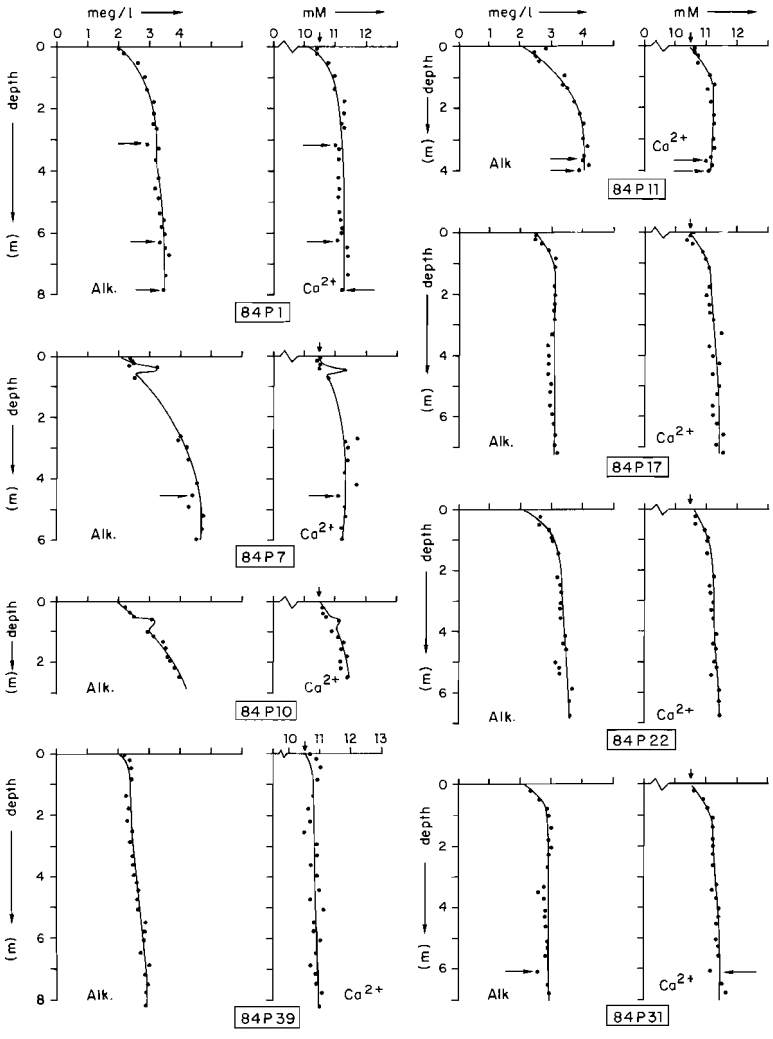

Fig. 4-5. Distribution of total alkalinity and dissolved calcium; vertical arrows indicate bottom-water concentrations; horizontal arrows indicate samples originating from sediment intervals with enhanced carbonate content.

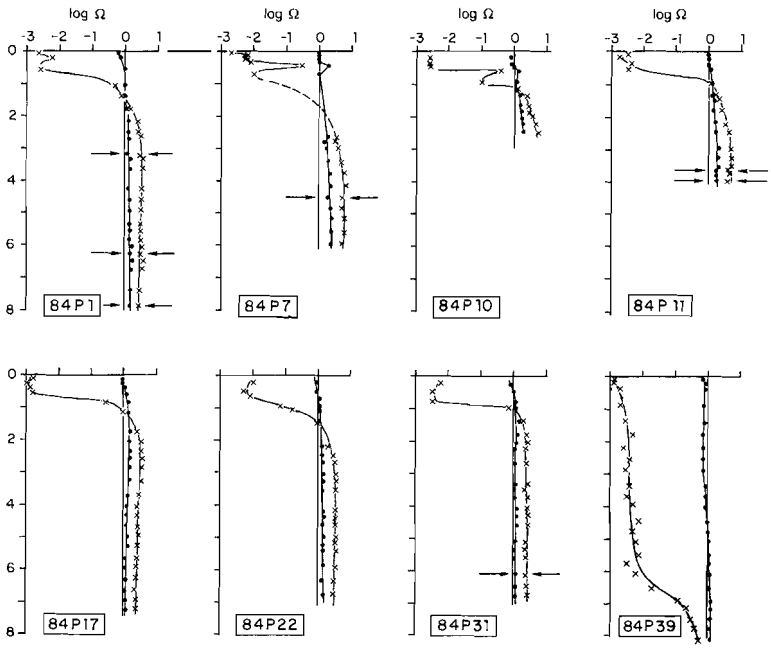

Fig. 4-6. Degree of saturation (log Ω) with respect to rhodochrosite [x] and calcite [o] (see Appendix 4-1, 4-2) versus depth in the sediment, log Ω = log [IP/K'$_{so}$(i.s.)] ; horizontal arrows indicate samples originating from sediment intervals with enhanced carbonate content.

(MURRAY et al., 1980). For example in core 84P7 in the sediment interval containing 15% $CaCO_3$, at a depth of 4.6 m, a slight decrease in alkalinity and Ca^{2+} is visible (Fig. 4-5). However, this decrease is hardly visible in the degree of saturation (Fig. 4-6). Therefore even if any local pressure artifact has occurred in the sediments of this study, it does not visibly effect the calculated degree of saturation.

It is known that rhodochrosite is rarely formed as a pure phase in marine sediments (SUESS, 1979; PEDERSEN & PRICE, 1982; SAYLES, 1985). Solid solutions with a molar ratio of Mn/Ca of up to 1/1 have been found (SUESS, 1979; PEDERSEN & PRICE, 1982). It has been suggested that an abundant presence of calcite is necessary for the in situ formation of rhodochrosite. Such a situation clearly does not exist in the sediments that are discussed here; they contain only low quantities (if any) of calcite (Fig. 4-2). The calculated degree of saturation indicates super-saturation with respect to the apparent solubility product of pure rhodochrosite.

Core 84P39, which has an extremely low average sedimentation rate, is the only core (with the exception of the uppermost part) for which kinetic

control of dissolution/precipitation reactions can be ruled out. Saturation with respect to $MnCO_3$ is not achieved in this core. However, the degree of saturation with respect to $CaCO_3$ is interesting in this context. If the top metre is excluded from the discussion, then it is only at a depth of 4-7 m that the sediment contains some solid-phase $CaCO_3$ (Fig. 4-2), and from 7 m downwards the concentration of dissolved manganese is higher than 1 µM. A stepwise increase in the degree of saturation with respect to $CaCO_3$ is observed (Fig. 4-6) : down to a depth of 4 m the pore water is under-saturated, between 4 and 7 m saturated, and from 7 m downwards super-saturated with respect to $CaCO_3$. The latter observation supports the hypothesis put forward by SAYLES (1985) and suggested earlier by others (e.g. EMERSON et al., 1980), namely that in the presence of Mn^{2+} pore water can become supersaturated with respect to pure $CaCO_3$.
For a mixed Mn,Ca-CO_3, EMERSON et al. (1980) suggest a resulting lower saturation, and SAYLES (1985) reports a possible twofold increase in the solubility product. In a recent paper MIDDELBURG et al. (1987) conclude that three possible Mn-phases (namely Mn-calcite, kutnohorite and calcic-rhodochrosite) may control the solubility of Mn and may consequently account for the observed variation in the equilibrium product. The degree of super-saturation with respect to pure $MnCO_3$ seems to differ slightly per core, with a possible dependence on redox conditions or related parameters. The pore water in cores 84P17 and 84P31, where the sediment is slightly less reducing than in the other turbiditic cores, show a somewhat lower supersaturation with respect to rhodochrosite. The concentration of Ca^{2+} is similar for all turbiditic cores, within the analytical error.
In coastal areas with much higher reducing conditions the degree of super-saturation reported with respect to pure rhodochrosite can be much higher ($\log \Omega = 1.2$) (BERNER, 1980[b] and references therein). Therefore the degree of saturation seems to depend on redox conditions possibly because of some diagenetic constituent (e.g. inhibition of precipitation by the presence of dissolved organic matter; BERNER, 1980[b], referring to HOLDREN et al., 1975) or is kinetically controlled. It is noteworthy that cores with a higher average sedimentation rate (84P7 $>$ 84P10 $\approx$ 84P11 $>$ 84P1 $\approx$ 84P22 $>$ 84P17 $>$ 84P31 $>>$ 4P39; DUIN, 1985; KUIJPERS, 1985) generally show a higher degree of saturation. A possible indication for a kinetic control is the slight decrease in the degree of saturation observed in the lower parts of cores 84P17 and 84P22. The differences in the degree of saturation with respect to $MnCO_3$ as observed in the turbiditic cores in the Nares Abyssal Plain, however, seem minor when compared to the difference between the present data and those of PEDERSEN & PRICE (1982). If their apparent saturation is converted into $\log \Omega$ (see appendix 4-1) a value of -0.7 to -0.2 is obtained. The difference between the values calculated for the degree of saturation as presented by PEDERSEN & PRICE in their perspicuous paper (1982) and in

the present study, are, however, determined solely by the choice of constants used in the calculations (appendix 4-2). Introduction of the data from their core P8 into our model in fact yields values for the degree of saturation that are almost identical to those given in this study.
If rhodochrosite equilibrium exists in the interstitial water, then some precipitation can be expected in the sediment. Although many sharp peaks do occur in the solid-phase Mn content, it has not been possible to confirm the presence of Mn,Ca-CO_3 by conventional techniques (XRD). It is also possible that the major part of these Mn peaks are expressions of former diagenetic oxidation/reduction fronts (FROELICH et al., 1979).

Phosphorus

The concentration/depth profile of dissolved phosphate is very irregular in almost all cores from the Nares Abyssal Plain. Irregular profiles of dissolved phosphate have also been reported for the turbiditic sediments of the Madeira Abyssal Plain and a close relationship was shown there between dissolved phosphate and the organic carbon content of the sediment (DE LANGE, 1984[a]). No such clear relation exists in the sediments discussed in this chapter. Nevertheless there is some correlation between the occurrence of sediment intervals with a relatively high organic carbon content and the presence of a maximum in the concentration of dissolved phosphate. There seems to be a connection between the concentration of dissolved phosphate and the Eh of the sediment (Fig. 4-4[e]), but it is evident that Eh conditions do not determine the presence and the level of the concentration of dissolved phosphate.
Dissolved phosphate in the pore water of marine sediments is generally considered to be the product of early diagenetic reactions during the decomposition of organic material (Table 4-3). To verify whether the irregular profile of dissolved phosphate is entirely due to an irregular distribution of the rate of diagenetic reactions, the 'potential' phosphate increase was calculated.
The stoichiometric reactions of Table 4-3 were taken to be representative of the processes that occur, and include the assumptions that there is no bioturbation, that the organic material is of 'Redfield" composition (REDFIELD et al. (1963), that equilibrium is maintained with respect to $CaCO_3$, and that the possibility of manganese and/or iron precipitation can be neglected. The latter assumption is not entirely true: as was shown above precipitation of rhodochrosite ($MnCO_3$) is likely to occur, and as was shown elsewhere (DE LANGE & RISPENS, 1986) some precipitation of an iron-silicate phase occurs. In view of the large uncertainties, the use of a sophisticated equilibrium model (e.g. EMERSON et al., 1982) will not

improve the approximation made by using the simple stoichiometric model values, nor will it alter the conclusions that are drawn from this model. The potential phosphate increase can be calculated from the stoichiometric reactions in Table 4-3:

$$\Delta[PO_4]_{pot} = +(1/138)*\Delta[O_2] + (1/94.4)*\Delta[NO_3^-] + (1/236)*[Mn^{2+}] +$$

$$+ (1/424)*[Fe^{2+}] + (1/53)*[HS^-] \qquad (1)$$

As discussed above sulphate reduction was found to be insignificant in the cores from the Nares Abyssal Plain. Therefore the last term of equation 1 can be omitted. The different diffusion coefficients from the constituents under discussion have to be taken into account (e.g. BERNER, 1977; EMERSON et al., 1980), which transforms equation 1 into :

$$\Delta[PO_4]_{pot} = +(1/138)*(D_{O2}/D_{HPO4})*\Delta[O_2] + (1/94.4)*(D_{NO3}/D_{HPO4})*\Delta[NO_3^-] +$$

$$+(1/236)*(D_{Mn}/D_{HPO4})*[Mn^{2+}] + (1/424)*(D_{Fe}/D_{HPO4})*[Fe^{2+}]$$

(2)

in which : $D_{O2} = 23*10^{-6}$ cm^2.s^{-1})
$D_{HPO4} = 7*10^{-6}$ cm^2.s^{-1})
$D_{NO3} = 19*10^{-6}$ cm^2.s^{-1})--all at 25°C (LI & GREGORY, 1974;
$D_{Mn} = 6.9*10^{-6}$ cm^2.s^{-1}) EMERSON et al., 1980)
$D_{Fe} = 7.2*10^{-6}$ cm^2.s^{-1})

Substitution into equation 2 results in :

$$\Delta[PO_4]_{pot} = +0,024*\Delta[O_2] + 0,029*\Delta[NO_3^-] + 0,0041*[Mn^{2+}] + 0.0024*[Fe^{2+}]$$

(3)

In the above equations the production of nitrate during the reduction of oxygen (reaction 1 of Table 4-3) has not yet been taken into account. If the sediment depth where oxygen becomes zero is assumed to coincide with the depth at which the maximum in the concentration of nitrate occurs, then the situation above the nitrate maximum can be differentiated from the situation below it. In the former situation only reaction 1 of Table 4-3 has to be considered. Oxygen has not been determined in the pore water, so the decrease in the concentration of oxygen has to be estimated from the increase in nitrate as outlined above. However, concentrations of dissolved oxygen which go to zero at nearly the same depth as nitrate have been reported. (WILSON et al., 1985). Even if such an oxygen profile is assumed

it would not make much difference to the general picture.
Including the assumptions made above one obtains the next equation :

$$\Delta [O_2] = (138/16) * \Delta [NO_3^-] * (D_{NO3}/D_{O2}) \qquad (4)$$

in which $\Delta [NO_3^-] = [NO_3^-]_{measured} - [NO_3^-]_{bottom\ water}$ (5)
with $[NO_3^-]_{bottom\ water} = 20.2\ \mu M$ (Table 4-4)

Substitution of equations 4 and 5 in equation 3, yields for the situation above the nitrate maximum :

$$\Delta [PO_4]_{pot} = 0,17 * ([NO_3^-]_{measured} - 20.2) \qquad (6)$$

For the nitrate maximum a potential nitrate concentration can be calculated according to :

$$[NO_3^-]_{max} = (16/138) * [O_2]_{bottom\ water} * (D_{O2}/D_{NO3}) + [NO_3^-]_{bottom\ water}$$

with $[O_2]_{bottom\ water} = 130\ \mu M$ (Table 4-4)

After substitution of the appropriate values a maximum potential nitrate concentration of 38.4 µM is obtained; this yields the following equation for the situation below the nitrate peak :

$$\Delta [PO_4]_{pot} = 0,024 * \Delta [O_2] + 0,029 * (38.4 - [NO_3^-]_{measured}) + 0,0041 * [Mn^{2+}] + 0,0024 * [Fe^{2+}] \qquad (7)$$

In the following discussion only the cores 84P1 and 84P39 will be dealt with, the former being representative for the cores mainly composed of turbiditic sediments, and the latter consisting largely of pelagic deposits.

Pelagic sediments

The potential phosphate concentration in the pore water of core 84P39 as calculated according to the above equations is visualized in Fig. 4-8[b]. In the top 2 m of core 84P39 the increase in the calculated potential phosphate concentration is three times larger than the increase in the measured concentration. This difference can be attributed either to the adsorption of phosphate into the sediment, or to incorrect assumptions in the calculation of the potential increase in phosphate concentration. The

assumptions that the organic matter is of Redfield composition and that no bioturbation occurred are possibly incorrect in the case of the sediments of core 84P39.

In their excellent compilation of phosphorus constituents and fluxes in marine sediment, FROELICH et al. (1982) state that most of the phosphorus in the marine system does not accumulate in the sediments. If this is true, then the slowly accumulating sediments of core 84P39 are unlikely to have adsorbed large quantities of phosphorus. The C:N:P ratio calculated from the increase in dissolved HCO_3^-, nitrate and phosphate in the top 2 m of core 84P39 is 106:15:0.9, which indicates that the assumption that the organic matter is of Redfield composition is approximately valid. Decomposition of 0.2% organic carbon in the top part of core 84P39 by reaction with dissolved oxygen (Table 4-3) would consume at least thousand times as much dissolved oxygen as deduced from the measured phosphate profile. The most plausible explanation is that oxygen has continuously been brought into the uppermost part of the slowly accumulating sediment of core 84P39, caused by biological action. Reworking of the sediment or biological pumping between bottom and pore water yields apparent diffusion coefficients for dissolved oxygen and phosphate for the top part of core 84P39 which are equal. A similar explanation was given by EMERSON et al. (1980) for their alkalinity / nitrate data in slowly accumulating Pacific sediments. For the top section of this core equation 2 can then be rewritten :

$\Delta[PO_4]_{pot} = (1/138) * \Delta[O_2]$, which yields after substitution of eq. 4 and 5

$$\Delta[PO_4]_{pot} = 0{,}063*([NO_3^-]-20.2) \qquad (8)$$

Equation 7 for the situation below the nitrate maximum transforms into :

$$\Delta[PO_4]_{pot} = 0{,}007*\Delta[O_2] + 0{,}029*(38.4-[NO_3^-]+0{,}0041*[Mn^{2+}] \qquad (9)$$

Introduction of the appropriate concentrations into equations 8 and 9 yields values for the concentration of "corrected" potential phosphate which match the measured concentrations almost exactly (Fig. 4-8^b). From 3 m downwards in core 84P39 there seems to be a slightly increasing difference between the potential and the measured concentration of dissolved phosphate. If this observation is correct, then adsorption is the likely cause.

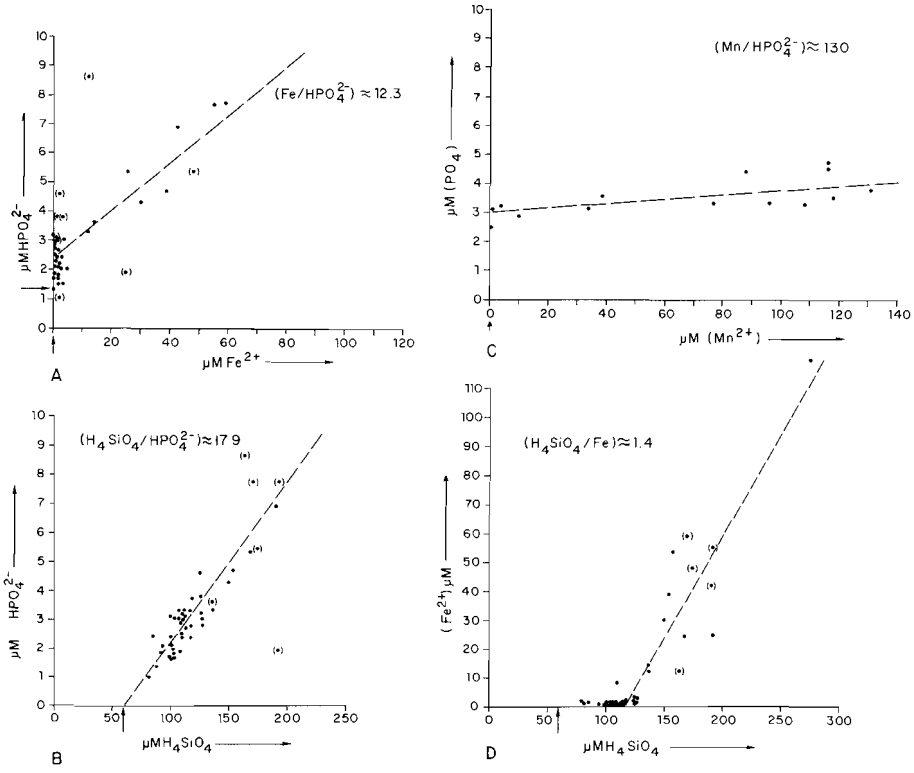

Fig. 4-7. Concentrations in the interstitial water for a. Iron vs phosphate; b. Silica vs phosphate; c. Manganese vs phosphate; d. Silica vs iron. (data for plot with manganese come from cores 84P17 and 84P31 only); all other data come from the upper part of the "major peak" of iron/silica at 1.5 m in the other turbiditic cores. Peak values are indicated in between brackets.

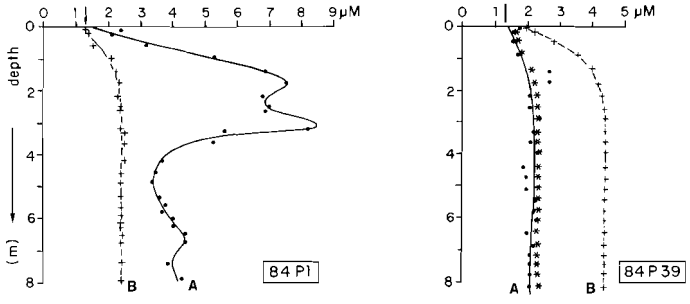

Fig. 4-8. Distribution of pore-water phosphate and potential phosphate concentrations in: a. Core 84P1, and b.Core 84P39. [o]= measured phosphate, [+]= potential phosphate, [*]= corrected potential phosphate (see text).

Turbiditic sediments

In core 84P1 the concentration/depth profile of dissolved phosphate and of the potential dissolved phosphate are very different (Fig. 4-8[a]). A distinct maximum in the concentration of dissolved phosphate in core 84P1 (and in the other turbiditic cores) can be seen just below the major maximum in the concentration of dissolved silica and iron at approximately 1.5 m (Fig. 4-3). If the excess dissolved phosphate is attributed to early diagenetic reactions involving the reduction of Mn and Fe, then much more Mn^{2+} and Fe^{2+} must have been liberated than can be deduced from the measured concentrations in the pore water. This excess Mn^{2+} and Fe^{2+} must then have precipitated as $MnCO_3$ (see above) and as $FeSiO_3$ (DE LANGE and RISPENS, 1986). If equilibrium with $CaCO_3$ is assumed, then both precipitates result in an alkalinity decrease. However, a gradual increase is found, which means that precipitation apparently is not important. The increase in alkalinity in the depth interval from 1 to 4 m therefore indicates that the major part of the excess phosphate probably has a different origin.

Dissolved phosphate can be produced not only by oxidation of organic matter but also as a result of adsorption/desorption and related processes (e.g. see KROM & BERNER, 1981). Results obtained with selective extraction techniques for different phosphate phases indicate a decrease especially in adsorbed phosphate and in phosphate related to iron/manganese hydroxides (DE LANGE, 1988)(in preparation). The observed decrease in adsorbed phosphate (Fig. 4-9) is more than sufficient to explain the increase in dissolved phosphate. However, the main decrease in the adsorbed phosphate content in the sediments of core 84P1 is found at a depth of 50 to 300 cm, whereas the maximum in the dissolved phosphate is between 50 and 400 cm. It should be realized however that, unlike the pore-water composition, the sediment composition does not reflect the present situation. Therefore at 140 - 180 cm a considerable amount of adsorbed and hydroxide -bound phosphate must have been liberated, and subsequently readsorbed above and below this depth interval. Dissolved phosphate is known to adsorb rapidly onto the surface of fresh iron hydroxides. Above the iron maximum the formation of iron hydroxide is likely, whereas below it an iron-silicate phase precipitates (DE LANGE & RISPENS, 1986). The

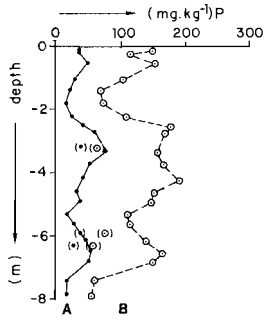

Fig. 4-9. Distribution of adsorbed phosphate [A] and phosphate bound to iron/manganese oxihydroxides [B]. Samples with silt-stringers are indicated in between brackets.

sediment below 180 cm has now become more reducing than it was before, and part of the earlier adsorped phosphate is liberated again.
In order to assess to what phase phosphorus is bound, the relationship between dissolved phosphate and some constituents was studied (Fig. 4-7). For the cores without a major peak in the concentration of dissolved iron and silica at 1.5 m (cores 84P17 and 84P31) a HPO_4^{2-}/Mn ratio of 1/130 can be deduced (Fig. 4-7). In the other turbiditic cores a much higher ratio is found for phosphate and dissolved silica and iron. Apparently phosphate is not so much associated with Mn, as it is with iron (Fig. 4-7). Such a close association of adsorbed phosphate and iron oxihydroxide is well-known for an estuarine environment (e.g. POMEROY et al., 1965; HEARN et al., 1983) and has also been reported for a marine environment (e.g. BERNER, 1973; KROM & BERNER, 1980). Diffusion coefficients for Fe^{2+} and HPO_4^{2-} are similar; therefore the HPO_4^{2-}/Fe^{2+} ratio in the pore water must reflect the composition of that fraction of the solid phase that is being reduced. The P/Fe ratio (g/g) of 1/12 that is found is close to the ratio of 1/16 reported by FROELICH et al. (1973) for oxalate-extractable P and Fe ("Fe-hydroxide fraction") in metalliferous sediments from the East Pacific Rise, but differs largely from the ratio of 1/40 found in pelagic sediment (e.g. core 84P39) and in average shale (WEDEPOHL, 1971). The turbiditic sediments considered here, however, are not likely to have a ridge-crest /hydrothermal origin, but are reported to originate from the American continental slope (TUCHOLKE, 1980). In estuarine and coastal marine sediments too, high P/Fe ratios have been reported (e.g. POMEROY et al., 1965; HEARN et al., 1983); therefore a coastal area is the most likely origin of these turbiditic sediments.
Profiles of dissolved phosphate and silica similar to the ones discussed above have been published recently by WATANABE & TSUNOGAI (1984). Unfortunately however, these authors give no data for dissolved iron and manganese. They attributed the maximum in dissolved phosphate to desorption during sulphate reduction. Their description leads one to believe that there may be a relation with Fe/Mn-hydroxide in their cores too.

4-4 CONCLUSIONS

In the turbiditic sediments a fair correlation was found between redox conditions and the highly variable pore-water concentrations of nitrate, manganese and iron , in accordance with the order of oxidants during the early diagenetic degradation of organic matter : $O_2 > NO_3^- > MnO_2 > Fe_2O_3 > SO_4^{2-}$. In the turbiditic cores nitrate goes to zero within a sediment depth of 1 m, whereas dissolved manganese increases down to a depth of 3 m and from thereon remains nearly constant. Reduction of

sulphate was found to be negligible.

Although organic carbon is a minor constituent in the turbiditic sediments from the Nares Abyssal Plain, it is of major importance in early diagenetic reactions that determine the pore-water and sediment composition of several constituents. The sediments from "turbiditic cores" are characterized by turbiditic intervals interbedded with pelagic units which are mostly of limited extent. In these cores some intervals contain a much higher organic carbon content than others, causing locally enhanced degradation of organic matter; this in turn leads to more reducing conditions and elevated pore-water concentrations of manganese, iron, silica and phosphate in these specific intervals. The combination of low porosity and relatively high sedimentation rates of the sediments in the Nares Abyssal Plain makes them an ideal subject for the study of interbedded sequences of sediments of different composition and with largely different reaction rates.

The "diagenetic spikes" in the top metre of 2 turbiditic cores are the only features that reveal the influence that an irregular distribution of organic carbon with depth in the sediment has on the concentration of dissolved nitrate and manganese. The interbedded nature of the sediments is demonstrated not only by these small diagenetic spikes, but also by major peaks in the pore-water concentration of iron and silica. These peaks coincide with a relatively high organic carbon, and a low manganese oxide content of the solid phase. The major peak at approximately 1.5 m in the turbiditic cores has been discussed in relation to the organic carbon content, redox potential and the stoichiometric reactions involved.

The nearly constant concentration of dissolved manganese from 3 m downwards is described in relation to saturation with respect to rhodochrosite ($MnCO_3$); in the same cores the pore water was found to be saturated with respect to calcite ($CaCO_3$).

The highly irregular concentration/depth profile of dissolved phosphate is shown to originate partly from the oxidation of organic matter. The major part of "excess" dissolved phosphate, however, is attributed to desorption from iron oxihydroxide in the solid phase. The P/Fe ratios as well as the possible origin of the sediment have been discussed.

APPENDIX 4-1

A. Calculation of the degree of saturation of rhodochrosite ($MnCO_3$) :

The degree of saturation with respect to pure rhodochrosite can be calculated; details will be given below.

The basic reaction for the equilibrium of pure $MnCO_3$ is :

$$MnCO_3 \quad \langle\text{-----}\rangle \quad Mn^{2+} + CO_3^{2-} \qquad (10)$$

$K'_{so} = 3.27*10^{-9}$, which is the apparent solubility product at 25°C and 1 bar (JOHNSON, 1982). This value converted into a thermodynamic K gives : $2.6*10^{-11}$, which is in accordance with the thermodynamic data from ROBIE et al., (1978; see also JOHNSON, 1982) and is smaller than the values found in experiments by Morgan (used by PEDERSEN & PRICE, 1982) and by GARRELS & CHRIST (1965)(used by LI et al., 1969).
The apparent solubility product is a function of temperature, salinity and pressure; therefore K'_{so}(25°C, 1 bar) must be corrected for in situ conditions. In the calculations the composition of the pore water is assumed to be the same as that of average sea water. The fact that complexation parameters due to differences in the composition of pore water and sea water have not been incorporated in the calculations might lead to some deviation.
All cores except for 84P39 are located in the same area which has an almost uniform depth (5850 m) and temperature (1.5°C) distribution; therefore the calculation of only one apparent solubility product for in situ conditions will be shown.
Temperature correction after JOHNSON (1982) yields :

K'_{so}(1.5°C, 1 bar) = $2.20*10^{-9}$

Correction for the effect of pressure can be done by the method of MILLERO (1979; 1982; 1983) according to equation 11. The pressure correction includes the change in apparent partial molar volume ($-\Delta V1(p-1)/RT$) and the change in the apparent adiabatic compressibility of the constituents involved. If at an in situ pressure of 600 bar the adiabatic compressibility correction for the apparent solubility product is not included, this could cause an error of 30% (MILLERO, 1983).

$$K'_{so}(\text{in situ}) = K'_{so}(1.5°C,\ 1\ \text{bar}) * \exp[(-\Delta V_1 (p-1)/RT) + 0.5 * \Delta K_1 (p-1)^2/RT]$$

(11)

where R = 83.15 $cm^3.bar.K^{-1}.mole^{-1}$ = gas constant
T = in situ temperature, in K
p = in situ pressure, in bar
ΔV_1 = apparent partial volume change for reaction 10
ΔK_1 = apparent adiabatic compressibility change for reaction 10
$\Delta V_1 = V(Mn^{2+}) + V(CO_3^{2-}) - V(MnCO_3)$
$V(Mn^{2+}) = -13.08\ cm^3.mole^{-1}$ (MILLERO, 1982)
$(CO_3^{2-}) = +7.4 + 0.3725*t - 5.653*10^{-3}*t^2\ cm^3.mole^{-1}$ (MILLERO, 1982)
where t = in situ temperature in °C
$V(MnCO_3) = +31.07\ cm^3.mole^{-1}$ (MILLERO, 1983)

After substitution of the in situ temperature a value of -36.2 $cm^3.mole^{-1}$ is obtained for ΔV_1.

$$\Delta K_1 = K(Mn^{2+}) + K(CO_3^{2-}) - K(MnCO_3)$$

where $K(Mn^{2+}) = -7.16*10^{-3}$) (MILLERO, 1982)
$K(CO_3^{2-}) = (-7.88 + 0.1673*t)*10^{-3}$ (MILLERO, 1982)
$K(MnCO_3) = 0$

The resulting value for ΔK_1 is $-14.79*10^{-3}$ $cm^3.mole^{-1}.bar^{-1}$
No corrections have been made for the pressure dependence of ΔK_1, since the resulting error is less than 4% (MILLERO, 1982), which is insignificant in comparison to the other uncertainties (see text, and appendix 4-2).
Substitution of all values into equation 11 yields the following apparent in situ solubility product for $MnCO_3$: $K'_{so}(i.s.) = 5.07*10^{-9}$
The degree of saturation with respect to pure rhodochrosite is defined here as :

$$\log \Omega = \log [IP/K'_{so}(i.s.)]$$

where IP = $[Mn^{2+}]*[CO_3^{2-}]$ is the ion product
with $[Mn^{2+}]$ = total or "analytical" concentration of dissolved Mn^{2+} in the pore water
and $[CO_3^{2-}]$ = in situ concentration of CO_3^{2-} calculated according to :
$[CO_3^{2-}] = CA*C_2/([H+]+2*C_2)$
where $CA = [HCO_3-] + 2*[CO_3^{2-}]$.

CA has been calculated according to :

$$CA = TA + [H^+] + [HSO_4^-] + [HF] + [H_3PO_4] - [HPO_4^{2-}] - 2*[PO_4^{3-}] - [OH^-] - [NH_3] - [H_3SiO_4^-] - [H_4BO_4^-] - [HS^-] - 2*[S^{2-}] \quad (12)$$

The CA, as calculated from the above equation, has not been corrected for pressure effects, but possible changes are expected to be minor.
In equation 12 the total alkalinity (TA), as measured on-board ship, is defined according to DICKSON (1981).
C_2(i.s) = $9.97*10^{-10}$ = the second apparent equilibrium constant of carbonic acid, which has been calculated for in situ temperature and pressure from the thermodynamic constant ($4.67*10^{-11}$; MEHRBACH et al., 1973) according to MILLERO (1979; 1983) after data from MEHRBACH et al. (1973) and CULBERSON & PYTKOWICZ (1968).
$[H^+]$ = in situ activity of H^+ as calculated according to MILLERO (1979) for NBS scale from the on-board pH measurements :

temperature correction :

$$pH(t) = pH(25°C) + A*(t-25) + B*(t-25)^2$$
$$\text{where } A = [-9.702 - 2.378(pH(25) - 8)]*10^{-3}$$
$$\text{and } B = [1.123 - 0.003(pH(25) - 8) + 0.933(pH(25) - 8)^2]*10^{-4}$$

pressure correction :

$$pH(i.s.) = pH(t) + A*(p-1)$$
$$\text{where } A = -[0.424 - 0.0048(S-35) - 0.00282*t - 0.0816(pH(t) - 8]*10^{-3}$$
where S = salinity (‰)

The degree of saturation (log Ω) as calculated for all the samples is plotted in Fig. 4-6.

B. The calculation of the equilibrium of $CaCO_3$:

The basic reaction for the calcite equilibrium is :

$$CaCO_3 \langle\text{-----}\rangle Ca^{2+} + CO_3^{2-} \quad (13)$$

$K_{s\,o}$(25°C, 1 bar) = $3.80*10^{-9}$ = the thermodynamic solubility product for calcite at 25°C and 1 bar (JACOBSON & LANGMUIR, 1974).

K_{so}(25°C, 1 bar) is converted into the apparent solubility product by means of the temperature and pressure corrections from MILLERO (1979; 1982) after data from INGLE et al. (1973) and INGLE (1975).
The calculation is outlined in detail by MILLERO (1979; 1982; 1983); therefore only the result for the in situ apparent solubility product will be given here : $K'_{so}(i.s.) = 1.22*10^{-6}$
The degree of saturation with respect to pure calcite is defined here :

$$\log \Omega = \log [IP/K'_{so}(i.s.)]$$

where IP = ion product = $[Ca^{2+}]*[CO_3^{2-}]$
$[Ca^{2+}]$ = total or analytical concentration
$[CO_3^{2-}]$ = calculated in situ concentration (see above under the calculation of $MnCO_3$ equilibration)

The degree of saturation ($\log \Omega$) as calculated for all the samples is plotted in Fig. 4-6.

APPENDIX 4-2.

JOHNSON (1982) found excellent agreement between the experimentally determined apparent solubility product and the thermodynamic solubility product as calculated from the data of ROBIE et al. (1978). His value, however, deviates from the value used by PEDERSEN & PRICE (1982) and LI et al.(1969), see also discussion by POSTMA (1981) on this subject. It seems inappropriate to discuss the choice of the constants used in the calculation of the degree of saturation, particularly because the differences cannot be attributed to a single parameter. A comparison of the set of constants used by PEDERSEN & PRICE (1982) with the set used in the present study shows, amongst others, the following differences : thermodynamic solubility product (difference 30%), total activity coefficient of Mn^{2+} (0.08 versus 0.22), (not) including of the adiabatic compressibility effect (difference of up to 30%). Evidently some fundamental research remains to be done on this subject.
To a certain extent a similar situation exists with regard to calcite equilibrium (BROECKER & TAKAHASHI, 1977). If the equilibrium constants of PLUMMER & SUNDQUIST (1982) had been used to calculate the degree of saturation with respect to calcite the supersaturation would have been slightly greater.

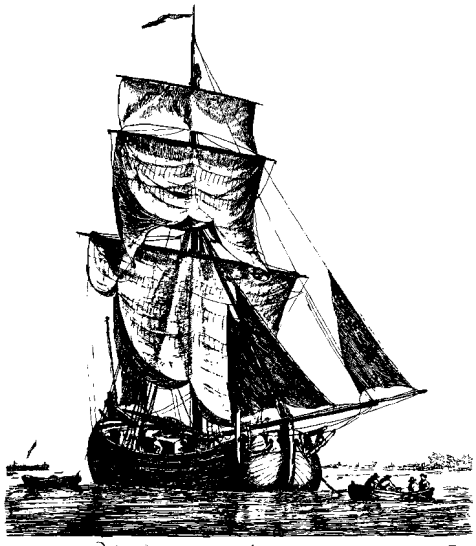

E Hoeker zyn Zeilen dragende 3

Chapter 5

GEOCHEMICAL CHARACTERISTICS AND PROVENANCE OF LATE-QUATERNARY SEDIMENTS FROM THE MADEIRA AND NARES ABYSSAL PLAINS (NORTH ATLANTIC)

ABSTRACT

Late-Quaternary sediments of the Madeira Abyssal Plain consist predominantly of metre-thick turbidites interbedded with thin layers of pelagic sediment. The chemical composition of the turbiditic sediments is determined mainly by their provenance. On the basis of the geochemical data three separate groups of turbidites can be recognized : 1. **organic-rich turbidites**, *2.* **turbidites with a volcanic component**, *and 3.* **carbonate-rich turbidites**. *The organic-rich turbidites originate from the continental margin off NW Africa. Much of the material in the volcanic turbidites originates from the oceanic islands of the Canaries, Madeira and possibly the Azores. A few carbonate-rich (>75% $CaCO_3$) turbidites on the other hand, originate from an "oceanic" area situated above lysocline depth, such as the Great Meteor-Cruiser seamounts to the west of the Madeira Abyssal Plain. Diagenetic alteration is only of secondary importance with respect to the bulk chemical composition.*

In contrast to the well-defined metre-thick turbidites in the Madeira Abyssal Plain, the sediments from the Nares Abyssal Plain consist of numerous thin turbidites (mostly less than 0.5 m thick). These sediments are interbedded with a more pelagic-type sediment. The main source area for the turbidites in the Nares Abyssal Plain is the North American continent and adjacent continental slope areas. On the basis of the geochemical data, statistical partitioning into two groups occurs, possibly reflecting pelagic and turbiditic sediments. At present it seems not possible to recognize separate provenance groups for the turbidites in the Nares Abyssal Plain, which is in sharp contrast to those from the Madeira Abyssal Plain.

5-1. INTRODUCTION

In the present study the geochemical characteristics of sediments and their related provenance will be discussed for two North Atlantic abyssal plains, namely the Madeira Abyssal Plain and the Nares Abyssal Plain (Fig. 2-1). Comparison of the two abyssal plains is interesting, since both are covered mainly by turbiditic sediments but show marked differences in geochemical and sedimentological characteristics.

Madeira Abyssal Plain

The Madeira Abyssal Plain (MAP) lies 700 km west of Madeira and the Canary Islands, approximately half-way between the NW African Continental Shelf

Fig. 5-1. a. Sediment pathways of the Canary Basin (After EMBLEY, 1982). b. Study area with the location of cores that are discussed in the text. P indicates occurrence of phosphorite nodules (CRONAN, 1980).

and the Mid Atlantic Ridge. The MAP is situated in the deepest part (average depth 5400 m) of the Canary Basin, forming a narrow stripe of flat (average slope <1:2000) seafloor about 200 km wide (Fig. 5-1). Studies of the NW African continental margin (SEIBOLD & HINZ, 1974; UCHUPI et al., 1976; JACOBI, 1976; EMBLEY & JACOBI, 1977; EMBLEY 1980; 1982; VON RAD & HINZ, 1982) have demonstrated that submarine slides, slumps, debris flows and turbiditic currents carry sediment from the continental slope onto the deep ocean floor. Sediment slides, and large turbidity current pathways that continue down the continental slope to the eastern margin of the MAP have recently been mapped in some detail (Fig, 5-1) (EMBLEY 1982; JACOBI & HAYES, 1982; KIDD & SEARLE, 1984). Turbidites derived from the African continental rise have been shown to occur immediately south of the MAP (BELDERSON & LAUGHTON, 1966). Late Quaternary sediments in the MAP consist of alternating thick (up to 6 m) distal turbidites and thin (centimetre to decimetre) pelagic deposits. Individual beds have

distinctive colours and lithologies, and contain diagnostic coccolith assemblages. These characteristics have enabled the development of a detailed litho- and biostratigraphy for the cored part (uppermost 15 m) of the sediment column (WEAVER & KUIJPERS, 1983).

The turbidites in the MAP are highly distal, and consist mostly of nearly homogenous massive silty clays (E3 division of PIPER, 1978) but having laminated silty bases of sometimes up to 50 cm thick (e.g. MCCAVE and JONES, 1988; JONES et al., 1988). The sediment consists of 40-85% biogenic calcite (predominantly coccoliths), with the remainder composed predominantly of quartz and clay minerals (illite, smectite and chlorite/ kaolinite). Basal sediments contain significant amounts of basalt fragments, heavy minerals and foraminifera. Turbidites are lettered consecutively from the top downwards (a to u in this paper), with thin turbidites which cannot be traced across the whole area being given numbered suffixes (e.g. a_1). This stratigraphy (WEAVER & KUIJPERS, 1983) has been used to correlate individual turbidites over distances of > 300 km (KUIJPERS et al., 1984a; KUIJPERS & WEAVER 1985; SEARLE et al., 1985; WEAVER et al., 1986; WEAVER & ROTHWELL, 1987; DE LANGE et al., 1987[a]). The various turbidites in the MAP are generally easy to recognize and have been discussed recently in a number of papers (WEAVER & KUIJPERS, 1983; KUIJPERS et al., 1984a; KUIJPERS & WEAVER, 1985). The provenance of these turbidites has been investigated recently by WEAVER & ROTHWELL (1987) and by DE LANGE et al. (1987[a]).

Pelagic sediments in the MAP are readily distinguished by their brown colours, strong bioturbation and variable compositions. They vary from thin dark brown clays (< 3% $CaCO_3$), to thicker, very pale brown, marly carbonate oozes (>75% $CaCO_3$). Variations in the carbonate content is related to the seafloor's position immediately above the present-day calcite compensation depth (CCD). During glacial periods the level of the CCD rose above the depth of the MAP (GARDNER, 1975; CROWLEY, 1983) causing dissolution of carbonate and the deposition of pelagic clays. Small fluctuations in the CCD during the late Pliocene and Quaternary, therefore, have produced an alternating succession of marls and clays which reflects climatic shifts caused by glacial-interglacial cyclicity (WEAVER & KUIJPERS, 1983; KUIJPERS et al., 1984[b]; WEAVER et al., 1986).

Nares Abyssal Plain

The Nares Abyssal Plain (NAP) is situated in the western North Atlantic, approximately 300 km north of Puerto Rico (Fig. 2-1, 5-2). The abyssal plain is bounded to the west and south by the Greater Antilles Outer Ridge, to the north by the Bermuda Rise, and to the east by the lower flank of the

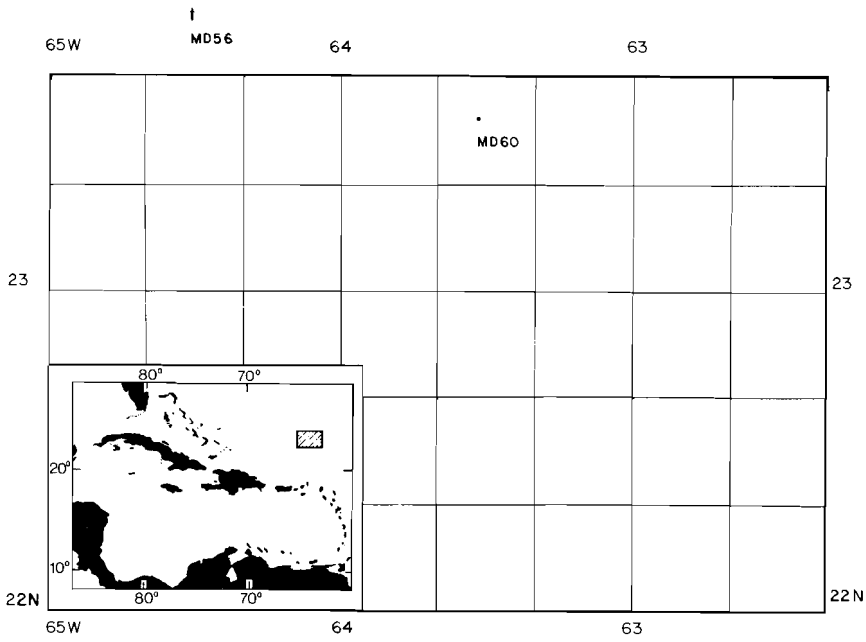

Fig. 5-2. Turbidite distribution in the Hatteras Abyssal Plain. Marked are the main sediment sources, and the sediment outlet into the Nares Abyssal Plain : the Vema Gap.

Mid-Atlantic Ridge. The Vema Gap connects the western part of the NAP with the Hatteras Abyssal Plain (Fig. 5-3). The average depth of the southern NAP is approximately 5860 m, which is below the CCD depth. Therefore, the sediments in this plain are virtually carbonate depleted, with the exception of only a few turbiditic intervals.

Features of massive transportation of sediment similar to those reported for the MAP, have been recognized on the East American continental slope (Fig. 5-3; e.g. TUCHOLKE, 1980). Turbiditic sediments are reported to cover the major part of the southern NAP (SHIPLEY, 1978; KUIJPERS et al., 1984[a]; KUIJPERS & DUIN, 1986; KUIJPERS et al., 1987). Most of the turbidites present in the southern NAP are reported to originate from northern latitudes (KUIJPERS & DUIN, 1986). The thickness of the turbidites varies between a few cm to an exceptional 1.3 m; on the average it is less than 0.5 m. The colouring of the turbiditic sediments is much less distinct than it is for turbiditic sediments in the MAP. Transport of sediment is reported to occur through the Hatteras Abyssal Plain, via the Vema Gap into the NAP (Fig. 5-3). The areal distribution of the sediment in the NAP is very irregular. The average sedimentation rates for turbiditic sediments in the NAP can show great variations (KUIJPERS et al., 1987) and correlations

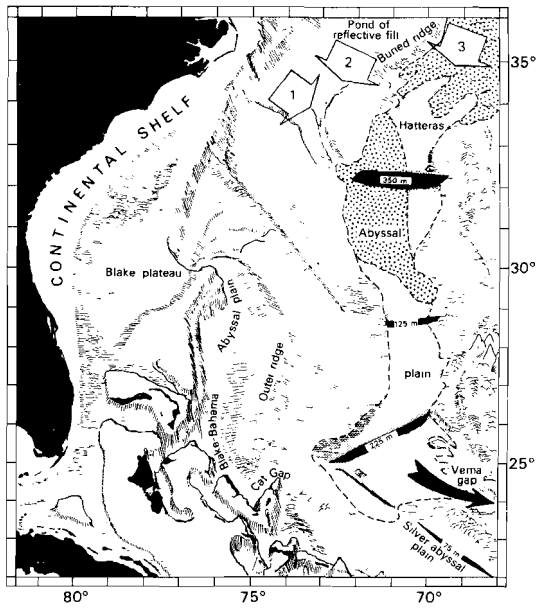

Fig. 5-3. Nares Abyssal Plain area. The location of the cores discussed in the text are indicated.

between turbidites in different cores cannot readily be made (KUIJPERS, 1985); this is in sharp contrast to the turbidites in the MAP which can be correlated easily.

Pelagic sediments in the NAP are distinguished by their brown colour, and their bioturbated inhomogeneous composition. Their colour ranges from pale brown (>75% $CaCO_3$) to dark brown (<3% $CaCO_3$). The sediments of the NAP have always been situated below the CCD, and therefore would not be expected to contain any carbonate. Turbiditic deposits, however, have entrained some carbonate material from shallower depths, which undergoes only slow partial dissolution once deposited (DE LANGE, 1986[b]). The very low primary carbonate content of the pelagic intervals could therefore have been enhanced by mixing with turbidite carbonate during bioturbation.

In this Chapter we examine the geochemical characteristics of turbidites and pelagic sediments from the MAP and NAP in relation to their provenance. This comparison is interesting in view of the contrasting differences that exist between the sediments of these two abyssal plains, despite the fact that both are covered mainly by turbiditic deposits. Besides using a conventional approach, we have chosen to apply a statistical approach too. The results obtained for the two areas are compared and discussed in relation to the sediment source areas, the thickness and composition of the various turbidites, and the area of deposition.

TABLE 5-1. Number, location and water depth of cores that are discussed in the text.

Core	Location	Water depth
MD10	31° 16,70'N 25° 23,33'W	5450 m
D10688	32° 03,0 'N 24° 12,1 'W	5428 m
MD56	23° 59,38'N 64° 30,78'W	5845 m
MD60	23° 34,49'N 63° 31,30'W	5855 m

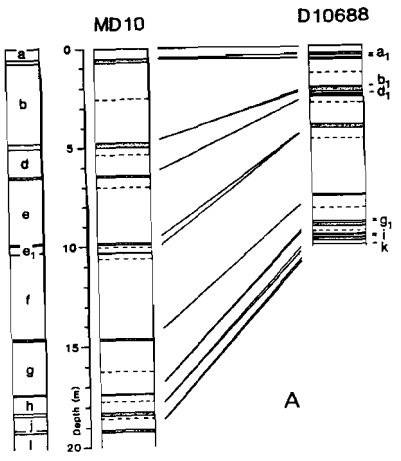

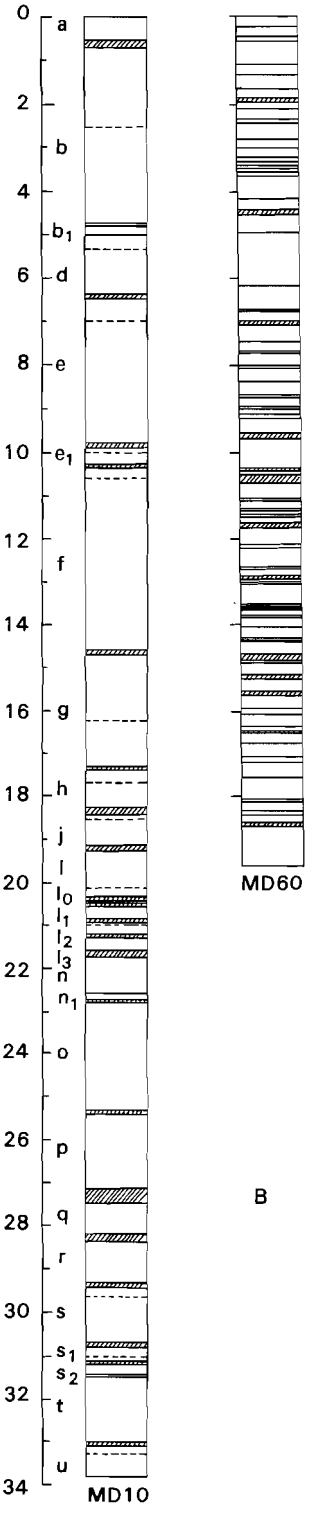

Fig. 5-4. Schematic representation of turbidites and pelagic intervals in cores MD10, MD60, and core D10688; pelagic intervals are stippled or shaded. The positions of major colour changes in two-tone turbidites (those having brown coloured tops and green bases) are indicated by broken lines. These boundaries are interpreted as relic redox fronts. a. Lithostratigraphic correlation of turbidites in core MD10 and core D10688. b. core MD60 (NAP) with all turbidites unidentifiable; core MD10 (MAP) with all turbidites identified and lettered consecutively from the top downwards (a to u in this paper. Thin turbidites which cannot be traced across the whole area have been given numbered suffixes (e.a. a1).

5-2. SAMPLES

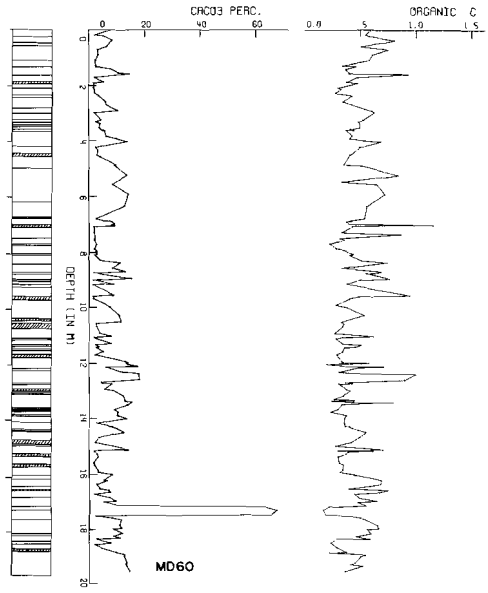

Fig. 5-5. Total carbonate content as calculated from the total Ca concentration, and the organic carbon content of core MD60, NAP.

The discussion will be restricted to two cores from each area. Cores MD10, MD56 and MD60 were taken in 1985 during the International ESOPE expedition on the R.V. Marion Dufresne cruise MD 45, and core D10688 was taken in 1983 during RRS Discovery Cruise 134 (Fig. 5-1,2,3, Table 5-1). Core MD10 from the MAP, taken at a water depth of 5450 m, recovered 34 m of sediment and includes more than 24 major turbiditic events (Fig. 5-4b). Core D10688 from the same abyssal plain is 10 m long and comes from a water depth of 5428 m. (Fig. 5-4; Table 5-1).
Cores MD60 (and MD60), from the NAP taken at a waterdepth of 5860 m, recovered approximately 20 m of sediment and contain a large number (> 55) of turbidites too (Fig. 5-4,5).
Until recently the maximum recovered core length in the MAP was generally less than 20 m (down to the k-turbidite (Fig. 5-4a), and in the NAP the maximal recovery was only 13 m. With the improved coring equipment (STACOR) (MONTARGES et al., 1983) available during the 1985 cruise a much deeper penetration of excellent quality was obtained. These cores therefore provide a unique opportunity for studying turbiditic and pelagic intervals in a longer sedimentary column.

5-3. METHODS

Geochemical techniques

The samples for this study were taken directly from the split cores on-board ship and kept at +4°C until further elaboration in our laboratory. Samples were dried at 105°C and thoroughly ground in an agate mortar, and mixed prior to acid-destruction (for ICP) or pressing into pellets

(XRF). Subsamples (0.25 g) from cores MD10, MD56 and MD60 were digested in an HF- $HClO_4$ - HNO_3 mixture and evaporated, final solutions being made up in 50 ml 1 N HCl. Subsamples (0.5 g) from core D10688 were dissolved in HF-$HClO_4$ mixture (method modified after JARVIS 1985) and evaporated, final solutions being made up in 50 ml 1 N HNO_3. Most elements discussed here were determined simultaneously using an ARL 34.000 Inductively Coupled Plasma (ICP) atomic-emission spectrometer at the University of Utrecht (MD10, MD56 and MD60 samples), and on a Philips PV8210 ICP at King's College London (D10688 samples). All S determinations were made at Utrecht. Calibration curves were constructed using artificial composite standards. Nb was determined in pressed pellets by X-Ray Fluorescence (XRF), using a Philips PW1400 spectrometer.

Analytical precision (1 σ) as determined by replicate analyses is better than 5% for all elements except Zr (10%). Detection limits are below 5 ppm for all elements determined by ICP. By reference to international standards (Table 5-2), absolute accuracy is judged to be within limits indicated by the precision, with good agreement between results from the two laboratories. Analytical accuracy of ICP results was additionally checked using X-ray fluorescence at the Institute of Earth Sciences, Utrecht and at the Institute of Oceanographic Sciences, Wormley (IOS). These also showed good agreement with ICP data. With the exception of Nb (XRF), only ICP results are discussed here.

Organic carbon (C_{org}) in cores MD10 and MD60 was determined on samples which had previously been squeezed for pore-water analysis. In these samples C_{org} was analysed at Utrecht by wet chemical oxidation (after SIMS and HABY, 1971) and by dry-oxidation at 1000°C after removal of carbonate; results were similar, except in the case of some sulphur-rich

TABLE 5-2. Geochemical analyses of standard rocks determined by ICP.

Element	Standard					
	AGV-1			SCO-1		
	Utrecht[1]	London[2]	Recommended	Utrecht[1]	London[2]	Recommended
Major elements (%)						
TiO_2	0.95	1.05	1.05	0.55	0.61	0.62
Al_2O_3	15.9	17.3	17.2	13.3	14.6	13.7
Fe_xO_3	6.76	6.56	6.78	5.13	5.49	5.22
MgO	1.41	1.50	1.52	2.75	2.79	2.76
MnO	0.093	0.099	0.097	0.049	0.061	0.050
CaO	4.76	4.90	4.94	2.52	2.55	2.64
Na_2O	4.06	4.37	4.32	0.96	0.92	0.95
K_2O	2.73	2.90	2.92	2.70	2.74	2.82
Trace elements (ppm)						
Li	8	9	12	44	47	44
Zr	239	226	230	110	110	135

Determinations made on HF-$HClO_4$ digestions using [1] : ARL 34000 and [2] : Philips PV8210 ICP spectrometers. See text for details.

samples. For these samples we used the results obtained with the dry-oxidation technique.
C_{org} determinations for core D10688 were done at IOS. After removal of $CaCO_3$ by dissolution in hot phosphoric acid with N_2 pumping, C_{org} in a 1 g sample was oxidised to CO_2 with boiling phosphoric acid containing $K_2Cr_2O_7$ and determined gravimetically (COLLEY & THOMSON, 1985).

Statistical analysis

In the statistical approach, one of the basic assumptions is that the degree of similarity between pairs of samples will be inversely related to their distance in a multidimensional space. Of the algorithms available to portray interrelationships between samples, we have chosen the Fuzzy-C-Means (FCM) clustering algorithm (BEZDEK et al., 1984). This method has already been outlined (BEZDEK et al., 1984), and tested for geochemical data (VRIEND et al., 1988). Therefore, we will only briefly re-state the basic principles :
Similar to other clustering methods, FCM is meant to determine sub-structures in a set of data. However, FCM does not allocate samples to a cluster; it only expresses the similarity of sample and cluster in a continuous function (membership) between the values zero (not alike) and one (identical). The significance of the obtained cluster model can be obtained from cluster validity criteria (BEZDEK, 1981; BEZDEK et al., 1984). For FCM the classification entropy H and the partition coefficient F are such criteria. F is closest to 1 and H approaches zero for the most significant clustering, but will only approach these values in an absolutely ideal (*i.e.* 'unnatural') case (VRIEND et al., 1988).
In the statistical approach, only data of turbidites (200 samples) have been used for core MD10. Turbidites and pelagites are sometimes difficult to distinguish in cores MD56 and MD60 from the NAP; therefore all data have been used for those cores.

5-4. RESULTS

Madeira Abyssal Plain

In the sediments from the MAP both the carbonate and the organic carbon contents fluctuate considerably (Fig. 5-6). Individual turbidites, however, exhibit nearly homogenous carbonate contents throughout their thickness, and also display an almost constant composition over wide areas. Consequently, the carbonate values may be used for the recognition

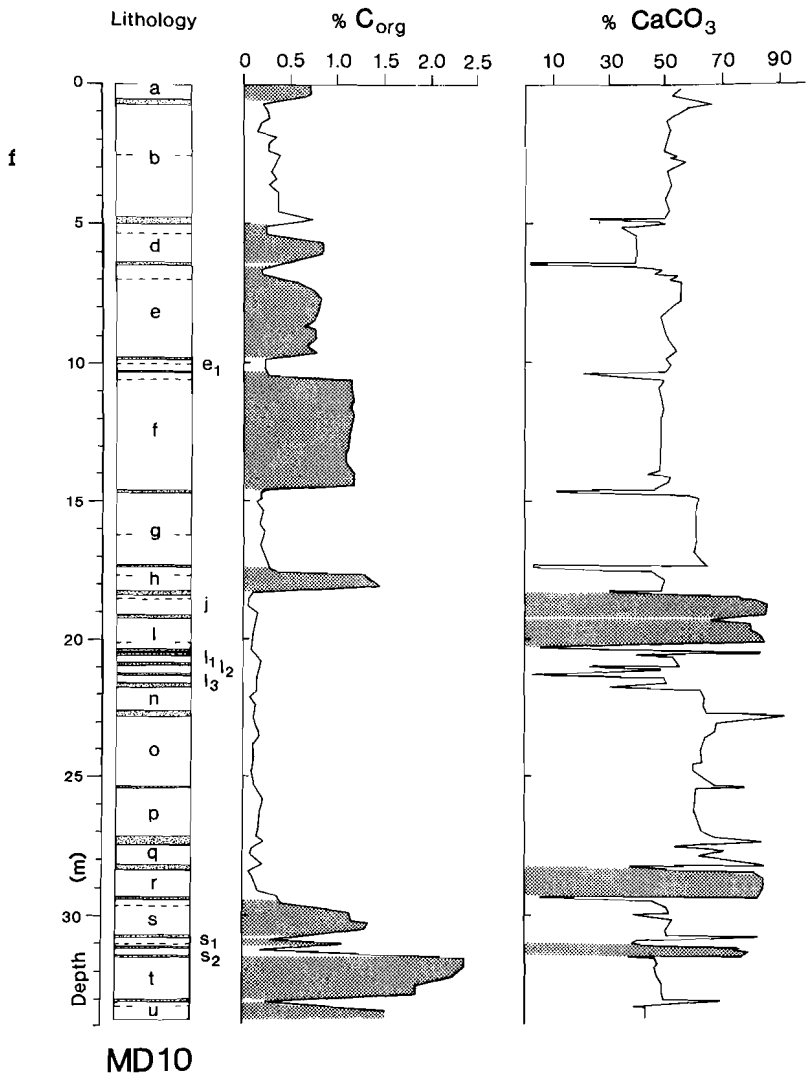

Fig. 5-6. Total carbonate content as calculated from the total Ca content, and organic carbon content of core MD10, MAP. For turbidite lettering see caption of

and correlation of individual beds over most of the MAP.

The distribution of C_{org} is more complex, because after emplacement the tops of organic-rich turbidites have been oxidised by oxygen diffusing into the sediment from the overlying sea water (COLLEY et al., 1984; COLLEY & THOMSON, 1985; THOMSON et al., 1984[a]; WILSON et al., 1985; 1986; THOMSON

TABLE 5-3. Geochemistry of major turbidites in core MD10 recalculated on a carbonate-free basis*.

Element	Turbidite											
	a (n=3)	*b* (n=13)	*d* (n=6)	*e* (n=13)	*e₁* (n=2)	f (n=14)	*g* (n=9)	*h* (n=8)	*j* (n=3)	*l* (n=5)	*l₁* (n=5)	*l₂* (n=5)
Major elements (%)												
TiO_2	0.73±0.04	1.50±0.07	0.73±0.03	0.79±0.02	0.76±0.02	0.67±0.03	1.32±0.03	0.74±0.03	0.63±0.08	0.74±0.03	0.86±0.06	0.97±0.08
Al_2O_3	15.0±1.6	13.6±0.5	16.4±0.3	15.2±0.4	17.5±0.4	15.1±0.9	15.0±0.3	16.0±0.7	12.6±1.6	13.8±0.5	19.3±0.6	19.1±1.0
Fe_2O_3	5.92±0.33	8.06±0.27	6.60±0.16	6.10±0.20	7.42±0.23	6.97±1.10	7.52±0.18	6.02±0.38	5.32±0.60	6.32±0.45	8.28±0.50	8.01±0.50
MnO	0.117±0.022	0.201±0.010	0.094±0.004	0.119±0.003	0.124±0.003	0.095±0.003	0.258±0.007	0.124±0.012	0.689±0.030	0.442±0.002	0.155±0.003	0.113±0.004
MgO	3.87±0.18	4.42±0.17	4.46±0.16	4.13±0.06	4.50±0.30	3.37±0.18	3.92±0.04	3.77±0.19	3.73±0.23	3.67±0.17	4.72±0.09	3.90±0.21
Na_2O	7.37±0.40	6.79±0.33	3.19±0.31	4.33±0.08	3.77±0.08	3.75±0.12	6.16±0.13	3.45±0.10	8.34±0.28	7.39±0.14	3.55±0.10	3.15±0.19
K_2O	3.15±0.24	2.54±0.10	3.42±0.36	2.99±0.19	2.61±0.44	3.29±0.48	3.14±0.03	2.88±0.34	2.95±0.25	3.22±0.18	4.49±0.28	4.02±0.33
$CaCO_3$*	56.3±2.2	52.3±0.8	38.3±1.0	51.0±1.5	51.3±1.0	45.3±2.3	61.0±0.7	48.0±1.5	85.8±0.5	81.0±1.0	49.8±2.7	38.3±4.2
C_{org}	1.32	0.40±0.06	1.15±0.06	1.44±0.28	ND	1.80±0.05	0.16±0.02	2.11±0.15	0.15±0.02	0.16±0.03	0.26	0.45
S	0.50±0.02	0.28±0.02	0.24±0.08	0.41±0.06	0.16±0.01	1.74±0.92	0.22±0.01	0.73±0.04	0.43±0.04	0.31±0.02	0.12±0	0.11±0.01
Trace elements (ppm)												
Li	64±4	42±1	84±2	82±4	90±1	73±5	46±5	85±6	70±7	74±0	100±2	94±5
Zr	94±7	174±10	109±6	124±10	160±0	137±15	377±11	160±11	147±21	179±21	157±14	181±16

Element	Turbidite										
	l₃ (n=3)	*n* (n=3)	*o* (n=11)	*p* (n=9)	*q* (n=4)	*r* (n=5)	*s* (n=8)	*s₁* (n=8)	*s₂* (n=2)	*t* (n=8)	*u* (n=7)
Major elements (%)											
TiO_2	0.85±0.14	1.55±0.04	1.52±0.09	1.66±0.08	0.69±0.18	0.51±0.09	0.71±0.03	0.72±0.01	0.45±0.01	0.56±0.01	0.62±0.03
Al_2O_3	19.8±2.4	16.8±0.8	16.3±0.5	14.3±0.3	13.6±3.7	10.0±1.9	15.5±0.9	17.0±0.4	8.6±0.1	11.8±0.2	13.7±0.7
Fe_2O_3	7.71±1.30	9.22±0.23	8.53±0.78	8.00±0.29	5.88±1.60	4.22±0.70	5.61±0.39	5.70±0.16	3.02±0.06	4.48±0.05	5.19±0.30
MnO	0.122±0.008	0.296±0.003	0.330±0.027	0.300±0.012	0.178±0.012	0.396±0.007	0.113±0.010	0.105±0.008	0.409±0.29	0.093±0.002	0.103±0.010
MgO	4.80±0.30	4.61±0.09	4.17±0.13	4.47±0.13	3.30±0.60	3.30±0.40	4.50±0.20	4.52±0.13	2.59±0.07	3.19±0.06	3.36±0.17
Na_2O	3.12±0.23	6.17±0.88	6.59±0.26	6.35±0.24	5.96±0.30	7.64±0.49	3.14±0.25	2.81±0.06	6.95±0.06	3.26±0.07	3.12±0.07
K_2O	4.44±0.76	3.56±0.13	3.71±0.13	2.76±0.09	3.08±0.76	2.44±0.22	3.68±0.33	3.99±0.18	2.10±0.05	2.33±0.09	2.54±0.12
$CaCO_3$*	43.3±6.7	63.8±0.5	63.8±1.2	61.8±1.0	73.5±5.2	83.8±1.0	46.3±3.0	40.5±1.0	78.3±0.5	47.0±0.5	43.3±1.7
C_{org}	ND	0.21	0.26±0.03	0.24±0.02	0.24	0.10	1.95±0.08	1.62	0.23	3.70±0.10	2.61
S	0.09±0.02	0.19±0.02	0.21±0.02	0.22±0.01	0.21±0.02	0.32±0.03	0.43±0.20	0.39±0.05	0.46±0.01	1.44±0.04	0.54±0.14
Trace elements (ppm)											
Li	97±12	76±3	63±5	57±1	60±15	45±8	87±2	92±3	41±4	65±1	79±3
Zr	178±12	313±16	353±41	217±13	174±41	92±25	136±9	118±2	106±4	109±1	109±5

Turbidite tops and bottoms excluded; ND, not determined; standard deviations quoted as σ_n.
*Values not recalculated on a CFB.

et al., 1987). Oxidation of sediment results in the discoloration of turbidite summits from olive green to light brown, and causes the redistribution of Mn and many trace elements (JARVIS & HIGGS, 1987). Consequently, the C_{org} content of the upper portions of some turbidites has been reduced to very low levels (JARVIS & HIGGS, 1987; DE LANGE et al., 1987[a]), although in most cases the C_{org} content of the lower portion reflects the original composition. Despite these modifications, turbidites of the MAP are characterised by distinctive primary C_{org} contents which may also be used in their identification and correlation (KUIJPERS & WEAVER, 1985). In addition, the statistical approach seems to be able to distinguish organic-rich turbidites even if the C_{org} content has decreased.

TABLE 5-4. Geochemistry of pelagite groups in core MD10 recalculated on a carbonate-free basis.

Element	Pelagite group		
	P1 (n=2)	*P2* (n=9)	*P3* (n=9)
Major elements (%)			
TiO_2	0.48±0	0.83±0.26	0.84±0.18
Al_2O_3	9.9±1.0	15.7±5.0	15.0±2.4
Fe_2O_3	3.44±0	6.33±2.04	6.36±1.37
MnO	0.730±0.042	0.201±0.033	0.059±0.008
MgO	3.24±0.35	3.40±0.88	3.23±0.52
Na_2O	9.02±0.35	4.91±0.76	3.18±0.39
K_2O	2.39±0.23	3.06±0.78	3.10±0.56
$CaCO_3$*	82.9	57.8	17.5
C_{org}	ND	ND	ND
S	0.43±0.03	0.33±0.13	0.16±0.06
Trace elements (ppm)			
Li	66±3	69±28	67±19
Zr	102±2	139±62	158±33

Pelagite groups based on carbonate contents: P1, >75% $CaCO_3$; P2, 40-75% $CaCO_3$; P3, < 40% $CaCO_3$. ND, not determined; standard deviations quoted as σ_n. * Values not re-calculated on a CFB.

Our analyses (Tables 5-3,4,5; Appendix 5-1) indicate that turbidites of the MAP contain 25-86% $CaCO_3$ and 0.02-1.96% C_{org} (Fig. 5-6), and that individual turbidites in both cores contain very similar carbonate and organic carbon contents. Five turbidites (j, l, l_0, r, s_2) are distinguished by containing extremely high carbonate contents (>75% $CaCO_3$), and a second group (a, a_1, d, e, f, h, s, s_1, t and u) is characterised by high (> 0.3% C_{org}) levels of organic carbon (i.e. above that occurring in oxidising pelagic sediments). Remaining turbidites exhibit moderate carbonate (≈ 50%) and low organic carbon (< 0.3%) contents.

The extreme range of carbonate contents in MAP turbidites makes it difficult to assess variations in the distributions of other elements. All elements, therefore, have been recalculated (Tables 5-3,4,5) on a carbonate free base (CFB) or are normalised to Al (Figs. 5-7,8) in order to facilitate comparisons between turbidites. These recalculations are based on the assumption that carbonate and aluminium have no geochemical link with any of the variables. To avoid any *a priori* assumption, or other possibly subjective choices, we have chosen to use unrecalculated data for the statistical approach.

The CFB data demonstrate that most of the turbidites which do not fall into the calcareous or organic-rich group (Fig. 5-7) are characterised by high average Ti (1.5% TiO_2), compared with the other turbidites which have only moderate Ti contents (0.75% TiO_2). The group of Ti-rich turbidites (b, b_1, d_1, g_1, i, n, o, f) is further distinguished by high Zr and low Li concentrations (Fig. 5-7; JARVIS & HIGGS, 1987; DE LANGE et al.,

TABLE 5-5. Geochemistry of major turbidites in core D10688 recalculated on a carbonate-free basis*.

Element	Turbidite						
	a (n=3)	*a*$_1$ (n=4)	*b* (n=6)	*b*$_1$ (n=2)	*d* (n=2)	*d*$_1$ (n=2)	*e* (n=17)
Major elements (%)							
TiO_2	0.81±0.02	0.81±0.01	1.95±0.05	2.32±0	0.78±0.01	1.34±0.03	0.83±0.03
Al_2O_3	15.6±0.1	19.3±0.5	15.1±0.4	14.0±0.1	18.2±0.1	15.1±0.3	16.7±0.6
Fe_2O_3	6.07±0.04	7.12±0.31	8.80±0.26	8.52±0.10	7.38±0.31	7.13±0.03	5.94±0.32
MnO	0.150±0.020	0.130±0.100	0.230±0.030	0.203±0.006	0.350±0.310	0.250±0.010	0.160±0.010
MgO	3.94±0.08	2.79±0.03	4.81±0.12	5.03±0.06	4.44±0.01	4.19±0.03	4.26±0.13
Na_2O	6.57±0.53	3.87±0.36	7.23±0.53	5.30±0.31	3.35±0.23	6.49±0.13	4.73±0.36
K_2O	3.00±0.01	2.20±0.03	2.62±0.08	2.23±0.01	4.06±0.06	3.08±0.04	3.49±0.14
$CaCO_3$*	58.2±0	24.5±5.2	53.5±0.7	48.9±6.2	38.0±0.2	55.9±0.9	53.0±1.1
C_{org}	1.24±0.22	1.52±0.49	0.43±0.04	ND	0.44±0.05	0.54±0	1.19±0.51
S	ND	ND	(0.30)	ND	(0.18)	ND	(0.64)
Trace elements (ppm)							
Li	72±1	94±2	52±2	32±1	89±1	68±3	87±7
Zr	184±28	139±7	472±23	486±36	118±6	271±43	164±25

Element	Turbidite						
	f (n=23)	*g* (n=4)	*g*$_1$ (n=2)	*h* (n=7)	*i* (n=2)	*j* (n=3)	*k* (n=4)
Major elements (%)							
TiO_2	0.70±0.01	1.41±0.02	0.97±0.01	0.80±0.02	1.59±0.13	0.75±0.10	0.74±0.02
Al_2O_3	16.1±0.05	16.2±0.2	17.7±0.2	17.1±0.4	16.1±0.3	14.4±0.12	18.0±0.8
Fe_2O_3	5.82±0.34	7.11±0.16	6.13±0.25	5.98±0.64	7.95±0.16	5.76±0.09	8.10±0.33
MnO	0.130±0.010	0.280±0.010	0.120±0	0.170±0.010	0.250±0.020	0.610±0	0.160±0.010
MgO	3.63±0.14	3.77±0.10	3.37±0.10	3.66±0.10	4.18±0.12	3.63±0.06	3.10±0.05
Na_2O	4.81±0.21	7.13±0.32	3.61±0.17	3.30±0.15	5.66±0.27	6.51±0.48	3.40±0.12
K_2O	2.80±0.10	3.31±0.03	3.38±0.01	2.88±0.07	2.96±0.08	2.85±0.03	2.69±0.06
$CaCO_3$*	50.0±1.1	57.4±1.1	32.7±1.8	46.6±1.4	53.9±2.5	81.4±0.4	47.1±2.9
C_{org}	1.40±0.64	0.42±0.05	ND	ND	0.39	0.59	ND
S	(0.80)	(0.18)	ND	ND	ND	ND	ND
Trace elements (ppm)							
Li	84±6	59±4	81±0	86±4	80±2	60±2	97±9
Zr	132±10	628±115	211±19	142±10	382±17	140±21	126±2

Turbidite tops and bottoms excluded; ND, not determined; standard deviations quoted as σ_n; sulphur values in parentheses based on single determinations only. *Values not recalculated on a CFB.

1987[a]), when recalculated on a CFB (Tables 5-3,4,5). Turbidites which do not clearly fall into the calcareous, C_{org}-rich or Ti-rich groups (e_1, g_1, k, l_1, l_2, l_3, q) are all thin (- 70 cm). The primary sediment of these units, therefore, may have been contaminated by mixing with pelagic and other sediment during transit of the turbidity current across the ocean floor, or has been modified subsequently by bioturbation and/or diagenetic processes. The relationship between the minor turbidites and the main three groups of turbidites can best be demonstrated on an expanded triangular diagram (Fig. 5-9). The parameters used in the construction of this diagram were chosen to give maximum separation between the three turbidite groups. Each of the corners of the triangle shows the element ratio that is most characteristic for one of the three main groups :

Calcareous turbidites are distinguished by their high $CaCO_3/Fe_2O_3$ ratios

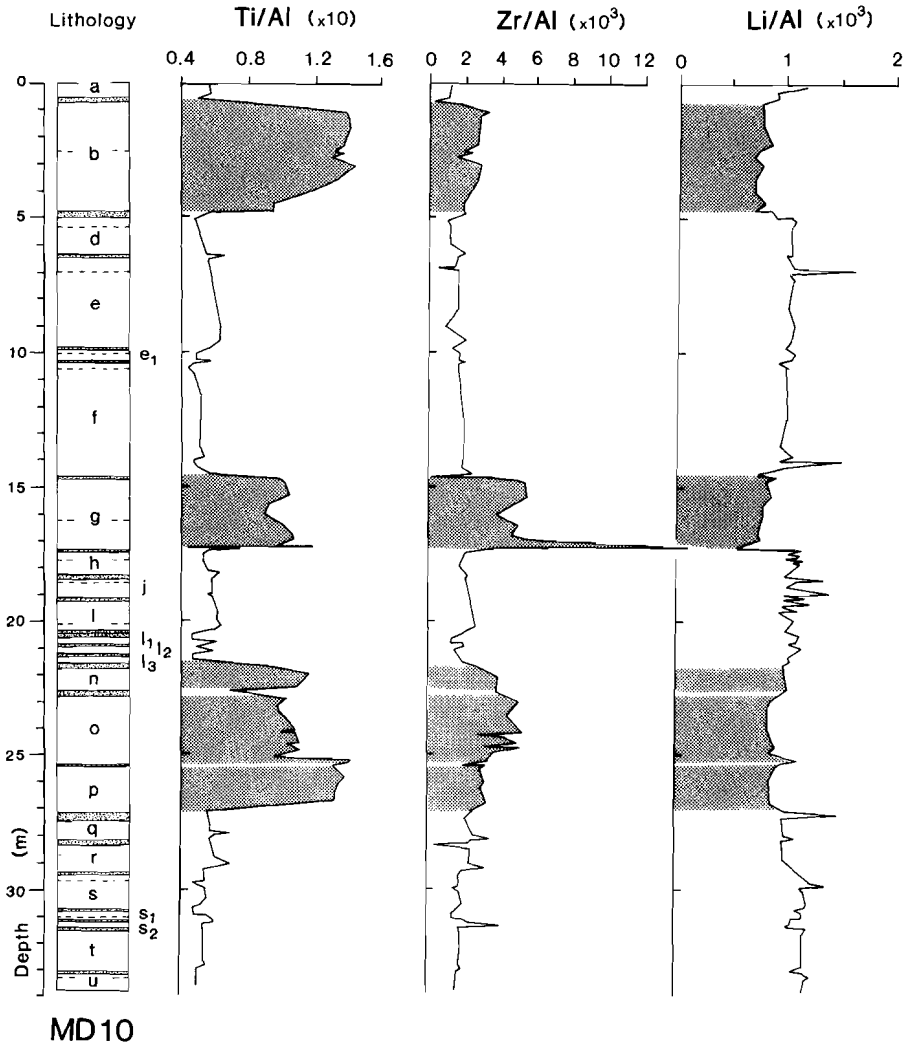

Fig. 5-7. The Ti/Al, the Zr/Al ratio and the Li/Al ratio versus depth for core MD10. Stippled units are 'volcanic' turbidites (see text for discussion). For turbidite lettering see caption of Fig. 5-4.

(Fig. 5-9). The carbonate in these turbidites is essentially of pelagic origin, dominantly coccolith with subordinate foraminiferal calcite (WEAVER & KUIJPERS, 1983; KUIJPERS et al., 1984[a]; SEARLE et al., 1985).
The distribution of Fe in pelagic sediments is predominantly related to detrital minerals, where the area is in close proximity to an active sea-floor hydrothermal system (e.g. JARVIS, 1985). This is a predictable consequence of the highly insoluble nature of Fe under oxic conditions. Evidence from both MAP pore waters (DE LANGE, 1984[a]; WILSON et al., 1986)

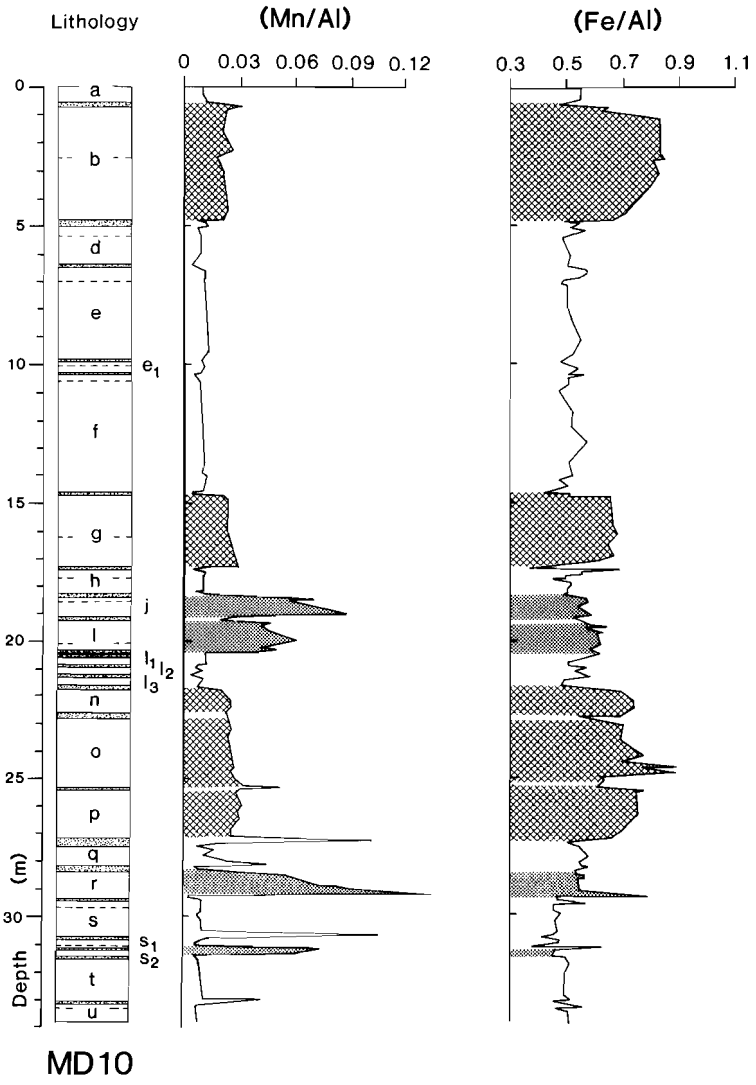

Fig. 5-8. The Mn/Al ratio and the Fe/Al ratio versus depth for core MD10. Stippled areas are 'calcareous' turbidites, and the cross-hatched areas are 'volcanic' turbidites. Note the high manganese contents of all calcareous turbidites; additional peaks are pelagic carbonate ooze. Volcanic turbidites have high iron and intermediate manganese contents. Manganese and iron are lowest in the 'organic-rich' turbidites (a, d, e, f, h, s, s_1, t, u).

and sediments (JARVIS & HIGGS, 1987) indicates that there is limited redox-driven relocation of Fe within organic-rich turbidites during early diagenesis. The proportion of the total Fe affected by these processes, however, is insignificant when the bulk composition of the sediment is considered (Fig. 5-8). The $CaCO_3/Fe_2O_3$ ratio, therefore, strongly

differentiates between pelagic carbonates and those sediments containing a significant proportion of detrital clay minerals and other siliciclastic components.

Organic turbidites are represented by high S/MnO ratios (Fig. 5-9). This is because S and Mn have an antipathetic relationship during early diagenesis of organic-rich sediments (BERNER, 1970; 1980[b]; 1981; 1982). Anoxic conditions are established rapidly in these lithologies, and consequently S is fixed as sulphides during sulphate reduction, thereby producing elevated S concentrations in the sediment. Prior to sulphate reduction Mn is redissolved and diffuses upwards towards the sediment/water interface, and is therefore removed from the older sediment. Consequently, upon redeposition the sediments of these organic-rich turbidites contain relatively low concentrations of Mn, and relatively high concentrations of S. It must be noted, however, that these relationships may be modified by the complex behaviour of Mn in MAP turbidites. Firstly, although pore-water data (DE LANGE, 1984[a]; WILSON et al.,1985; 1986; THOMSON et al., 1986; 1987) confirm that Mn is remobilised in some turbidites, most of this Mn is likely to be reprecipitated in the upper part of the same turbidite by oxygen diffusing downwards from the overlying sea water (WILSON et al., 1985; JARVIS & HIGGS, 1987). These Mn concentrations, however, are then themselves dissolved and relocated higher in the sequence after the turbidite has been buried by deposition of a subsequent turbidity flow (THOMSON et al., 1987). Manganese, therefore, displays a sequence of dissolution-reprecipitation events which ultimately control the Mn content of the sediment.

A further complication results from the interaction of Mn with calcite. Once in solution, some Mn^{2+} is sorbed by calcite surfaces and is not re-mobilised later (THOMSON et al., 1986; JARVIS & HIGGS, 1987; MIDDELBURG & DE LANGE, 1988[b]). This process results in higher than average Mn/Al contents in carbonate-rich turbidites (Fig. 5-8) and therefore increases the separation of the calcareous and organic-rich groups in Fig. 5-9.

The history of S in MAP turbidites is also not entirely clear. There is no evidence from pore-water sulphate concentrations (DE LANGE, 1984[a]) that sulphate reduction is currently active in the cored part of the succession. Nevertheless, metastable black discolorations associated with faint H_2S odours, which are detectable when the cores are split, occur in the upper parts of some organic-rich turbidites (KUIJPERS et al., 1984[a]; JARVIS & HIGGS, 1987). These features suggest that restricted local sulphate reduction has once occurred, or is still occurring at these levels. Therefore, it seems probable that the high S concentrations in the organic-rich turbidites are predominantly relic features, inherited from the primary sediment prior to its deposition as a turbidite.

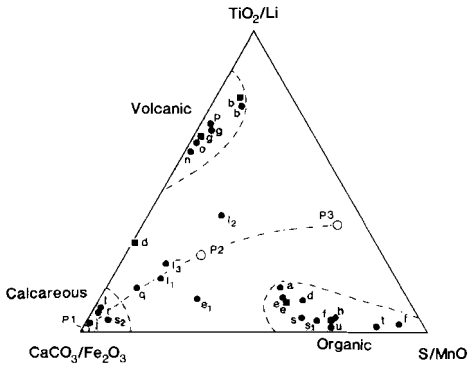

Fig. 5-9. Expanded triangular diagram of MAP turbidite average compositions. 'Calcareous', 'organic' and 'volcanic' turbidites all fall in distinct fields (stippled areas).(see text for discussion).

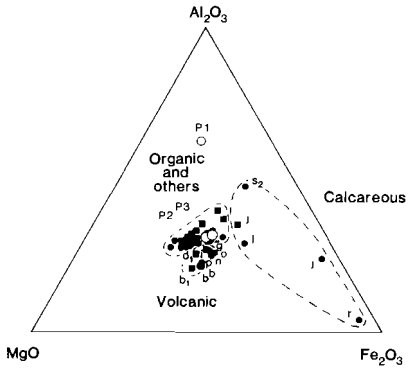

Fig. 5-10. Expanded triangular diagram of Al_2O_3-MgO-Fe_2O_3 contents. For symbols and conventions see below.

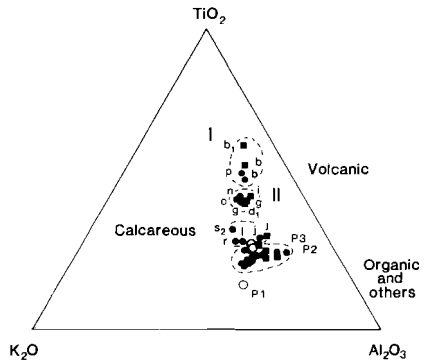

Fig. 5-11. Expanded triangular diagram of TiO_2-K_2O-Al_2O_3 contents. For symbols and conventions see below.

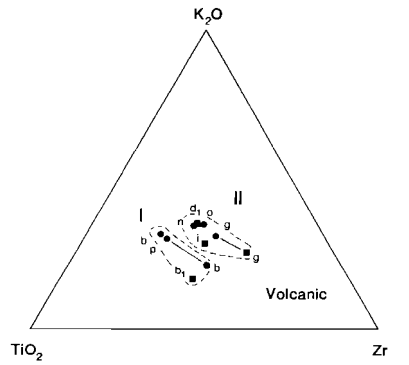

Fig. 5-12. Expanded triangular diagram of K_2O-TiO_2-Zr contents. For symbols and conventions see below.

Figs. 5: 9-12. The averages of MD10 turbidites (Table 5-3) are indicated by full circles and the averages of D10688 turbidites (Table 5-5) by full squares. Some D10688 turbidites could not be plotted on this Fig. because the sulphur data were not available. The positions of the circles and squares represent turbidite compositions; adjacent letters refer to Weaver's turbidite designations (see caption of Fig. 5-4). Large open circles represent averages of : high-carbonate (P1, more than 75% $CaCO_3$), medium-carbonate (P2, 40-75% $CaCO_3$) and low-carbonate (P3, less than 40% $CaCO_3$) pelagites (Table 5-4). The broken line joining these values indicates the position of intermediate compositions. Element ratios are plotted using the following formulae :

$$A^* = \frac{A - A^{min}}{A^{max} - A^{min}} \qquad A^c = \frac{A^*}{A^* + B^* + C^*}$$

Where A, B and C are the three element ratios, A^* is the recalculated value and A^c is the plotted value. A^{min} is 0.99 times the minimum concentration of A in cores MD10 and D10688; A^{max} is the maximum value of A in the cores. Plotted values of B and C are calculated in the same way.

Despite these modifications of the normal behaviour of S and Mn in sediments of organic-rich turbidites, it is apparent that all C_{org}-rich MAP turbidites are tightly clustered in the S/Mn corner of the triangular diagram (Fig. 5-9). This confirms the validity of this parameter as a means of distinguishing between turbiditic groups.

Volcanic-type turbidites. Separation of the volcanic-type turbidites is enhanced by plotting TiO_2/Li ratios (Fig. 5-9), because Li is an incompatible element and is most depleted in basalt, whereas TiO_2 has maximum abundance in basalts. This inverse variation of Ti and Li in volcanic-type turbidites is clearly visible in Fig. 5-7. (see also Tables 5-3,4,5. The high Ti content of these sediments exceeds that, which can be attributed to the clay mineral component (DEER et al., 1962; WEAVER & POLLARD, 1973). These turbidites contain a high proportion of igneous material (see below).

Three groups of pelagic sediments are also plotted in Fig. 5-9. These are average compositions of High-carbonate (P1, >75% $CaCO_3$), medium carbonate (P2, 40-75% $CaCO_3$), and low carbonate (P3, <40% $CaCO_3$) pelagites. The compositions of these pelagites (Table 5-4) can then be directly compared with those of the turbidites.

The high-carbonate pelagites (P1) fall in the $CaCO_3/Fe_2O_3$ corner of the triangular diagram (Fig. 5-8) close to the position of the calcareous turbidites. The other groups of pelagites (P2, P3) lie in the lower half of the diagram and are clearly distinct from the main turbidite groups. It is not clear if this deviation of the less-calcareous pelagites (P2, P3) results from a lower sedimentation rate and consequently a more intense mixing with turbiditic material (caused by bioturbation), or if it results from more intense diagenetic changes (such as carbonate dissolution).

Some turbidites (d, e_1, l_1, l_3 and q) evidently fall outside the three distinct turbidite areas; these turbidites are all relatively thin.

In general, turbiditic averages from core MD10 (Fig. 5-9, filled circles) plot close to averages for corresponding turbidites in core D10688 (Fig. 5-9, filled squares). A notable exception is turbidite d from core D10688 which falls on the opposite side of the diagram from the same turbidite in core MD10 (Fig. 5-9). Turbidite d is very thin in core D10866 (Fig. 5-4[a]). As a result C_{org} and S have been completely oxidised during early diagenesis by diffusion of seawater oxygen, and now these elements are only present at refractory levels (Table 5-5). In addition, relocation of Mn during the oxidation process has produced a concentration of Mn oxi-hydroxides in the upper part of the bed (JARVIS & HIGGS, 1987). This results in a high average Mn concentration in the unit (Table 5-5). Extreme diagenetic modification, therefore, causes turbidite d in core D10866 to plot away from other members of its group (Fig. 5-9). This

specific phenomenon of oxidation and provenance will be discussed in more detail in the section on *statistical approach.*

Of course, the intensity of such a postdepositional modification is also dependent of the time interval between the deposition of two consecutive turbidites. Therefore, some thin turbidites may show all the characteristics of oxidised organic-rich turbidites, whereas some others may not.

Compositional differences between the three turbidite groups are also apparent from the distributions of other elements. All three groups are again clearly defined on an Al_2O_3-MgO-Fe_2O_3 triangular diagram (Fig. 5-10). Volcanic turbidites are here differentiated by their high Fe and Mg contents, which are a consequence of the higher percentages of ferromagnesian minerals which they contain. Calcareous turbidites have the lowest Mg concentration, but show a wide range of Fe contents (Fig. 5-10). Remaining turbidites and most pelagites (P2, P3) have intermediate positions on the Al_2O_3-MgO-Fe_2O_3 diagram. The compositions of pelagic carbonate oozes (P1), however, are distinct from all other sediments and are distinguished by low Mg and Fe concentrations relative to Al. These pelagites must contain only a small percentage of ferromagnesian minerals. Scatter on the Al_2O_3-MgO-

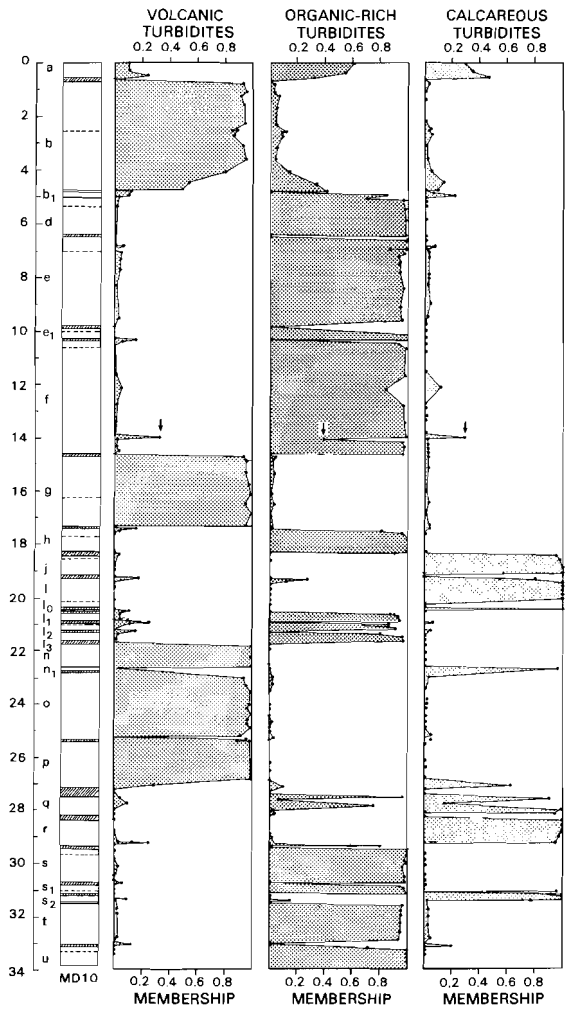

Fig. 5-13. Representation of the three groups as distinguished by the statistical analysis for samples from core MD10, MAP. 'Volcanic', 'organic-rich' and 'calcareous' turbidites are stippled on the relevant statistical logs (see text for discussion). Arrows indicate an extreme sample with a high pyrite contents.

Fe_2O_3 plot (Fig. 5-10) may be attributed to the presence of Fe (and to a lesser extent Mg) in a wide range of minerals, including silicates, oxides, oxihydroxides and sulphides. The same turbidite groups, however, are picked out more coherently on a triangular diagram of TiO_2-K_2O-Al_2O_3 (Fig. 5-11). In this plot the volcanic turbidites are characterised by high Ti and low K contents, while organic-rich turbidites have low Ti and high K concentrations. Calcareous turbidites are of intermediate composition. Most pelagites (P2, P3) are compositionally on the boundary between the calcareous and organic-rich turbidite groups on the TiO_2-K_2O-Al_2O_3 diagram (Fig. 5-11). Pelagic carbonate oozes (P1), however, are characterised by very low Ti and high K contents, and again do not fall close to the fields of other sediments.

The clustering of turbidite compositions within each group of the TiO_2-K_2O-Al_2O_3 plot (Fig. 5-11) is generally better than for the Al_2O_3-MgO-Fe_2O_3 diagram (Fig. 5-10). The former additionally distinguishes two subgroups of volcanic turbidites. Subgroup I consists of turbidites b, b_1 and p, and is distinguished from subgroup II (turbidites d_1, g, i, n, o) by higher Ti and lower K contents. It is noteworthy that, despite variations between cores MD10 and D10688, in all cases individual turbidites have very similar proportions of Ti, K and Al.

The two suites of volcanic turbidites seen in the TiO_2-K_2O-Al_2O_3 plot are also separated by a TiO_2-K_2O-Zr ternary diagram (Fig. 5-12). Additionally, however, this combination of parameters separates turbidite compositions from the core MD10 and core D10688. Where comparative data are available (turbidites b and g only), turbidites from the latter core are characterised by higher Zr contents (Tables 5-3,4,5). Some discrepancies were encountered with Zr during our interlaboratory calibration exercise, but it is considered unlikely that analytical differences could explain the large shift of compositions in Fig.5-12. The higher Zr levels in core D10688 turbidites b and g, therefore, are probably attributable to higher percentages of zircon (WEAVER & ROTHWELL, 1987) in these sediments.

Statistical approach

From all turbiditic intervals in core MD10 the chemical data of 200 samples in total have been used in a Fuzzy C-Means cluster analysis (see METHODS and see MIDDELBURG & DE LANGE, 1988[a]). Cluster validity

TABLE 5-6. Cluster validity criteria for samples from core MD10, MAP.

Number of clusters	Total data set (n=200)		Volcanic only (n=55)		Organic-rich only (n=101)	
	F	H	F	H	F	H
2	0.832	0.276	0.709	0.456	0.826	0.287
3	0.903	0.199	0.743	0.469	0.742	0.466
4	0.859	0.286	0.735	0.523	0.675	0.613
5	0.824	0.352	0.744	0.533	0.698	0.595

Run parameters : Weighting exponent (QQ) = 1.5; Norm = Diagonal norm.

criteria, both the classification entropy (H) and partition coefficient (F), strongly favour a division into three groups (Table 5-6). The cluster centres of these groups, corresponding with the average composition of each group, are given in Table 5-7. The resultant membership profiles are displayed in Fig. 5-13. The membership distribution clearly shows the different turbidites. The internal homogeneity of the turbidites is evident from the consistency of the memberships. The great similarity of samples within a turbidite and the differences between turbidites indicate the importance of provenance for the geochemical variations that are found. The results from the statistical approach applied on the whole data-set of core MD10 of the MAP (Fig. 5-13) are in general similar to those that come from the triangular diagrams (see above and Fig. 5-9. The groups of turbidites that are found, are identical for conventional and statistical approach, and only in the case of some thin turbidites differences do occur. All turbidites, except a and q, seem to have a similarity with one type only. The a and q turbidites seem to be intermediate between the calcareous and organic-rich turbidites.

TABLE 5-7. Cluster compositions for samples from core MD10, MAP.

Element	Volcanic	Organic	Calcareous
Fe (%)	2.39	2.33	0.93
Al (%)	3.32	4.50	1.45
Ca (%)	23.4	18.3	31.1
K (%)	1.08	1.48	0.52
Na (%)	1.91	1.41	1.07
Mg (%)	1.06	1.29	0.45
Ti (%)	0.36	0.24	0.09
Sr	1209	922	1344
Co	22	17	14
Ba	287	407	154
Mn	775	436	601
P	617	520	358
S	1540	3055	2208
V	67	73	27
Zn	51	63	22
Cu	73	53	83
Li	21	44	13
Zr	113	74	31
Ni	38	41	26
Y	20	21	15
Cr	57	80	24

(All in ppm, except major elements)

Nares Abyssal Plain

In the sediments from the southern NAP, the carbonate and organic carbon concentrations fluctuate to a much lesser extent than in the MAP (DE LANGE, 1986[b]; DE LANGE et al., 1987). Similar to the sediments of the MAP, no sulphate reduction could be demonstrated for the cored sediment interval in the NAP (DE LANGE, 1986[a]). Individual turbidites are mostly thin, ranging from a few cm to an exceptional 1.4 m and an average thickness of 0.3 m (Fig. 5-5). Pelagic intervals are often entirely bioturbated. The lateral continuity of turbidites seems to be very limited (KUIJPERS, 1985; KUIJPERS & DUIN, 1986; KUIJPERS et al., 1987) Lateral correlation of turbidites in the southern NAP has not been possible so far (KUIJPERS, 1985). Due to the large number of thin turbidites inter-

TABLE 5-8. Cluster validity criteria for samples from core MD60, NAP.

number of clusters	F (n=181)	H
2	0.760	0.386
3	0.609	0.656
4	0.548	0.829
5	0.504	0.970

TABLE 5-9. Cluster compositions for samples from core MD60, NAP.

Element	Cluster 1	Cluster 2
Fe (%)	5.22	3.70
Al (%)	8.56	6.78
Ca (%)	2.0	5.2
K (%)	3.03	2.47
Na (%)	2.00	1.93
Mg (%)	2.11	1.86
Ti (%)	0.46	0.38
S (ppm)	960	1510

bedded with mostly thin pelagic sections, the conventional methods which have been successfully applied to samples of the MAP, did not result in any clear conclusion. It must be noted that the visual distinction between turbidites and pelagites is often difficult to make for sediments of the southern NAP.

When the statistical approach is applied to the data-set of cores MD56 and MD60 of the southern NAP, it shows that the only possible partitioning is in 2 clusters (Table 5-8; Fig. 5-14). Although only the results from the statistical analysis of core MD60 are shown, it is important to remark that the results for core MD56 were exactly the same. The cluster centres of these groups, corresponding with the average composition of each group, are given in Table 5-9. The resultant membership profiles are displayed in Fig. 5-14.

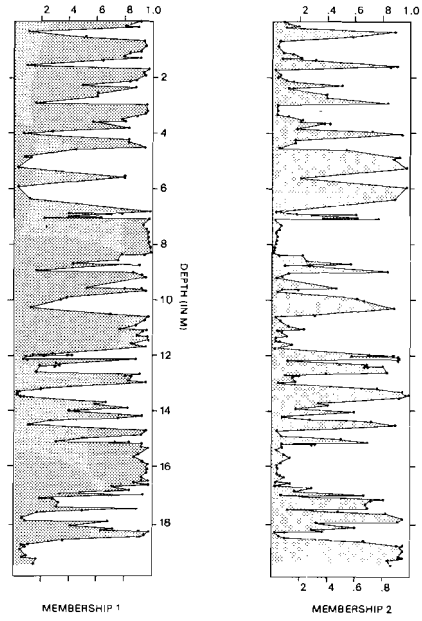

Fig. 5-14. Representation of the two groups as found by the statistical analysis for samples from core MD60, southern NAP. Conventions as in Fig. 5-13.

5-5. DISCUSSION

Madeira Abyssal Plain

The general provenance of the younger turbidites (a - k) of the MAP has been discussed previously (KUIJPERS, 1982; KUIJPERS et al., 1984[a]; WEAVER et al., 1986; WEAVER & ROTHWELL, 1987). These authors conclude from mineralogical, grain size and isopach data that the NW African continental slope is the main source area for the turbiditic sediments of the MAP. Our geochemical and statistical data, however, define three distinct compositional groups and two subgroups of turbidites, which must be related to changing sediment provenance. We will now discuss the constraints which our and other data place on the probable locations of sediment source areas.

Organic-rich turbidites (a, a_1, d, e, e_1, f, h, l_1, l_2, l_3, q, s, s_1, t, u) These turbidites are almost all characterised by having C_{org} contents of higher than 0.3%. Pyrolysis studies of organic matter in some of the

younger turbidites (DE LEEUW et al., 1982) demonstrate that most of the organics are of marine origin, with little or no terrestrial material. Some of the organic-rich turbidites (notable a, d, f, t and u ; KUIJPERS et al., 1984[a]; WEAVER & ROTHWELL, 1987; ESOPE, 1986) also contain large amounts of biogenic silica, such as diatoms and radiolarians. The relatively high proportion of preserved marine organic matter and the presence of siliceous microplankton are characteristic of sediments below areas of high surface productivity, such as those currently present under the Canary Current off the NW African Shelf. Such sediments are restricted to this environment, because high sedimentation rates are necessary for the preservation of significant amounts of C_{org} in the sediment. Elsewhere in the oceans, burial rates are low, and organic matter is rapidly oxidised on the sea floor.

Burial of labile organic matter generally results in the establishment of sulphate reducing conditions and the precipitation of sulphides. Most of the organic turbidites are characterised by high S values, and two rounded pyritic (≈ 17% FeS_2) lumps were found at the base of turbidite f in core MD10. There is no evidence of significant amounts of sulphate reduction currently active in the turbidites (DE LANGE, 1984[a]; see also Chapter 6) so that sulphides were probably redeposited with their parent sediment.

Studies of the NW African continental margin (HARTMANN et al., 1976) indicate that between 15° and 28°N lower slope sediments contain 1-2% C_{org} and upper slope sediments have 4% C_{org}. Organic carbon contents also generally increase in a southerly direction (SEIBOLD & BERGER, 1982). In the same area, the sediments also display geographical variations in carbonate content (MÜLLER, 1975), with those sediments north of 20°N containing 40-85% $CaCO_3$, while those to the south of this latitude generally contain less than 35% carbonate.

The organic turbidites of the MAP in general have less than 2% C_{org} and contain 40-50% $CaCO_3$. It can be concluded that they originate from the lower continental slope of NW Africa, north of 20°N. A single exception is turbidite a_1 which contains only 25% $CaCO_3$, and was probably derived from south of this latitude.

Isopach data for turbidites d, e and f (KUIJPERS et al., 1984[a]; WEAVER & ROTHWELL, 1987) demonstrate that these beds thicken and become finer grained towards the western part of the MAP. The thickness and grainsize of their silty bases, however, increases towards the east. This conforms with our knowledge of sediment transport pathways coming from that direction onto the MAP (Fig. 5-1).

Turbidite a_1, however, is restricted to the axial part of the MAP (KUIJPERS et al., 1984[a], KUIJPERS & WEAVER, 1985). This supports the carbonate data which indicate a different, more southerly source for that

turbidite. To a lesser extent, differences in organic carbon content between the organic turbidites may also relate to provenance. Turbidites with the highest C_{org} contents (> 1% C_{org} : a_1, f, h, s, s_1, t, u) may have been derived from more southerly or higher parts of the slope than others (a, d, e) in the group. This difference in C_{org} contents may also be caused by post-depositional diagenetic changes (see below). It is noteworthy that the statistical analysis indicates that some thin turbidites which presently contain only low amounts of C_{org} (such as l_1, l_2, l_3 and the top of d) should be classified under the organic-rich group.

TABLE 5-10. Cluster compositions for the volcanic type samples of core MD10, MAP (see discussion in text).

Element	Volcanic I	Volcanic II	Volcanic III
Fe (%)	2.08	2.28	2.58
Al (%)	2.94	3.17	3.29
Ca (%)	24.94	24.96	22.93
K (%)	0.93	1.09	1.08
Na (%)	1.76	1.84	2.29
Mg (%)	0.98	0.97	1.21
Ti (%)	0.35	0.33	0.45
Sr	1294	1269	1141
Co	16	25	23
Ba	262	291	271
Mn	843	808	723
P	603	597	634
S	846	822	1356
V	62	60	84
Zn	45	48	55
Cu	63	86	56
Li	21	22	18
Zr	96	134	91
Ni	40	36	38
Y	18	20	19
Cr	55	52	59

All in ppm, except major elements

Organic turbidites are also differentiated by their major and trace element compositions, having the lowest Fe, Mg, Ti and Zr on a CFB, and the highest Al, K, S, Cr and Li of the three turbidite groups. These differences are also reflected in the average cluster composition that is found in the statistical approach (Table 5-7; MIDDELBURG & DE LANGE 1988[a]). The increased proportion of Al and alkali metals is indicative of a continental provenance for the aluminosilicate phases, and confirms a continental slope source region suggested by other data.

The organic carbon contents of the organic-rich turbidites exhibit a large range of values; it seems reasonable therefore to search for subgroups. On cluster validity criteria (Table 5-6) a twofold sub-partitioning appears to be the most suitable. The composition of the two cluster centres is given in Table 5-10, and Figure 5-15 demonstrates the resultant membership profiles. For each turbidite the FCM clustering separates the top few samples from the rest of the turbidite. In addition, the sub-partitioning within the group of organic-rich turbidites (Fig. 5-15) contrasts sharply to the main partitioning. In the latter (Fig. 5-13) large differences between turbidites and homogeneity within each individual turbidite were found, whereas in the former the opposite occurs, namely the differences between the turbidites appear to be minor compared to the chemical variation within each turbidite. We interpret this to be the result of post-depositional alteration of the top part of organic-rich turbidites (COLLEY et al., 1984; WILSON et al., 1985). The deposition of an organic-rich turbidite generally initiates the development of a downward progressing oxidation front. The front deepens the upper oxidized layer by progressive downward oxidation of organic carbon and other reduced species

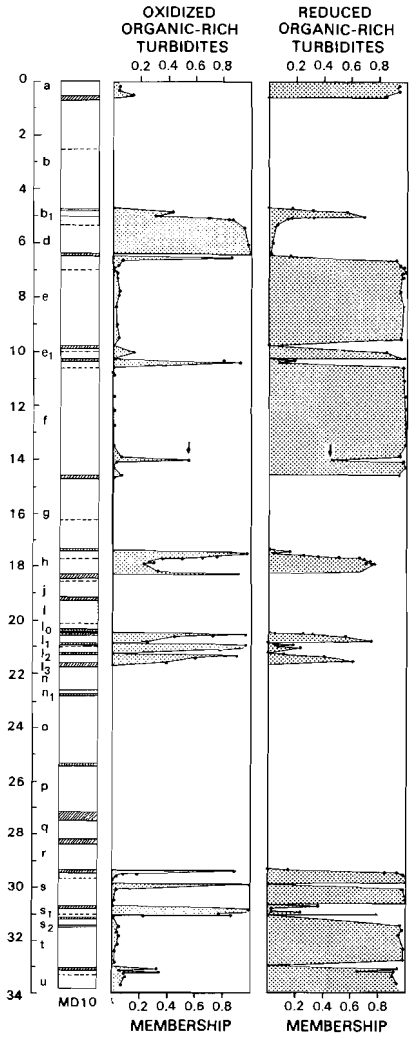

Fig. 5-15. Sub-partitioning within the organic-rich group, as found by the statistical analysis of core MD10, MAP. Conventions as in Fig. 5-13.

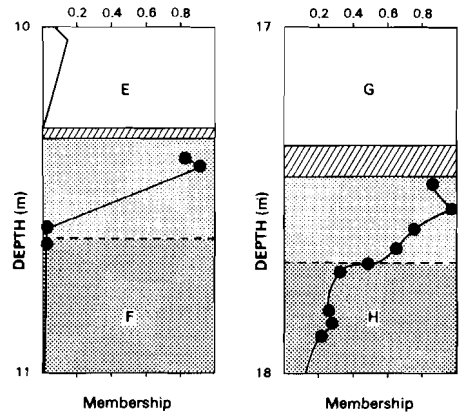

Fig. 5-16. Detailed representation of the sub-partitioning within the organic-rich group, at the colour transition in turbidites f and h in core MD10, MAP. Pelagites (hatching), oxidized interval (light stipples) and reduced interval (heavy stipples) of two 'organic-rich' turbidites are indicated. In addition the location of the samples (crosses) is shown.

('burning down'). The progress of this oxidation front is marked by a sharp colour contrast in the sediments. Upon the arrival of the next turbidite, the diffusive flux of oxidants will cease and consequently the downward penetration of the oxidation front will also cease (COLLEY & THOMSON, 1985). Relict fronts are generally marked by colour changes. The transition from samples with great similarity to cluster 1 (oxidised) to those with great similarity to cluster 2 (reduced) generally coincides with a colour change (Fig. 5-15) within a turbidite. The redox front transition of the f and h turbidites displayed in Fig.5-16 clearly shows the partitioning into oxidized (i.e. burnt down) and reduced samples. The samples in the oxidized parts of the turbidites (great similarity with cluster 1) are rich in Fe, Ti, Co, K and Al and low in Ca, Sr and S (Table 5-10). The slight decrease in Ca and Sr is believed to be due to carbonate dissolution as a result of the production of CO_2 during

organic carbon oxidation by means of oxygen (FROELICH et al., 1979; DE LANGE, 1986 a,b).
The thin turbidites (d, l_1, l_2, l_3 and s_1) are distinctive, because of their relatively low C_{org} throughout (Fig. 5-6), and their similarity with the 'burnt down' cluster (1) (Fig. 5-15). We, therefore, suggest that all labile C_{org} of these turbidites has been oxidized. This implies that redox fronts have passed down through these turbidites and may now be located in the underlying units (e.g. COLLEY & THOMSON, 1985). However, as shown in Figure 5-15, the diagenetically 'burnt down' organic-poor turbidites are still classified as organic-rich turbidites in the present approach. Notice that in the conventional approach (Fig. 5-9,10,11) the turbidites l_1, l_2 and l_3 are not recognized as organic-rich turbidites. We therefore conclude that the statistical partitioning method enables us to distinguish the original characteristics of these turbidites despite post-depositional changes.

Volcanic-rich turbidites (b, b_1, d_1, g, i, n, o, p)

These turbidites are best differentiated by their high TiO_2 and Zr contents (Table 5-3,5,7). In addition, these turbidites contain only refractory levels of organic matter (< 0.3% C_{org}) and have moderate carbonate contents of 50-60 %. The mineral compositions of turbidites b, b_1 and g have been studied previously (KUIJPERS et al., 1984[a]; GEEL & JONGERIUS, 1984; WEAVER et al., 1987). In the area around and to the north of core D10688 (Fig. 5-1), turbidites b and b_1 are characterised by centimetre to decimetre thick basal volcanoclastic sands containing less than 20% of the clay fraction (GEEL & JONGERIUS, 1984). These sands are well sorted, fine upwards and are commonly laminated. Laminations are caused by alternating layers of foraminifera-rich and heavy mineral-rich sediment. The sands fine and thin to the south and west and are absent in core MD10. The coarse nature of the basal sands make them ideally suited to heavy mineral analysis. Detailed work (GEEL & JONGERIUS, 1984) has identified euhedral-anhedral grains of clinopyroxenes (augite, titanoaugite), olivine, and volcanic glass as the dominant phases. Subsidiary minerals include amphiboles (hornblende), orthopyroxenes (hypersthene), epidote and biotite. Zircons, green tourmaline and magnetite (WENSINK, 1984) occur in the finer fractions. More general analysis of turbidites b and g (WEAVER & ROTHWELL, 1987) has identified sodic pyroxenes (e.g. aegirine) and some alkali feldspars (microcline, sanidine) in these beds. The chemistry of the volcanic glass shards in turbidites b, e (an organic turbidite) and g from core D10688 (WEAVER & ROTHWELL, 1987) indicate a trachytic-

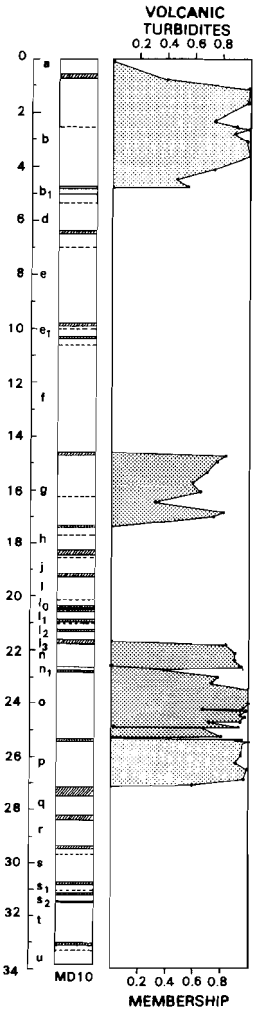

Fig. 5-17. Sub-partitioning within the volcanic group, as found by the statistical analysis of core MD10, MAP. Group I volcanic turbidites (relatively high Ti contents) in light stipples; group II volcanic turbidites (relatively high Zr and K contents) in heavy stipples.

trachyandesitic composition for the parent magma. We have observed cm-sized pebbles of pumice at the bases of the b and g turbidites in cores from the NE part of the MAP (KUIJPERS, 1982; KUIJPERS et al., 1984[a]). There is no doubt, therefore, that turbidites identified as falling within our volcanic group contain considerably more volcanogenic and other igneous material than the other turbidites in the MAP. The high proportion of basic and intermediate igneous minerals clearly explains the high Fe, Mg, Ti and Zr levels (Figs. 5-7,8,10,11) in these turbidites. The mineralogy and chemistry of the igneous material are typical of oceanic islands such as the Quaternary of the Canaries (SCHMINKE & VON RAD, 1979; WOLFF, 1985) and Madeira. These islands lie 700 km east of the MAP, close to the probable source areas for MAP turbidites, *i.e.* the NW African continental margin (EMBLEY, 1982). Volcanic material in sediments from the northern part of the MAP has been reported to originate from the Azores, located 600 km north of the MAP (MONNIOT & SEGONZAC, 1985). An island source is supported by shallow water benthonic foraminifera populations which occur in the basal sands of these turbidites (TROELSTRA, 1984).

Isopach and grain size data for turbidites b, b_1 and g (KUIJPERS, 1982; KUIJPERS et al., 1984[a]; KUIJPERS & WEAVER, 1985; WEAVER & ROTHWELL, 1987) indicate that these turbidites were emplaced from the NE part of the MAP (32°30'N). Turbidite b, however, shows an additional SE component which was probably a continuation of a debris flow which occurs in the eastern part of the MAP (31°N) (SIMM & KIDD, 1984). This debris flow was emplaced during the Sahara Slide Event, 15-16,000 years ago (EMBLEY, 1982).

Our geochemical data demonstrate that two subgroups exist within the volcanic group of turbidites (Figs. 5-11,12,17), with b, b_1 and p (subgroup I) being distinguished by higher Ti values than other volcanic turbidites (subgroup II). Using the plot of Zr/TiO_2 versus Nb/Y, which has been reported to differentiate between various magma series (WINCHESTER & FLOYD, 1977; HUFF & TURKMENOGLU, 1981) confirms that volcanic turbidites of subgroup I (b and p) are likely

to have a different source than the other volcanic turbidites of subgroup II (Fig. 5-18).

Samples from volcanic turbidites (b, g, n, n_1, o and p), 55 in total, were submitted to another FCM analysis, to look for further sub-partitioning. Cluster validity criteria for the volcanic sediments (Table 5-6) do not clearly favour a sub-partitioning into 2 or 3 clusters criteria (Table 5-6) therefore demonstrate much lower significance levels than those of the previous (main) partitioning. The cluster centres for a three-cluster model are given in Table 5-11, and the major membership profiles are shown in Figure 5-17. The different turbidites are easily recognized from the membership distributions, although some inhomogeneity within a turbidite is indicated by memberships of much less than 1. The b and p turbidites (subtype 1 and 3), which show a close resemblance, are chemically distinct from the n, n_1, o, and g (subtype 2) turbidites. The latter group is relatively enriched in Zr and poor in Ti compared to the former group (Table 5-11).

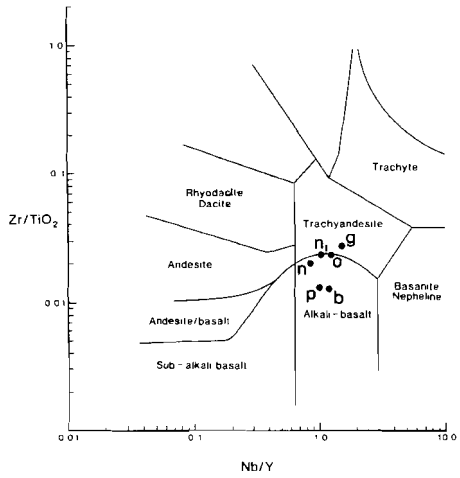

Fig. 5-18. WINCHESTER & FLOYD (1977) diagram illustrating Zr/TiO_2 versus Nb/Y of the volcanogenic turbidites of core MD10, MAP. Note the distinct grouping of b and p volcanic turbidite averages (group I) away from the group II volcanic turbidites (g,n, n_1 and o).

In addition to geochemical differences between turbidites, Zr and Ti data (Figs. 5-11, 12) indicate that turbidites b and g are compositionally distinct in core MD10 and and core D10688. The higher Zr content of these turbidites in core D10688 is related to increased proportions of zircon in the sediments, and probably reflects the increased proximity to the source of the depostis in that area, *i.e.* heavier grains settle closer to the source area. Two distinct provinces are suggested for turbidite b by GEEL & JONGERIUS (1984), namely a north-eastern area 32°N and a southern area 31°N. The basal sands of this turbidite in the north-eastern area are finer grained, contain more volcanic glass, and yield less augite and titanoaugite than those to the south. These authors suggest that Madeira

TABLE 5-11. Cluster composition of samples from the organic-rich group, from core MD10, MAP.

Element	Oxidized	Reduced
Fe (%)	2.84	2.11
Al (%)	5.32	4.05
Ca (%)	16.17	19.51
K (%)	1.76	1.34
Na (%)	1.39	1.42
Mg (%)	1.47	1.20
Ti (%)	0.28	0.21
Sr	817	990
Co	24	14
Ba	348	453
Mn	469	417
P	558	498
S	3027	3893
V	83	68
Zn	73	59
Cu	55	49
Li	50	40
Zr	85	66
Ni	47	37
Y	22	20
Cr	91	76

All in ppm, except major elements

is the main source area for the north-eastern province, while the Canary Islands provide the source for the southern province. These different provenances might also explain the differences in the b and g turbidites between the two cores studied here, but this suggestion cannot be confirmed without further data.
Centimetre-sized phosphorite nodules have been found in the basal part of the b turbidite (KUIJPERS, 1982; KUIJPERS et al., 1984[a]) in cores taken to the north of D10688. In addition, relatively large quantities of apatite-associated P are found in all of the volcanic turbidites (DE LANGE, unpublished data). The occurrence of phosphates in these turbidites clearly indicates the addition of a continental shelf/upper slope-derived component to the sediment (CRONAN, 1980).

Calcareous turbidites (j, l, l_o, r, s_2)

These turbidites are characterised by very high carbonate contents (>75% $CaCO_3$), but they also have distinctive major and trace element compositions (Figs. 5-9,10,11; Tables 5-3,5,7). They exhibit marginally higher Ti contents than the organic-rich turbidites, but are distinct from the volcanic group (Fig. 5-9). The calcareous turbidites show some affinities to MAP pelagic sediments (Figs. 5-9,10,11). Previous workers (WEAVER & ROTHWELL, 1987) have studied only the youngest of the calcareous turbidites (j). Isopach data for this turbidite indicate that it is thickest in core MD10, where it contains a 24 cm thick basal layer of foraminiferal sand. The turbidite thins to the north and east, indicating a western or south-western provenance.
In the MAP, turbidites are absent on the small abyssal hills, which exhibit continuous successions of pelagic clays and marls (average carbonate contents <60%). These hills have remained within the lysocline for most of their recent history, and have never accumulated sufficient carbonate to be potential source areas for the calcareous turbidites (carbonate contents >75%).
However, approximately 350 km west of the MAP, the Great Meteor - Cruiser Seamount Chain (Fig. 5-1) rises to within 300 m of the ocean surface. These seamounts are currently accumulating thick sequences of carbonate ooze, providing ample source material for MAP calcareous turbidites (cf. WEAVER & ROTHWELL, 1987). Possible flow path-ways for these turbidites have recently been demonstrated (SCHÜTTENHELM et al., 1988). It must be concluded that the calcareous turbidites are the only group with a western oceanic source, all other turbidites being derived from the margins of NW Africa, to the east.

Nares Abyssal Plain

The correlation of turbidites in the southern NAP presents major problems because of their mixed origin, their limited thickness and the fact that their deposition was probably more sensitive to small differences in topography: it seems as if depth variations of only a few metres are sufficient to prevent deposition of most turbidites on the slightly elevated areas. Sediments in cores taken within a mile of each other at almost identical water depths, range from mainly pelagic to mainly turbiditic (KUIJPERS, 1985; DE LANGE 1986[a], 1986[b]).
It is surprising that two abyssal plains, consisting mainly of turbiditic sediments, can be different from each other in so many respects. Apart from the earlier mentioned limited thicknesses of turbidites, another complication arises from the large range of inferred average sedimentation rates for the southern NAP. These have been reported to range from less than 0.5 cm/1000 yrs to more than 50 cm/1000 yrs (KUIJPERS et al., 1987).
Only by means of the more sophisticated statistical approach have we been able to distinguish different groups in the sediments from the southern NAP (Table 5-8,9). It must be noted, that for the samples from the southern NAP we have used all (e.g. turbiditic and pelagic) samples for the FCM cluster analysis. There is a clear partitioning into two groups; the main difference between these groups coming from the elements Ca, S and Fe. In cluster 2 the first two elements are relatively enriched, which might represent the turbiditic group, whereas the group 1 cluster with a lower Ca content (< 4% $CaCO_3$) may represent the pelagic samples.
The total absence of a clear partitioning for the turbiditic sediments of the southern NAP is a clear illustration of the large differences that exist between sediments from both areas (*i.e.* the MAP and the NAP).

5-6. CONCLUSIONS

Madeira Abyssal Plain

Geochemical data (both by conventional and statistical approach) from core MD10 and core D10688 from the MAP indicate that late Quaternary turbidites in this area fall into three distinct compositional groups :

1. *Calcareous turbidites* (j, l, l_o)

These sediments of more than 75% carbonate contents are thought to originate from the Great Meteor - Cruiser Seamount chain to the west of the MAP.

2. *Organic-rich turbidites* (a,a_1, d, e, f, h, s, s_1, u)

High percentages of organic matter and diatoms / radiolarians and the occurrence of a high sulphur content indicate that this sediment was derived from a highly productive area of the NW African Continental Margin. Organic carbon and carbonate contents suggest that this area was the lower continental slope north of 20°N, although turbidite a_1 probably originated from south of this latitude.

Statistical sub-partitioning within the organic-rich group clearly distinguishes between oxidised and reduced parts of individual turbidites, and even classifies the entirely 'burnt down' organic-rich turbidites in the "organic-rich" provenance group.

3. *Volcanic turbidites* (b, b_1, g, i, n, o, p)

The distinctive geochemistry of the volcanic turbidites is caused by the increased abundance of igneous material in these sediments. Heavy mineral suites, feldspar compositions and the geochemistry of volcanic glasses all indicate that this material was derived from an oceanic island source, probably the Canaries, and Madeira / Azores. The presence of derived phosphorite nodules in some turbidites of this group, however, indicates the addition of a continental shelf / upper slope component to the sediment.
Within the volcanogenic group two main sub-groups can be distinguished, relating to different source areas.

Nares Abyssal Plain

The interpretation of the geochemical results for sediments of the southern NAP is much more complicated. Visual distinction between turbidites and pelagites is often difficult to make, and lateral continuity of individual turbidites has not been found.
For sediments of the southern NAP, only the partitioning done by statistical analysis led to two distinct groups, probably representing pelagic and turbiditic sediments.
Therefore, in contrast to the well-defined turbiditic sediments of the MAP, at present it seems not possible to recognize separate provenance groups for the NAP turbidites.
The total absence of such a partitioning is a clear illustration of the large differences that exist between the turbiditic material from both study areas (*i.e.* the MAP and the NAP).

APPENDIX 5-1

TABLE 5-1. Geochemistry of major turbidites in core MD10.

Element	Turbidite											
	a (n=3)	*b* (n=13)	*d* (n=6)	*e* (n=13)	e_1 (n=2)	*f* (n=14)	*g* (n=9)	*h* (n=8)	*j* (n=3)	*l* (n=5)	l_1 (n=5)	l_2 (n=5)
Major elements (%)												
TiO_2	0.32±0.02	0.72±0.03	0.45±0.02	0.39±0.01	0.37±0.01	0.37±0.02	0.51±0.01	0.38±0.02	0.09±0.01	0.14±0.01	0.43±0.03	0.60±0.05
Al_2O_3	6.60±0.70	6.50±0.20	10.1±0.2	7.40±0.20	8.50±0.20	8.30±0.50	5.90±0.10	8.30±0.40	1.80±0.20	2.60±0.10	9.70±0.30	11.8±0.6
Fe_2O_3	2.59±0.14	3.84±0.13	4.07±0.10	2.99±0.10	3.61±0.11	3.81±0.60	2.93±0.07	3.13±0.20	0.76±0.09	1.20±0.09	4.16±0.25	4.94±0.31
MnO	0.051±0.001	0.096±0.005	0.058±0.003	0.058±0.002	0.060±0.004	0.052±0.002	0.101±0.003	0.065±0.006	0.098±0.0004	0.084±0.000	0.078±0.002	0.070±0.003
MgO	1.69±0.08	2.11±0.08	2.75±0.10	2.03±0.03	2.19±0.15	1.84±0.10	1.53±0.02	1.96±0.10	0.53±0.03	0.70±0.03	2.37±0.05	2.41±0.13
Na_2O	3.22±0.17	3.24±0.16	1.97±1.91	2.12±0.04	1.83±0.04	2.05±0.07	2.40±0.05	1.80±0.05	1.18±0.04	1.40±0.03	1.78±0.05	1.94±0.12
K_2O	1.38±0.10	1.21±0.05	2.11±0.22	1.46±0.09	1.27±0.21	1.80±0.26	1.22±0.01	1.50±0.18	0.42±0.04	0.61±0.03	2.25±0.14	2.48±0.20
CaO	31.5±1.2	29.3±0.5	21.5±0.6	28.6±0.8	28.7±0.6	25.4±1.3	34.2±0.4	26.9±0.8	48.1±0.3	45.4±0.6	27.9±1.5	21.5±2.4
C_{org}	0.58	0.19±0.03	0.71±0.04	0.70±0.14	ND	0.98±0.03	0.06±0.01	1.10±0.08	0.02±0.00	0.03±0.01	0.13	0.28
S	0.22±0.01	0.13±0.01	0.15±0.05	0.20±0.03	0.08±0.00	0.95±0.50	0.09±0.00	0.38±0.02	0.06±0.01	0.06±0.00	0.06±0.00	0.07±0.01
Trace elements (ppm)												
Li	28±2	20±0	52±1	40±2	44±0	40±3	18±2	44±3	10±1	14±2	50±1	58±3
Zr	41±3	83±5	67±4	61±5	78±0	75±8	147±6	83±6	21±3	34±4	79±7	112±10

Element	Turbidite										
	l_3 (n=5)	*n* (n=3)	*o* (n=11)	*p* (n=9)	*q* (n=4)	*r* (n=5)	*s* (n=8)	s_1 (n=8)	s_2 (n=2)	*t* (n=8)	*u* (n=7)
Major elements (%)											
TiO_2	0.48±0.08	0.57±0.01	0.55±0.03	0.63±0.03	0.18±0.05	0.08±0.01	0.38±0.02	0.43±0.01	0.10±0.00	0.30±0.01	0.35±0.02
Al_2O_3	11.2±1.4	6.20±0.30	5.90±0.20	5.50±0.10	3.60±1.00	1.60±0.30	8.30±0.50	10.1±0.2	1.90±0.00	6.30±0.10	7.80±0.40
Fe_2O_3	4.37±0.74	3.38±0.08	3.08±0.28	3.06±0.11	1.56±0.42	0.68±0.11	3.01±0.21	3.39±0.10	0.66±0.01	2.37±0.03	2.94±0.17
MnO	0.070±0.005	0.101±0.001	0.120±0.010	0.115±0.005	0.047±0.003	0.064±0.001	0.061±0.005	0.063±0.005	0.089±0.006	0.049±0.001	0.058±0.006
MgO	2.72±0.17	1.69±0.03	1.51±0.05	1.71±0.05	0.87±0.16	0.53±0.06	2.42±0.11	2.69±0.08	0.56±0.02	1.69±0.03	1.91±0.10
Na_2O	1.77±0.13	2.26±0.32	2.39±0.09	2.43±0.09	1.58±0.08	1.24±0.08	1.69±0.13	1.67±0.04	1.51±0.01	1.73±0.04	1.77±0.04
K_2O	2.52±0.43	1.31±0.05	1.34±0.05	1.05±0.03	0.82±0.20	0.39±0.04	1.98±0.18	2.38±0.11	0.45±0.01	1.24±0.05	1.44±0.07
CaO	24.3±3.8	35.5±0.3	35.7±0.7	34.6±0.6	41.2±2.9	47.0±0.6	25.9±1.7	22.7±0.6	43.9±0.3	26.3±0.3	24.3±1.0
C_{org}	ND	0.08	0.09±0.01	0.09±0.00	0.06	0.02	1.05±0.04	0.96	0.05	1.96±0.05	1.48
S	0.05±0.01	0.07±0.01	0.08±0.01	0.09±0.00	0.06±0.00	0.05±0.00	0.23±0.11	0.23±0.03	0.10±0.00	0.76±0.02	0.31±0.08
Trace elements (ppm)											
Li	55±7	28±1	23±2	22±0	16±4	7±1	47±1	55±2	9±1	34±1	45±2
Zr	101±7	115±6	128±15	83±5	46±11	15±4	73±5	70±1	23±1	58±1	62±3

Turbidite tops and bottoms excluded; ND, not determined; standard deviations quoted as σ_n.
*Values not recalculated on a CFB.

APPENDIX 5-2.

TABLE 5-2. Geochemistry of major turbidites in core D10688 recalculated on a carbonate-free basis*.

Element	Turbidite						
	a (n=3)	*a*$_1$ (n=4)	*b* (n=6)	*b*$_1$ (n=2)	*d* (n=2)	*d*$_1$ (n=2)	*e* (n=17)
Major elements (%)							
TiO_2	0.34±0.01	0.63±0.05	0.91±0.02	1.19±0.0	0.48±0.01	0.59±0.02	0.39±0.01
Al_2O_3	6.51±0.05	14.6±1.4	6.99±0.10	7.20±0.10	11.3±0.3	6.69±0.25	7.82±0.29
Fe_2O_3	2.54±0.02	5.40±0.60	4.09±0.11	4.35±0.05	4.58±0.19	3.15±0.07	2.79±0.16
MnO	0.061±0.007	0.105±0.082	0.105±0.013	0.104±0.031	0.217±0.189	0.109±0.002	0.075±0.003
MgO	1.65±0.03	2.11±0.13	2.24±0.04	2.57±0.03	2.75±0.01	1.85±0.02	2.00±0.04
Na_2O	2.75±0.22	2.91±0.16	3.36±0.24	2.71±0.16	2.07±0.13	2.87±0.11	2.22±0.14
K_2O	1.26±0.01	1.66±0.12	1.22±0.02	1.14±0.01	2.52±0.03	1.36±0.04	1.64±0.07
CaO	32.6±0	13.7±2.9	30.0±0.4	27.4±3.5	21.3±0.1	31.3±0.5	29.7±0.6
C_{org}	0.52±0.09	1.15±0.37	0.20±0.02	ND	0.27±0.03	0.24±0.0	0.56±0.24
S	ND	ND	(0.13)	ND	(0.11)	ND	(0.30)
Trace elements (ppm)							
Li	30±0	71±6	24±1	16±1	55±1	30±3	41±3
Zr	77±12	105±10	220±11	248±18	73±4	120±21	77±11

Element	Turbidite						
	f (n=23)	*g* (n=4)	*g*$_1$ (n=2)	*h* (n=7)	*i* (n=2)	*j* (n=3)	*k* (n=4)
Major elements (%)							
TiO_2	0.35±0.01	0.60±0.01	0.65±0.02	0.43±0.01	0.74±0.09	0.14±0.00	0.39±0.01
Al_2O_3	8.02±0.37	6.88±0.16	12.0±0.5	9.16±0.17	7.45±0.26	2.68±0.07	9.51±0.36
Fe_2O_3	2.91±0.23	3.02±0.04	4.13±0.27	3.21±0.41	3.68±0.27	1.07±0.04	4.29±0.36
MnO	0.063±0.004	0.120±0.003	0.078±0.00	0.090±0.010	0.115±0.001	0.113±0.003	0.086±0.003
MgO	1.82±0.10	1.61±0.01	2.27±0.06	1.96±0.04	1.94±0.16	0.67±0.02	1.64±0.07
Na_2O	2.40±0.07	3.03±0.11	2.43±0.05	1.76±0.06	2.62±0.26	1.18±0.09	1.80±0.11
K_2O	1.40±0.07	1.41±0.05	2.25±0.06	1.53±0.06	1.37±0.04	0.53±0.01	1.42±0.07
CaO	28.0±0.6	32.2±0.6	18.3±1.0	26.1±0.8	30.2±1.4	45.6±0.2	26.4±1.6
C_{org}	0.70±0.32	0.18±0.02	ND	ND	0.18	0.11	ND
S	(0.40)	(0.08)	ND	ND	ND	ND	ND
Trace elements (ppm)							
Li	42±3	25±2	55±2	46±2	37±1	11±0	51±6
Zr	66±5	264±43	142±9	76±5	177±17	26±4	67±3

Turbidite tops and bottoms excluded; ND, not determined; standard deviations quoted as σ_n; sulphur values in parentheses based on single determinations only.

APPENDIX 5-3.

TABLE 5-3. Geochemistry of pelagite groups in core MD10.

Element	Pelagite group		
	P1 (n=2)	*P2* (n=9)	*P3* (n=9)
Major elements (%)			
TiO_2	0.08±0.00	0.35±0.11	0.69±0.15
Al_2O_3	1.70±0.20	6.60±2.10	12.4±2.0
Fe_2O_3	0.59±0.00	2.67±0.86	5.26±1.13
MnO	0.125±0.007	0.085±0.014	0.048±0.007
MgO	0.55±0.06	1.43±0.37	2.66±0.43
Na_2O	1.54±0.06	2.07±0.32	2.62±0.32
K_2O	0.42±0.04	1.29±0.33	2.56±0.46
$CaCO_3$*	46.4	32.4	9.80
C_{org}	ND	ND	ND
S	0.07±0.01	0.14±0.06	0.13±0.05
Trace elements (ppm)			
Li	11±0	29±12	55±16
Zr	17±0	59±26	130±27

Pelagite groups based on carbonate contents: P1, >75% $CaCO_3$; P2, 40-75% $CaCO_3$; P3, < 40% $CaCO_3$. ND, not determined; standard deviations quoted as σ_n.

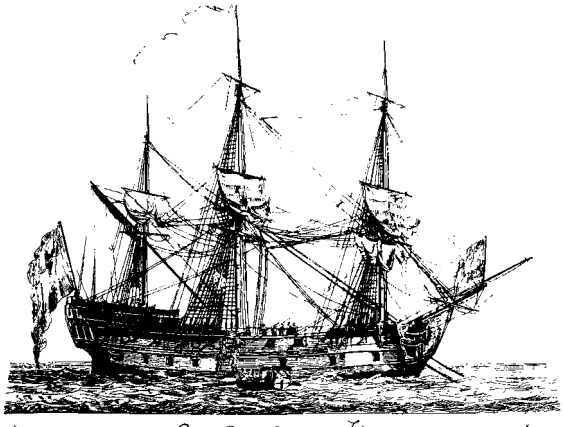

A Oostindesch Compagnie Schip 4

Chapter 6

DISTRIBUTION OF NITROGEN COMPOUNDS

(as found by selective extraction)

ABSTRACT

Nitrogen compounds that occur in the sediment of core MD10 MAP can be divided in separate extracted fractions such as 'exchangeable nitrogen' (N_{ex}), fixed nitrogen (N_{fix}) and organic nitrogen (N_{org}). N_{ex} is found to be directly proportional to the amount of organic matter (C_{org}) present in the sediment and is not related to the amount of ammonium present in the pore water. Only at a relatively low C_{org} content is the N_{ex} determined by the mineralogy of the sediment. The N_{org} as determined from N_{org}= (N_{tot} - N_{fix} - N_{ex}) is strongly related with C_{org}. The N_{fix} content and the N_{fix}/Al ratio for organic-rich sediments is high relative to other sediments and has not changed upon post-depositional oxidation of the organic matter. Post-depositional oxidation of organic matter through oxygen does lead to a decrease in the C/N ratio of the remaining organic matter in the organic-rich turbidites. The C/N ratio calculated for the organic matter that has been decomposed through oxygen is similar to that calculated through stoichiometric modelling for decomposition under reducing circumstances (C/N ratios of ≈17 and ≈18 respectively). This implies that the C/N ratio of decomposing organic matter is not influenced by the redox conditions in the sediment.

6-1. INTRODUCTION

Nitrogen (N) is one of the major constituents of organic matter. The average C:N:P composition of organic matter in living marine plankton has been reported to be close to the molar ratio of 106:16:1 (REDFIELD et al., 1963; see also Chapter 4). Organic matter is being degraded upon settling through the water column and after deposition in the sediment. Preferential decomposition of especially N- and P-rich organic matter has been reported (e.g. GORDON, 1971; HARTMANN et al., 1976; WALSH et al., 1985). The relative concentrations of C,N and P in organic matter in the sediment may therefore be altered through early diagenetic reactions in the sediment. These changes depend on parameters such as the environment of deposition, the organic-matter content, the composition of the organic matter at deposition and the sedimentation rate. Through study of N and its relationship to C and P, various authors have tried to unravel the origin and diagenetic reactions of organic matter in the marine environment. In addition, it was attempted to relate the results of such studies to paleo productivities and past environments.

In the literature controversy exists concerning the question if P or N is the limiting nutrient for primary production. In a recent paper CODISPOTI (1988) gives an excellent review of these opposing opinions. Although

BROECKER (e.g. 1982) and others conclude that P must be the limiting nutrient, CODISPOTI demonstrates that on a time-scale of several thousands of years imbalances between nitrogen fixation and denitrification may cause large changes in the primary productivity of the open ocean. In his opinion, N is the limiting nutrient for the growth of plankton in the present open ocean. However, in some exceptional environments (e.g. estuaries, Mediterranean Sea, Red Sea) and during warmer epochs in the past ocean, P may have been the limiting nutrient (e.g. CODISPOTI, 1988 and refs therein). The on-going discussion on this matter underlines the importance of processes involving N (and P) for the primary production in the oceans. The brief introduction given in this chapter is not meant to be complete, but merely to put the study of N (& P) compounds in a wider perspective.

Marine plankton is produced (and for the greater part consumed) in the top 200 m of the water column (the euphotic zone). Less than 5% of the primary production escapes from the euphotic zone (ROMANKEVITCH, 1984; EPPLEY, 1988). A large part of this "export production" reaches the sea-floor, where most of it decomposes in a period of less than a year (REIMERS, 1988; JUMARS et al., 1988). Therefore, in slowly accumulating sediments such as those in the Central Pacific, very little organic carbon is buried; the organic carbon (C_{org}) content is in general less than 0.1%. Oxygen penetrates down to several meters depth in these sediments, that are therefore exposed to oxygen during 10^5 to 10^6 years. In contrast, near upwelling areas and in near-coastal areas sedimentation rates and organic carbon content are extremely high, resulting in anoxic sediments below a depth of a few cm or less. Highly reactive organic matter (such as that from fresh plankton) has been reported to be decomposed at similar rates (within a factor of 2 to 3) under oxic and under anoxic conditions (WESTRICH & BERNER, 1984; REIMERS, 1988) (see Chapter 1). However, the decomposition rate of part of the organic matter in the sediment seems to be highly oxygen-dependent. Under anoxic conditions the decomposition rate of this oxygen-dependent organic fraction must be at least some orders of magnitude smaller than under oxic conditions (JUMARS et al., 1988; Chapter 1). In organic-rich deposits, such as near upwelling areas or Cretaceous black shales, it is mainly this fraction that is or has been buried. The organic matter of the organic-rich turbidites in the Madeira Abyssal Plain falls in the same category. These turbidites represent the distal part of turbidity-current transported organic-rich sediments which originate from near-coastal or upwelling-related areas (see Chapter 5). Upon deposition of each of the fairly homogeneous organic-rich turbidites penetration of oxygen and consequent decomposition of the top-most organic matter is started and gradually this oxidation front migrates downward until the supply of oxygen is cut off by the next turbidite being deposited (see Chapter 5). Therefore, with the exception of the C_{org} and the trace element

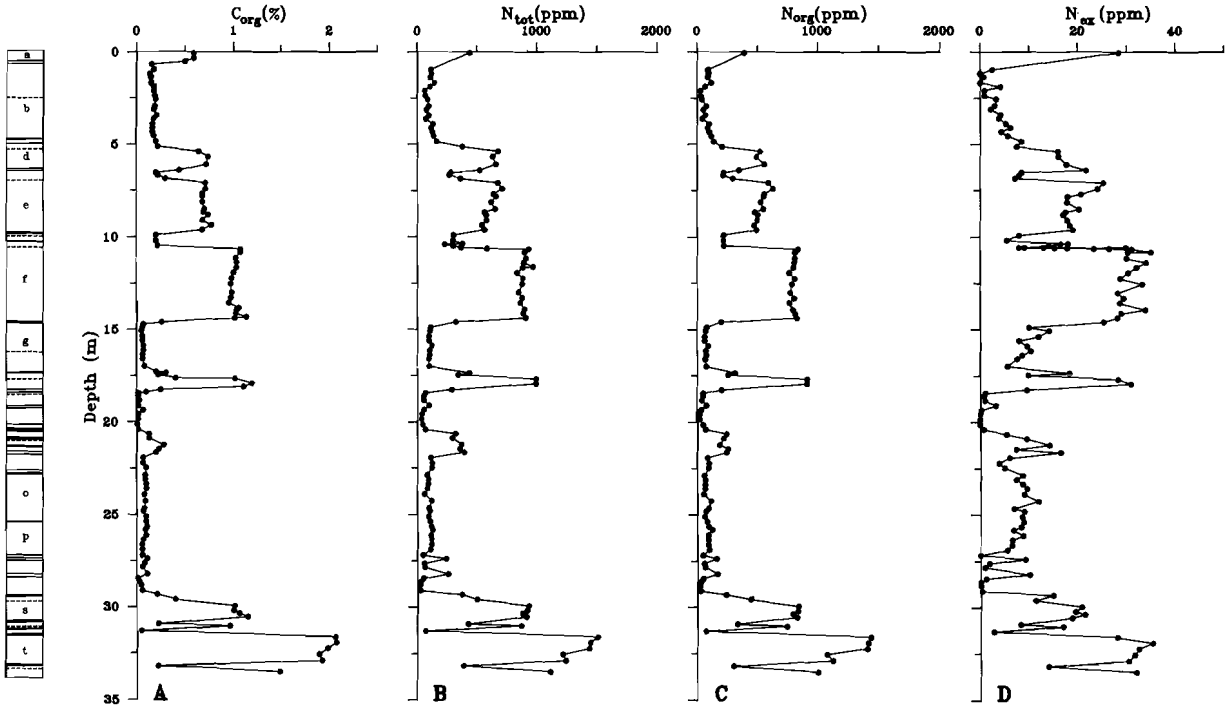

Fig. 6-1. Stratigraphic variation of organic carbon (a), total nitrogen (b), organic nitrogen (c) and 'exchangeable' nitrogen (d) in the sediment of core MD10 (see also text). In addition, a lithological representation of core MD10 is given; approximate turbidite boundaries are indicated. For turbidite lettering see Fig. 5-4.

content, each turbidite can be considered homogeneous in composition. These sediments offer a unique opportunity to study the composition of those sedimentary constituents, that are related to organic carbon. Such study leads to a better understanding of the decomposition of organic matter and the related diagenetic reactions (e.g. JUMARS et al., 1988). In view of the time needed for these "in situ experiments" (1 - 50 ky) identical laboratory simulation experiments are not likely to be ever done. It is not only because of this intra-turbidite comparison that the turbidites of the Madeira Abyssal Plain are interesting, but also because of inter-turbidite comparison. Distinct groups of turbidites having very different composition and origin can be distinguished (see Chapter 5). This distinction is not only visible in the major element composition, but also in the C_{org} content and in the various fractions of N that have been extracted (Fig. 6-1).
The various N compounds as found by selective extraction of samples from core MD10, MAP (Fig. 2-1, 5-1) will be discussed in this chapter. The analytical details of the extractions are given in Appendices 6-1,2. Briefly, exchangeable nitrogen (N_{ex}) is defined here as the amount of NH_4^+ extracted by a 2 N KCl solution; fixed ammonium (N_{fix}) as the fraction which is not extracted by 2 N KCl, but which is liberated with a HF/HCl solution after destruction of the organic matter with a hypobromite solution. Organic nitrogen (N_{org}) is defined here as the difference between total nitrogen (N_{tot}) and inorganic nitrogen ($N_{fix} + N_{ex}$) :

$$N_{org} = N_{tot} - N_{fix} - N_{ex}$$

In the literature some controversy seems to exist about the possible effect of drying of the sediment on its N_{ex} content. Changes in N_{ex} and N_{fix} have also been reported to occur during the wet-storage of the sediment (KEMP & MUDRUCHOVA, 1973). Others claim that wet storage at 4°C does not significantly alter the N_{ex} content of the sediment (ROSENFELD, 1979[a]; MACKIN & ALLER, 1984). Preliminary experiments done in our laboratory did not indicate detectable differences in the various N-fractions between wet, freeze-dried and oven-dried samples. Therefore,all extractions were done on dried (24 hours at 105°C) and powdered sediment. No correction was made for the possible contribution of pore-water NH_4^+ to N_{ex}, as some uncertainty exists in the literature about this contribution (STEVENSON & CHENG, 1972; ROSENFELD, 1979[a]). Both no contribution at all, due to volatilization during drying (STEVENSON & CHENG, 1972) and a full contribution have been assumed. The highest pore-water ammonium concentrations are found in the bottom part of core MD10. For these sediments the highest contribution of pore-water NH_4^+ to N_{ex} may amount to 6 ppm N (cf. Fig. 6-1).
The various N compounds in core MD10 are strongly related to the C_{org} content (Fig. 6-1; Table 6-1). Only for N_{fix} there is some relation with

TABLE 6-1. Correlation diagram of some relevant sediment constituents in core MD10. Fe Mg Al clay

	Ca	Sr	S	C_{org}	N_{tot}	N_{org}	N_{ex}	N_{fix}	K	ill	kao	smec	chl				
Ca	1.0																
Sr	0.95	1.0															
S	-0.17	-0.17	1.0														
C_{org}	-0.31	-0.30	0.91	1.0													
N_{tot}	-0.41	-0.39	0.90	0.97	1.0												
N_{org}	-0.34	-0.32	0.91	0.98	0.99	1.0											
N_{ex}	-0.46	-0.40	0.80	0.87	0.91	0.90	1.0										
N_{fix}	-0.82	-0.85	0.27	0.41	0.52	0.44	0.47	1.0									
K	-0.87	-0.84	0.06	0.20	0.34	0.27	0.37	0.83	1.0								
ill	-0.86	-0.87	0.14	0.15	0.26	0.19	0.30	0.81	0.84	1.0							
kao	-0.71	-0.73	0.41	0.43	0.50	0.46	0.51	0.68	0.71	0.67	1.0						
smec	-0.47	-0.40	-0.05	0.01	0.08	0.03	0.28	0.49	0.34	0.25	0.29	1.0					
chl	-0.75	-0.78	0.12	0.21	0.30	0.26	0.32	0.77	0.72	0.71	0.55	0.08	1.0				
Fe	-0.85	-0.77	-0.15	0.00	0.09	0.03	0.19	0.63	0.82	0.73	0.54	0.44	0.74	1.0			
Mg	-0.87	-0.79	0.13	0.27	0.37	0.31	0.36	0.76	0.89	0.82	0.66	0.31	0.77	0.88	1.0		
Al	-0.92	-0.89	0.13	0.26	0.39	0.32	0.46	0.86	0.94	0.85	0.70	0.48	0.77	0.88	0.89	1.0	
clay	0.16	0.18	-0.11	-0.13	-0.12	-0.12	-0.10	-0.08	-0.18	-0.19	-0.21	-0.08	-0.27	-0.22	-0.22	-0.17	1.0
vsp	-0.39	-0.38	-0.09	-0.12	-0.09	-0.10	-0.05	0.21	0.46	0.39	0.36	0.25	0.31	0.39	0.30	0.36	-0.31

vsp= feldspar; clay= fraction < 4µm; ill,kao,smec and chl= resp. relative % illite, kaolinite,smectite and chlorite (AUFFRET et al., 1988)

pelagic intervals concurring with a higher relative illite content (see section 6-3). In order to facilitate comparison between and within different types of turbidites, this study will focuss on the 5 to 18 m depth interval in core MD10 containing relatively thick and well-defined turbidites of different nature.

6-2. EXCHANGEABLE NITROGEN (N_{ex})

Exchangeable nitrogen (N_{ex}) is defined here as the amount of N extracted by a 2 N KCl solution (for details of method see Appendix 6-1).
The adsorption of ammonium has been reported to depend on grain size, mineralogy, organic matter content and the concentration of ammonium in the pore water (ROSENFELD, 1979[a]; 1981; BOATMAN & MURRAY, 1982; MACKIN & ALLER, 1984). In most studies of natural systems more than one of these parameters vary simultaneously, which makes it difficult to distinguish the impact of each separately. For the sediments of the MAP it is only the organic matter content that changes within each turbidite, whereas between turbidites (and pelagic sediments) it is the mineralogy and sometimes the grain size that vary too.

Impact of the sediment composition

The profile of N_{ex} versus depth in core MD10 (Figs. 6-1,2) clearly demonstrates that the N_{ex} co-varies with the C_{org} content (R=0.87; Table 6-1). However, C_{org} also co-varies with the sulphur content (in the organic-rich intervals mainly present as sulphide) of the sediment (R=0.91).

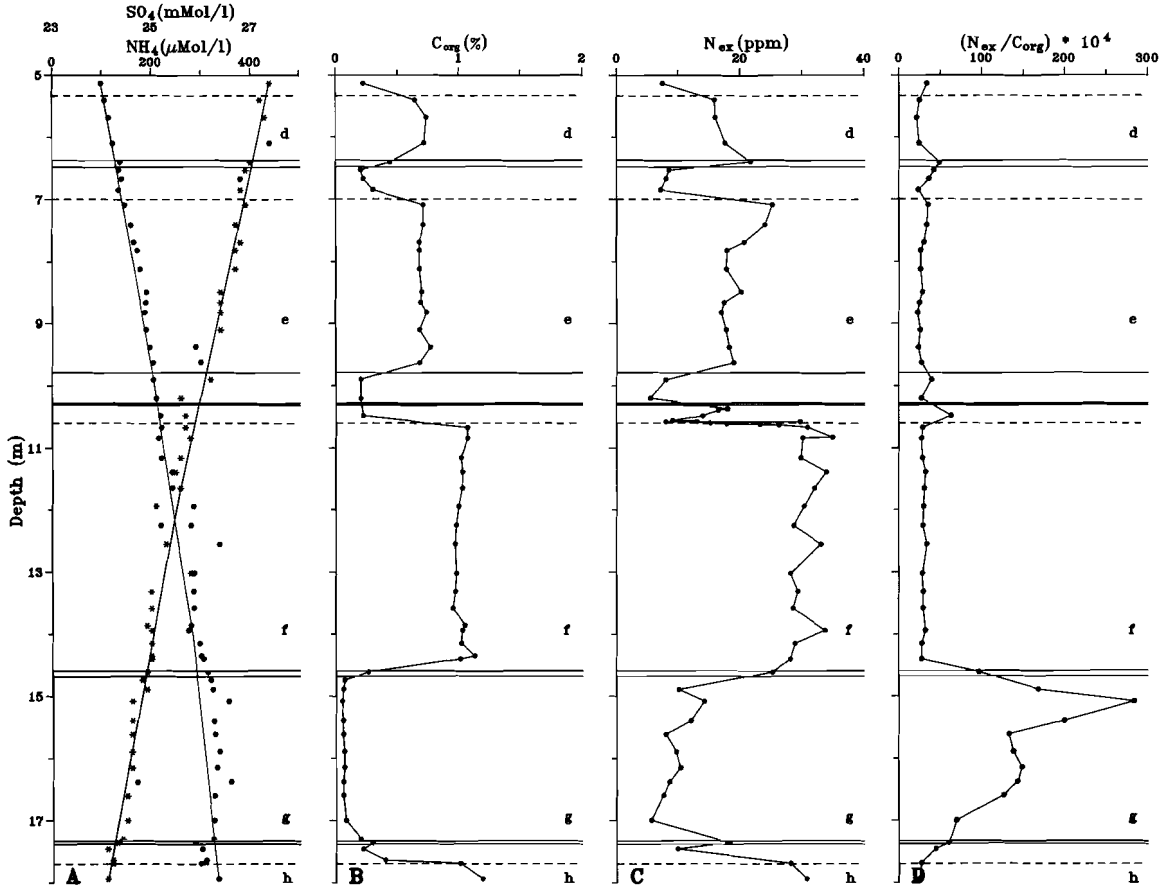

Fig. 6-2. Pore-water concentration versus depth profiles of ammonium (o) and sulphate (*) (a); profiles versus depth for the concentration in the sediment of organic carbon (b), exchangeable nitrogen (c) and the ratio of exchangeable nitrogen/organic carbon (d). All profiles are for the interval of 5-18 m in core MD10 ; approximate turbidite boundaries have been indicated, dashed lines represent redox boundaries. For turbidite lettering see Fig. 5-4.

Sulphides are reported to adsorb only cations which form insoluble sulphides; this excludes NH_4^+ (BOATMAN & MURRAY, 1982 + refs herein). The shape of the C_{org} plot is not influenced by carbonate dilution (plot not shown in Fig., but see Table 6-1, Section 6-3 and Figs. 6-2^b,9^b). Therefore, the N_{ex} must result from adsorption of ammonium on organic matter or organic-clay complexes (BOATMAN & MURRAY, 1982). By 'normalizing' the N_{ex} to the C_{org} content, for example by taking the ratio (N_{ex}/C_{org}), possible relationships in addition to those with organic matter can be emphasized. Despite the fact that the much higher analytical error at lower concentrations certainly influences the shape of the plot, the relatively high values of (N_{ex}/C_{org}) in pelagic intervals and in turbidite g are obvious (Fig. 6-2). As discussed in Chapter 5, the mineralogy and composition of turbidite g deviate from those of turbidites d,e,f and h.

In summary, organic matter is the major sedimentary constituent that determines the N_{ex} content of the sediment in the MAP. Only at relatively low organic matter content it is the mineralogy that determines the N_{ex} content. On the basis of the correlation diagram (Table 6-1), kaolinite seems to be the most favourable clay mineral for NH_4^+ adsorption, which agrees with findings of others (BOATMAN & MURRAY, 1982).

Large differences in N_{ex} content occur between the oxidized (organic-poor) upper part and the reduced (organic-rich) lower part within each organic-rich turbidite. These differences are caused by a different C_{org} content, because the N_{ex}/C_{org} ratio remains constant across these redox boundaries.

However, important differences exist in the N_{ex}/C_{org} ratio in particular between the organic-rich turbidites above 20 m and those below that depth in core MD10. These differences may be illustrated by the following example : The N_{ex} content of samples in the f-and t-turbidite is similar, whereas the C_{org}-content in the t-turbidite is twice as high as that in the f-turbidite (Fig. 6-3; Appendix 5-1). Therefore, the N_{ex}/C_{org} ratio in the t-turbidite is only half as high as that in the f-turbidite. In addition, the pore-water concentration of ammonium in the samples of the t-turbidite is twice as high as those

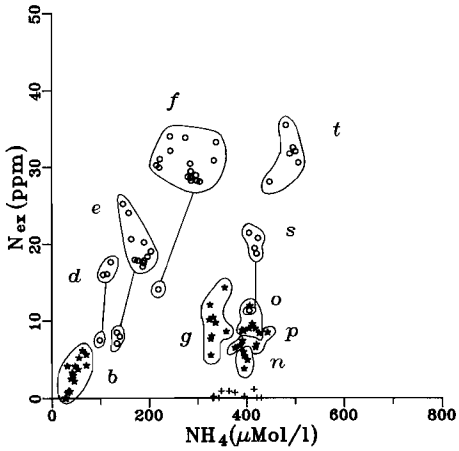

Fig. 6-3. Plot of dissolved ammonium versus exchangeable ammonium for samples of core MD10. Symbols indicate different types of turbidites, (*): volcanic, (o): organic-rich and (+): carbonate-rich. Letters indicate different turbidites (cf. Fig. 6-1); the reduced (high N_{ex}) and the oxidized (low N_{ex}) part of each organic-rich turbidite has been connected.

of the f-turbidite (see next paragraph). This difference in N_{ex} content must be caused by a different composition of the organic matter. At present there are no other observations (such as C/N ratio) that could confirm this difference in organic matter. However, the observed large differences indicate that not only a different mineral composition may result in a different N_{ex} content, but also different types of organic matter may be associated with different quantities of N_{ex}.

Impact of the pore-water ammonium concentration

The quantity of N_{ex} within one sediment type has been reported to be related to the NH_4^+ concentration in the pore water and to be exchanged rapidly and reversibly (e.g. ROSENFELD, 1979[a]). The absence of a visible relationship between pore-water ammonium and N_{ex} in this study (Figs. 6-2,3) seems to be in sharp contrast to the reported data for near-coastal sediments (e.g. ROSENFELD, 1979[a]; MACKIN & ALLER, 1984). In view of the differences in N_{ex} content that have been reported to occur between various sediment types, in core MD10 such a correlation may only be visible within each turbidite. This does not seem to be the case (Fig. 6-3).
The C_{org} content in the reduced parts of each of the organic-rich turbidites is relatively constant, whereas the pore-water ammonium concentration increases with depth. For example, in the reduced part of the f-turbidite the C_{org} content is fairly constant (0.98 ± 0.03), whereas the pore-water ammonium concentration increases from 220 to 300 µM. Yet, in the plot of N_{ex} versus pore-water ammonium no correlation is visible (Fig. 6-3). In fact, b and g may be the only turbidites for which this correlation may exist. For the b-turbidite the C_{org} content is relatively constant too (0.18 ± 0.02 for the upper part and 0.19 ± 0.02 for the lower part), but the N_{ex} content increases with increasing ammonium content. It must be noted that the N_{ex}/NH_4^+ ratio for the b-turbidite is high relative to those reported for near-coastal or deep-sea sediments of similar water content (ROSENFELD, 1979[a]; BOATMAN & MURRAY, 1982; MACKIN & ALLER, 1984). As the C_{org} content of this turbidite is relatively low, it seems likely that a different mineralogical composition is the cause for this deviation.

6-3. FIXED NITROGEN (N_{fix})

Fixed ammonium (N_{fix}) is defined here as the fraction which is not extracted by 2 N KCl, but which is liberated with a HF/HCl solution after destruction of the organic matter with a hypobromite solution.
N_{fix} may make up a large part of the total N content of the sediment:

reported values range from 18-96% (e.g. LEW, 1981). The N_{fix} values for core MD10 range from 4-94%, the lowest percentage corresponding to organic-rich sediments and the highest to organic-poor sediments. Most N_{fix} values are below 100 ppm. Variations in the N_{fix} content of sediment have been reported to be related to the clay mineral composition of the sediment. Illite is known to retain large amounts of non-exchangeable ammonium whereas smectite and kaolinite contain only low concentrations of N_{fix} (e.g. STEVENSON & DHARIWAL, 1959; STEVENSON & CHENG, 1972). In the distal turbidites of the MAP with a clay content of generally more than 60%, the relative % illite varies fig. 6-4 between 25 and 50% with most values lying between 30 and 40% (App. 7-3; AUFFRET et al., 1988). The preferential fixing of ammonium in illite is caused by the almost similar cationic radii of ammonium (1.43 Å) and of potassium (1.33Å) in the unhydrated state (MÜLLER, 1977; LEW, 1981 and refs therein). In these papers potassium has been used as a measure for the illite content of the sediment. This approach seems to be supported by the good correlation between the relative % illite, K, and N_{fix} in this study (Table 6-1; Fig.6-4). The slope in the N_{fix} versus K plot (Fig. 6-5) found here (≈100 ppm N_{fix}/1% K) is identical to that reported by MÜLLER (1975; 1977). However, N_{fix} correlates also with Al, Li, Mg, Zn and Be (R= 0.71 - 0.90), and all plots of these constituents versus N_{fix} have a non-zero intercept on the constituents' axis (not shown in Fig.). Furthermore, all these constituents demonstrate a strong negative correlation with Ca and Sr

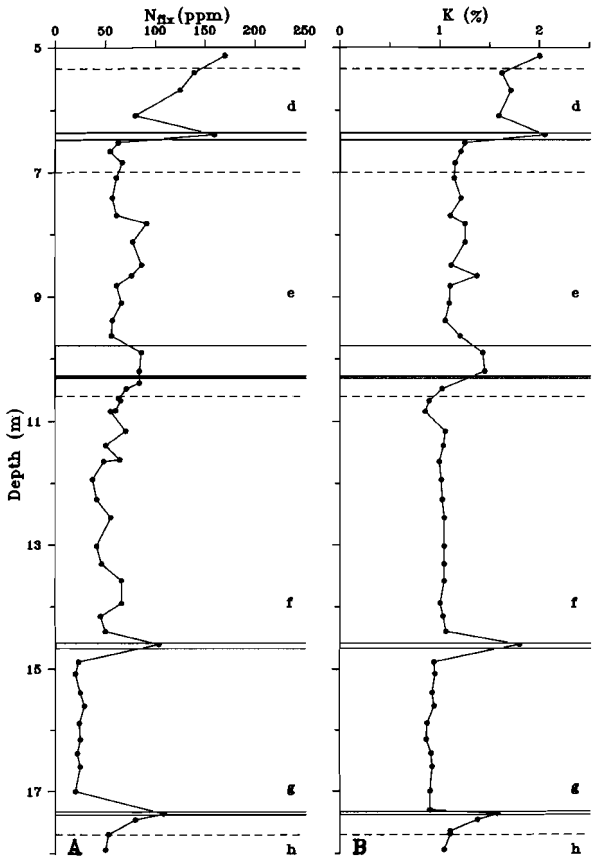

Fig. 6-4. The concentration of fixed ammonium (a) and of K (b) (see text) versus depth in the sediment interval from 5-18 m in core MD10. For turbidite lettering see Fig. 5-4.

(R=-0.82-0.85), pointing to a major influence of carbonate dilution, with a possible minor effect of the illite content of the sediment (Table 6-1). A way to compensate for the effect of carbonate dilution is to discuss the constituent-to-aluminium ratio in stead of the constituent itself (see also Chapter 5). Implicit in this 'correction' is the assumption that the aluminium content of the non-carbonate fraction is constant.

In contrast to the results of MÜLLER (1977) no correlation is found between N_{fix}/Al and K/Al (Fig. 6-5). It is remarkable that the relatively high K/Al ratio found for the samples in core MD10 corresponds to N_{fix}/Al values (Fig. 6-5) that are half as high as could be expected from published relationships (see MÜLLER, 1977). If the N_{fix} concentration is mainly determined by the illite content (see above) then, K or K/Al is not solely associated with illite in the present sediments. The non-zero intercept in the N_{fix}/K plot may indicate such a non-illite contribution to K, such as K-feldspars or zeolites. This would imply that K or K/Al is not a good measure for the illite concentration in the sediments of the MAP.

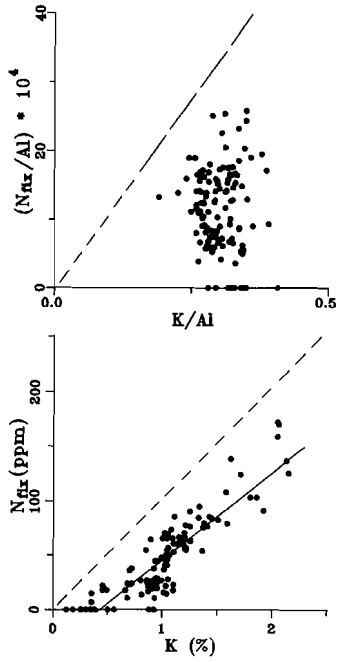

Fig. 6-5. Plot of K versus N_{fix} and of K/Al versus N_{fix}/Al for core MD10. Dashed lines are regression lines through data of MÜLLER (1977).

Although the sediments of organic-rich turbidites have in general a high N_{fix} content (and N_{fix}/Al ratio), it is clearly not the organic matter in these sediments that determines the N_{fix} content. Upon post-depositional oxidation of the organic matter there seems to be no change in the N_{fix} content (Fig. 6-4). However, the relative % illite in organic-rich turbidites is in general higher and the carbonate content lower than in other turbidites (Appendices 7-3,5-1). It must be noted that the relative % illite is expressed as % relative to the total clay mineral content as determined by XRD. This implies that for example at high carbonate content the "absolute" amount of illite is very low. (In fact, it is not possible to convert relative % of clay minerals into absolute quantities due to the limitations of the detection technique). The above-mentioned differences in relative % of illite that exist between organic-rich and volcanic turbidites will become even larger if the differences in carbonate content are taken into account. The "carbonate-corrected" relative % of illite for samples in the f-turbidite would then be twice as high as those in the g-

turbidite (see Appendices 7-3, 5-1). These differences between turbidites are not visible in the K content (cf. turbidites f and g in Fig. 6-4) or in the K/Al ratio (not shown in Fig.). This observation is another indication that K or K/Al is not a good measure for the illite content in these samples.
The simultaneous occurrence of high N_{fix} and K concentrations in some pelagic intervals agrees with the high relative % of illite and the low carbonate content reported for these intervals (AUFFRET et al., 1988). However, in the plot of N_{fix}/Al versus K/Al the pelagic samples deviate from the reported correlation (MÜLLER (1977) in a way similar to that discussed earlier for the turbiditic samples (Fig. 6-5). It is unlikely that this deviation (and those discussed earlier) could be attributed to errors in the analysis of N_{fix}. Therefore, this deviation must be caused by a non-illite contribution of K, such as from K-feldspars or zeolites.

6-4. ORGANIC NITROGEN (N_{org})

Organic nitrogen (N_{org}) is defined here as the difference between total nitrogen (N_{tot}) and inorganic nitrogen (N_{fix} + N_{ex}) :

$$N_{org} = N_{tot} - N_{fix} - N_{ex}.$$

The total nitrogen concentration of the sediment does not represent the nitrogen content of the organic matter because N_{fix} in particular may make up a large part of the N_{tot} (see section 6-3). Therefore, the C_{org}/N_{org} ratio (from hereon referred to as the C/N ratio) gives a much better measure for the C/N ratio of the organic matter than does the often used C_{org}/N_{tot} ratio. This is especially true for sediments with a relatively low organic matter content.
The profile of N_{org} versus depth in core MD10 closely resembles that of C_{org} versus depth (Figs. 6-1,6). For the organic-rich turbidites an average C/N molar ratio of ≈17 can be deduced from the strong correlation demonstrated in Fig. 6-7. In addition, the near-zero intercept in the latter figure shows that organic matter is likely to be the only source for N_{org}. This finding confirms that N_{org} as defined above is a good measure for the organic nitrogen content of the samples in this study.
In the oceans nitrogen is present in all sorts of organic compounds/ organisms in various concentrations. The distribution of organic N is related to the occurrence of plankton and its concentration depends on factors such as primary productivity and water depth. The C/N ratio of various organisms may be very different. For example protein-rich phyto-plankton has a relatively low ratio (e.g. 6.5 for blue-green algae and 5.5-

7.5 for diatoms; BORDOWSKIY, 1965[a]), whereas protein-poor terrestrial plants have a relatively high ratio (14-30; BORDOWSKIY, 1965[b]). Animal organisms in particular are rich in protein and exhibit C/N ratios of near 3 (polychaetes 3.4, fish 3.9, copepods 4.3) (MÜLLER, 1977 + refs therein). The average ratio of marine plankton has been reported to be 6.6 (Molar ratio) (e.g. REDFIELD et al., 1963; WALSH et al., 1985). The C/N ratio of plankton found in the euphotic zone commonly corresponds closely to this value (e.g. GORDON, 1971 ; WALSH et al. , 1985). However, at greater depths in the water column this ratio increases progressively from 10 (≈1000 m) to 15 (>3000 m) (e.g. GORDON, 1971; MÜLLER, 1977). A similar increase in C/N with depth seems to occur in organic-rich continental slope sediments (SHOLKOVITZ, 1973; WALSH et al., 1985; HARGRAVE, 1988; WALSH, 1988). This increase in the C/N_{tot} ratio has been attributed to the preferential release of organic nitrogen relative to organic carbon during decomposition of organic matter. The C/N ratio has been reported to depend also on the fig 6-7 organic matter content of the sediment, in that a high organic matter content corresponds to a relatively high C/N_{tot} ratio, whereas a low organic

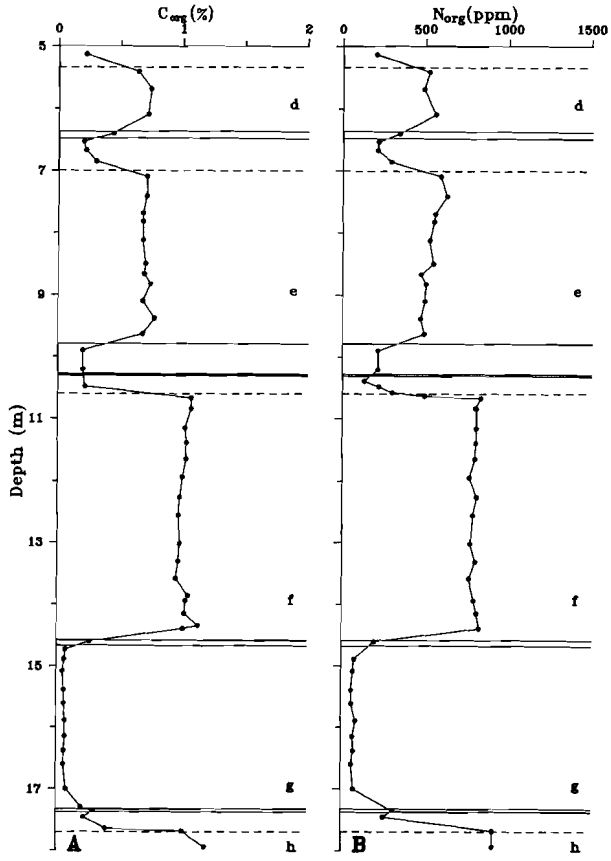

Fig. 6-6. The concentration of organic carbon (a) and organic nitrogen (b) versus depth in the sediment interval from 5-18 m in core MD10.

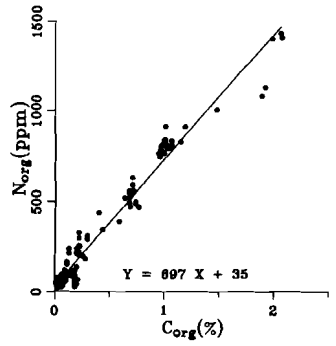

Fig. 6-7. Plot of C_{org} versus N_{org} for core MD10. A Molar C/N ratio of 16.8 is calculated from the regression line (R=0.98).

matter content corresponds to a low C/N_{tot} ratio (MOHAMED, 1949; ARRHENIUS, 1950; MÜLLER, 1975; HARTMANN et al., 1976). This may in part be explained by a contribution of N from N_{fix} to N_{tot} (Section 6-3; see discussion below).

C/N ratio in the sediments

In the sediments of core MD10 the C/N ratio for the organic-rich turbidites is clearly higher than that for the organic-poor turbidites (Fig. 6-8). This observation seems to agree with the earlier mentioned reports (e.g. MOHAMED, 1949 and others). Low C_{org}/N_{tot} ratios in marine sediments (as low as ≈1) have been reported to be partly caused by relatively high amounts of N_{fix} (e.g. MÜLLER, 1977; see section 6-3). In the completely oxidized Pacific sediments, studied by MÜLLER (1977), the organic carbon content of 0.3% at the surface decreased to less than 0.1% at a depth of 3 m, in the absence of carbonate and in the abundant presence of smectites. At the same time the C/N ratio decreased from ≈5 to ≈2.2. In these organic-poor sediments the N_{org} is preferentially preserved, which seems in contrast to the reported preferential decomposition of N_{org} in organic-rich sediments (e.g. HARTMANN et al., 1976). The residual organic matter fraction in the former sediments is sorbed / complexed to smectites and is thus protected against microbial oxidation. The low C/N ratio of the residual organic matter (≈ 2.5) could indicate N-compounds

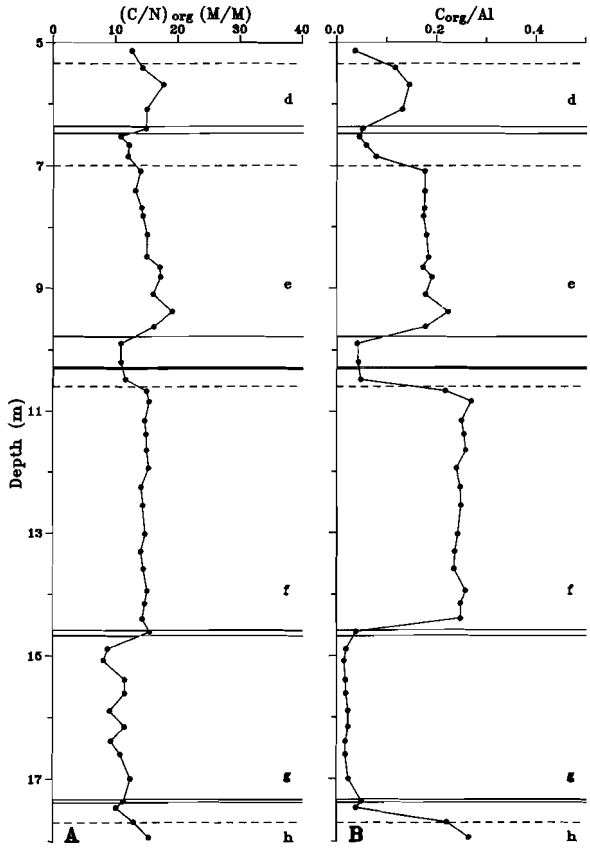

Fig. 6-8. The molar C/N ratio (a) and the C_{org}/Al ratio (b) versus depth in the sediment interval from 5-18 m in core MD10.

such as amino acids, which have been reported to adsorb strongly on to clay fig 6-8 minerals (MÜLLER, 1977; ROSENFELD, 1979[b]). For organic-poor but carbonate-rich sediments relatively high C/N ratios (≈10) have been reported (SUESS, 1973). It seems therefore, that a low amount of organic matter can be protected against microbial decomposition provided that a sufficient amount of clay minerals, specifically smectite (MÜLLER, 1977), is present.

A remarkable phenomenon in the organic-rich turbidites of the MAP is the occurrence of an oxidized top layer (see Chapter 5). The C/N ratio in the oxidized part is low compared to the reduced part within the same turbidite (Fig. 6-8). The 'residual' organic matter fraction in the oxidized part is near 0.2% with a carbonate content of near 50% and a relative percentage of smectite of near 30%. The occurrence of 'residual' organic matter in these sediments could be explained in two different ways, namely by 'smectite protection' or by 'kinetic considerations'. If the 'residual' organic matter is related to the smectite content in a ratio similar to that reported for the Pacific sediments, then one would expect a 'residual' organic carbon content of at most 0.02% for the sediments of the organic-rich turbidites in this study. Smectites seem to be the most suitable clay minerals for complexation with organics (e.g. BRINDLEY & SUITO, 1971), for example smectite-protein complexes have been reported (ENSMINGER & GIESEKING, 1939). Recently also kaolinite has been reported to adsorb readily some amino acids (HEDGES & HARE, 1987). In smectites stable complexes can form between silicate layers and organic molecules by means of N-H...O or O-H...O hydrogen bonds (e.g. YAMANAKA et al., 1971). Not all organic matter has the same affinity for complexation with clay minerals. If the 0.2% of organic matter in the oxidized top part of the organic-rich turbidites in core MD10 represents the 'residual' fraction of organic matter, then the higher amount in these sediments relative to the Pacific sediments can only be explained by differences in the composition of the organic matter. This implicitly means that the 'protection' capacity of smectites would not be the limiting factor for the amount of 'residual' organic matter in the sediment. The presence (sort and amount) of functional groups in organic matter may determine the capacity of organic matter to form complexes with smectites and thereby also determine the protection against microbial oxidation. High amounts of organic matter that is suitable for adsorption are more likely to be present in organic-rich than in organic-poor sediments. Therefore, upon oxidation of organic-rich sediments a higher C_{org}/Al ratio is expected to remain in the sediment than upon oxidation of organic-poor sediments. This difference is in fact observed in core MD10 between turbidites d,e,f (organic-rich) and g (organic-poor) (Fig. 6-8). If this is true in general, then for <u>oxidized</u> sediments the 'residual' organic matter content would be proportional to

the original organic matter content. However, the C/N ratio of the 'residual' organic matter in core MD10 is much higher than the ratio in the Pacific sediments. This observation would imply that dramatically different compounds are involved, which makes this option less likely.
An alternative explanation is that the 'residual' organic matter in the oxidized part of the organic-rich turbidites can only be decomposed in the presence of oxygen and at relatively low rates (kinetic considerations). Consequently, only part of this 'residual' organic matter may be really protected by smectites whereas the rest is still slowly decomposing. On the basis of reported results from the Pacific (MÜLLER, 1977) and the present data, the last explanation seems the most likely.
It is remarkable that in organic-rich turbidites post-depositional decomposition of organic matter through oxygen leads to a decrease in the C/N ratio of the remaining organic matter (Fig. 6-8). The C/N ratio of the organic matter decomposed in the upper part of each organic-rich turbidite must therefore be higher than that of the un-decomposed organic matter in the lower part. For example in the f-turbidite the C/N ratio of the un-decomposed organic matter (0.98% C_{org}) in the lower reduced part is 14.7, whereas the ratio for the remaining organic matter (0.22% C_{org}) in the upper oxidized part is 11.6. The C/N ratio of the decomposed organic matter can then be calculated as follows :

$$(C/N)_{decomposed} = \frac{0.98 * 14.7 - 0.22 * 11.6}{0.98 - 0.22} = 15.2$$

The calculated C/N ratios for the decomposed organic matter in the top part of the organic-rich turbidites ranges from 15 to 18, the average being ≈17. The release of N from organic matter requires the breaking of C-N bonds, which are much weaker than C-C bonds (e.g. TOTH & LERMAN, 1977). This accords with the higher C/N ratio and lower decomposition rates of the decomposed organic matter of the 'labile' fraction (C/N≈17; found in sediments of core MD10) relative to the 'very labile' fraction (C/N≈5-16; reported for near-coastal sediments). BLACKBURN (1980) made similar observations, i.e. fresh organic matter with low C/N ratio (≈8) being mineralized at the sediment surface and older organic matter with high C/N ratio (≈17) in deeper sediment layers.

Stoichiometric modelling

A different way to determine the C/N ratio of decomposing organic matter is through stoichiometric modelling. During the microbial oxidation of organic matter various decomposition products are formed, such as ammonium, phosphate, bicarbonate etc. (see also Table 4-1). The SO_4^{2-}/NH_4^+ ratio resulting from the decomposition of organic matter through sulphate reduction, has been used previously to ascertain the C/N ratio of the decomposing organic matter (HARTMANN et al., 1973; 1976; BERNER, 1977; MARTENS et al., 1978; ROSENFELD, 1981; KLUMP & MARTENS, 1987). Pore-water NH_4^+ is produced during the decomposition of organic matter through reduction of Feoxihydroxides or sulphate (see reactions 4 and 5, Table 4-1). Sulphate reducing conditions do not occur in the sediments of core MD10, with the possible exception of some micro-reducing environments. (e.g. KUIJPERS et al., 1984[a]; DE LANGE et al., 1984[a]). Fe-oxihydroxide reduction seems to occur only in some specific intervals (e.g. 15-17 m and 24-27 m; Fig. 2-7), with the highest measured Fe^{2+} concentration in the pore water being in the range of 40-50 µM (DE LANGE, 1984[a]; DE LANGE et al., 1988[a,b]). The regular increase of the concentration of dissolved NH_4^+ with depth in core MD10 does not allow for a major NH_4^+ contribution through Fe-oxihydroxide reduction. On the other hand, the good correlation between the SO_4 and NH_4^+ concentrations in the pore water (Fig. 6-9) indicates that the profile of NH_4^+ is more likely to be caused by decomposition of organic matter through sulphate reduction below a depth of 35 m and subsequent upward diffusion of the NH_4^+. This is illustrated by the pore-water concentrations of sulphate and ammonium that decrease respectively increase steadily with depth in the sediment (Fig. 6-2). These observations all imply that the pore-water profiles of ammonium and sulphate are diffusion controlled. Therefore, the diffusion coefficients have to be taken into account when modelling these compounds. The slope of the ammonium versus sulphate plot demonstrates the good correlation between these two compounds (Fig. 6-9). Because sedimentation rates are relatively low, the C/N ratio of the decomposing organic matter (at depths below 35 m)

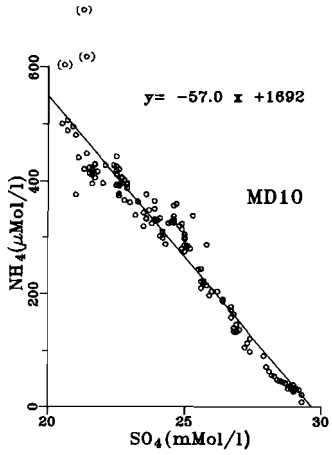

Fig. 6-9. Plot of the pore-water concentration of ammonium versus that of sulphate for core MD10 (R=-0.96).

can be calculated from the slope as follows (BERNER, 1977; MARTENS et al., 1978; see also Section 6-2) (see Table 4-1) :

$$C/N = \frac{2 * SO_4^{2-}}{NH_4^+} * \frac{D_{SO4}}{D_{NH4}}$$

in which :
D_{NH4} = molecular diffusion coefficient for NH_4^+
D_{SO4} = molecular diffusion coefficient for SO_4^{2-}
and the factor 2 originates from reaction 5 of Tabel 2-1, in which 106 C corresponds with 53 SO_4^{2-}.

The resulting C/N ratio of 18 is only slightly higher than the ratio observed for the organic matter in the organic-rich turbidites in the top 35 m of this core (e.g. Figs. 6-8,10). This ratio also corresponds with the C/N ratio of 17 calculated for the decomposed organic matter of the oxidized top part of the organic-rich turbidites. In view of the similar C/N ratios in all the organic-rich turbidites in the top 35 m, it is likely that this ratio will not be much different below 35 m (Fig. 6-10). The C/N ratio of organic matter which has been decomposed through oxygen is very similar to that which is being decomposed through sulphate reduction (17 and 18 respectively). This implies that the C/N ratio of decomposing organic matter is not much influenced by sedimentary redox conditions.

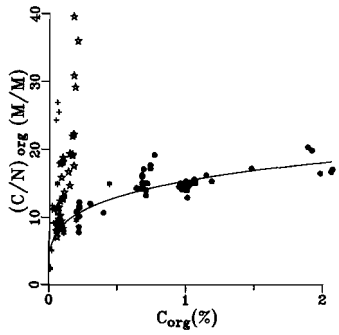

Fig. 6-10.Plot of the molar C/N ratio versus the concentration of C_{org} in samples of core MD10; symbols as in Fig. 6-4.

6-5. CONCLUSIONS

The exchangeable ammonium (N_{ex}) in MAP is directly proportional to the amount of C_{org} present in the sediment and is not related to the amount of ammonium present in the pore water. Only at relatively low organic matter content it is the mineralogy that determines the N_{ex} content. Kaolinite seems to be the clay mineral that is slightly favourable to NH_4^+ adsorption.
There seems to be no difference in the 'quality' of organic matter with respect of NH_4^+-adsorption between the oxidized and reduced parts of each

turbidite, as illustrated by the fairly constant N_{ex}/C_{org} ratio versus depth (Fig. 6-2).

In general, the sediments of the organic-rich turbidites have a relatively high N_{fix} content and N_{fix}/Al ratios, which do not change upon post-depositional oxidation of the organic matter. If the carbonate content is taken into account, then the relative % of illite in the organic-rich turbidites is much higher than in the other turbidites. Therefore, N_{fix} is not associated with organic matter, but with illite.

In the sediments of core MD10 there is a strong correlation between C_{org} and N_{org} (as determined from : $N_{org}=N_{tot}-N_{ex}-N_{fix}$). Post-depositional decomposition of organic matter through oxygen leads to a decrease in the C/N ratio of the remaining organic matter in the upper part of the organic-rich turbidites of the MAP. The decomposed organic matter must therefore have had a relatively high C/N ratio (≈17).

By stoichiometric modelling a C/N ratio of 18 has been derived for the organic matter that is decomposing through sulphate reduction below a depth of 35 m. The identical C/N ratios calculated for organic matter that is decomposed under oxidized and under reduced conditions indicate that redox conditions in the sediment do not affect this C/N ratio.

APPENDIX 6-1.

Details of the N-extraction analytical methods

All extractions have been done on oven-dried sediment (105°C); reported results are the mean of at least duplicate analyses. The concentration of ammonium in blanks that were run occasionally was always non-detectable.

Total Nitrogen (N_{tot}) [after HARTMANN et al., 1971]

To 1 g of sample 6 ml concentrated H_2SO_4 and 0.5 g Se-mix katalyser (Merck) were added; under regular mixing the solutio was gently boiled for half an hour. The colour of the solution changes to white-greenish. The sample-holder was connected to the steamdestillation unit, 25 ml 10 N KOH were added and the ammonium was destilled into 25 ml 1% H_3BO_3 to which 5 drops of mix-indicator A (Merck) were added. The destilled ammonium was determined by back-titration with 0.01 N HCl.

Exchangeable nitrogen (N_{ex}) [after KEENEY & BREMNER, 1966]

After shaking of 3 g of sediment with 10 ml 2N KCl solution, 0.1 g MgO was added followed by flushing with a few ml of bidest. The sample-holder was connected to the steamdestillation unit, 10 ml 10 N KOH were added and the ammonium was destilled as described under N_{tot}.

Fixed Nitrogen (N_{fix}) [after SILVA & BREMNER, 1966]

To 1 g of sample 20 ml of a KOBr/KOH solution (6 ml of Br_2 in 200 ml of 2 N KOH, freshly prepared every day) are added and mixed. After 2 hours the solution is boiled during 1 minute. With 20 ml 0.5 N KCl solution the mixture is flushed into a 50 ml centrifuge tube, which is centrifuged during 10 minutes. The liquid is decanted and the sediment is mixed again with 20 ml 0.5 N KCl solution followed by centrifuging and decanting again. Approximately 20 ml of a HF/HCl (5N HF/ 1N HCl) solution are added to the remaining sediment, which is subsequently shaken for 24 hours. The suspension is then transferred quantitatively into a kjeldahl flask as little water as possible, and after the addition of 20 ml 10 N KOH solution the ammonium is destilled as described previously under N_{tot}.

Organic Nitrogen (N_{org})

The organic nitrogen content of the sediment is calculated according to

$$N_{org} = N_{tot} - N_{fix} - N_{ex}$$

APPENDIX 6-2.

TABLE
Analytical errors of in-house standard that has been analysed in the same series as the reported samples.

	NAP84 (n=6)
N_{ex}	11.4 ± 2.6
N_{fix}	294 ± 14
N_{tot}	1930 ± 72

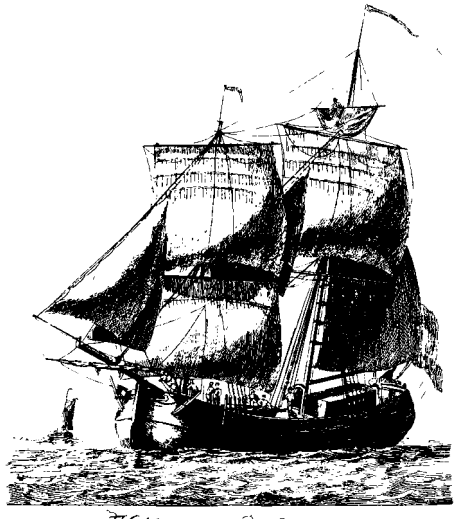

B een Hoeker met een Barkentyn tuyg 7

Chapter 7

PHOSPHORUS COMPOUNDS

(as found by selective extraction)

ABSTRACT

For most samples in core MD10 'carbonate-associated + exchangeable phosphate' (P_{ex}) forms a minor fraction of the total sedimentary phosphorus. The relatively high P_{ex} and the moderately high 'apatite-P' (P_{HCl}) for the sediment of turbidite e may point to a source area that is possibly upwelling-related. For most samples apatite-P (P_{HCl}) represents near 80% of the total-P content of the sediment (P_{tot}). The high P_{HCl} for the sediments of the volcanic turbidites (b,g,n,o,p) is caused by a similar provenance area for the volcanic material and for the possibly near-coastal apatite-P.
In addition to the major impact of inherited P to P_{tot}, only some contribution comes from post-depositional re-allocation of Fe and associated P (P_{OH}). This results in a slightly higher P_{OH} concentration in the oxidized parts relative to the reduced parts of turbidites and possibly in enhanced Fe, P levels in some pelagic intervals.
The C/P molar ratio for organic matter in these sediments is much higher than that reported for average marine plankton (1200 versus 106), which may be caused by differential decomposition. The relatively large error in the P_{org} content - a major problem for all P_{org} values reported in the literature - does not permit more firm conclusions to be drawn in this respect.

7-1. INTRODUCTION

Phosphorus is a nutrient which may limit primary productivity in the oceans (see Section 6-1). Unlike nitrogen which has important transfers between the atmosphere and the ocean, phosphorus is added to the ocean primarily by run off and is removed by sedimentation. Through early diagenetic reactions in the sediment, part of the sedimentary P may be regenerated to the sea water. Remobilization of sedimentary P depends on the form in which P occurs in the sediment and on the environmental conditions of the sediment. During decomposition of organic matter in oxidizing sediments part of the released phosphate adsorbs on Fe-oxihydroxides, carbonates and clay minerals (e.g. BERNER, 1973; PRICE, 1976; KROM & BERNER, 1981; DE LANGE, 1986[b]; LUCOTT & d'ANGLEJAN, 1988). In some (mainly estuarine) reducing environments the precipitation of vivianite (Fe[II]-phosphate) and of struvite ($MgNH_4PO_4$) has been reported (e.g. NRIAGU, 1972; MARTENS et al., 1978; POSTMA, 1981). In other environments (mainly upwelling areas) P may precipitate (possibly after initial adsorption on to carbonate) as apatite (e.g. CALVERT, 1976; PRICE & CALVERT, 1978; SUESS, 1981; LUCAS & PREVOT, 1984). During the anoxic reduction of iron, phosphate may be released again

from the Fe-oxihydroxides, whereas apatite is reported to be stable during both oxidizing and reducing conditions. Therefore, depending on the environmental conditions prevailing in the sediment, phosphate may either be released or immobilized. Study of early diagenetic reactions of P and of the various forms of P in the sediment is important to establish the contribution of sediment-derived phosphate to the global fluxes of this essential nutrient for biological growth. Such study is not easy due to the many geochemical variables that affect the partition of P between the different phases in the sediment and to the generally low concentrations of P in these phases. This partly explains the limited number of studies on the distribution of P in the marine environment.

Phosphorus may be associated with various components in the sediment. On a global scale approximately 40% has been reported to occur in the form of organic matter, another 40% in the form of biogenic carbonate, 10% associated with (hydrothermal) Fe-oxihydroxides, 10% as phosphorite deposits and less than 2% in fish debris (FROELICH et al., 1982; MACH et al., 1987; CODISPOTI, 1988). Some controversy seems to exist in the literature on the exact fractions and on the descriptions of the various modes of occurrence of P (e.g. FROELICH et al., 1982; MACH et al., 1987 and refs herein). It is beyond the scope of this thesis to discuss this matter extensively. In this paragraph, only a brief introduction is given of some of the modes of occurrence of phosphorus, on a global scale. The phosphorite and fish-debris deposits often occur within or near zones of upwelling where they may constitute the major form of occurrence of sedimentary P (e.g. SUESS, 1981). For example, in sediments of the Peru continental margin the re-generation of phosphate from fish debris is about 4 times more important than that from decomposing organic matter (SUESS, 1981). In normal hemi-pelagic or continental margin sediments decomposition of organic matter is the major source for dissolved phosphate.

In contrast, during some past epochs enormous phosphorite deposits were formed such as the Permian Phosphoria Formation (e.g.

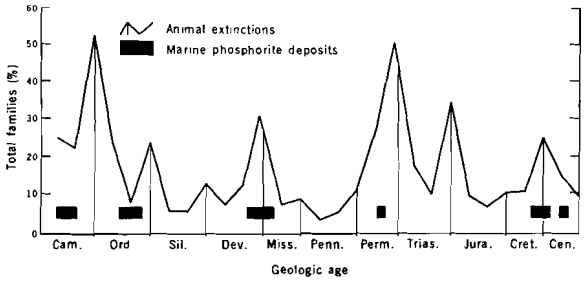

Fig. 7-1. Episodes of extinction in the animal kingdom, and approximate ages of extensive marine phosphorite deposits. The last appearances of animal families through geologic time are given in percentages. Main episodes of extinction occurred near the close of the Cambrian, Devonian, Permian, Triassic, and Cretaceous periods. The size of the symbols designating the age of phosphorite deposits is not intended as an estimate of their relative economic importance nor of their amount of total phosphorus (PIPER & CODISPOTI, 1978).

BATURIN & POKRYSHKIN, 1980; CODISPOTI, 1988), which contain several times as much phosphorus as is present in the present-day ocean (FROELICH et al., 1982). The Cretaceous and Tertiary phosphorite deposits near Marocco/ Mauretania (CRONAN, 1980) may be noteworthy with respect to the present study (see Fig. 5-1; Section 7-4). Major intervals of phosphorite deposits of marine origin have accumulated during only a few intervals of geologic time. These deposits are usually associated with black shales and seem to have formed under reducing conditions in areas of high productivity or upwelling. A correlation has been suggested between periods of extensive phosphorite deposition and the occurrence of animal extinction (Fig. 7-1; PIPER & CODISPOTI, 1975). During these past epochs phosphate instead of nitrate may have been the limiting nutrient for primary productivity in the oceans (CODISPOTI, 1988).

Selective extractions

This study will focuss on the various forms of P in the sediment as found by selective extraction. Such a study will not only give insight into the early diagenesis of P, but may also indicate past environmental conditions or possible source areas for the sediment. In a preliminary study, using some representative samples of core MD10, the effect of drying on the various forms of P extracted from the sediment had been tested. Prior to extraction these samples had been freeze-dried (with all handling under nitrogen), oven-dried at 40°C or oven-dried at 105°C. The results were compared with those obtained from extraction of identical but untreated ('wet') samples. No significant deviations were found between results from identical samples that had undergone different pre-treatments. Therefore, all extractions for the present study were done on oven-dried (24 hours, 105°C) and powdered sediment. The selective extractions that will be discussed in this chapter have been reported to discriminate between the various modes of occurrence of P in marine and fresh-water sediments (e.g. HIELTJES, 1980; VAN ECK, 1981). This method is an adaption of previously published methods, mainly originating from analytical techniques in soil science (WILLIAMS et al., 1967; WILLIAMS et al., 1976; HIELTJES & LIJKLEMA, 1980 + refs herein). The latter authors have demonstrated the suitability of this method compared to other methods by

TABLE 7-1. Percent of ortho-phosphate extracted from dry, powdered synthetic and natural P-compounds by various reagents.

Extractant	(1)	(2)	(3)	(4)	(5)
1*N* NH_4Cl (pH7)	3-6	4-6	5-7	4-6	10
0.1*N* NaOH	<1	<1	98.9	91.0	4
0.5*N* HCl	100.8	98.9	98.6	100.0	92

Total amounts of P in samples varied between 0.2 and 4 mg; 50 ml of reagent in each extraction. (1): hydroxy-apatite ($Ca_5(PO_4)_3OH$; Riedel-de Haen A.G., chem. pure). (2): calcium phosphate ($Ca_3(PO_4)_2$;Merck, chem. pure). (3): ironhydroxy-phosphate ('Fe-P';see HIELTJES & LIJKLEMA, 1980) (4): aluminium ortho-phosphate ($AlPO_4.H_2O$; BDH, chem. pure). (5): phosphorite nodule originating from the base of the b-turbidite, core 82PCS16; 31°20,8' N, 24°16,6' W; results from this study, cf text). Table after HIELTJES & LIJKLEMA, 1980)

extracting synthetic phosphate compounds using the different methods (Table 7-1). In the present study the selective extractions have also been applied to a phosphorite nodule that was found near the base of the b-turbidite in core 82PCS16 (31°20,8' N, 24°16,6' W; KUIJPERS et al., 1984[a]). Most of the P of the phosphorite nodule (containing ≈10% apatite) has been extracted with the 'apatite-P' extraction step. The fractionation procedure used in this study is indicated in Table 7-2; details on the extraction and on the analytical errors are given in Appendix 7-1,2. Only a brief summary is given here, for a more extensive discussion reference is made to HIELTJES & LIJKLEMA (1980) and VAN ECK (1981). The NH_4Cl extraction has been reported

TABLE 7-2. Extraction procedure used in this study.

Extractant	Form of phosphorus extracted
2*N* NH_4Cl	Loosely bound (exchangeable + carbonate-associated) [P_{ex}]
0.1*N* NaOH	Fe,Al-associated [P_{OH}]
0.5*N* HCl	Ca-associated (apatite) [P_{HCl}]
$K_2S_2O_8/H_2SO_4$	Rest [P_R]
$K_2S_2O_8/H_2SO_4$	Total [P_{tot}]

TABLE 7-3. Correlation Matrix of extracted P-phases and some major and trace elements for samples of core MD10

	C_{org}	P_{ex}	P_{OH}	P_{org}	P_{HCl}	P_R	P_{sum}	P_{tot}	Sr	Na	Ti	Zr	Li	V
C_{org}	1.00													
P_{ex}	.02	1.00												
P_{OH}	-.11	-.16	1.00											
P_{org}	.34	-.12	.24	1.00										
P_{HCl}	-.23	.16	.24	.18	1.00									
P_R	.14	-.01	.31	.47	.40	1.00								
P_{sum}	-.19	.20	.44	.25	.97	.53	1.00							
P_{tot}	-.07	.18	.39	.31	.92	.54	.95	1.00						
Sr	-.30	.17	-.61	-.42	-.10	-.33	-.24	-.30	1.00					
Na	-.14	.30	.13	.14	.65	.49	.67	.66	-.17	1.00				
Ti	-.22	.05	.44	.22	.72	.43	.76	.75	-.42	.73	1.00			
Zr	-.22	.03	.36	.19	.66	.36	.69	.66	-.30	.61	.75	1.00		
Li	.44	-.15	.53	.51	-.01	.35	.13	.22	-.86	.07	.23	.16	1.00	
V	.10	-.23	.62	.44	.35	.55	.48	.52	-.76	.45	.69	.51	.73	1.00
Fe	.00	-.09	.65	.42	.50	.57	.63	.66	-.77	.53	.82	.62	.71	.89
Mn	-.62	.03	-.12	-.23	.41	-.00	.33	.24	.57	.26	.34	.26	-.65	-.16
Mg	.27	.06	.49	.48	.41	.46	.52	.58	-.79	.49	.64	.46	.83	.82
Zn	.33	-.11	.62	.53	.25	.49	.40	.48	-.85	.28	.52	.39	.92	.84
Al	.26	-.13	.65	.51	.18	.50	.35	.41	-.89	.27	.49	.39	.94	.86
K	.19	-.08	.58	.51	.21	.40	.35	.40	-.84	.22	.45	.35	.91	.79
Y	-.02	-.27	.71	.36	.30	.48	.44	.45	-.69	.27	.50	.46	.69	.76
Ni	.19	-.39	.57	.35	.10	.40	.22	.28	-.57	.13	.40	.25	.62	.72
N_{ex}	.87	-.03	.02	.44	-.19	.32	-.12	.00	-.40	-.02	-.09	-.08	.57	.26
N_{fix}	.41	-.05	.52	.36	-.05	.22	.09	.16	-.83	.07	.23	.16	.87	.65
N_{org}	.98	-.01	-.10	.38	-.26	.16	-.22	-.10	-.32	-.18	-.25	-.24	.52	.14
N_{tot}	.97	-.01	-.04	.40	-.25	.18	-.20	-.07	-.39	-.16	-.21	-.21	.58	.20
Ca	-.31	.05	-.59	-.48	-.23	-.44	-.37	-.45	.95	-.31	-.55	-.41	-.86	-.81

	Fe	Mn	Mg	Zn	Al	K	Y	Ni	N_{ex}	N_{fix}	N_{org}	N_{tot}	Ca
Fe	1.00												
Mn	-.12	1.00											
Mg	.89	-.32	1.00										
Zn	.86	-.46	.90	1.00									
Al	.88	-.47	.89	.97	1.00								
K	.82	-.43	.89	.93	.94	1.00							
Y	.78	-.27	.62	.79	.81	.74	1.00						
Ni	.61	-.12	.52	.69	.67	.56	.67	1.00					
N_{ex}	.19	-.65	.36	.49	.46	.36	.18	.29	1.00				
N_{fix}	.61	-.61	.73	.81	.84	.81	.61	.55	.47	1.00			
N_{org}	.03	-.67	.31	.39	.32	.27	.03	.22	.90	.44	1.00		
N_{tot}	.09	-.70	.37	.45	.39	.34	.09	.27	.91	.52	.995	1.00	
Ca	-.85	.48	-.87	-.91	-.92	-.87	-.69	-.58	-.46	-.81	-.34	-.41	1.00

(n=130)

to remove exchangeable and carbonate-associated phosphate. Incomplete removal of carbonate may result in resorption of phosphate liberated during the NaOH extraction. Therefore the NH_4Cl extraction must be prior to the other extractions. The NaOH extraction has been reported to remove Fe- and Al-associated phosphate. Only a minor fraction of apatite-P is removed during this extraction. The HCl-extraction has been reported to remove quantitatively the apatite-P but also Fe- and Al-associated P. Therefore, this extraction must follow the NaOH extraction.

The various P phases only demonstrate relatively low correlations with other sediment constituents (Table 7-3). This could in part be due to the relatively low concentrations in some fractions and the concurrent analytical problems. However, a high correlation exists between total-P (P_{tot}) and the sum of the extracted P (P_{sum}) (R=0.95; Table 7-3). In addition, the slope of the regression line in the plot of P_{tot} versus tab 7-3 P_{sum} is 1 and passes through the origin. Therefore, no large errors may have been introduced during the extractions.

Factor analysis resulted in 3 main factors (Table 7-4, 5) which seem to represent 'carbonate-dilution / clay-fraction' (Factor 1), 'apatite / volcanic fraction' (Factor 2) and 'organic fraction' (Factor 3) respectively. In factor 1 all carbonate-associated elements have a negative loading (Ca, Sr, Mn and P_{ex}), whereas the Fe,Al-oxihydroxide/silicate associated elements have a positive loading (Al, Fe, Mg, Zn,....N_{fix} and P_{OH}. Factor 2 includes high loadings for elements related to the volcanic turbidites tab 7-4 (Ti, Zr, P_{HCl},.). In factor 3 the constituents related to organic matter give a high loading (C_{org}, N_{ex}, N_{org}, but also P_{org}). The various P-fractions show up in different factors just as could be expected, although not always with a high factor loading. Therefore, the available extraction technique for distinguishing different P-phases yields results that are much more informative than total analysis only. The results of the individual extractions will be discussed in the next sections. It must be realized that the P-phases removed by the various extraction

TABLE 7-4. Eigenvalue (Ev), percentage of variance (%V) and cumulative percentage (%C) for the factor analysis shown in Table 7-3.

Factor	Ev	%V	%C
1	12.7	47.1	47.1
2	6.2	22.6	69.7
3	2.4	9.0	78.7

TABLE 7-5. Rotated Factor Matrix of extracted P-fractions together with some major- and trace-constituents for samples of core MD10 (n=130).

	Factor 1	Factor 2	Factor 3
C_{org}	0.10	-0.12	0.95
P_{ex}	-0.12	0.24	0.06
P_{OH}	0.70	0.19	-0.21
P_{org}	0.30	0.30	0.47
P_{HCl}	0.03	0.91	-0.14
P_R	0.23	0.61	0.30
P_{sum}	0.20	0.92	-0.12
P_{tot}	0.24	0.90	-0.00
Sr	-0.91	-0.09	-0.21
Na	0.12	0.81	-0.05
Ti	0.40	0.79	-0.21
Zr	0.29	0.72	-0.19
Li	0.89	0.00	0.40
V	0.77	0.43	0.08
Fe	0.78	0.56	-0.00
Mn	-0.51	0.44	-0.56
Mg	0.79	0.45	0.26
Zn	0.87	0.29	0.31
Al	0.92	0.23	0.24
K	0.90	0.21	0.18
Y	0.77	0.28	-0.05
Ni	0.59	0.16	0.14
N_{ex}	0.25	-0.04	0.90
N_{fix}	0.87	-0.06	0.31
N_{org}	0.15	-0.16	0.96
N_{tot}	0.24	-0.16	0.94
Ca	-0.89	-0.27	-0.27

Factor 1 indicates: carbonate dilution/ Fe,Al-oxihydroxide/silicate. Note P_{OH} and N_{fix}. Factor 2 indicates: apatite/ volcanic group. Factor 3 indicates: organic group.

steps are operationally defined. They must, therefore, be interpreted with some caution. The analytical data have not been included in this chapter because in general they contribute little to the conclusions. Instead of analytical data, statistical and graphical representations have been used in reporting the results.

7-2. EXCHANGEABLE AND CARBONATE-ACCOCIATED PHOSPHATE (P_{ex})

The NH_4Cl extraction at pH 7 has been reported to remove the exchangeable and the carbonate-associated phosphate (e.g. HIELTJES & LIJKLEMA, 1980). According to these authors, incomplete removal of carbonate may result in resorption of phosphate liberated in the following (NaOH-) extraction.
Initial tests had demonstrated total dissolution of carbonate using 50 mg of sample and 25 ml of extractant, while the extracted phosphate was still detectable. Using larger volumes of extractant resulted in lower concentrations of phosphate in the extract which increased the analytical error. However, only ≈30% carbonate has been dissolved during the extractions of the present study, whereas on average 50% carbonate is present in the samples. Incomplete dissolution could be due to (Fe,Mn) coatings which have been reported to account for most of the P-content in foraminifera (PALMER, 1985; SHERWOOD et al., 1987). In view of the relatively constant amount of carbonate that has been dissolved even for the carbonate-rich intervals, a 'saturation' of the extraction solution seems more likely despite contrary results obtained during preliminary test runs. This discrepancy is not yet understood. The amount of phosphate released during the NH_4Cl extraction is minor and the plot of P_{ex} versus depth shows almost no fluctuation (Fig. 7-2[a]). In contrast, the plot of P_{ex}/Al versus depth clearly demonstrates not only distinct differences between turbidites, but also the association of part of the P_{ex} with carbonate (Fig. 7-2[b]). However, the low carbonate content of some samples does not correspond to a similarly low value of P_{ex} (Fig. 7-2). Therefore, carbonate-associated P accounts for only part of the P_{ex}. The concentration of phosphate in the pore water has been reported to be always below ≈12 µM (DE LANGE et al., 1988; see also Chapter 2). The contribution of the pore-water phosphate to the first extraction step is therefore undetectable.
Reported values for carbonate-associated phosphate are near 160 ppm P calculated for pure $CaCO_3$ (ARRHENIUS, 1959 [Pacific Ocean]; MORSE & COOK, 1978 [Atlantic Ocean]). This value lies between the reported values of phosphate associated with foraminifera (50 ppm) and coccoliths (400 ppm) (FROELICH et al., 1982). It must be noted here, that even lower values have been reported for carbonate-associated P (or carbonate-lattice P) in thoroughly cleaned foraminifera (PALMER, 1985 [< 3 ppm P] and SHERWOOD et

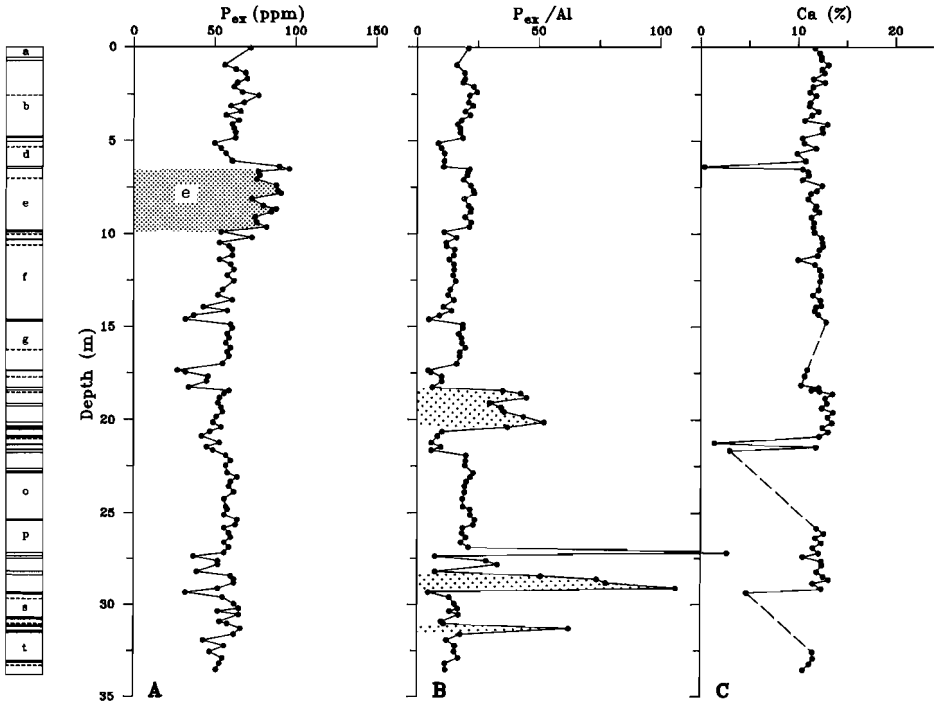

Fig. 7-2. Profiles versus depth in core MD10 of NH_4Cl-extracted: a. phosphate (P_{ex}), c. Ca (mainly as $CaCO_3$), and of the (P_{ex}/total-Al) ratio (b). The average amount of extracted Ca (12%) corresponds to approximately 30% $CaCO_3$. 'Calcareous' turbidites are stippled on the relevant geochemical logs.

al., 1987 [18 ppm P]). If the reported average value of 160 ppm P in carbonate is valid for samples of the MAP too, then the in-house MAP standard MM82 (12% $CaCO_3$) would have a content of 19 ppm carbonate-associated-P. This value is in fact identical to the value found in a NaAc/HAc pH5 'carbonate' extraction (Table 7-6). This extraction was preceded by a NH_4Ac pH8.2 'exchangeable' extraction. The sum of these 2 steps for MM82 is similar to the phosphate extracted by a 2 N NH_4Cl 'exchangeable + carbonate' extraction. This finding confirms the relative magnitude of the carbonate-P contribution.

During the NH_4Cl extraction of the samples only approximately 30% carbonate has dissolved (Fig. 7-2). Following the above-made assumption, this would represent a release of ≈48 ppm carbonate-associated phosphate, provided that no significant (re-)adsorption has occurred on the remaining carbonate. The small differences between calculated and measured P_{ex} concentration suggest that adsorption is minor (Fig. 7-2). The observation that the negative

TABLE 7-6. Some extraction results of in - house standard MM82 (n=6).

Extractant	ppm P
NH_4Cl pH7	40 ± 4 (a)
NH_4Ac pH8.2	21 ± 5 (b)
NaAc/HAc pH5	19 ± 1 (b)

a. colorimetric analysis
b. ICPES analysis
indicated error: 1σ

carbonate spikes do not show up in the profile of P_{ex} versus depth (Fig. 7-2) indicates that in these samples (with complete carbonate dissolution [Fig.7-3]) the relative contribution of non-carbonate-associated P is at least as important as the carbonate-associated P is in other samples. For most samples there seems to be a source of P in excess of the calculated 48 ppm 'carbonate-associated P', especially for the samples of turbidite e (Fig. 7-2[a],4). The excess-P of almost all samples can easily be explained by a minor (2-5%) contribution from apatite-P (see section 7-1). For samples from the e-turbidite a 10% contribution would be necessary. The relatively high excess-P values for this turbidite compared to others could be caused by a different apatite, or alternatively could be explained by a relatively higher content of coccoliths versus foraminifera compared to other turbidites (see above). At present, no quantitative data are available on the relative abundance (including fragments) of coccoliths versus foraminifera (VERBEEK, 1984; TROELSTRA, 1984). On the basis of diatom assemblages the e-turbidite has been reported to be distinctly different from other turbidites (i.e. turbidites a,b,d,f,g; KUIJPERS et al., 1984[b]). In addition, the diatom assemblages in the e-turbidite seem upwelling-related. The different diatom

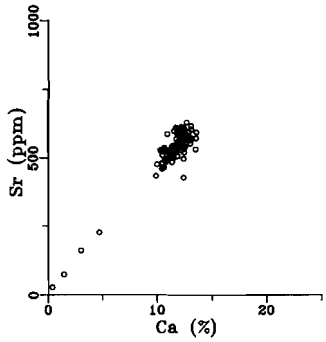

Fig.7-3. Plot of NH_4Cl-extracted Ca versus Sr. The carbonate of the 4 samples near the origin has been totally dissolved, whereas the carbonate dissolution of the other samples seems to demonstrate 'saturation'.

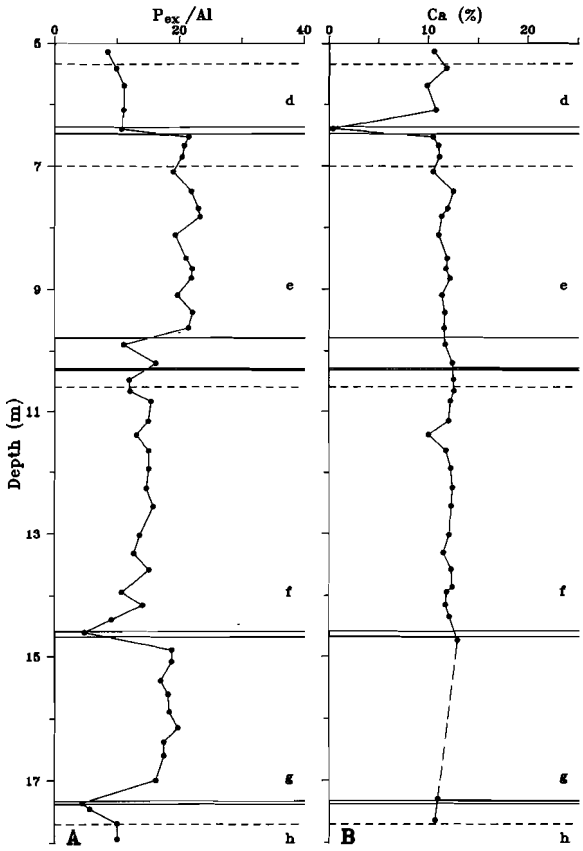

Fig. 7-4. Profiles versus depth in the interval from 5-18 m in core MD10 for: a. (P_{ex}/total-Al), and b. NH_4Cl-extracted Ca.

assemblages and the influence of upwelling could be in support of both options discussed above, namely a different micro-fossile composition and an apatite of different composition (e.g. fish bones). Therefore, at present no firm conclusions can be drawn concerning the possible cause of the relatively high P_{ex} content of samples from the e-turbidite. In view of the findings in the HCl extraction (Section 7-4), a different apatite composition seems the most likely.
Phosphate adsorption in laboratory experiments has been reported to show large differences between oxic and anoxic conditions (LUCOTTE & d'ANGLEJAN, 1988). In the sediments of core MD10 no such differences are observed in the P_{ex} or in the P_{ex}/Al within each turbidite (Fig. 7-4). It is only within each turbidite that (paleo-) redox conditions may change , whereas the mineral composition -including the carbonate content- remains relatively constant. Differences in P_{ex}/Al are only observed between turbidites, i.e. between samples with a different mineral composition. Therefore, in contrast to N_{ex} (see Section 6-2), P_{ex} and P_{ex}/Al are obviously not influenced by redox conditions in the sediment but only by the mineral composition.

7-3. IRON- AND ALUMINIUM-ASSOCIATED PHOSPHATE (P_{OH})

The 0.1 N NaOH extraction has been reported to remove the Fe- and Al-associated phosphate (e.g. WILLIAMS et al., 1976; HIELTJES & LIJKLEMA, 1980; LINDSTRÖM, 1980; VAN ECK, 1981). This extraction may also remove some organic-P, which may not be determined in the analysis of ortho-phosphate (see Section 7-6, and Appendix 7-1). The NaOH extraction seems suitable for synthetic and natural P-compounds (Table 7-1) in that almost all of the Fe- and Al-associated P are extracted, but only small fractions of apatite-P.
The plots of P_{OH} and of P_{OH}/Al versus depth in core MD10 demonstrate only a few significant fluctuations (Fig. 7-5). Pelagic intervals have high concentrations of P_{OH} , whereas the carbonate-rich intervals ($CaCO_3$ > 80%) have high P_{OH}/Al ratios (Fig. 7-5,6). The high values for P_{OH}/Al could indicate that part of the extracted phosphate is carbonate-related. An alternative explanation could be that a small fraction of the carbonate-associated phosphate that had been liberated during the NH_4Cl extraction and had re-adsorbed on the large amount of $CaCO_3$ still present (50%), has been released again during the NaOH extraction. These two possibilities are highly unlikely, because during the NaOH extraction no carbonate has dissolved and adsorption (on carbonate) rather than desorption is likely to occur (HIELTJES & LIJKLEMA, 1980). A small 'excess' fraction will show up especially in the low-Al-containing (i.e. carbonate-rich) samples. A minor contribution from possibly extracted apatite (2% or less of the total

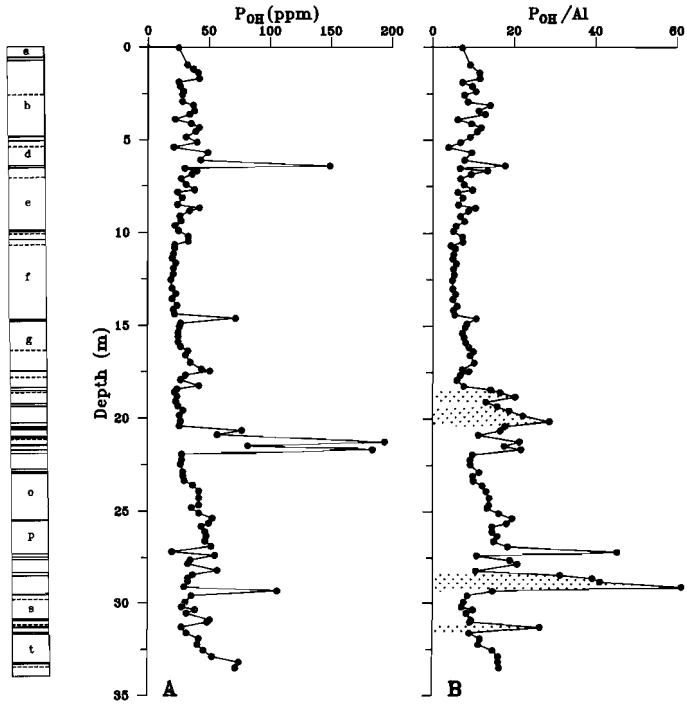

Fig.7-5. Profiles versus depth in core MD10 of : a. NaOH-extracted phosphate (P_{OH}) and of : b. the (P_{OH}/ total-Al) ratio. Stippled areas are 'calcareous' turbidites.

apatite would suffice) would have this effect. The most likely explanation, however, is the occurrence of (Fe,Mn) coatings on carbonate micro-fossiles. These coatings have been reported to account for most of the P present in carbonate-rich sediments (SHERWOOD et al., 1987). In addition, it must be noted that a P_{OH} concentration of approximately 20 ppm P_{OH} has been found in the reducing (pyrite containing) sediments near the base of core MD10, which cannot be attributed to the presence of Fe(III)-oxihydroxide/ phosphate phases. Therefore, also here it is necessary to assume a phosphate-containing phase (possibly a minor fraction of apatite) that has been liberated during the NaOH extraction.

There seems to be a positive relationship between P_{OH} and the total Fe and Al concentration (Fig. 7-7). In contrast there is a negative correlation with total Ca (most of which is present as $CaCO_3$), demonstrating the effect of carbonate dilution. To eliminate the effect of carbonate dilution variables can be plotted as their ratio to Al (see Chapter 5; Fig. 7-8). The resulting plots clearly demonstrate that P_{OH} is related to the sum of the different P fractions (P_{sum}), but is not related to the total Fe content of the sediment. The apparent correlation in Fig. 7-7 is therefore

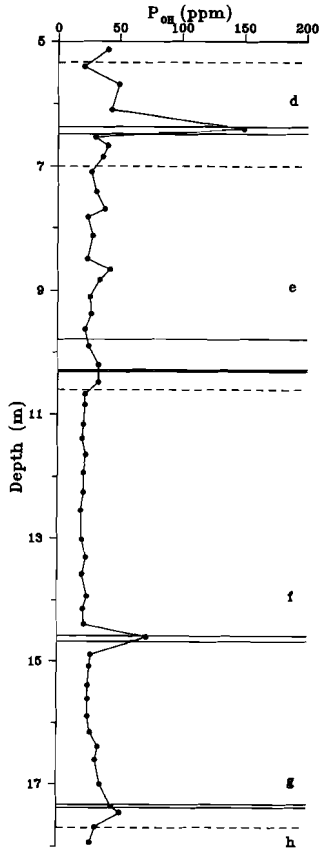

Fig. 7-6. Profile of P_{OH} versus depth in the interval from 5-18 m in core MD10.

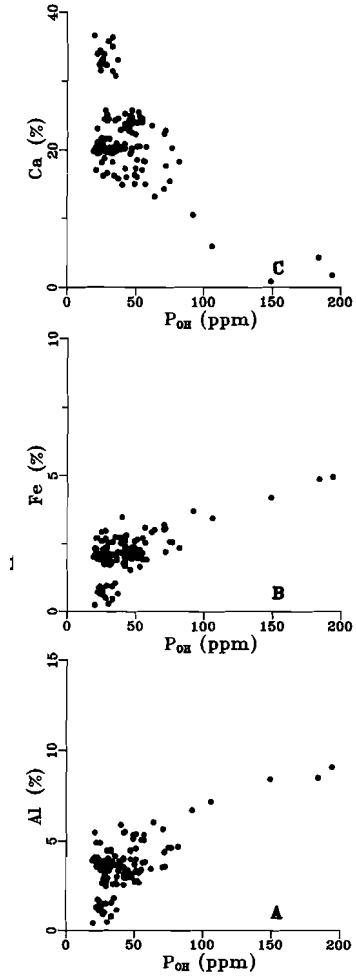

Fig. 7-7. Plots of P_{OH} versus: a. total-Al, b. total-Fe, and c. total-Ca.

entirely due to carbonate dilution which affects these sediment constituents in a similar way. The lack of correlation with Fe (or Fe/Al) is caused by the large amount of Fe to which no phosphate is likely to be associated, such as magnetite-Fe (reported for the volcanic turbidites) and pyrite-Fe (reported for the organic-rich turbidites). (WENSINK, 1984; DE LANGE et al., 1987[a]; Chapter 5). Obviously, these high amounts of Fe and of Al (not shown in plot) that are not associated to P may obscure such relationships.

For most organic-rich turbidites the concentration of P_{OH} within each turbidite is slightly higher in the upper, oxidized part, than in the

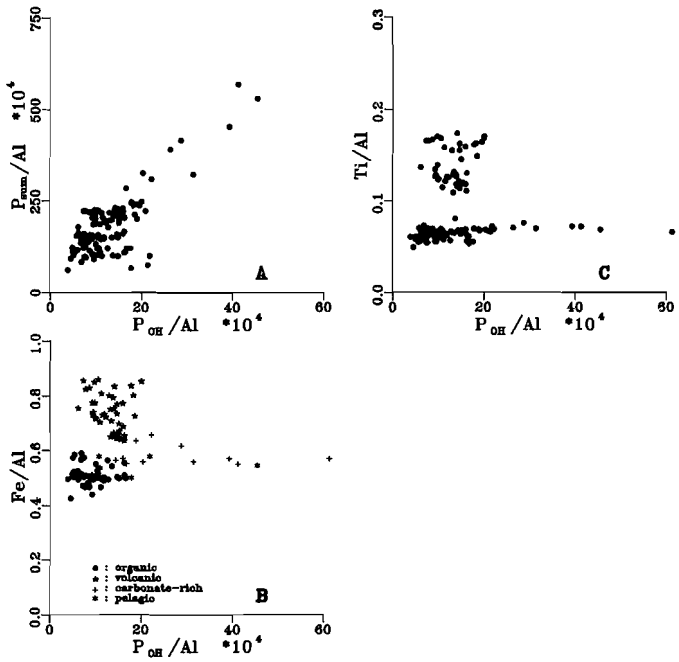

Fig. 7-8. Plots of (P_{OH}/total-Al) versus: a. (P_{sum}/total-Al), b. (total-Fe/total-Al), and c. (total-Ti/total-Al).

lower, reduced part (Fig. 7-6). Turbidite d is the only exception. Some elements have been reported to indicate a complete 'burn-down' of this turbidite, although in the lower part the organic C content is still relatively high (DE LANGE et al., 1987[a]; JARVIS & HIGGS, 1987). In the provenance study of the sediments of core MD10, but more specifically in the statistical sub-partitioning within the organic-rich group, deviations have been reported for turbidite d too (see also below). The general observation is that the P_{OH} content in the organic-rich turbidites is slightly higher in the oxidized part than in the reduced part.
Upon deposition in the MAP the turbiditic sediments of core MD10 must have contained relatively low concentrations of P_{OH}. This seems plausible, because :

- the ***organic-rich reducing sediments*** lack the presence of Fe(III)-oxihydroxides as a carrier/catalytic phase

- the ***organic-poor, oxidized sediments*** contain low concentrations of P_{OH} at present and are unlikely to have decreased in P_{OH} content ever since their deposition

Therefore, the only change that seems to have occurred in the P_{OH} content of the turbiditic sediments in core MD10 is a slight increase in the oxidized parts of the organic-rich turbidites. Part of the phosphate and iron generated during early diagenetic reactions may have been immobilized in the oxidized parts of these turbidites.

High absolute P_{OH} values are mainly confined to pelagic intervals (Figs. 7-5,6). Results obtained on recent to sub-recent pelagic sediments from the South Atlantic with 50% $CaCO_3$ give values of near 30 ppm as P_{OH}, whereas those for Tertiary pelagic sediments in the Atlantic and Pacific Ocean are much higher (300-800 ppm) (FROELICH et al., 1982; DE LANGE, unpublished results). Most pelagic sediments on the present ocean floor are not so much enriched in P or P_{OH}. However, considerable enrichment in total P may occur in pelagic sediments with a large hydrothermal Fe-oxihydroxide component on to which large amounts of seawater-phosphate have been scavenged (BERNER, 1973; FROELICH et al., 1973; FROELICH et al., 1982). For carbonate-depleted sediments from the NAP P_{OH} is approximately 200 ppm. This value is close to that found for carbonate-poor pelagic intervals in core MD10. It seems therefore, that origin and composition of pelagic sediments may in part explain their P_{OH} content. If a hydrothermal component of the presently studied pelagic sediments is excluded, then their excess-P_{OH} -when compared to earlier mentioned (sub-) recent pelagic sediments- is likely to have originated from post-depositional early diagenetic reactions. The concentration of total Fe in some of these intervals is relatively high too (not shown in Fig.). For pelagic sediments from the South Atlantic, NAP and MAP a relatively constant Fe_{tot}/P_{tot} ratio of ≈40 has been found which is identical to the average ratio reported for shale (WEDEPOHL, 1971; DE LANGE, 1986[b]; DE LANGE et al., 1988[b] and unpublished results). However, this ratio is much higher for some of the pelagic intervals in core MD10. This deviation could indicate that post-depositional precipitation of Fe-oxihydroxides or a Fe,Al-silicate phase has occurred in these intervals (Fig. 7-9; and see below). Apparently some P is entrained in such precipitation, but the amount is not necessarily comparable to that scavenged from seawater during extended periods of exposure (i.e. low sedimentation rates). Some re-allocation of iron resulting from reductive dissolution followed by diffusion and subsequent oxidation/precipitation in a more oxidized zone, is known to occur in the sediments of the MAP (DE LANGE, 1984[a]; THOMSON et al., 1987). The reported occurrence of high (total-) P peaks near relic redox boundaries, coinciding with large enrichments of redox-sensitive elements, is further evidence for the re-allocation of phosphate in the MAP sediments (JARVIS & HIGGS, 1987).

In the sediments of NAP similar processes have been shown to occur (see Chapter 4). Reduction of Fe-oxihydroxides has resulted in the generation of Fe^{2+} and of phosphate (e.g. at 1.4 and at 8 m in core 84P1; see Figs. 5-

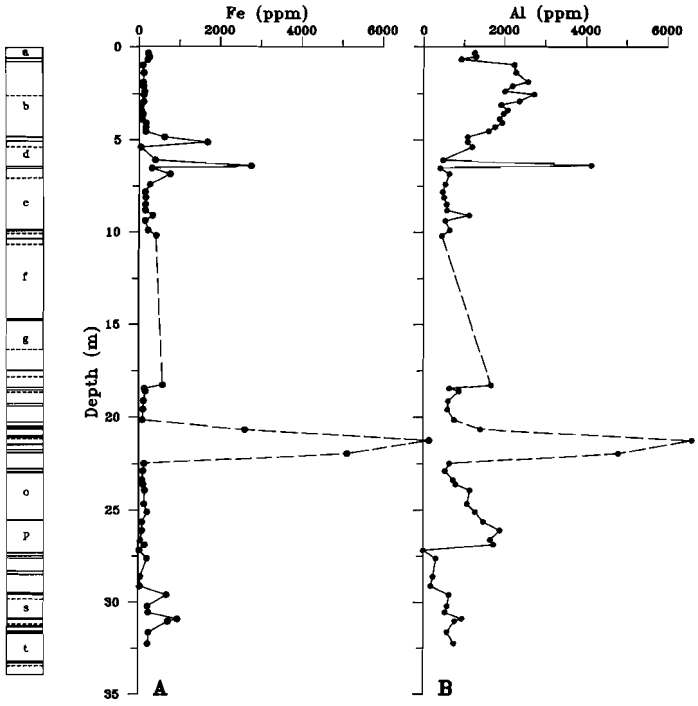

Fig. 7-9. Profiles versus depth in core MD10 for NaOH-extracted: a. Fe, b. Al. Not all extracts could be analysed; no data are available for the interval from 10-18 m.

3a,9), which subsequently have diffused upward and downward until they have precipitated in a more oxidizing environment. This process has resulted in relatively low concentrations of P_{OH} at 1.4 and at 8 m in core 84P1 and in relatively high concentrations in the oxidized zones just above and below these depth intervals (Fig. 5-9). The process of re-allocation of Fe and of phosphate in core 84P1 forms a good example of the early diagenetic mobility of these elements. For the sediments in core MD10 a similar early diagenetic mobility may be able to explain the fluctuations that are observed in the P_{OH} content of these sediments.

7-4. CALCIUM-ASSOCIATED PHOSPHATE / APATITE (P_{HCl})

The 0.5 N HCl solution has been reported to remove quantitatively the apatite-P (CHANG & JACKSON, 1957; WILLIAMS et al., 1967; 1976; LINDSTRÖM 1980; HIELTJES & LIJKLEMA, 1980; VAN ECK, 1981).
The profile of P_{HCl} and of P_{HCl}/Al versus depth in core MD10 demonstrate clear differences that seem to be turbidite-related (Figs. 7-10,11). In the

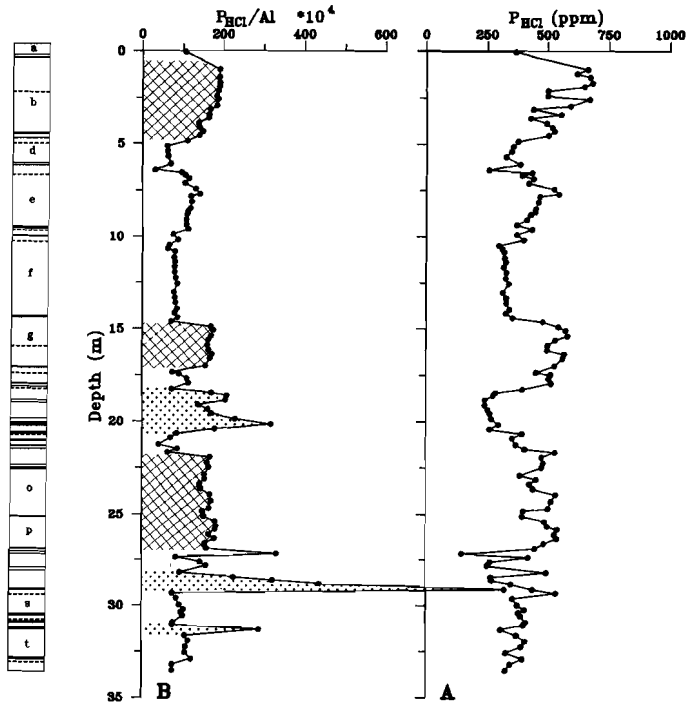

Fig. 7-10. Profiles versus depth in core MD10 of a. HCl-extracted phosphate (P_{HCl}) and b. (P_{HCl}/total-Al). Stippled areas are 'calcareous' turbidites and 'cross-hatched' areas are 'volcanic' turbidites.

P_{HCl}/Al plot the values for carbonate-rich samples are relatively high (see Section 7-3). This must indicate a carbonate-associated apatite-P. The apatite association with carbonate has been observed for lake sediments and in laboratory experiments (see DE KANEL & MORSE, 1978 and refs herein). Even a minor contribution of apatite-P associated with carbonate would show up especially in the samples low in Al (i.e. carbonate-rich samples) (Fig. 7-10). It is unfortunate that on average 1/3 of the total carbonate has dissolved in the HCl extraction, because of incomplete dissolution in the first extraction step (see Section 7-2) (Fig. 7-12). In view of the relatively low concentrations of carbonate-associated P found in the NH_4Cl extraction, only a minor contribution would be expected in the HCl extraction too (at most 40 ppm, see Section 7-2).

The amount of HCl-extracted P that originates from apatite can in general be confirmed by comparison of P_{HCl} and simultaneously extracted Ca, provided that no carbonate is present. However, as a result of carbonate dissolution in the HCl extraction no correlation can be observed between P and Ca (Fig. 7-12).

In the natural sediments studied here not only carbonate and apatite, but

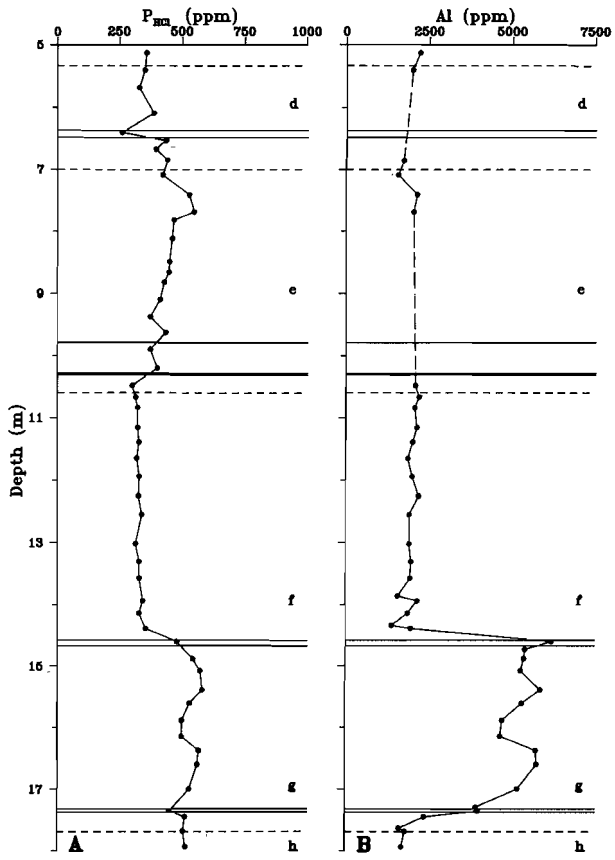

Fig. 7-11. Profiles versus depth in the interval from 5-18 m in core MD10 of HCl-extracted: a. P_{HCl}, and b. Al.

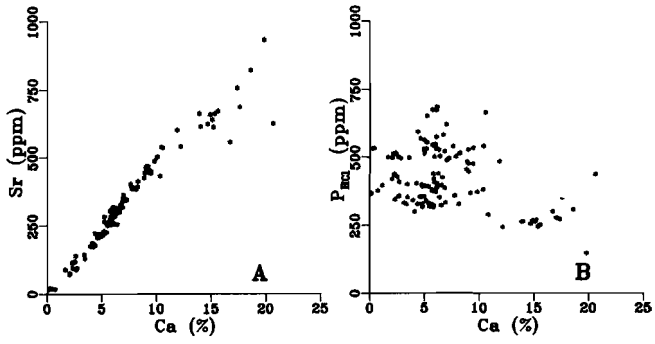

Fig. 7-12. Plots of HCl-extracted: a. Ca versus Sr, and b. Ca versus P_{HCl}. Most Ca and Sr result from carbonate dissolution.

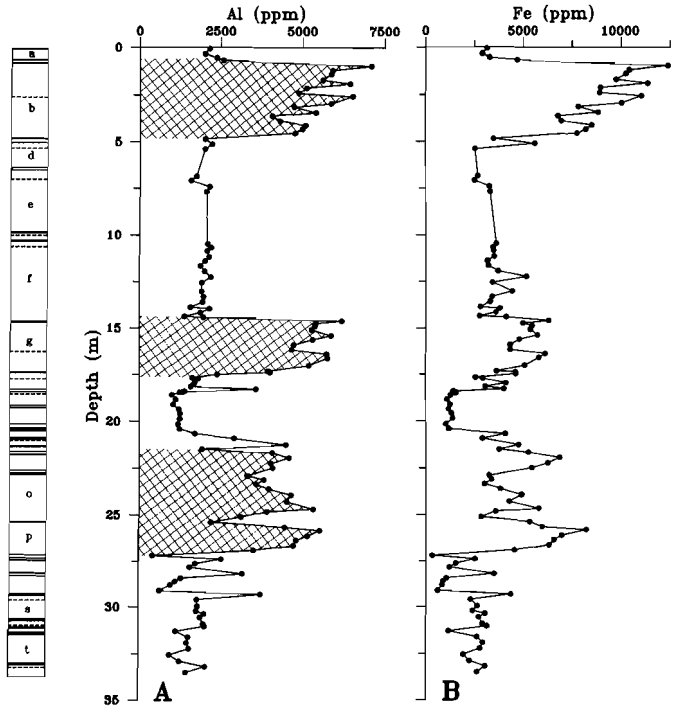

Fig. 7-13. Profiles versus depth in core MD10 of HCl-extracted: a. Al, and b. Fe. 'cross-hatched' areas are 'volcanic' turbidites.

also other minerals have been dissolved in the HCl extraction (Fig. 7-13). In specific for the volcanic turbidites large amounts of Fe, Al (Fig. 7-13) and P (but also Na, Si and to some extent Mg [not shown in Fig.]) have been extracted with HCl. It is therefore necessary to discuss briefly the relative mineral composition of the volcanic turbidites in order to assess a possible contribution of P from non-apatite minerals. The preceding NaOH extraction has been reported to remove quantitatively Fe,Al-phosphate. Therefore, a contribution from this fraction is unlikely. High relative concentrations of smectite have been reported for all volcanic turbidites, but also for all carbonate-rich turbidites and for the organic-rich f-turbidite (KUIJPERS et al., 1984[a]; AUFFRET et al., 1988; Appendix 7-3). Low amounts of P are known to be associated with smectite. The relatively low amount of P extracted from the f-turbidite confirms this finding. It seems therefore likely that the high amount of HCl-extracted P in the volcanic turbidites is not associated with the smectite content of these samples.
Although the extract of only a few samples of the e-turbidite could be analysed for major elements, it is obvious that the amount of extracted Fe and Al in this turbidite is not high, whereas the amount of P is (Figs. 7-10,11,13). Obviously, for this turbidite the amount of HCl-extracted P must

be related to the amount of apatite present in the sediment. In the volcanic turbidites the concentration of total Ti (expressed as Ti/Al in Fig. 5-7) is also considerably higher than in other turbidites and seems to correlate perfectly with the extracted P_{HCl}. The relatively high concentrations of Ti (and of Zr and Fe, compare Figs. 5-7,8,9) have been attributed to the (Ti-)magnetite and zircon content of these turbidites (Chapter 5). It seems therefore, that the simultaneous occurrence of high extracted concentrations of Fe, Al and P for samples from the volcanic turbidites are coincidental, and are only related through their similar provenance.

The acid extraction does not discriminate between various forms of apatite such as fish-debris and phosphorite-P. For example, the slightly enhanced concentration of P_{HCl} that has been found in turbidite e (Figs. 7-10,11; see also Section 7-2) could be fish-debris phosphate from upwelling areas. The in-situ formation of authigenic apatite is highly unlikely in view of the relatively low concentrations of phosphate in the pore water of core MD10.

There are a few other possible sources for P_{HCl} in the volcanic turbidites, namely fish-bone and igneous apatite-P. The scavenging of Zr onto fish-bone apatite has recently been reported for deep-sea sediments from the South Pacific (TLIG, 1988), whereas no Zr enrichment could be demonstrated for fish-bones near the SW African upwelling area (PRICE & CALVERT, 1978). For the base of the b-turbidite olivine, zircon and augite are amongst the minerals that have been reported (GEEL & JONGERIUS, 1984). Therefore, the Zr enrichment found in the volcanic turbidites of this study is likely to originate from an enrichment in heavy minerals and does not indicate a possible contribution of fish-bone apatite.

Apatite is also known to occur as a minor accessory mineral in igneous rocks, where the apatite content rarely exceeds 1% (MCCONNELL, 1973). The composition of the apatite phases in the volcanic turbidites strongly resemble those of a phosphorite pebble found at the base of the volcanic turbidite b (Table 7-7). The concentration of apatite in the phosphorite pebble (Ø 9 mm) is close to 10%, which makes a possible 'igneous origin' unlikely (M. VAN BERGEN, Pers. Commun.). The large resemblance of the b-turbidite and the other volcanic turbidites (as far as can be judged from extractions, total composition and sedimentary descriptions) would

TABLE 7-7. Extracted phosphate concentrations in % of the total extracted P (P_{tot}), average values are given for turbidites and for the phosphorite pebble. In addition the averages per provenance group have been given.

Turb.	p	n	P_{ex}	P_{OR}	P_{HCl}	P_R
b	v	16	9	6	78	7
g	v	9	9	7	78	7
n	v	3	9	5	79	7
o	v	9	10	6	77	7
p	v	6	9	7	77	7
avg.	v	43	9	6	78	7
d	o	4	11	8	74	7
e	o	14	14	7	73	7
f	o	15	12	6	71	10
h	o	3	7	9	76	9
s	o	5	12	7	74	8
t	o	5	10	8	74	8
u	o	2	11	15	69	5
avg.	o	48	12	7	73	8
j	c	3	15	6	70	9
l	c	4	14	7	73	5
r	c	4	14	8	76	3
avg.	c	11	14	7	73	5
phosphorite nodule		2	10	4	82	4

n=number of samples; p=provenance group; v=volcanic; o=organic-rich; c=carbonate-rich

similarly not allow for such an igneous source of apatite-P for these turbidites. The Canary Islands and Madeira have been suggested as source areas for the volcanic turbidites (e.g. DE LANGE et al., 1987). In the same ENE direction large near-coastal Tertiary phosphorite deposits are known to occur (e.g. CRONAN, 1980 and refs herein). A similar source area seems therefore the most likely explanation for the simultaneous occurrence of volcanic material, heavy minerals and apatite in the volcanic turbidites.

7-5. REMAINING PHOSPHORUS (P_R) AND TOTAL PHOSPHORUS (P_{sum} and P_{tot})

a. Remaining Phosphorus (P_R)

The phosphorus that remains in the sample after the HCl extraction has been dissolved in $K_2S_2O_8/H_2SO_4$ (see Appendix 7-1). The concentration of the remaining phosphate is relatively constant with depth at a value of near 50 ppm P (Fig. 7-14). It is only the carbonate-rich samples that have lower values. In view of their much lower non-carbonate mineral content this is not surprising. Accordingly, the low-carbonate pelagic intervals have

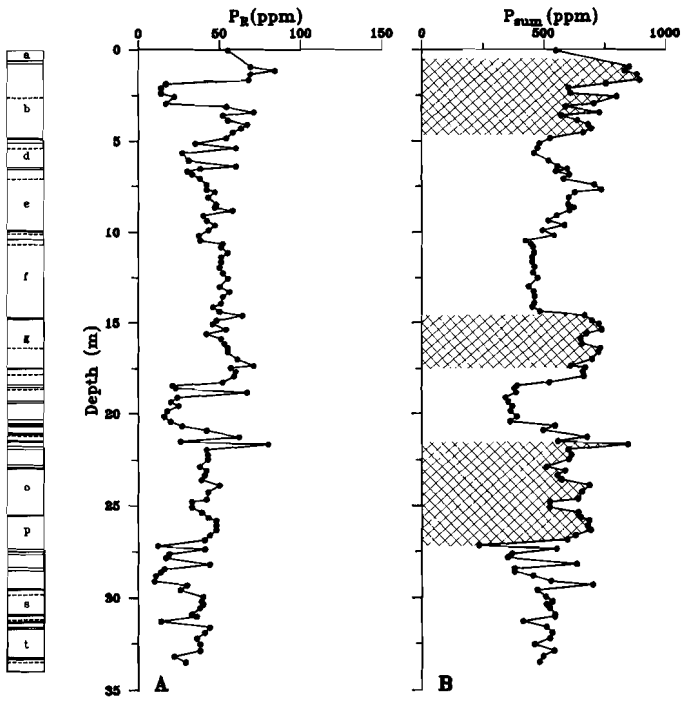

Fig. 7-14. Profiles versus depth in core MD10 for: a. remaining phosphate (P_R) and b. the sum of extracted P-fractions (P_{sum}). 'cross-hatched' areas are 'volcanic' turbidites.

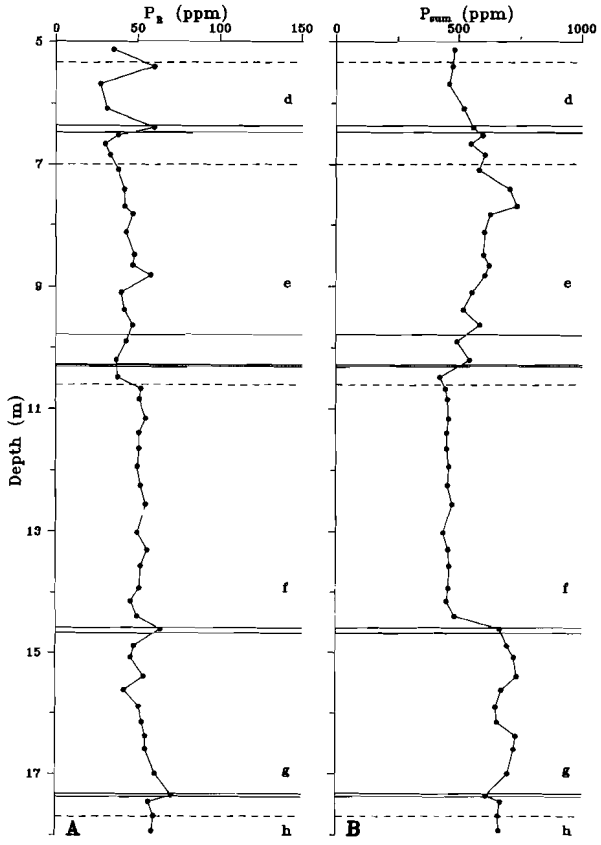

Fig. 7-15. Profiles versus depth in the interval from 5-18 m in core MD10 for a. P_R and b. P_{sum}.

slightly higher values (Figs. 7-14,15). There is no clear difference for P_R around the redox boundary within each of the organic-rich turbidites.

b. Total Phosphorus (P_{sum} and P_{tot})

The sum of the different P extractions (P_{sum}) demonstrates excellent correlation (R=0.95) with the independently determined total P content (Table 7-3). In addition, the slope of the regression line in the plot of

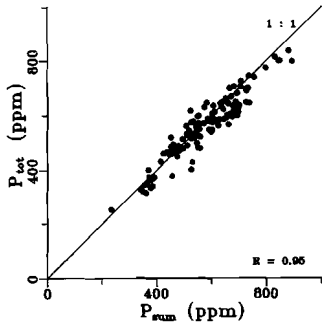

Fig. 7-16. Plot of total-phosphate (P_{tot}) versus the independently determined sum of extracted phosphate (P_{sum}).

P_{sum} versus P_{tot} is near 1 and passes through the origin (Fig. 7-16). The profiles of P_{sum} or P_{sum}/Al versus depth are very similar to those of P_{HCl} (Fig. 7-14,15) and to those of P_{tot} (not shown in Fig.). All three parameters are strongly related (Table 7-3).

7-6. ORGANIC-PHOSPHORUS (P_{org})

The concentration of organic phosphorus (P_{org}) has been calculated from the difference in concentration of acid-extracted phosphate between ignited (550°C) and the same un-ignited samples (after ASPILA et al., 1976). Summarizing most of the available organic-P data for marine sediments, FROELICH et al. (1982) have suggested that the P_{org} content in these sediments is nearly constant and independent of the C_{org} content. On the basis of the same data-set MACH et al. (1987) have concluded that the concentration of P_{org} is proportional to C_{org} with the exception of 'C_{org}-poor' sediments (defined by them as <2% C_{org}!). The poor relationship found between P_{org} and C_{org} in the latter sediments could in part be due to the difficulty of making sufficiently accurate measurements of P_{org} at low concentrations (Fig. 7-17). Unfortunately, almost all deep-sea sediments contain considerably less than 2% C_{org}. Therefore, a correlation could only be demonstrated for some upwelling-related and some near-coastal organic-rich sediments.

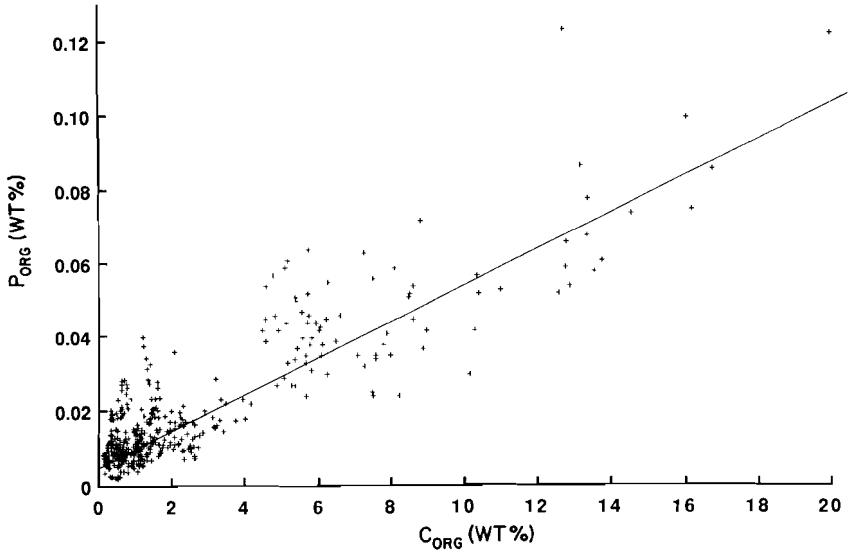

Fig. 7-17. Plot of organic phosphorus content (P_{org}) versus organic carbon content (C_{org}) in modern marine sediments (After MACH et al., 1987)

The sediments in this study all contain less than 2% C_{org} and the results of at least duplicate analysis of P_{org} show only a poor correlation with C_{org} (Table 7-3; Fig. 7-18). Almost all reported P_{org} data have been analysed by difference, using the ignition method (HARTMANN et al., 1976; ASPILA et al., 1976; see Appendix 7-1) or the acid-base extraction method (MEHTA et al., 1954; WILLIAMS et al., 1976). Application of the acid-base extraction to the sediments of this study did not yield sufficiently reproducible results and is therefore not reported here. The results obtained by the ignition method, although better, still show rather large errors (not shown in Fig.). These errors are mainly introduced as a consequence of substracting two large concentrations ('total' and 'inorganic' P; defined according to ASPILA et al., 1976, see Appendix 7-1) to obtain a relatively low concentration (P_{org}). Total-P analyses of the in-house standard MM84 (n=12) have shown a 2% error (543 ± 9 ppm P). It seems reasonable to assume an error of at least 3% for the result of duplicate analysis of 'total' and of 'inorganic' P for individual samples. Simple comparison of the estimated error in extracted 'total' and 'inorganic' P (3% of on average 550 ppm ≈17 ppm P each) and the calculated organic-P content (average ≈ 70 ppm P) learns that the sum of errors equals half of the calculated value for P_{org}. An additional source of error could result from the inclusion of some inorganic-P in the determination of organic-P (HARTMANN et al., 1976), or from the inclusion of organic-P in the determination of 'total' and 'inorganic' P due to hydrolysis (e.g. OLSON & DEAN, 1965). More meaningful data may be obtained by taking the average of groups of similar samples such as individual turbidites.

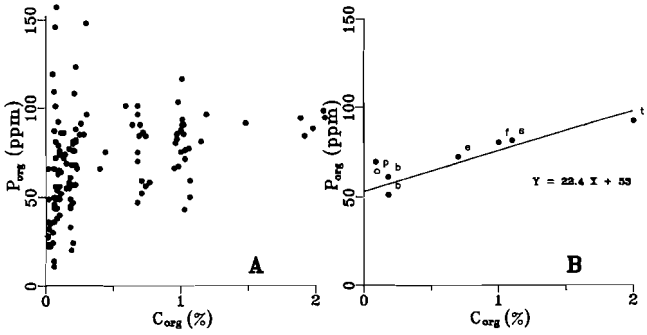

Fig. 7-18. Plots of P_{org} versus C_{org} for: a. all samples of core MD10, and b. turbidite-averaged data, in which only averages of at least 4 samples that have a C_{org} > 0.1% have been included. The resulting correlation is not caused by differences in carbonate content; letters indicate turbidites, numbers refer to total carbonate content: b (52%), e (50%), f (50%), o (57%), p (60%), s (50%) and t (50%).

Accepting turbidite averages of at least 4 samples with a C_{org} content greater than 0.1% only, then a relatively good correlation is obtained between C_{org} and P_{org} (Fig. 7-18). The non-zero intercept of ≈ 60 ppm P is similar to that reported by MACH et al. (1987; ≈70 ppm P) and can be attributed to a contribution of inorganic-P. The weight ratio C_{org}/P_{org} that can be calculated from the best fit line (Fig. 7-18) is near 450 (W/W), or 1200 on a molar basis. This ratio is much higher than that reported for marine sediments (MACH et al., 1987; 490 [M/M]) and for marine plankton (REDFIELD et al., 1963; 106 [M/M]). Most data of the organic-rich sediments reported by MACH et al. (1987) result from relatively recent sediment. The sediments of HARTMANN et al. (1976) included in this data set are among the oldest (< 150 ky BP; i.e. younger than the f-turbidite). The age of deposition of most turbidites that are discussed here, is higher (from turbidite f to u; i.e. 150 - 700 ky BP). In addition, in the volcanic turbidites with a relatively high inorganic P content not only the error in P_{org} will be much larger, but also the possible contribution of inorganic-P to P_{org} (see discussion above). However, despite these possible errors the C_{org}/P_{org} ratio found in this study is significantly larger than that reported for more recent sediments. It seems therefore, that in older sediments the C_{org}/P_{org} ratio increases, which could be caused by preferential decomposition of P_{org}-rich organic matter. The relatively large error in the P_{org} content - a major problem for all P_{org} values reported in the literature - does not permit more firm conclusions to be drawn in this respect.

Another way to estimate the composition of decomposing organic matter would be through stoichiometric modelling (see Section 6-4). Due to continuous generation / immobilization reactions that occur in the sediments from MAP similar to those reported for sediments in NAP (see Chapter 4), and due to oxidation problems during the handling of the samples (see Chapter 2) it is not possible to apply stoichiometric modelling to the phosphate concentrations in the pore water of core MD10. For example, if the 'diagenetic spike' at 30 cm depth in core MD10 is assumed not to be influenced by oxidation artifacts, then the contribution of 'organic'-P to the pore-water phosphate concentration is at most 10% (see similar calculations done in Chapter 4). The rest (90%) must originate from dissolving Fe-oxihydroxides and the simultaneous release of associated phosphate.

The oxidized parts of turbidites in general contain lower C_{org} and P_{org} concentrations than the reduced part of the same turbidite (only turbidite d forms an exception) (not shown in Fig.). However, based on the present P_{org} data no firm conclusions can be drawn as far as the relative importance of post-depositional oxidation effects on the C_{org}/P_{org} ratio are concerned.

7-7. CONCLUSIONS

In contrast to N_{ex}, the concentration of P_{ex} and the P_{ex}/Al ratio in core MD10 are not influenced by redox conditions but only by the mineral composition of the sediment. For most samples there is a source of P_{ex} in excess of the calculated 48 ppm 'carbonate-associated P', especially for the samples of turbidite e. The excess-P of almost all samples could be explained by a minor (2-5%) contribution from apatite-P. For samples from the e-turbidite a 10% contribution would be necessary. The relatively high excess-P values for this turbidite compared to others could be caused by a different apatite or by a relatively high content of coccoliths with respect to foraminifera.

High absolute P_{OH} values are mainly confined to pelagic intervals. The only change that seems to have occurred in the P_{OH} content of the turbiditic sediments in core MD10 is a slight increase in the oxidized parts of the organic-rich turbidites. Part of the phosphate and iron generated during early diagenetic reactions may have been immobilized in the oxidized parts of these turbidites.

Some re-allocation of iron resulting from reductive dissolution followed by diffusion and subsequent oxidation/precipitation in a more oxidized zone, is known to occur to some extent in the sediments of the MAP. Such early diagenetic mobility can explain the fluctuations that have been observed in the P_{OH} content of these sediments.

Relatively high P_{OH}/Al ratios for carbonate-rich samples have been explained by (Fe,Mn) coatings on carbonate micro-fossiles. These coatings have been reported to account for most of the P present in carbonate-rich sediments.

The relatively high amounts of apatite-P in the volcanic turbidites indicate a similar source area for volcanic material and apatite. The apatite-P present in the organic-rich turbidite e is likely to be upwelling-related (possibly fish-bone apatite).

The concentration of the remaining phosphorus (P_R) is relatively constant with depth and does not significantly change across redox boundaries.

The sum of the extracted P fractions (P_{sum}) is in excellent agreement with the independently determined total phosphorus content (P_{tot}).

The large error that is introduced in the analysis of organic phosphorus (P_{org}) does not permit a discussion of individual samples. A relatively good correlation exists between C_{org} and P_{org} values of turbidites that consist of at least 4 samples and that contain at least 0.1% C_{org}. The resulting C/P molar ratio of ≈1200 is much higher than that reported for marine sediments (490) or marine plankton (106). The average composition that can be deduced for the organic matter in this study is approximately $C_{106}N_{5.9}P_{0.09}$ as compared to to $C_{106}N_{16}P_1$. The higher C/P ratio for the

relatively old samples of this study could point to a preferential decomposition of P_{org}-rich organic matter.
The concentrations of C_{org} and P_{org} in the oxidized upper parts of turbidites are generally lower than those in the reduced lower parts of the same turbidite. Due to the large error in the analysis of P_{org} it is not possible to make a firm statement on the C/P ratio across redox boundaries.

APPENDIX 7-1

Some details of the P extraction analytical methods

The extraction schedule has been adapted after Hieltjes (1980) en Van Eck (1981). All extractions have been done in screw-capped centrifuge tubes with conical bottom using oven-dried sediment (105°C). Reported values are the mean of at least duplicate extractions and analyses. The extracted ortho-phosphate has been analysed according to standard spectrophotometric techniques (e.g. STRICKLAND & PARSONS, 1968; VAN ECK, 1981). The ascorbic acid/molybdate colouring reagent has been prepared fresh daily, although over a period of 4 days undetectable/negligible deterioration occurred. The pH at colouring has always been closely watched, because in the presence of high Si concentrations large deviations can be expected at too high pH values, whereas no colouring occurs at too low pH values. Therefore, the NaOH and HCl extracts have been back-titrated to neutral pH, prior to the addition of the colouring reagent. For the extracted samples the pH values at colouring were always between 1.0 and 1.2. The concentration of phosphate in blanks was always negligible.

a. *Total Phosphorus (P_{tot})* [after ASPILA et al.,1976]

Colorimetric determination of the liberated ortho-phosphate after destruction of 50 mg sample with $K_2S_2O_8/H_2SO_4$ during 1 hour at 2 atm and 131°C.

b. *Exchangeable and carbonate-associated phosphate (P_{ex})*

Approximately 50 mg accurately weighed sample was mixed with 50 ml 2 N NH_4Cl solution in a well-closing centrifuge tube with conical bottom. After shaking for one night the tubes were centrifuged and the clear liquid was carefully decanted in a 50 ml volumetric flask. After thoroughly mixing of the remaining sediment with 15 ml bi-distilled water, centrifuging and careful decanting, the volume of the flasks is made up to 50 ml. The analysis of ortho-phosphate was done as above.

c. *Iron- and aluminium-associated phosphate (P_{OH})*

After the addition of 25 ml of a 0.1 N NaOH solution and shaking for 24 hours, the tubes were centrifuged and decanted in a way similar to that described under the former extraction. However, washing of the remaining sediment was done with 10 instead of 15 ml bi-distilled water, followed by the same centrifuge/decanting procedure as described above. The extract in the flasks was then titrated to pH≈7±0.5 using ca. 5 ml of a 0.5 N HCl solution and the volume was made up to 50 ml. The analysis of ortho-phosphate was done as above.

d. *Calcium-associated phosphate / apatite (P_{HCl})*

After the addition of 25 ml of a 0.5 N HCl solution and shaking for 24 hours, the tubes were centrifuged and decanted in a way similar to that described under the former extraction. However, washing of the remaining sediment was done twice each time using 20 instead of 10 ml bi-distilled water, followed by the same centrifuge/decanting procedure as described above. The extract in the 100 ml flasks was then titrated to pH≈7±0.5 using 10% ammonium and the volume was made up to 100 ml. The analysis of ortho-phosphate was done as above.

e. *Residual phosphate (P_R)*

Destruction of the remaining sediment was done in a way similar to that for the determination of P_{tot}, followed by the analysis of ortho-phosphate.

f. *Organic phosphorus by extraction (P_{org})*

During the extraction of P_{OH} and P_{HCl} also some organic-P may be extracted, which will (partly) not be analysed in the ortho-phosphate determination. It is known that some organic-P compounds gradually hydrolyze in an acid solution (e.g. OLSON & DEAN, 1965). The P_{org} concentration may be estimated after complete destruction (see under P_{tot}) of part of the P_{OH} and P_{HCl} extracts and by substracting the phosphate concentrations found after and before destruction of the extract (with the proper volumetric corrections). However, the concentration of P_{org} found in the P_{OH} and P_{HCl} extracts did in general not give reproducible results and will therefore not be discussed in this Chapter.

g. *Organic phosphorus (P_{org})* [after ASPILA et al., 1976]

Approximately 100 mg accurately weighed sample was heated for 2 hours at 550°C, then transferred into a centrifuge tube. After over-night extraction with 25 ml of a 1 N HCl solution, centrifugation and washing done in a way similar to that for the extractions above, the volume was made up to 100 ml. Substraction of the measured ortho-phosphate in this extract from that in the extract of the same but un-ignited sample gives a measure of the concentration of organic phosphorus. See also note on possible errors under f.

APPENDIX 7-2.

TABLE. Analytical results and errors (1σ) of in-house standards that have been analysed in the same series as the reported samples.

Extraction	MM82 (n=6)	MM84 (n=26)	Phosphorite pebble (n=2)
P_{ex}	40 ± 4	43 ± 8	669 ± 1
P_{OH}	88 ± 6	145 ± 25	282 ± 38
P_{HCl}	405 ± 20	369 ± 22	5711 ± 350
P_{R}	40 ± 6	52 ± 12	307 ± 55
P_{sum}	576 ± 25	613 ± 40	6974 ± 260

APPENDIX 7-3.

TABLE Relative clay mineral composition (in %) in turbidites of core MD10.

Turb.	n	I	M	K	C
b	3	23	37	19	19
d	1	35	8	19	37
e	3	43	21	21	15
f	5	33	31	21	15
g	2	31	43	14	12
j	1	28	39	19	14
l	1	26	42	21	11
n	1	33	37	20	10
o	3	36	32	17	15
p	2	35	28	20	17
r	1	38	32	15	15
s	1	45	22	20	13
t	3	36	24	23	17

data after AUFFRET et al., 1988. n=number of samples; I=illite; M=smectite; K=kaolinite; C=chlorite

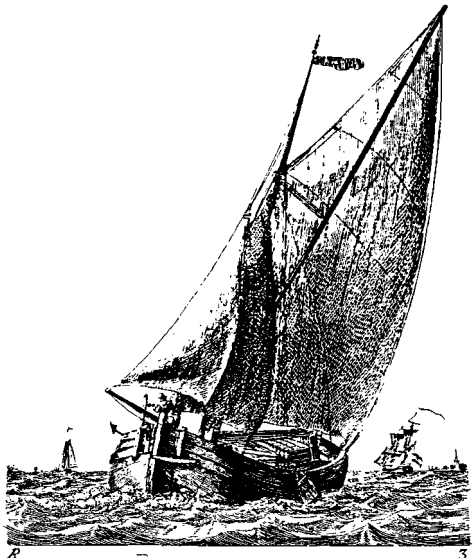

B 3
een Water schip Zout water voor de Zoutketen haleñde

REFERENCES

ARRHENIUS G. (1950) Carbon and nitrogen in subaquatic sediments. Geochim. Cosmochim. Acta 1, 15-21.

ARRHENIUS G.O. (1959) Sedimentation on the ocean floor. In: Researches in Geochemistry (Abelson P.H., ed.), p.1-24 (Wiley).

ASPILA K.I., AGEMIAN H., and CHAU A.S.Y. (1976). A semi-automated method for the determination of inorganic, organic and total phosphate in sediments. Analyst 101, 187-197.

AUFFRET et al. (1988) Geology, lithostratigraphy of STACOR cores from the Madeira (GME) and Southern Nares Abyssal Plains, In: Schüttenhelm R.T.E. et al (eds.), JRC Series (in press).

BARNES R.D. (1974). An in situ interstitial water sampler for use in unconsolidated sediments. Deep-Sea Res. 21, 1125-1128.

BATLEY G.E. and GILES M.S. (1979). Solvent displacement of sediment interstitial waters before trace metal analysis. Water Res. 13, 879-886.

BATURIN G.N. and POKRYSHKIN (1980) Upwelling and the formation of phosphorites. Oceanology 20, 56-61.

BELDERSON R.H. and LAUGHTON A.S. (1966) Correlation of some Atlantic turbidites. Sedimentology 7, 103-116.

BENDER M., MARTIN W., HESS J., SAYLES F., BALL L. and LAMBERT C. (1987) A whole-core squeezer for interfacial pore-water sampling. Limnol. Oceanogr. 32, 1214-1225.

BERNER R.A. (1970) Sedimentary pyrite formation. Am. J. Sci. 268, 1-23.

BERNER R.A. (1973) Phosphate removal from sea water by adsorption on volcanogenic ferric oxides. Earth Planet. Sci. Lett. 18, 77-86.

BERNER R.A. (1977) Stoichiometric models for nutrient regeneration in anoxic sediments. Limnol. Oceanogr. 22, 781-786.

BERNER R.A. (1980[a]) A rate model for organic matter decomposition during bacterial sulfate reduction in marine sediments. In: Biogéochimie de la matière organique à l'interface eau-sédiment marin. Colloq. Int. CNRS 293, 35-44.

BERNER R.A. (1980[b]) Early diagenesis, Princeton Press, 241p.

BERNER R.A. (1981) A new geochemical classification of sedimentary environments. J. Sed. Petrol. 51, 359-365.

BERNER R.A. (1982) Burial of organic carbon and pyrite sulfur in the modern ocean : its geochemical and environmental significance. Am. J. Sci. 282, 451-473.

BEZDEK J.C. (1981) Pattern recognition with fuzzy objective function algorithm. New York, Plenum Press. pp. 256.

BEZDEK J.C., EHRLICH R. and FULL W. (1984). The Fuzzy C Means clustering algorithm. Computers & Geoscience 10, 191-203.

BILLEN G. (1975) Etude écologique des transformations de l'azote dans les sédiments marins. Ph.D. dissertation, Univ. de Bruxelles, pp. 266.

BISCHOFF J.L., GREER R.E. and LUISTRO A.O. (1970) Composition of interstitial water of marine sediments : temperature of squeezing effect. Science 167, 1245-1246.

BLACKBURN T.H. (1980) Seasonal variations in the rate of organic-N mineralization in anoxic marine sediments. In: Biogéochimie de la matière organique à l'interface eau-sédiment marin. Colloq. Int. CNRS 293, 173-183.

BOATMAN C.D. and MURRAY J.W. (1982) Modeling exchangeable NH_4^+ adsorption in marine

sediments: Process and controls of adsorption. Limnol. Oceanogr. 27, 99-110.
BORDOWSKIY O.K. (1965[a]) Sources of organic matter in marine basins. Mar. Geol. 3, 5-31.
BORDOWSKIY O.K. (1965[b]) Accumulation of organic matter in bottom sediments. Mar. Geol. 3, 33-82.
BOUST D. (1986) Les terres rares au cours de la diagenèse des sédiments abyssaux; analogies avec un transuran : l'américium. Thesis Un. Caen, France, pp. 297.
BRAY J.T., BRICKER O.P. and TROUP B.N. (1973) Phosphate in interstitial waters of anoxic sediments : oxidation during sampling procedure. Science 180, 1362-1364.
BRECK W.G. (1974) Redox levels in the sea. In The Sea (ed. E.D. Goldberg), 5, pp. 153-179. Wiley Interscience.
BRINDLEY G.W. and SUITO E. (1971) Seminar on clay-organic complexes. Aug. 1971; pp.124.
BROECKER W.S. and TAKAHASHI T. (1977) The solubility of calcite and aragonite in seawater at atmospheric pressure and 34.5 %. salinity. In : Thermodynamics in Geology (ed. D.G. Fraser), pp.713-730. Reidel.
BROECKER W.S. (1982) Glacial to interglacial changes in the ocean chemistry. Progr. Oceanog. 11, 151-197.
BROECKER W.S. and PENG T.-H. (1982) Tracers in the sea, Lamont Doherty, 690p.
BROOKS R.R., PRESLEY B.J. and KAPLAN I.R. (1967) APDC-MIBK extraction systems for the determination of trace elements in saline waters by atomic absorption spectrophotometry. Talanta 14, 809-816.
BURDIGE D.J. and GIESKES J.M. (1983) A pore water/solid phase diagenetic model for manganese in marine sediments. Am. J. Sci. 283, 29-47.
CALVERT S.E. (1976) The mineralogy and geochemistry of near-shore sediments. In: Chemical Oceanography (Riley J.P. and Chester R., eds.) vol. 6, 187-280 (Academic Press).
CANFIELD D.E. (1988) Sulfate reduction and the diagenesis of iron in anoxic marine sediments. Ph. D. Thesis. Yale Un.
CHANG S.C. and JACKSON M.L. (1957) Fractionation of soil phosphorus. Soil Sci. 84, 133-144.
CODISPOTI L.A. (1988) Phosphorus versus nitrogen limitation of new (export) production. In : Productivity of the ocean: present and past. Dahlem Conf. April 1988 (in press).
COLLEY S., THOMSON J., WILSON T.R.S. and HIGGS N.C. (1984) Post-depositional migration of elements during diagenesis in brown clay and turbidite sequences in the North East Atlantic. Geochim. Cosmochim. Acta 48, 1223-1235.
COLLEY S. and THOMSON J. (1985) Recurrent uranium relocations in distal turbidites emplaced in pelagic conditions. Geochim. Cosmochim. Acta 49, 2339-2348.
CRONAN D.S. (1980) Underwater Minerals. Academic Press, London. pp.362.
CROWLEY T.J. (1983) Calcium-carbonate preservation patterns in the central North Atlantic during the last 150,000 years. Mar. Geol. 51, 1-14.
CULBERSON C. and PYTKOWICZ R.M. (1968) Effect of pressure on carbonic acid, boric acid, and pH in seawater. Limnol. Oceanogr. 13, 403-417.
DEER W.A., HOWIE R.A. and ZUSSMAN J. (1962) In : Rock-forming minerals, volume 3 : Sheet silicates. London, Longmans, Green & Company, 270p.
DE KANEL J and MORSE J.W. (1978) The chemistry of orthophosphate uptake from seawater on to calcite and aragonite. Geochim. Cosmochim. Acta 42, 1335-1340.
DE LANGE G.J. (1983) Geochemical evidence of a massive slide in the southern

Norwegian Sea. Nature 305, 420-422.
DE LANGE G.J. and TEN HAVEN H.L. (1983) Recent sapropel formation in the eastern Mediterranean. Nature 305, 797-798.
DE LANGE G.J. (1984[a]) Chemical composition of interstitial water in cores from the Madeira Abyssal Plain (Eastern North Atlantic). Meded. Rijks Geol. Dienst 38, 199-207.
DE LANGE G.J. (1984[b]) Shipboard pressure-filtration system for interstitial water extraction. Meded. Rijks Geol. Dienst 38, 209-214.
DE LANGE G.J., DEKKER H., EBBING J., VAN ZESSEN T. and VAN ALPHEN M. (1985) Chemical composition of interstitial water in cores from the Nares Abyssal Plain (western North Atlantic). Progress Report RGD 1984, 81-94.
DE LANGE G.J. (1986[a]) Chemical composition of interstitial water in cores from the Nares Abyssal Plain (western North Atlantic). Oceanol. Acta 9, 159-168.
DE LANGE G.J. (1986[b]). Early diagenetic reactions in interbedded pelagic and turbiditic sediments in the Nares Abyssal Plain (western North Atlantic) : Consequences for the composition of sediment and interstitial water. Geochim. Cosmochim. Acta 50, 2543-2561.
DE LANGE G.J. and RISPENS F.B. (1986) Indication of a diagenetically induced precipitate of an Fe,Si mineral in sediment from the Nares Abyssal Plain, western North Atlantic. Mar. Geol. 73, 85-97.
DE LANGE G.J., JARVIS I. and KUIJPERS A. (1987[a]) Geochemical characteristics and provenance of late quaternary sediments from the Madeira Abyssal Plain, North Atlantic. In : Weaver P.P.E. and Thomson J. (eds.) Geology and Geochemistry of Abyssal Plains. Proc. Geol. Soc. 31, 147-165.
DE LANGE G.J., VAN DER WEIJDEN C.H., MIDDELBURG J.J. AND VAN DER SLOOT H.A. (1987[b]) Chemical profiles in the water columns of two anoxic basins in the Mediterranean : Tyro and Bannock Basins. EOS 68, 1682.
DE LANGE G.J., CRANSTON R.E., HYDES D.H. and BOUST D. (1988[a]) Problems that can be encountered during the extraction of pore water from marine sediments. In: Schüttenhelm R.T.E. et al (eds.), JRC Series (in press).
DE LANGE G.J., VAN DIJK A., EUSSEN G., VAN INGEN R., NEDERLOFF H., VAN OS B. AND POORTER R. (1988[b]) Pore-water and sediment from a manganese-nodule-covered submarine hill in the Madeira Abyssal Plain (eastern North Atlantic) : some geochemical results. In Internal Report RGD, 1988 (in press).
DE LANGE G.J., MIDDELBURG J.J. and P.J. PRUIJSERS (1988[c]) Middle and Late Quaternary depositional sequences and cycles in the eastern Mediterranean : Discussion paper. Sedimentology (in press).
DE LANGE G.J., JARVIS I., MIDDELBURG J.J. and KUIJPERS A. (1988[d]) Geochemical characteristics and provenance of late quaternary sediments from the Madeira Abyssal Plain, North Atlantic. In: Schüttenhelm R.T.E. et al (eds.), JRC Series (in press).
DE LANGE G.J., MIDDELBURG J.J., POORTER R.P. and SOFIYAH S. (1988[e]) Geochemistry of manganese encrustations on the sea-bed west of Misool. Neth. J. Sea Res. (in press).
DE LANGE G.J., KOK P.T.J., EBBING J. and VAN DER KLUGT P. (1988[f]) Microfault-like structures in unconsolidated upper quaternary sediments from the Madeira Abyssal Plain (eastern North Atlantic) Mar. Geol. 80, 155-159.
DE LEEUW J.W., VIETS T.C. and SCHENCK P.A. (1982) Een vergelijkend onderzoek van 8 sedimentmonsters uit het Canary Basin en 9 sedimentmonsters uit het Angola Basin met Curie-punt Pyrolyse Massaspectrometrie. Internal Report of the TH-Delft-FOM Institute for Atomic and Molecular Physics, Amsterdam, p. 1-6.

DICKSON A.G. (1981) An exact definition of total alkalinity and a procedure for the estimation of alkalinity and total inorganic carbon from titration data. Deep-Sea Res. 28, 609-623.
DUIN E.J.T. (1985) Geophysics of the southern Nares Abyssal Plain, western North Atlantic. In : Progress report RGD, 1984 (ed. A. Kuijpers), 5-38.
EDMOND J.M. (1970) High precision determination of titration alkalinity and total carbon dioxide content of sea water by potentiometric titration. Deep-Sea Res. 17, 737-750.
EDMUNDS W.M. and BATH A.H. (1976) Centrifuge extraction and chemical analysis of interstitial waters. Environm. Sci. Techn. 10, 467-472.
EMBLEY R.W. and JACOBI R. D. (1977) Distribution and morphology of large submarine sediment slides and slumps on Atlantic continental margins. Marine Geotechnology 2, 205-228.
EMBLEY R.W. (1980) The role of mass transport in the distribution and character of deep-ocean sediments with special reference to the North Atlantic. Mar.Geol. 38, 23-50.
EMBLEY R.W. (1982) Anatomy of some Atlantic margin sediment slides and some comments on ages and mechanisms. - In (Saxov S., Nieuwenhuis J.K., eds.) : Marine slides and other mass movements , London, Plenum Press, 189-213.
EMERSON S., JAHNKE R., BENDER M., FROELICH P., KLINKHAMMER G., BOWSER C. and SETLOCK G. (1980) Early diagenesis in sediments from the Eastern equatorial Pacific I. Pore water nutrient and carbonate results. Earth Planet. Sci. Lett. 49, 57-80.
EMERSON S.R., GRUNDMANIS V. and GRAHAM D. (1982) Carbonate chemistry in marine pore waters : MANOP sites C and S. Earth Planet. Sci. Lett. 61, 220-232.
EMERSON S. (1985) Organic carbon preservation in marine sediments. In: The carbon cycle and atmospheric CO_2: Natural variations Archaen to Present. (Sundquist E.T. and Broecker W.S., eds.) Geophysical Monograph 32, 78-88 Washington D.C., AGU.
EMERSON S., STUMP C., GROOTES P.M., STUIVER M., FARWELL G.W. and SCHMIDT F.H. (1987) Estimates of degradable organic carbon in deep-sea surface sediments from ^{14}C concentrations. Nature 329, 51-53.
EMERY K.O. and RITTENBERG S.C. (1952) Early diagenesis in California basin sediments in relation to origin of oil. Bull. Am. Ass. Petrol. Geol. 36, 735-806.
ENSMINGER L.E. and GIESEKING J.E. (1939) The adsorption of proteins by montmorillonitic clays. Soil Sci. 48, 467-473.
EPPLEY R.W. (1988) Communicated at Dahlem Conf. April 1988, on : Productivity of the ocean: present and past.
ESOPE (1986) Cruise Data Report.
FANNING K.A. and PILSON M.E.Q. (1971) Interstitial silica and pH in marine sediment : some effect of sampling procedure. Science 173, 1228-1231.
FROELICH P.N., BENDER M.L. and HEATH G.R. (1973) Phosphorus accumulation rates in metalliferous sediments on the East Pacific Rise. Earth Planet. Sci. Lett. 34, 351-359.
FROELICH P.N., KLINKHAMMER G.P., BENDER M.L., LUEDTKE N.A., HEATH G.R., CULLEN D., DAUPHIN P., HAMMOND D., HARTMAN B. and MAYNARD V. (1979) Early oxidation of organic matter in pelagic sediments of the eastern equatorial Atlantic : suboxic diagenesis. Geochim. Cosmochim. Acta 43, 1075-1090.
FROELICH P.N., BENDER M.L., LUEDTKE N.A., HEATH G.R. and DEVRIES T. (1982) The marine phosphorous cycle. Am. J. Sci. 282, 474-511.
GARDNER J.V. (1975) Late Pleistocene carbonate dissolution cycles in the eastern

equatorial Atlantic. In Sliter W.V., Be A.W.H. and Berger W.H. (eds.), Dissolution of Deep-sea Carbonates : Spec. Publ. of the Cushman Found. for Foraminiferal Res. 13, 129-141.
GARRELS R.M. and CHRIST G.L. (1965) Solutions, Minerals, and equilibria, Harper and Row, 450p.
GEEL C.R. and JONGERIUS P. (1984) A sedimentological study of a coarse grained sediment of the Madeira Abyssal Plain. Meded. Rijks Geol. Dienst, 38, 119-128.
GIESKES J.M. (1973) Interstitial water studies leg 15 - alkalinity, pH,Mg,Ca, Si,PO4 and NH4. Init. Repts. DSDP, Wash. (U.S. Govt. Print. Office) 20, 813-829.
GORDON D.C., Jr (1971) Distribution of particulate organic carbon and nitrogen at an oceanic station in the central Pacific. Deep-Sea Res. 18, 1127-1134.
GROENEWEGEN G. (1789) Verzameling van 84 Hollandsche Schepen, geteekend en in koper gebragt. (J. Van Den Brink, Rotterdam).
HARDER H. (1965) Experimente zur "Ausfallung der Kieselsaure. Geochim. Cosmochim. Acta 29, 429-442.
HARDER H.and FLEHMIG W. (1970) Quartzsynthese bei tiefen Temperaturen. Geochim. Cosmochim. Acta 34, 295-305.
HARDER H. (1978) Synthesis of iron layer silicate minerals under natural conditions. Clays Clay Minerals 26, 65-72.
HARGRAVE B.T. (1988) Communicated at Dahlem Conf. April 1988, on : 'Productivity of the ocean: present and past'.
HARTMANN M. (1965) An apparatus for the recovery of interstitial water from recent sediments. Deep-Sea Res. 12, 225-226.
HARTMANN M., LANGE H., SEIBOLD E. and WALGER E. (1971) Oberflächensedimente im Persischen Golf und Golf von Oman I. Geologisch-hydrologischer Rahmen und erste sedimentologische Ergebnisse. Meteor Forsch. Ergebn. C4, 1-76.
HARTMANN M., MÜLLER P., SUESS E. and VAN DER WEIJDEN C.H. (1973) Oxidation of organic matter in recent marine sediments. Meteor Forsch. Ergebn. C12, 74-86.
HARTMANN M., MÜLLER P.J., SUESS E., and VAN DER WEIJDEN C.H. (1976) Chemistry of late quaternary sediments and their interstitial waters from the NW African Continental Margin. Meteor Forsch. Ergebn. C24, 1-67.
HARTMANN M. (1979) Evidence for early diagenetic mobilization of trace metals from discoloration of pelagic sediments. Chem. Geol. 26, 277-293.
HEARN P.P., PARKHURST D.L. and CALLENDER E. (1983) Authigenic vivianite in Potomac river sediments : control by ferric oxy-hydroxides. J. Sedim. Petrol. 53, 165-177.
HEDGES J.I. and HARE P.E. (1987) Amino acid adsoption by clay minerals in distilled water. Geochim. Cosmochim. Acta 51, 255-259.
HELDER W. and DE VRIES R.T.P. (1979) An automatic phenol-hypochlorite method for the determination of ammonia in sea- and brackish waters. Neth. J. Sea Res. 13, 154-160.
HENRICHS S.M. and REEBURGH W.S. (1987) Anaerobic mineralization of marine sediment organic matter: rates and the role of anaerobic processes in the oceanic carbon economy. Geomicrobiol. Jour. 5, 191-237.
HIELTJES A.H.M. (1980) Eigenschappen en gedrag van fosfaat in sedimenten. Ph.D. Thesis, Twente Un., pp. 307.
HIELTJES A.H.M. and LIJKLEMA L. (1980) Fractionation of inorganic phosphates in calcareous sediments. J. Environ. Qual. 9, 405-407.
HOLDREN G.R.jr., BRICKER O.P.III. and MATSOFF G. (1975) A model for the control of dissolved manganese in the interstitial waters of Chesapeake Bay. In Marine Chemistry in the Coastal Environment (ed. T.M. Church), pp. 364-381. Amer. Chem. Soc.

HOROWITZ R.M., WATERMAN L.S. and BROECKER W.S. (1973) Interstitial water studies, leg 15, new procedures and equipment. Init. Repts. DSDP, Washington (U.S. Print. Office) 20, 757-763.
HUFF W.D. and TURKUNENOGLU A.G. (1981) Chemical characteristics and origin of Ordovician K-bentonites along the Cincinnati Arch. Clays Clay Miner. 19, 113-123.
HURD D.C. (1973) Interactions of biogenic opal, sediment and seawater in the Central Equatorial Pacific. Geochim. Cosmochim. Acta 37, 2257-2282.
HYDES D.J., DE LANGE G.J. and DE BAAR H.J.W. (1988) Dissolved aluminium in the Mediterranean. Geochim. Cosmochim. Acta 52, 2107-2114.
INGLE S.E., CULBERSON C.H., HAWLEY J.E. and PYTKOWICZ R.M. (1973) The solubility of calcite in seawater at atmospheric pressure and 35 ‰ salinity. Mar. Chem. 1, 295-307.
INGLE S.E. (1975) The solubility of calcite in the oceans. Mar. Chem. 3, 301-319.
JACOBI R.D. (1976) Slides on the northwestern continental margin of Africa. Mar.Geol. 22, 157-173.
JACOBI R.D., and HAYES D.E. (1982) Bathymetry, microphysiography andreflectivity characteristics of the west African margin between Sierra Leone and Mauretania. In : von Rad, Hinz K., Sarntheim M. and Seibold E. (eds.) Geology of the Northwest African Continental Margin. Berlin, Springer-Verlag. p. 181-212.
JACOBSON R.L. and LANGMUIR D. (1974) Dissociation constants of calcite and $CaHCO_3^+$ from 0 to 50°C. Geochim. Cosmochim. Acta 38, 301-318.
JAHNKE R., HEGGIE D., EMERSON S., GRUNDMANIS V. and GRAHAM D. (1982) Pore waters of the central Pacific Ocean: nutrient results. Earth Planet. Sci. Lett. 61, 233-256.
JARVIS I. (1985) Geochemistry and origin of Eocene-Oligocene metalliferous sediments from the central equatorial Pacific : Deep Sea Drilling Project Sites 573 and 574. In Mayer L., Theyer F. et al., Init. Rept. DSDP 85, 781-804.
JARVIS I., and HIGGS N.C. (1987) Trace-element mobility during early diagenesis in distal turbidites : late Quaternary of the Madeira Abyssal Plain, North Atlantic. In : Weaver P.P.E. and Thomson J. (eds.) Geology and Geochemistry of Abyssal Plains. Proc. Geol. Soc. 31, 179-213.
JOHNSON R.G. (1967) Salinity of interstitial water in a sandy beach. Limnol. Oceanogr. 12, 1-7.
JOHNSON K.S. (1982) Solubility of rhodochrosite ($MnCO_3$) in water and seawater. Geochim. Cosmochim. Acta 46, 1805-1809.
JONES K.P.N., MCCAVE I.N. and PATEL P.D. (1988) A computer-interfaced sedigraph for modal size analysis of fine-grained sediment. Sedimentology 35, 163-172.
JONGSMA D., FORTUIN A.R., HUSON W., TROELSTRA S.R., KLAVER G.T., PETERS J.M., VAN HARTEN D., DE LANGE G.J. and TEN HAVEN (1983) Discovery of an anoxic basin within the Strabo Trench, eastern Mediterranean. Nature 305, 797-798.
JØRGENSEN B.B. (1979) A comparison of methods for the quantification of bacterial sulfate reduction in coastal marine sediments. II. Calculation from mathematical models. Geomicrobiol. J. 1, 29-47.
JUMARS P.A., ALTENBACH A.V., DE LANGE G.J., EMERSON S.R., HARGRAVE B.T., MÜLLER P.J., PRAHL F.G., REIMERS C.E., STEIGER T. and SUESS E. (1988) Transformation of seafloor-arriving fluxes into the sedimentary record. In : Productivity of the ocean: present and past. Dahlem Conf. April 1988 (in press).
KALIL E.K. and GOLDHABER M. (1973) A sediment squeezer for removal of pore waters without air contact. J. Sed. Petrol. 43, 553-557.
KEENEY D.R. and BREMNER J.M. (1966) Determination and isotope-ratio analysis of different forms of nitrogen in soils: 4. Exchangeable ammonium, nitrate, and nitrite

by direct distillation methods. Soil Sci. Soc. Amer. Proc. 30, 583-587.
KEMP A.L.W. and MUDROCHOVA A. (1973) The distribution and nature of amino acids and other nitrogen-containing compounds in Lake Ontario surface sediments. Geochim. Cosmochim. Acta 37, 2191-2206.
KHARAKA Y. and BERRY F.A.F. (1973) Simultaneous flow of water and solutes through geochemical membranes. I. Experimental investigation. Geochim. Cosmochim. Acta 37, 2577-2603.
KIDD R.B. and SEARLE R.C. (1984) Sedimentation in the southern Cape Verde Basin : regional observations by long-range sidescan sonar. In : Stow D.A.V. and Piper D.J.W. (eds.) Fine-grained Sediments. Proc. Geol. Soc. 15, 145-152.
KLUMP J.V. and MARTENS C.S. (1987) Biogeochemical cycling in an organic-rich coastal marine basin. 5. Sedimentary nitrogen and phosporus budgets based upon kinetic models, mass balances, and the stoichiometry of nutrient regeneration. Geochim. Cosmochim. Acta 51, 1161-1173.
KRIUKOV P.A. and KOMAROVA N.A. (1954) On squeezing fluids from clays at very high pressures (Russ.). Doklady Akad. Nauk. SSSR 99, 617-619.
KRIUKOV P.A. and MANHEIM F.T. (1982) Extraction and investigative techniques for study of interstitial waters of unconsolidated sediments: A review. In: The dynamic environment of the ocean floor (eds. FANNING K.A. and MANHEIM F.T.) (D.C. Heath Co) 1-26.
KROM M.D. and BERNER R.A. (1980) Adsorption of phosphate in anoxic marine sediments. Limnol. Oceanogr. 25, 797-806.
KROM M.D. and BERNER R.A. (1981) The diagenesis of phosphorus in nearshore marine sediment. Geochim. Cosmochim. Acta 45, 207-216.
KUIJPERS A. (1982) Sediment studies in the western Madeira Abyssal Plain. Internal Report RGD, 1982, 41-107.
KUIJPERS A., RISPENS F.B. and BURGER A.W. (1984[a]) Late Quaternary sedimentation and sedimentary processes on the Madeira Abyssal Plain, Eastern North Atlantic. Meded. Rijks Geol. Dienst, 38, 91-118.
KUIJPERS A., TROELSTRA S.R., VERBEEK J.W., WENSINK H. and DE WOLF H. (1984[b]) Paleoceanic conditions in the Canary Basin, eastern North Atlantic, since 1.4 Ma BP: Evidence from the deep-water sedimentary record. In: Geological Studies in the eastern North Atlantic (Kujpers et al., eds.) Meded. Rijks Geol. Dienst 38, 215-230.
KUIJPERS A. (1985) Geological studies of the southern Nares Abyssal Plain, western North Atlantic. Progress Report 1984, Haarlem, Rijks Geologische Dienst , 39-73.
KUIJPERS A. and WEAVER P.P.E. (1985) Deep sea turbidites from the Northwest African Continental margin. Dt. hydrogr. Z. 38, 147-164.
KUIJPERS A. and DUIN E.J.T. (1986) Boundary current-controlled turbidite deposition : a sedimentation model for the southern Nares Abyssal Plain, western North Atlantic. Geo-Marine Lett. 6, 21-28.
KUIJPERS A., DE LANGE G.J., and DUIN E.J.T. (1987) Areal sedimentation rate patterns of the southern Nares Abyssal Plain, western North Atlantic. In : Weaver P.P.E. and Thomson J. (eds.) Geology and Geochemistry of Abyssal Plains. Proc. Geol. Soc. 31, 13-22.
LEW M. (1981) The distribution of some major and trace elements in sediments of the atlantic ocean (DSDP samples) 2.The distribution of total, fixed and organic nitrogen. Chem. Geol. 33, 225-235.
LI Y.-H., BISCHOFF J., MATHIEU G. (1969) The migration of manganese in the arctic basin sediment. Earth Planet. Sci. Lett. 7, 265-270.

LI Y.-H. and GREGORY S. (1974) Diffusion of ions in seawater and in deep-sea sediments. Geochim. Cosmochim. Acta 38, 703-714.
LINDSTRÖM C.H.M. (1980) Transformations of iron constituents during early diagenesis. -In situ studies of a Baltic Sea sediment-water interface. Ph. D. Thesis,Stockholm Un., pp. 162.
LODER T.C., LYONS W.B., MURRAY S. and MCGUINESS H.D. (1978) Silicate in anoxic pore waters: oxidation effects during sampling. Nature 273, 373-379.
LUCAS J. and PREVOT L. (1984) Les synthèses de l'apatite, données nouvelles pour un modèle de genèse des phosphorites sédimentaires. In: Proc. 27th Int. Geol. Congress, Moscow 4-14 Aug. 1984, Vol. 15 'Non-metallic Mineral Ores', VNU Science Press, Utrecht).
LUCOTTE M. and d'ANGLEJAN B. (1988) Processes controlling phosphate adsorption by iron hydroxides in estuaries. Chem. Geol. 67, 75-83.
LYLE M. (1983) The brown-green color transition in marine sediments : A marker of the Fe(III)-Fe(II) redox boundary. Limnol. Oceanogr. 28, 1026-1033.
MACH D.L., RAMIREZ A. and HOLLAND H.D. (1987) Organic phosphorus and carbon in marine sediments. Am. J. Sci. 278, 429-441.
MACKENZIE F. and GEES R. (1971) Quartz : synthesis at earth-surface conditions. Science 173, 533-535.
MACKIN J.E. and ALLER R.C. (1984) Ammonium adsorption in marine sediments. Limnol. Oceanogr. 29, 250-257.
MACKIN J.E. (1987) Boron and Silica behavior in salt-marsh sediments : implications for paleo-boron distributions and the earley diagenesis of silica. Am. J. Sci. 287, 197-214.
MACKIN J.E., ALLER R.C. and ULLMAN W.J. (1988) The effects of iron reduction and nonsteady-state diagenesis on iodine, ammonium, and boron distributions in sediments from the Amazone continental shelf. Continent. Shelf Res. 8, 363-386.
MANGELSDORF P.C., WILSON T.R.S. and DANIELL E. (1969) Potassium enrichments in interstitial water of recent marine sediments. Science 165, 171-173.
MANHEIM F.T. (1966) A hydraulic squeezer for obtaining interstitial water from consolidated and unconsolidated sediments. U.S. Geol. Survey Prof. Paper 550-C, 171-174.
MANHEIM F.T. (1974) Comparative studies on extraction of sediment interstitial waters : discussion and comment on the current state of interstitial water studies. Clays Clay Miner. 22, 337-343.
MANHEIM F.T. and SAYLES F.L. (1974) Composition and origin of interstitial waters of marine sediments, based on Deep Sea Drilling cores. In: The Sea (ed. E.D. GOLDBERG; Wiley Interscience) 5, 527-568.
MANHEIM F.T. (1976) Interstitial waters of marine sediments. In : Chemical Oceanography (RILEY J.P. and CHESTER R., eds.) Academic Press , 115-186.
MARTENS C.S., BERNER R.A. and ROSENFELD J.K. (1978) Interstitial water chemistry of anoxic Long Island Sound sediments. 2. Nutrient regeneration and phosphate removal. Limnol. Oceanogr. 23, 605-617.
MASUZAWA T., KANOMORI S. and KITANO Y. (1980) The reversible effect of temperature on the chemical composition of interstitial water of marine sediment. J. Oceanogr. Soc. Japan 36, 68-72.
MCCAVE I.N. and JONES K.P.N. (1988) Deposition of ungraded muds from high-density non-turbulent turbidity currents. Nature 333, 250-252.
MCCONNELL D. (1973) Apatite. Applied Mineralogy, 5. Springer, N.Y.pp.111.

MEHRBACH D., CULBERSON C.H., HAWLEY J.I. and PYTKOWICZ R.M. (1973) Measurement of the apparent dissociation constants of carbonic acid in seawater at atmospheric pressure. Limnol. Oceanogr. 18, 897-907.
MEHTA N.C., LEGG J.O., GORING C.A.I. and BLACK C.A. (1954) Determination of organic phosphorus in soils: I. Extraction method. Soil Sci. Amer. Proc. 18, 443-449.
MIDDELBURG J.J., DE LANGE G.J. and VAN DER WEIJDEN C.H. (1987) Manganese solubility control in marine pore waters. Geochim. Cosmochim. Acta 51, 759-763.
MIDDELBURG J.J. and DE LANGE G.J. (1988[a]) Geochemical characteristics as indicators of the provenance of Madeira Abyssal Plain turbidites. A statistical approach. Oceanol. Acta 11, 159-165.
MIDDELBURG J.J. and DE LANGE G.J. (1988[b]) Manganese (II) equilibria in the interstitial waters of the Madeira and Nares Abyssal Plains. In: Schüttenhelm R.T.E. et al (eds.), JRC Series (in press).
MIDDELBURG J.J. and DE LANGE (1988[c]) Interstitial water chlorinity. Evidence for the isolation of Kau Bay during the last glaciation. Neth. J. Sea Res. (in press).
MIDDELBURG J.J., DE LANGE G.J., VAN DER SLOOT H.A., VAN EMBURG P.R. and SOFIYAH S. (1988[a]) Particulate manganese and iron framboids in Kau Bay, Halmahera (eastern Indonesia). Mar. Chem. 23, 353-364.
MIDDELBURG J.J., DE LANGE G.J., VAN DER WEIJDEN C.H. and SOFIYAH S. (1988[b]) Preliminary results of Kau Bay sediment chemistry. Neth. J. Sea Res. (in press).
MILLERO F.J. (1979) Thermodynamics of the carbonate system in seawater. Geochim. Cosmochim. Acta 43, 1651-1661.
MILLERO F.J. (1982) The effect of pressure on the solubility of minerals in water and seawater. Geochim. Cosmochim. Acta 46, 11-22.
MILLERO F.J. (1983) Influence of pressure on chemical processes in the sea. In Chemical Oceanography (eds. J.P. Riley and R. Chester) 8, 2-88.
MOHAMED A.F. (1949) The distribution of organic matter in sediments from the Northern Red Sea. Amer. J. Sci 247, 116-127.
MONNIOT C. and SEGONZAC M. (1985) La campagne ocanographique abyssale Abyplaine. Caractristique des stations et des peuplements bentiques. Oceanol. Acta 8, 67-76.
MONTARGES R., LE TIRANT P., WANNESSON J., VALERY P. and BERTHON J.-L. (1983) Large-size stationary-piston corer. In Proc. Deep Offshore & Technology, 2[nd] Conference, Malta, p. 63-74.
MORSE J.W. and COOK N. (1978) The distribution and form of phosphorus in North Atlantic Ocean deep-sea and continental slope sediments. Limnol. Oceanogr. 23, 825-830.
MÜLLER P.J. (1975) Zur Diagenese stickstoffhaltiger Substanzen in marinen Sedimenten unter oxidierenden and reduzierenden Bedingungen. Thesis, Kiel University, pp.179.
MÜLLER P.J. (1977) C/N ratios in Pacific deep-sea sediments: Effect of inorganic ammonium and organic nitrogen compounds sorbed by clays. Geochim. Cosmochim. Acta 41, 765-776.
MÜLLER P.J. and MANGINI A. (1980) Organic carbon decomposition rates in sediments of the Pacific manganese nodule belt dated by ^{230}Th and ^{231}Pa. Earth Planet. Sci. Lett 51, 94-114.
MURRAY J. and IRVINE R. (1895) On the chemical changes which take place in the composition of the sea water associated with blue muds on the floor of the ocean. Trans. Royal Soc. Edinburgh 37, 481-507.
MURRAY J.W., EMERSON S. and JAHNKE R. (1980) Carbonate saturation and the effect of pressure on the alkalinity of interstitial waters from the Guatemala Basin.

Geochim. Cosmochim. Acta 44, 963-972.
MURTHY A.S.P. and FERRELL R.E. Jr. (1972) Comparative chemical composition of sediment interstitial waters. Clays Clay Miner. 20, 317-321.
NRIAGU J.O. (1972) Stability of vivianite and ion-pair formation in the system $Fe_3(PO_4)_2$-H_3PO_4-H_2O. Geochim. Cosmochim. Acta 36, 459-470.
OLSON S.R. and DEAN L.A. (1965) Organic phosphorus. In: Methods of Soil Analysis (Black C.A. et al., eds.) Agronomy 9(2), 1038-1040 (Am. Soc. Agron. Inc., Madison USA).
PALMER M.R. (1985) Rare earth elements in foraminifera tests. Earth Planet. Sci. Lett. 73, 285-298.
PEDERSEN T.F. and PRICE N.B. (1982) The geochemistry of manganese carbonate in Panama Basin sediments. Geochim. Cosmochim. Acta 46, 59-68.
PIPER D.Z. and CODISPOTI L.A. (1975) Marine phosphorite deposits and the nitrogen cycle. Science 188, 15-18.
PIPER D.J.W. (1978) Turbidite muds and silts on deep-sea fans and abyssal plains. In Stanley D.J. and Kelling G. eds., Sedimentation in submarine canyons, fans and trenches, Stroudsberg Pa, Hutchinson and Ross, 163-176.
PLUMMER L.N. and SUNDQUIST E.T. (1982) Total individual ion activity coefficients of calcium and carbonate in seawater at 25°C and 35‰ Salinity, and implications to the agreement between apparent and thermodynamic constants of calcite and aragonite. Geochim. Cosmochim. Acta 46, 247-258.
POMEROY L.R., SMITH E.E. and GRANT C.M. (1965) The exchange of phosphate between estuarine water and sediments. Limnol. Oceanogr. 10, 167-172.
POSTMA D. (1981) Formation of siderite and vivianite and the pore-water composition of a recent bog sediment in Denmark. Chem. Geol. 31, 225-244.
POSTMA D. (1985) Concentration of Mn and separation from Fe in sediments - I. Kinetics and stoichiometry of the reaction between birnessite and dissolved Fe(II) at 10°C. Geochim. Cosmochim. Acta 49, 1023-1033.
POWERS M.C. (1957) Adjustment of land derived clays to the marine environment. J. Sediment. Petrol. 27, 355-372.
PRESLEY B.J., BROOKS R.R. and KAPPEL H.M. (1967) A simple squeezer for removal of interstitial water from ocean sediments. J. Mar. Res. 25, 355-357.
PRICE N.B. (1976) Chemical diagenesis in sediments. In: Chemical Oceanography (eds. Riley J.P. and Chester R.), vol. 6, 1-58 (Academic Press).
PRICE N.B. and CALVERT S.E. (1978) The geochemistry of phosphorites from the Namibian shelf. Chem. Geol. 23, 151-170.
REDFIELD A.C., KETCHUM B.H. AND RICHARDS F.A. (1963) The influence of organisms on the composition of seawater. In The Sea (ed. M.N. Hill) 2, 26-77. Wiley.
REEBURGH W.S. (1967) An improved interstitial water sampler. Limnol. Oceanogr. 12, 163-170.
REIMERS C.E. and SUESS E. (1983) partitioning of organic fluxes and sedimentary organic decomposition rates in the oceans. Mar. Chem. 13, 141-168.
REIMERS C.E. (1988) The control of benthic fluxes by particulate supply. In : Productivity of the ocean: present and past. Dahlem Conf. April 1988 (in press).
RIDOUT P.S. (1981) A shipboard system for extracting interstitial water from deep ocean sediments. IOS, report 121, pp.13.
RIDOUT P.S. and PAGETT R.M. (1984) A large volume sediment squeezing system for the analysis of rare earth elements in deep ocean pore waters. Mar. Chem. 15, 193-201.

RITTENBERG S.C., EMERY K.O., HULSEMANN J., DEGENS E.T., FAY R.C., REUTER J.H., GRADY J.R., RICHARDSON S.H. and BRAY E.E. (1963) Biogeochemistry of sediments in experimental Mohole. J. Sed. Petrol. 33, 140-172.

ROBBINS J.A. and GUSTINIS J. (1976) A squeezer for efficient extraction of pore water from small volumes of anoxic sediment. Limnol. Oceanogr. 21, 905-909.

ROBIE R.A., HEMINGWAY B.S. and FISHER J.R. (1978) Thermodynamic properties of minerals and related substances at 298.15 K and 1 bar (10^5 Pascals) pressure and at higher temperatures. Geol. Surv. Bull. 1452, 456p. (U.S. Govt Printing Office).

ROMANKEVITCH E.A. (1984) In: Geochemistry of Organic Matter in the Ocean, p. 334 (Springer Verlag).

ROSENFELD J.K. (1979[a]) Ammonium adsorption in nearshore anoxic sediments. Limnol. Oceanogr. 24, 356-364.

ROSENFELD J.K. (1979[b]) Amino acid diagenesis and adsorption in nearshore anoxic sediments. Limnol. Oceanogr. 24, 1014-1021.

ROSENFELD J.K. (1981) Nitrogen diagenesis in Long Island Sound sediments. Am. J. Sci 281, 436-462.

ROZANOV A.G., MISCHENOKO V.V. and YAHKICHEV V.I. (1978) The 'pneumo-press' - a device for extracting interstitial water. Oceanology 18, 229-231.

SALOMONS W. and FÖRSTNER U. (1984) Metals in the hydrocycle, Springer, 349p.

SANTSCHI P.H., BAJO C., MANTOVANI M., ORCIUOLO D., CRANSTON R.E. and BRUNO J. (1988) Uranium in pore waters from North Atlantic (GME and Southern Nares Abyssal Plain) sediments. Nature 331, 155-157.

SAWLAN J.L. and MURRAY J.W. (1983) Trace metal remobilization in the interstitial waters of red clay and hemipelagic marine sediments. Earth Planet. Sci. Lett. 64, 213-230.

SAWLAN J.J. (1982) Early diagenetic remobilization of some transition metals in hemipelagic sediments. Ph.D. Thesis, Un. of Washington, pp. 251.

SAYLES F.L. (1970) Preliminary geochemistry - in : (Bader R.G., et al., eds), Init. Repts. DSDP, Washington, U.S. Govt. Print. Office) 4, 645-655.

SAYLES F.L., WILSON T.R.S., HUME D.N. and MANGELSDORF P.C. Jr. (1973[a]) In situ sampler for marine sedimentary pore waters : evidence for potassium depletion and calcium enrichment. Science 181, 154-156.

SAYLES F.L., MANHEIM F.T. and WATERMAN L.S. (1973[b]) Interstitial water studies on small core samples. Init. Rept. DSDP, Wash. (U.S. Print. Office) 20, 783-805.

SAYLES F.L. and MANHEIM F.T. (1975) Interstitial solutions and diagenesis in deeply burried marine sediments : results from the Deep Sea Drilling Project. Geochim. Cosmochim. Acta 39, 103-127.

SAYLES F.L., MANGELSDORF P.C., WILSON T.R.S. and HUME D.N. (1976) A sampler for the in situ collection of marine sedimentary pore waters. Deep-Sea Res. 23, 259-264.

SAYLES F.L. (1979) The composition and diagenesis of interstitial solutions - I. Fluxes across the seawater-sediment interface in the Atlantic Ocean. Geochim. Cosmochim. Acta 43, 527-545.

SAYLES F.L. (1981) The composition and diagenesis of interstitial solutions -II. Fluxes and diagenesis at the water-sediment interface in the high-latitude North and South Atlantic. Geochim. Cosmochim. Acta 45, 1061-1086.

SAYLES F.L. (1985) $CaCO_3$ solubility in marine sediments : Evidence for equilibrium and non-equilibrium behavior. Geochim. Cosmochim. Acta 49, 877-888.

SCHMINKE H.U. and VON RAD U. (1979) Neogene evolution of Canary Islands volcanism

inferred from ash layers and volcaniclastic sandstones of DSDP Site 397 (Leg 47A). In von Rad U., Ryan W.B.F. et al., eds. Init. Rep. DSDP 47, 703-725.
SCHOLL D.W. (1963) Techniques for removing interstitial water from coarse-grained sediments for chemical analysis. Sedimentology 2, 156-163.
SCHÖTTENHELM R.T.E. et al. (1988) Shipboard report (in press).
SEARLE R.C., SCHULTHEISS P.J., WEAVER P.P.E., NOEL M., KIDD R.B., JACOBS C.L. and HUGGETT Q.J. (1985) Great Meteor East (distal Madeira Abyssal Plain) : geological studies of ints suitibility for disposal of heat-emitting radioactive wastes. Rep. 193, Wormley, Institute of Oceanographic Sciences.
SEIBOLD E.and HINZ K. (1979) Continental slope construction and destruction. In : Burke C. et al. (eds.) The Geology of Continental Margins, Berlin, Springer., p. 179-196.
SEIBOLD E. and BERGER W.H. (1982) The Sea floor. Berlin, Springer Verlag, p.288.
SHERWOOD B.A., SAGER S.L. and HOLLAND H.D. (1987) Phosphorus in foraminiferal sediments from North Atlantic Ridge cores and in pure limstones. Geochim. Cosmochim. Acta 51, 1861-1866.
SHIPLEY T.H. (1978) Sedimentation and echo characteristics in the abyssal hills of the west-central North Atlantic. Geol. Soc. Amer. Bull. 89, 397-408.
SHISHKINA O.V. (1968) Metody issledovaniya morskikh i okeanicheskikh ilovykh vod (methods of studying marine and oceanic pore fluids). In : BOGOMOLOV G.V. (ed.) Porovye rastvory i metody ikh izucheniya (interstitial waters and methods of studying them), 167-177. Nauka i Tekhnika, Minsk.
SHISHKINA O.V. and TSVETKOV G.A. (1978) Separation of interstitial waters using a cooling system. Oceanology 18, 428-430.
SHOLKOVITZ E. (1973) Interstitial water chemistry of the Santa Barbara Basin sediments. Geochim. Cosmochim. Acta 37, 2043-2073.
SIEVER R. (1962) A squeezer for extracting interstitial waters. J. Sed. Petrol. 32, 329-331.
SILVA J.A. and BREMNER J.M. (1966) Determination and isotope-ratio analysis of different forms of nitrogen in soils. 5. Fixed ammonium. Soil Sci. Soc. Amer. Proc. 30, 587-594.
SIMM R.W. and KIDD R.B. (1984) Submarine debris flow deposits detected by long-range sidescan sonar 1000 km from source. Geo-mar. Lett. 3, 13-16.
SIMS J.R. and HABY V.A. (1971) Simplified colorimetric determination of soil organic matter. Soil Sci. 112, 137-141.
SINGER A., STOFFER P., HELLER-KALLAI L. and SZAFRANEK D. (1984) Nontronite in a deep-sea core from the South Pacific. Clays Clay Minerals 32, 375-383.
STEVENSON F.J. and DHARIWAL A.P.S. (1959) Distribution of fixed ammonium in soils. Soil Sci. Soc. Amer. Proc. 23, 121-125.
STEVENSON F.J. and C.-N. CHENG (1972) Organic geochemistry of the Argentine Basin sediments: carbon-nitrogen relationships and Quaternary correlations. Geochim. Cosmochim. Acta 36, 653-671.
STRICKLAND J.D.H. and PARSONS T.R. (1968) A practical handbook of seawater analysis. Fish. Board Canada Bull. 167, 311p.
STUMM W. and MORGAN J.J. (1970) Aquatic chemistry, Wiley Interscience, 583p.
SUESS E. (1973) Interaction of organic compounds with calcium carbonate -II. Organo-carbonate association in Recent sediments. Geochim. Cosmochim. Acta 37, 2435-2447.
SUESS E. (1979) Mineral phases formed in anoxic sediments by microbial decomposition of organic matter. Geochim. Cosmochim. Acta 43, 339-352.

SUESS E. (1981) Phosphate regeneration from sediments of the Peru continental margin by dissolution of fish debris. Geochim. Cosmochim. Acta 45, 577-588.
SWARZENSKI W.V. (1959) Determination of chloride in water from core samples. Bull. Am. Ass. Petrol. Geol. 43, 1995-1998.
TEBO B.M., NEALSON K.H., EMERSON S. and JACOBS L. (1984) Microbial mediation of Mn(II) and Co(II) precipitation at the O_2/H_2S interfaces in two anoxic fjords. Limnol. Oceanogr. 29, 1247-1258.
TEN HAVEN H.L., DE LANGE G.J., and KLAVER G.T. (1985) The chemical composition and origin of the Tyro brine, eastern Mediterranean. A tentative model. Mar. Geol. 64, 337-342.
TEN HAVEN H.L. (1986) Organic and inorganic geochemical aspects of Mediterranean late-Quaternary sapropels and Messinian evaporitic deposits. Ph. D. Thesis, Utrecht Un., pp. 203.
TEN HAVEN H.L., DE LANGE G.J. and MCDUFF R.E. (1987) Interstitial water studies of Late Quaternary eastern Mediterranean sediments with emphasis on early diagenetic reactions and evaporitic salt influences. Mar. Geol. 75, 119-136.
THIERSTEIN H.R. (1988) Inventory of paleoproductivity records : the Mid-Cretaceous enigma. In : Productivity of the ocean: present and past. Dahlem Conf. April 1988 (in press).
THOMSON J., WILSON T.R.S., CULKIN F. and HYDES D.J. (1984[a]) Non-steady state diagenetic record in eastern equatorial Atlantic sediments. Earth Planet. Sci. Lett. 71, 23-30.
THOMSON J., CARPENTER M.S.N., COLLEY S., WILSON T.R.S., ELDERFIELD H. and KENNEDY H. (1984[b]) Metal accumulation rates in northwest Atlantic pelagic sediments. Geochim. Cosmochim. Acta 48, 1935-1948.
THOMSON J., HIGGS N.C., JARVIS I., HYDES D.J., COLLEY S. and WILSON T.R.S. (1986) The behaviour of manganese in post-oxic Atlantic carbonate sediments. Geochim. Cosmochim. Acta 50, 1807-1818.
THOMSON J., COLLEY S., HIGGS N.C., HYDES D.J., WILSON T.R.S. and SØRENSEN J. (1987) Geochemical oxidation fronts in NE Atlantic turbidites and their effects in the sedimentary record. In : Weaver P.P.E. and Thomson J. (eds.) Geology and Geochemistry of Abyssal Plains. Proc. Geol. Soc. 31, 167-177.
TLIG S. (1988) Fish debris as chemical scavengers of zirconium and lanthanum in oceanic environments - Zr and Hf fractionation in marine phosphates. Chem. Geol. 69, 59-71.
TOTH D.J. and LERMAN A. (1977) Organic matter reactivity and sedimentation rates in the ocean. Am. J. Sci 277, 465-485.
TROELSTRA S.R. (1984) Foraminiferal studies on cores from the Madeira Abyssal Plain, eastern North Atlantic. In: Geological Studies in the eastern North Atlantic (Kujpers et al., eds.) Meded. Rijks Geol. Dienst 38, 153-168.
TROUP B.N., BRICKER O.P. and BRAY J.T. (1974) Oxidation effect on the analysis of iron in the interstitial water of recent anoxic sediments. Nature 249, 237-239.
TUCHOLKE B.E. (1980) Acoustic environment of the Hatteras and Nares Abyssal Plains, western North Atlantic Ocean, determined from velocities and physical properties of sediment cores. J. Acoust. Soc. Am. 68, 1376-1390.
TURNER D.R., WHITFIELD M. and DICKSON A.G. (1981) The equilibrium speciation of dissolved components in freshwater and seawater at 25°C and 1 atm pressure. Geochim. Cosmochim. Acta 45, 855-881.

UCHUPI E., EMERGY K.O., BOWIN C.O. and PHILLIPS J.D. (1976) Continental margin off western Africa; Senegal to Portugal. Bull. Am. Assoc. petrol. Geol. 60, 809-878.
VAN DER SLOOT H.A., HOEDE D., HAMBURG G., DE LANGE G.J., MIDDELBURG J.J. and SHOFIYAH S. (1988) Suspended manganese micro-nodules in Kay Bay Halmahera (eastern Indonesia). Mar. Geol. 80, 251-259.
VAN DER WEIJDEN C.H., SCHUILING R.D. and DAS H.A. (1970) Some geochemical characteristics of sediments from the North Atlantic Ocean. Mar. Geol. 9, 81-99.
VAN DER WEIJDEN C.H., DE LANGE G.J., MIDDELBURG J.J., HOEDE D., VAN DER SLOOT H.A., and SOFIYAH S. (1988[a]) Chemical characteristics of Kau Bay water. Neth. J. Sea Res. (in press).
VAN DER WEIJDEN C.H., DE LANGE G.J., MIDDELBURG J.J. and VAN DER SLOOT H.A. (1988[b]) The chemical composition of the hypersaline anoxic Tyro and Bannock Basins in the eastern Mediterranean. Chem. Geol. 70, 19.
VAN DER WEIJDEN C.H., DE LANGE G.J., MIDDELBURG J.J. and VAN DER SLOOT H.A. (1988[c]) Some marine geochemical aspects of Kau Bay : a tropical fjord-like anoxic basin. Chem. Geol. 70, 199.
VAN ECK G.T.M. (1981) Geochemie van zwevend materiaal en water in het Hollands Diep/Haringvliet. Ph.D. Thesis Utrecht University, pp.271.
VERBEEK J.W. (1984) The nannofossils from the western Madeira Abyssal Plain. In: Geological Studies in the eastern North Atlantic (Kujpers et al., eds.) Meded. Rijks Geol. Dienst 38, 137-151.
VON RAD U. and HINZ K. (1982) Geology of the Northwest African Continental Margin, Berlin, Springer.
VRIEND S.P., VAN GAANS P., MIDDELBURG J.J. and DE NIJS T. (1988) The application of non-linear mapping and Fuzzy-C-Means clustering to geochemical data sets. Applied Geochem. 3, 213-224.
WALSH J.J., PREMUZIC E.T. and WHITLEDGE T.E. (1985) Fate of nutrient enrichment of continental shelves as indicated by the C/N content of bottom sediments. In: Ecohydrodynamics, ed. J.H. Nihoul (Amsterdam, Elsevier), pp.13-49.
WALSH J.J. (1988) How much shelf production reaches the deep-sea In : Productivity of the ocean: present and past. Dahlem Conf. April 1988 (in press).
WATANABE Y. and TSUNOGAI S. (1984) Adsorption-desorption control of phosphate in anoxic sediment of a coastal sea, Funka Bay, Japan. Mar. Chem. 15, 71-83.
WEAVER P.P.E. and KUIJPERS A. (1983) Climatic control of turbidite deposition on the Madeira Abyssal Plain. Nature 306, 360-363.
WEAVER P.P.E., SEARLE R.C. and KUIJPERS A. (1986) Turbidite deposition and the origin of the Madeira Abyssal Plain. In : Summerhayes C.P. and Shackleton N.J.(eds.) North Atlantic Paleoceanography. Proc. Geol. Soc. 21, 131-143.
WEAVER P.P.E. and ROTHWELL R.G. (1987) Sedimentation on the Madeira Abyssal Plain over the last 300 000 years. In: Weaver P.P.E. and Thomson J. (eds) Geology and Geochemistry of Abyssal Plains. Proc. Geol. Soc. 31, 71-86.
WEAVER C.E. and POLLARD L.D. (1973) The Chemistry of Clay Minerals, Developments in Sedimentology 15, Amsterdam, Elsevier.
WEDEPOHL K.H. (1971) Environmental influences on the chemical composition of shales and clays. In: L.H. Ahrens, F. Press, S.K. Runcorn and H.C. Urey (eds.) Physics and Chemistry of the Earth 8, 307-333. Pergamon Press.
WENSINK H. (1984) Paleomagnetism of three deep-sea cores recovered from the Madeira Abyssal Plain. Meded. Rijks Geol. Dienst 38, 169-181.

WESTRICH J.T. (1983) The consequences and controls of bacterial sulfate reduction in marine sediments. Ph. D. Thesis, Yale Un., pp. 530.
WESTRICH J.T. and BERNER R.A. (1984) The role of sedimentary organic matter in bacterial sulfate reduction = The G model tested. Limnol. Oceanogr. 29, 236-249.
WHITFIELD M. and JAGNER D. (1981) Marine Electrochemistry, Wiley, 529p.
WILLIAMS J.D.H., SYERS J.K. and WALKER T.W. (1967) Fractionation of soil inorganic phosphate by a modification of Chang and Jackson's procedure. Soil Sci. Soc. Am. Proc. 31, 736-739.
WILLIAMS J.D.H., JAQUET J.M. and THOMAS R.L. (1976) Forms of phosphorus in the surfacial sediments of Lake Erie. Can. Fish. Res. Bd. J. 33, 413-429.
WILSON T.R.S., THOMSON J., COLLEY S., HYDES D.J., HIGGS N.C. and SØRENSEN J. (1985) Early organic diagenesis; the significance of progressive subsurface oxidation fronts in pelagic sediments. Geochim. Cosmochim. Acta 49, 811-822.
WILSON T.R.S., THOMSON J., HYDES D.J., COLLEY S., CULKIN F. and SØRENSEN J. (1986) Oxidation fronts in pelagic sediments : diagenetic formation of metal-rich layers. Science 232, 972-975.
WINCHESTER J.A.G. and FLOYD P.A. (1977) Geochemical discriminants of different magma series and their differentiation products using immobile elements. Chem. Geol. 20, 325-343.
WINTERS G.V. and BUCKLEY D.E. (1986) The influence of dissolved $FeSi_2O_3(OH)^\circ$ on chemical equilibria in pore waters from deep sea sediments. Geochim. Cosmochim. Acta 50, 277-288.
WOLFF J.A. (1985) Zonation, mixing and eruption of silica-undersaturated alkaline magma : a case study from Tenerife, Canary Islands. Geol. Mag. 122, 623-640.
WOLLAST R. (1974) The silica problem. In The Sea (ed. E.D. Goldberg) 5, pp. 359-392. Wiley Interscience.
YAMANAKA S., KANAMARU F. and KOIZUMI M. (1971) Reaction of montmorillonite with acrylonitrile In: US/Japan Seminar on clay-organic complexes, aug. 1971; 31-35.

Curriculum Vitae

Gerrit Jan de Lange werd geboren op 15 juni 1950 te Harderwijk. In 1969 behaalde hij het diploma hbs-B aan het Chr. College Nassau-Veluwe te Harderwijk. In 1977 werd aan de Rijks Universiteit Groningen het doctoraal examen Chemie met bijvak Geologie afgelegd. Van 1978 - 1979 was hij werkzaam bij het NIOZ (als tijdelijk wetenschappelijk medewerker voor het STUNET project), en van 1979-1980 bij de Gemeentelijke MTS te Vlissingen (als leraar Natuur- en Scheikunde). Vanaf 1980 werkt hij als wetenschappelijk ambtenaar, en vanaf 1987 als Universitair Docent Mariene Geochemie bij het Instituut voor Aardwetenschappen van de Rijksuniversiteit te Utrecht.